Characterisation of Pigmentation in a Novel Isolate of *Arthrobacter* Recovered from Soils of the Namib Desert

Jack Vasey

A thesis submitted to Auckland University of Technology in partial fulfilment of the requirements for the degree of Master of Science (Research) (MSc(Res))

2022

School of Science

Abstract

The high solar irradiation of desert systems is biologically stressful upon their indigenous soil bacteria, and has major influences on the complexity of their irradiation resistomes (Yuan et al. 2012; Paulino-Lima et al. 2013; Pavlopoulou et al. 2016; León-Sobrino et al. 2019). Characterising features of these bacterial resistomes which confer tolerance to irradiation stress develops our understanding of the breadth of survival systems utilised by extremophiles, and is thus valuable to the field of microbial ecology (Matallana-Surget and Wattiez 2013; Pérez et al. 2017).

Arthrobacter sp. NamB2 is a pink-pigmented bacterium from surface soils of the Namib Desert (Buckley 2020). This bacterium demonstrates substantial tolerance to ultraviolet irradiation, and has a corresponding multifaceted intrinsic irradiation resistome (Buckley 2020). The contribution of this bacterium's pink-pigmentation to its irradiation tolerance was the focus of investigation for this thesis, as pigmentation – particularly the red/yellow pigments of the carotenoid class – have been attributed as a major component in the tolerance of bacteria from other desert systems, including the Atacama and Antarctic deserts (Dieser et al. 2010; Silva et al. 2019; Flores et al. 2020). Despite the stable, demonstrably microbiologically-harmful solar irradiance of the Namib Desert, no similar investigations of pigmentation as a component of intrinsic bacterial resistomes in this environment have yet been performed. This thesis thus sought to expand knowledge on the breadth of irradiation tolerance systems utilised by extremophiles from regions of high solar irradiance by characterising the role of pigmentation in the irradiation-resistome of *Arthrobacter* sp. NamB2. To achieve this, the pigment was first identified, while its contributions to irradiation tolerance were investigated via analyses of its light-inducibility in biosynthesis, and pigment-specific mitigation of lethality arising under ultraviolet-A, -B and -C irradiation.

The pigmentation of *Arthrobacter* sp. NamB2 was extracted and subject to a series of analyses for identification. The extracted pigmentation produced characteristic carotenoid spectral responses under scanning ultraviolet-visible spectroscopy, confirming it was a carotenoid. Chromatographic separation of the pigment extract using thin-layer chromatography and high-performance liquid-chromatography demonstrated the pigment comprised six – eight polarity-discrete carotenoids, each possessing a chromophore thirteen conjugated double bonds in length. Subsequent mass-spectrometry confirmed the presence of the carotenoid bacterioruberin

within the extract, and provided evidence for the presence of a number of its commonly co-isolated dehydrated/glycosylated carotenoid variants. The pink-pigment of *Arthrobacter* sp. NamB2 was thus concluded as carotenogenic in nature, and comprised of a pigment complement specifically based around the carotenoid bacterioruberin.

The light-inducibility of pigment production by *Arthrobacter* sp. NamB2 was investigated as evidence of its function in irradiation-tolerance. The total pigment content produced by cultures grown at a series of light intensities was compared for evidence of light-responsive carotenoid biosynthesis. Results of these assays were supported by *in silico* examinations of the available *Arthrobacter* sp. NamB2 genome (GenBank: GCA_005281365.1) for the presence of candidate genes encoding homologues to known light-responsive regulators of carotenogenesis. This was used to establish if there was a genetic basis for light-responsive carotenoid production in *Arthrobacter* sp. NamB2. There was no significant difference between the pigment content of cultures grown under differing light conditions, indicating a lack of light-responsive carotenogenesis. This conclusion was supported by the absence of relevant homologues to known light-responsive carotenogenesis regulators within the *Arthrobacter* sp. NamB2 genome. Lack of light-responsive pigmentation in *Arthrobacter* sp. NamB2 did not discount its photoprotective role, but was a novel contribution to the study of photoinducibility within both *Arthrobacter* and desert organisms.

Finally, pigment-mediated protection against ultraviolet-irradiation was examined through survival comparisons of pigmented *Arthrobacter* sp. NamB2 cultures and their unpigmented variants generated via carotenoid inhibition. Pigmented and unpigmented cultures were exposed to high intensities of ultraviolet-A, -B and -C irradiation to determine within which waveband(s) the pigment was capable of cellular protection. Pigmented cells had significantly higher survival than unpigmented cells under ultraviolet-A and ultraviolet-B irradiation, with weakening protection afforded under higher doses of ultraviolet-B, and a total loss of protection under ultraviolet-C. Potential ultraviolet-screening protective roles of the pigment were investigated and dismissed from its lack of pronounced absorbance within the ultraviolet waveband. From the known damage modes of ultraviolet-irradiation, these findings indicated that pigmentation protected *Arthrobacter* sp. NamB2 only from ultraviolet-wavebands and dosages stimulating damage through the production of reactive oxygen species, with no capacity for the mitigation of direct DNA/protein damage. These inferred conclusions would be strengthened by specific investigations of the mechanisms of protection afforded by pigmentation, but did confirm the contribution of pigmentation to the ultraviolet-irradiation tolerance of *Arthrobacter* sp. NamB2.

The findings of this thesis demonstrated that the carotenoid pigmentation of *Arthrobacter* sp. NamB2 contributes meaningfully to its ultraviolet-irradiation resistome. Use of carotenoid pigmentation in irradiation-protection is consistent with findings in bacteria from other desert systems, while limitation of their protective capacity to the mitigation of damage inflicted by reactive oxygen species matches expectations of carotenoid photoprotection. This thesis demonstrates for the first time the contribution of pigmentation in a novel edaphic Namib Desert bacterium to its irradiation-resistome, and speculates a similar physiological utility in its natural environment.

Table of Contents

List of Figures

List of Equations

List of Tables

Attestation of Authorship

I hereby declare that this submission is my own work and that, to the best of my knowledge and belief, it contains no material previously published or written by another person (except where explicitly defined in the acknowledgements), nor material which to a substantial extent has been submitted for the award of any other degree or diploma of a university or other institution of higher learning.

Jack Vasey

Date: 29/09/2021

Acknowledgements

I could not have achieved a fraction of what I have within this work without some truly incredible people behind me. I hope that through acknowledgement, I can show you all some small part of my gratitude.

To my supervisor Dr Brent Seale, thank you for allowing me to study under you, and for granting me staunch guidance on my project with the levity to never make it intimidating. Your knowledge and patience with my concerns meant I was never truly lost, and never without encouragement. Thank you further to my secondary supervisor Dr Colleen Higgins. You consistently challenged me to push forward my thinking around my research, and held me accountable in my leaps of logic. The critical lens you turned towards my ideas, and the evident empathy behind it, have shaped my grasp of science in ways that I am quite certain, and contented, that I will hold forever.

To Dr Kevin Lee, I thank you for the extensive time you spent reading and re-reading every chapter I sent to you. Your consistent ability to make time for me, and the always-conversational critique you provided, has meaningfully influenced my writing, and supported me to take pride in my work.

I would like to thank the entire Molecular Genetics research group. Each of you granted me advice, support, and an audience through which my concerns could be reshaped (however successfully) into quips and jokes, to which I owe no small part of my sanity. To Dr Elizabeth Buckley, your constant advice and genuine, meaningful engagement with my research was consistently amazing, and helped me see things in ways I could not have alone. To Tay, I don't think I can thank you enough.

I owe rightful thanks to everyone who ever acted as a lab-buddy for me, from five-minute inoculations to six-hour irradiations. In-particular, I would like to extend my thanks to Kendall and Gayathri, who shared a breadth of their early mornings and late-evenings with me and my eternally time-sensitive and picky bacteria.

To my brother and sister Tom and Megan, I thank you for your endless confidence in me. For distracting me when I needed it, and celebrating every milestone, no matter how small, with an excitement that I found contagious.

To my Mum, I just honestly couldn't have done this without you. For every late night phonecall, sanity check and reassurance, I owe you more than I could possibly hope to articulate or repay. You helped me see the bigger picture, and remember my confidence when I needed it. I love you.

Finally, to Natalie. Thank you for every wonderful moment of respite you gave me from this beast. The genuine joy and freedom you shared with me always overshadowed my worries, and picked me up when I could not do so alone. Having you along for this journey has meant more to me than I can say here without finally exceeding my word limit, but understand that things are far brighter with you around. Weird and happy.

Abbreviations

%	Percentage
(6-4)PP	Pyrimidine-(6-4)-Pyrimidone Photoproducts
µA	Microamps
µM	Micromolar
µmol m^{-2} s^{-1}	Micromoles of Photons Per Meter Squared Per Second
aa	Amino-Acid
ABC	ATP-Binding Cassette
AdoB12	Adenosylcobalamin
ANOVA	Analysis of Variance
APCI	Atmospheric-Pressure Chemical Ionisation
BABR	Bisanhydrobacterioruberin
BER	Base-Excision Repair
BLAST	Basic Local Alignment Search Tool
bp	Base Pair
°C	Degrees Celsius
c.d.b.	Conjugated Double Bonds
cfu	Colony Forming Units
cm	Centimetre
CPD	Cyclobutane Pyrimidine Dimer
CrtR	Carotenogenesis Regulator
DAD	Diode-Array Detector
DPA	Diphenylamine
DU	Dobson-Units
EtOH	Ethanol
g	Grams
g	Gravity
HK	Histidine Kinase
HPLC	High-Performance Liquid Chromatography
HTH	Helix-Turn-Helix
ISC	Inter-System Crossing
IR	Infra-Red
J/cm^2	Joules Per Centimetre Squared
J/m^2	Joules Per Meter Squared
kV	Kilo-Volts
LC	Liquid Chromatography
LED	Light-Emitting Diode
LitR	Light-Induced Transcription Regulator
M	Molar
m/z	Mass to Charge Ratio
M^{-1} cm^{-1}	Moles Per Centimetre
MABR	Monoanhydrobacterioruberin
MarR	Multiple Antibiotic Resistance Regulator
MeOH	Methanol
MerR	Mercuric Resistance Repressor
mg/g	Milligram Per Gram

mL	Millilitre
MMPL	Mycobacterial Membrane Large
MS	Mass-Spectrometry
NER	Nucleotide-Excision Repair
nm	Nanometres
nt	Nucleotide
OD_{600}	Optical Density at 600 nm
OH	Hydroxyl
PAR	Photosynthetically-Active Radiation
PHR	Photoreactivation
psi	Pounds Per Square Inch
Rf	Retardation Factor
rpm	Revolutions Per Minute
RT-qPCR	Quantitative Reverse Transcription Polymerase Chain Reaction
ROS	Reactive Oxygen Species
RQ	Research Question
SOD	Superoxide Dismutase
TABR	Tetraanhydrobacterioruberin
TLC	Thin-Layer Chromatography
TRABR	Trisanhydrobacterioruberin
Tukey HSD	Tukey's Honest Significance Difference
UHPLC	Ultra-High-Performance Liquid Chromatography
UV	Ultraviolet
UVA	Ultraviolet-A
UVB	Ultraviolet-B
UVC	Ultraviolet-C
UV-Vis	Ultraviolet-Visible
W/m^2	Watts Per Meter Squared
wHTH	Winged Helix-Turn-Helix

Chapter 1 General Introduction and Literature Review

1.1 General Introduction

Solar irradiation is an abiotic stressor with significant influences on desert bacterial community compositions and the sophistication of their resistomes (Cary et al. 2010; Hernández et al. 2016). Prolonged, biologically stressful irradiation stimulates the development of complex and multifaceted irradiation tolerance systems in bacteria (Fernández Zenoff et al. 2006; Matallana-Surget and Wattiez 2013; Albarracín et al. 2016). As deserts are subject to stable, high-intensity surface irradiance resulting from atmospheric conditions common to arid environments, their edaphic bacterial communities demonstrate well-developed irradiation resistomes and complex damage tolerance systems (Yuan et al. 2012; Pavlopoulou et al. 2016; León-Sobrino et al. 2019). Understanding the irradiation-resistance mechanisms of bacteria from these regions of high solar insolation deepens our understanding of how extremophiles persist under such conditions, and is consequently of growing interest to the field of microbial ecology (Matallana-Surget and Wattiez 2013; Pavlopoulou et al. 2016).

Production of carotenoid pigmentation is an important strategy for irradiation tolerance in desert soil bacteria (Dieser et al. 2010; Yuan et al. 2012; Reis-Mansur et al. 2019). In these organisms, carotenoids provide cellular protection by quenching reactive oxygen species (ROS), generated from radiation-stimulated photochemical reactions (Dieser et al. 2010; Schwieterman et al. 2015; Sandmann 2019; Silva et al. 2019). Carotenoid pigmentation has been characterised repeatedly as a significant component of bacterial irradiation resistomes, with examples in soil organisms from the Atacama, Antarctic and Gobi deserts (Dieser et al. 2010; Yuan et al. 2012; Pavlopoulou et al. 2016; Silva et al. 2019; Flores et al. 2020).

Arthrobacter sp. NamB2 is a novel, pink-pigmented bacterium from soils of the Namib Desert, which presents a promising model with which to study the contribution of bacterial pigmentation to irradiation tolerance (Buckley 2020). *Arthrobacter* sp. NamB2 has presented a high tolerance to ultraviolet radiation, with suspicions of a complex, multifaceted intrinsic irradiation-resistome consistent with its prolonged solar exposure (Buckley 2020). The pink-pigmentation of this bacterium has been speculated to share identity with carotenoids of suspected but unproven function in the irradiation-protection of other *Arthrobacter* spp.,

suggesting it may contribute meaningfully to the intrinsic irradiation-resistome of *Arthrobacter* sp. NamB2 (Ii et al. 2019; Silva et al. 2019; Buckley 2020). Despite the stable, high-intensity solar-irradiance of the Namib Desert, there have not yet been any dedicated investigations into pigmentation as a mechanism of irradiation-tolerance in its edaphic bacteria (Warren-Rhodes et al. 2013; León-Sobrino et al. 2019; Cowan et al. 2020). As such, this organism presents a novel model from a yet-unstudied desert environment of stable, biologically-stressful irradiance with which to characterise contributions of pigmentation to the irradiation-resistomes of edaphic desert bacteria, and the genus *Arthrobacter*.

The irradiation tolerance mechanisms of bacteria subject to stable, high solar irradiation are sophisticated and multifaceted (Pavlopoulou et al. 2016). Characterising the systems used for irradiation tolerance by extremophiles aids scientific understanding of the intracellular resistance mechanisms controlling microbial ecology in biologically stressful environments. The value of the Namib Desert as a model system is provided through the high intensity and stability of its irradiation, combined with the yet-uncharacterised nature of tolerance systems used by its edaphic bacteria. This thesis will thus investigate the protective role of cellular pigmentation in *Arthrobacter* sp. NamB2 against solar irradiation.

1.2 Research Questions/Aims

Research Question 1: What is the likely identity of the pink-pigmentation produced by *Arthrobacter* sp. NamB2?

Aim 1.1: To extract and determine if the pigmentation of *Arthrobacter* sp. NamB2 is carotenogenic in nature.

Objective 1.1.1: To perform a methanolic extraction of cellular pigmentation from *Arthrobacter* sp. NamB2, with subsequent ultraviolet-visible spectroscopy of these pigment extracts used to determine the pigment class.

Aim 1.2: To determine the likely identity of individual pigments comprising the pigment complement of *Arthrobacter* sp. NamB2.

Objective 1.2.1: To use chromatographic separation, specifically thin-layer chromatography (TLC) and high-performance liquid-chromatography (HPLC), to resolve the pigment complement of *Arthrobacter* sp. NamB2 into individual fractions on the basis of polarity.

Objective 1.2.2: To identify the individual pigment fractions purified by the chromatographic separation of **Objective 1.2.1** via features of their ultraviolet-visible spectral response/polarity (TLC-separated fractions) or fragmentation patterns of their generated mass-spectra (HPLC-separated fractions).

Research Question 2: Is the production of the pink-pigmentation of *Arthrobacter* sp. NamB2 light-induced?

Aim 2.1: To determine whether *Arthrobacter* sp. NamB2 produces significantly higher pigment content when grown under carotenoid-stimulatory light conditions.

Objective 2.1.1: To quantify and compare the pigment production of *Arthrobacter* sp. NamB2 cultures grown under a range of visible-light intensities known to stimulate carotenoid biosynthesis.

Aim 2.2: To determine whether there is a genetic basis for light-responsive carotenogenesis in *Arthrobacter* sp. NamB2.

Objective 2.2.1: To identify candidate homologues to known regulators of light-responsive carotenogenesis from non-phototrophic bacteria within the available genome sequence of *Arthrobacter* sp. NamB2.

Objective 2.2.2: To investigate whether the candidate light-responsive regulators identified under **Objective 2.2.1** are likely to have function in regulating carotenogenesis within *Arthrobacter* sp. NamB2 through *in silico* analysis of protein alignments and genomic context.

Research Question 3: What contribution does pigmentation provide the ultraviolet irradiation resistome of *Arthrobacter* sp. NamB2?

Aim 3.2: To determine the protective role pigmentation serves in the ultraviolet-A (UVA), ultraviolet-B (UVB) and ultraviolet-C (UVC) tolerance of *Arthrobacter* sp. NamB2.

Objective 3.2.1: To generate unpigmented cultures of *Arthrobacter* sp. NamB2 via treatment of cells with the carotenoid inhibitor diphenylamine, and assess negative influences of this inhibitor treatment upon cell growth.

Objective 3.2.2: To determine if pigmentation has a protective screening capacity against ultraviolet irradiation by comparing ultraviolet-visible scanning spectra of total methanolic extracts from pigmented and unpigmented cultures.

Objective 3.2.3: To compare the survival of pigmented and unpigmented cultures of *Arthrobacter* sp. NamB2 under biologically-stressful intensities of UVA, UVB or UVC-irradiation for evidence of pigment-specific protection.

1.3 Literature Review

1.3.1 Desert Systems

Deserts constitute more than one-fifth of Earth's land surface area, and are characterised by a number of common climatic and spatial features which render them hostile to biotic life (Laity 2008; Pointing and Belnap 2012). Desert systems are limited in biologically-available water, and are classified as arid regions on the basis that their ratio of water input (precipitation) to output (potential evapotranspiration) is below 1.0 (United Nations Environmental Programme 1992; Pointing and Belnap 2012; Makhalanyane et al. 2015; Šťovíček et al. 2017). Alongside this desiccation stress, deserts are subject to wide variability in surface temperatures, and oligotrophic soils due to their aridity preventing the development of important soil chemical cyclers, such as higher plants (Pointing and Belnap 2012; Lee et al. 2016; Lebre et al. 2017; Steven 2017).

These abiotic features of deserts exert considerable stress upon indigenous soil bacteria, including xeric stress, imposition of freeze-thaw cycles and severe nutrient limitations (Dieser et al. 2010; Lebre et al. 2017; Cowan et al. 2020). Desert systems consequently present a restricted range of functional and taxonomic diversity in their soil bacterial communities relative to more temperate regions (Navarro-González et al. 2003; Fierer et al. 2012; Makhalanyane et al. 2015; Ramond et al. 2019). For example, the soils of the Atacama Desert have bacterial taxonomic diversities some four-fold lower than temperate terrestrial environments (Navarro-González et al. 2003; Fierer et al. 2012). Local climate stressors shape the biodiversity and distribution of the persisting desert bacterial communities, with solar irradiation in particular playing a significant role (Andrew et al. 2012; Vásquez-Dean et al. 2020).

1.3.1.1 Solar Irradiation as a Biological Stressor in Desert Systems

Desert systems are subject to high surface solar irradiation at intensities stressful for their indigenous microbiota (Cunningham 1998; Rondanelli et al. 2015; Cordero et al. 2016). Solar irradiation exerts stress on microorganisms through wavelength-dependent damage to DNA and other cellular components, and is lethal at sufficient incident intensities (Santos et al. 2013). In contrast to temperate regions, deserts present low atmospheric aerosol loadings, infrequent cloud coverages, low ozone column densities and low solar-zenith angles, ultimately resulting in low atmospheric sunlight-screening capacities, and unusually high surface irradiance (Dana et

al. 1998; Lacap et al. 2011; Rampelotto 2013; Cordero et al. 2014; Cordero et al. 2016; Kgabi et al. 2016). As a consequence of these atmospheric trends, desert systems such as the Atacama and Antarctic Deserts exhibit midday visible light and ultraviolet (UV) irradiation intensities 1.8 – 3.0 times higher than temperate regions such as New Zealand or European sites, and consistently in excess of intensities known to be lethal to microorganisms (Glaeser and Klug 2005; Huld et al. 2005; Paulino-Lima et al. 2013; Hernández et al. 2016; Shiona et al. 2016; Remund et al. 2020).

Due to its high intensity, solar irradiation has a considerable influence on the bacterial communities of desert systems (Cary et al. 2010; Wierzchos et al. 2015; Meslier et al. 2018). The study of Cowan et al. (2011) stressed that Antarctic bacterial community distributions are significantly influenced by local solar irradiation intensities, and specifically develop in a manner to avoid irradiation. This is supported by studies of bacterial community distributions within the Atacama and Namib Deserts, indicating that irradiance is a generalisable abiotic stressor for desert bacterial communities (Warren-Rhodes et al. 2013; Makhalanyane et al. 2015; Wierzchos et al. 2015). Furthermore, high solar irradiance shapes sky-exposed bacterial communities to favour the predominance of radiotolerant species, with bacteria from open desert soils frequently presenting solar irradiation tolerances some two to ten-fold higher than temperate terrestrial organisms (Makhalanyane et al. 2013; Montero-Calasanz et al. 2013; Paulino-Lima et al. 2013; Paulino-Lima et al. 2016; Pavlopoulou et al. 2016; Reis-Mansur et al. 2019; Silva et al. 2019). Understanding the mechanisms used by desert bacteria to tolerate irradiation stress directly informs our understanding of microbial ecology within these high irradiance environments, and the complexity of systems such organisms may use to persist under lethal irradiation (Makhalanyane et al. 2015; Pavlopoulou et al. 2016).

1.3.1.2 The Namib Desert

The Namib Desert is one of the oldest and driest deserts on Earth, and extends some 2,000 kilometres along the Atlantic coast of Southern Africa (Foissner et al. 2002; Eckardt et al. 2013; Goudie and Viles 2015a; Cowan et al. 2020). The interaction between the Atlantic Benguela current and South Atlantic high-pressure region means that the Namib Desert maintains a stable climatic zone, and an arid climate (Eckardt et al. 2013; Bliss 2018). The microbiota of the Namib Desert is subject to substantial abiotic stress consistent with other desert systems. Rainfall across the Namib is low (below 50 mm annually) and demonstrates high spatial variability, exerting xeric stress on edaphic bacteria (Schachtschneider and February 2010; Eckardt et al. 2013; Scola et al. 2018; Cowan et al. 2020). Furthermore, daily surface

temperatures fluctuate from 0 – 50 ºC, and the desert soil is oligotrophic, restricted in quantities of organic carbon and nitrogen, discouraging the growth of higher organisms and selecting against fastidious microbiota (Makhalanyane et al. 2013; Goudie and Viles 2015b; Makhalanyane et al. 2015; Gunnigle et al. 2017; Johnson et al. 2017; Ramond et al. 2018). These abiotic stressors result in the limited taxonomic diversity and abundance of bacterial communities within the Namib Desert (Ramond et al. 2019).

1.3.1.3 Solar Irradiation of the Namib Desert

The Namib Desert is subject to a high intensity of solar irradiance due to its sparse cloud coverage, low levels of air-borne particulate matter and low ozone column density (Cunningham and Bodeker 2000; Esposito et al. 2003; Rondanelli et al. 2015; Kgabi et al. 2016; Adesina et al. 2019). Consequently, the Namib Desert demonstrates a midday solar irradiation intensity comparable to, or surpassing those of the Antarctic and Atacama Deserts (Dana et al. 1998; Warren-Rhodes et al. 2013; Cordero et al. 2018; León-Sobrino et al. 2019). Indeed, the midday visible light intensity of the Namib Desert is five fold higher than temperate regions such as New Zealand, while ultraviolet-A and ultraviolet-B intensities are some three – four fold higher (Lange et al. 1990; Warren-Rhodes et al. 2013; Beckmann et al. 2014; Kgabi et al. 2016; Lucas et al. 2016; Remund et al. 2020). This high solar insolation exerts a notable selection pressure on bacteria within the Namib Desert, and has been shown to significantly influence bacterial community distributions, compositions, and the expression of genes facilitating irradiation survival (Makhalanyane et al. 2013; Warren-Rhodes et al. 2013; León-Sobrino et al. 2019).

Furthermore, the Namib Desert demonstrates a remarkable stability in its irradiance, resulting from its highly stable local climate and atmospheric composition (Cunningham and Bodeker 2000; Kgabi et al. 2016; Adesina et al. 2019). Indeed, the study of Cunningham and Bodeker (2000) denoted only minor shifts in total ozone column density and other atmospheric screening factors in the Namib Desert over the course of 21 years (1978 – 1999). The stability of the Namib Desert's atmospheric conditions creates a uniquely stable surface irradiance, thus rendering solar-irradiation a highly stable selection pressure on its bacterial communities (Cunningham 1998; Cunningham and Bodeker 2000; Hernández et al. 2016).

In terrestrial environments where solar irradiance consistently reaches stressful intensities, bacterial abundance is limited, and community compositions shift to favour limited diversities

of organisms with more sophisticated irradiation resistomes (Jacobs and Sundin 2001; Stark and Hart 2003; Farías et al. 2009; Ruiz Gonzalez et al. 2013). As the high surface-irradiance of desert systems necessitates the adaptation of their indigenous organisms for survival, the study of tolerance systems employed by bacteria capable of survival within environments such as the Namib is intrinsically valuable to our understanding of microbial ecology in conditions of extreme irradiation (Makhalanyane et al. 2015). To contextualise how bacteria from these environments specialise their irradiation tolerance, understanding first how solar irradiation exerts damage upon microorganisms is required.

1.3.2 Solar Irradiance as an Abiotic Stressor

The solar irradiation reaching Earth's surface is comprised of approximately 13 % UV radiation (< 400 nm), 44 % visible radiation (400 – 700 nm) (also known as photosynthetically-active radiation (PAR)), and 43 % infra-red (> 700 nm) (Pitts 1990). Of these, radiation within the UV and PAR wavebands are the most relevant as microbial stressors (Besaratinia et al. 2011; Santos et al. 2012).

Ultraviolet radiation is divided into four wavelength categories; Vacuum UV (< 200 nm), ultraviolet C (UVC) (200 – 280 nm), ultraviolet B (UVB) (280 – 320 nm), and ultraviolet A (UVA) (320 – 400 nm) (Cockell and Knowland 1999; Rastogi et al. 2010; Santos et al. 2013). Of the UV radiation reaching Earth's surface, 90 – 95 % comprises UVA, and 5 – 10 % comprises UVB, with UVC quantitatively screened by atmospheric ozone (Girard et al. 2011; Santos et al. 2013; Jones and Baxter 2017). Shorter irradiation wavelengths are considered more microbiologically stressful, with UVB and UVC irradiation inflicting higher rates of bacterial mutagenesis and inactivation than UVA in *in vitro* studies (Santos et al. 2013). However, as the UVA and PAR waveband comprises the greater component of terrestrial radiation, it is considered more important as a biological stressor in bacterial community development (Girard et al. 2011; Björn 2015a; Jones and Baxter 2017).

Irradiation inflicts bacterial cell damage in a wavelength-dependent manner (Santos et al. 2013). The main source of damage invoked by UVB and UVC radiation is considered to be upon the cellular DNA, in which they induce a variety of lethal/mutagenic lesions (Yoon et al. 2000; García-Gómez et al. 2012). Conversely, PAR and UVA predominantly induce oxygen-dependent photodynamic damage of cellular structures through the generation of reactive

oxygen species (ROS) (Yoon et al. 2000; He and Häder 2002a; He and Häder 2002b; Santos et al. 2013).

1.3.2.1 Ultraviolet B/C DNA Damage

Ultraviolet B and C irradiation inflict bacterial cell death predominantly through direct DNA damage (Santos et al. 2013). Both UVB and UVC are absorbed readily by bacterial DNA, generating DNA photoadducts (Taylor 2005; Santos et al. 2013). The best characterised of these are the cyclobutane pyrimidine dimers (CPDs) and pyrimidine (6-4)-pyrimidone photoproducts ((6-4) PPs) (Santos et al. 2013). Cyclobutane pyrimidine dimers are the most common form of DNA photoadducts, and occur through the absorption of UV by DNA, inducing the covalent bonding of adjacent pyrimidines to form four-membered rings (Yoon et al. 2000; Taylor 2005; Goosen and Moolenaar 2008; Rastogi et al. 2010). These CPDs are formed 20 – 40 times more abundantly than other photoadducts, and their quantification is thus often used as a marker of mutagenicity under UVB and UVC irradiation (Cadet et al. 1992; Yoon et al. 2000; Rastogi et al. 2010). Pyrimidine (6-4)-pyrimidone photoproducts are formed at a lower rate than CPDs, but have greater mutagenic importance (Yoon et al. 2000). Formation of (6-4)PPs similarly involves the covalent bonding of adjacent pyrimidines to form four-membered rings, albeit through different bonds (Taylor 2005; Rastogi et al. 2010).

Both CPDs and (6-4) PPs are capable of stimulating mutagenicity and lethality in irradiated bacteria. If these photoadducts are not repaired prior to DNA replication they may generate DNA mutations or cause cell death (Yoon et al. 2000; Rastogi et al. 2010; Ikehata and Ono 2011; García-Gómez et al. 2012). Generally, (6-4)PPs are more difficult for the cellular replication machinery to bypass, and thus provide a higher rate of mutagenicity (Yoon et al. 2000; Ikehata and Ono 2011). Other mutagenic damage induced by UVB/UVC irradiation includes DNA depurination/depyrimidisation (generating single-strand DNA breakages) hydrolytic deamination (causing base conversions), and double stranded DNA breaks – which are lethal to bacteria (Rastogi et al. 2010; Ikehata and Ono 2011).

While such DNA damage is typically attributed as the cause of UVB-lethality, at low UVB dosages, intracellular generation of ROS is known to predominate in cellular stress (Santos et al. 2012). This ROS generation occurs through UVB-mediated photodynamic reactions, similar in nature to those dominating the intracellular damage of UVA/PAR.

1.3.2.2 Photodynamic Damage from Visible Light and Ultraviolet A

Visible light and UVA irradiation cause microbial stress through a radiation-and-oxygen-dependent mechanism known as photodynamic damage (Matallana-Surget and Wattiez 2013; Song et al. 2019). Photodynamic damage is a form of oxidative stress resulting from light-stimulated intracellular production of ROS including singlet oxygen ($^1O_2$), hydrogen peroxide (H_2O_2), superoxide ($O_2^{\cdot -}$), and hydroxyl ($^{\cdot}OH$) radicals (Mathews-Roth and Krinsky 1970; Ziegelhoffer and Donohue 2009; Sandmann 2019). Here, ROS are formed by interactions between irradiation, a photosensitiser molecule, and oxygen (Sandmann 2019). Photosensitisers are organism-specific intracellular compounds capable of absorbing incident radiation and subsequently generating ROS (Ziegelhoffer and Donohue 2009, Sandmann 2019). Photosensitiser molecules are common within bacteria, and include quinones, flavins, bacteriochlorophylls and porphyrins (Amagasa 1981; Krinsky 1994; Ochsner 1997; Jori et al. 2006; Ziegelhoffer and Donohue 2009; Hope et al. 2016; Shleeva et al. 2019).

Upon absorption of light energy at the compatible wavelength, intracellular photosensitisers ascend from their ground state to an excited singlet state, from which they proceed to their triplet state via inter-system crossing (ISC) (**Figure 1.1)** (Ochsner 1997; Alves et al. 2014; Cadet et al. 2015). The triplet state of the photosensitiser generates ROS on its return to ground state through the transfer of electrons (Type I photosensitisation) or energy (Type II photosensitisation) (Krinsky 1994; Ochsner 1997; Matallana-Surget and Wattiez 2013).

Figure 1.1: Summary of the photosensitisation process occurring through the absorption of incident light by a photosensitiser. Asterisks represent unpaired electrons, while superscript numbers denote the energy state (singlet/triplet) of the molecule.

1.3.2.2.1 Type I and Type II Photosensitisation

Type I photosensitisation occurs when the photosensitiser donates an electron to a compatible substrate, generating a radical anion photosensitiser and cationic substrate, as demonstrated in **Figure 1.2-A** (Krinsky 1978; Ochsner 1997; Alves et al. 2014; Cadet et al. 2015). The radical cation undergoes further reactions in the presence of oxygen to produce ROS such as superoxide ($O_2^{\cdot -}$) or hydrogen peroxide (H_2O_2) (Ziegelhoffer and Donohue 2009; Cadet et al.

2015; Baptista et al. 2017). In the Type II mechanism (**Figure 1.2-B**) the triplet photosensitiser transfers its excitation energy directly to ground state molecular oxygen, producing oxygen in its first-excited state, known as singlet oxygen ($^1O_2$) (Edge et al. 1997; Ziegelhoffer and Donohue 2009). Singlet oxygen is the predominant ROS formed under both UVA/PAR exposure, and plays a major role in subsequent photodynamic damage (Girard et al. 2011; Cadet et al. 2015).

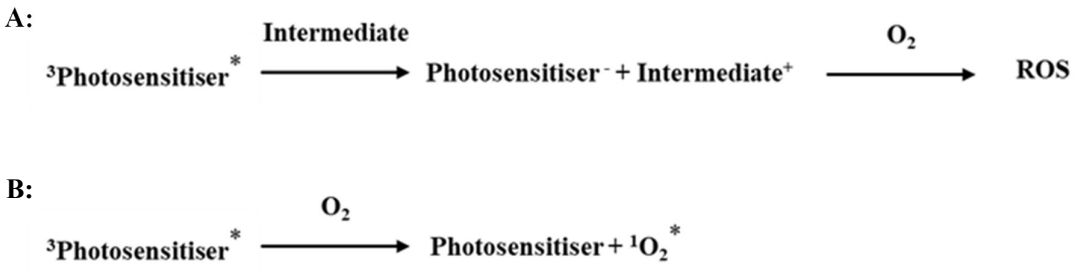

Figure 1.2: Reaction scheme for generation of reactive oxygen species via **A:** Electron transfer in Type I photosensitisation; **B:** Energy transfer in Type II photosensitisation. Asterisks represent unpaired electrons, while superscript numbers denote the energy state (singlet/triplet) of the molecule.

1.3.2.2.2 Cellular Targets of Photodynamic Damage

The ROS generated from UVA/PAR photosensitisation inflicts irreversible damage on bacterial cellular structures and viability (Sandmann 2019). The main cellular targets of ROS damage are the bacterial DNA, proteins and lipid-membranes (Zhao and Drlica 2014).

The damage stimulated by UVA/PAR on bacterial DNA predominantly relies on ROS-mediated base oxidation. While UVA is capable of creating DNA photoadducts through direct absorption by DNA, this absorption is inefficient, and typically produces photoadducts at a rate 10^5 times lower than UVB/UVC (Cadet et al. 1992; Ochsner 1997; Girard et al. 2011; Ikehata and Ono 2011). Instead, under UVA/PAR irradiation, ROS produced from photosensitisation directly react with and oxidise DNA bases to form purine/pyrimidine adducts, which can subsequently induce mutagenicity or single-strand breakages in the DNA during replication (Ochsner 1997; Eisenstark 1998; Rastogi et al. 2010; Alves et al. 2014; Cadet et al. 2015). For example, hydroxyl radicals can directly oxidise both purines and pyrimidines, and/or abstract hydrogen from sugars of the DNA backbone (Fang 2011; Girard et al. 2011; Cadet et al. 2015). These reactions produce base-adducts, DNA-DNA or DNA-protein cross-linkages, and single/double-

stranded DNA breakages, all of which are highly deleterious to cell survival (Cadet et al. 1992; Ochsner 1997; Cabiscol et al. 2000; Rastogi et al. 2010; Fang 2011; Alves et al. 2014).

Proteins are major targets of photodynamic damage due to their high intracellular abundance, frequent use of photosensitisers as prosthetic groups, and the susceptibility of amino acids to oxidation (Girard et al. 2011; Alves et al. 2014). Amino acid oxidation creates residue derivatives, which modify the protein structure, and cause loss-of-function (Cabiscol et al. 2000; Grosvenor et al. 2010; Alves et al. 2014; Dixon and Stockwell 2014). Enzyme loss-of-function is common under photodynamic stress, with studies such as Alves et al. (2014) characterising the inactivation of bacterial enzymes including lactate dehydrogenases, ATPases, NADH dehydrogenases and succinate dehydrogenase under UVA-irradiation. Particular susceptibility has been demonstrated for enzymes involved in cell division, oxidative stress responses, and sugar uptake, as well as DNA repair and photoreactivation (Alves et al. 2014; Song et al. 2019). The loss-of-function of critical bacterial proteins under photodynamic stress eventually stimulates cellular-lethality (Girard et al. 2011; Cadet et al. 2015).

The destruction of cell membranes is the predominant cause of bacterial cell death under photodynamic stress (Jori et al. 2006; Reis-Mansur et al. 2019). Membrane lipids are major targets of photodynamic damage due to the readiness by which the polyene chains of unsaturated fatty acids may be oxidised by ROS, and the membrane-localisation of most bacterial photosensitisers (Mathews 1963; Ochsner 1997; Jori et al. 2006; Alves et al. 2014). Bacterial lipid membranes contain a high density of unsaturated fatty acids, with large numbers of carbon-carbon double bonds which are highly vulnerable to ROS oxidation (Anderson and Krinsky 1973; Ziegelhoffer and Donohue 2009; Björn and Huovinen 2015). Reactions of these membrane lipids with hydroxyl radicals or singlet oxygen results in lipid peroxidation (Cadet et al. 1992; Cabiscol et al. 2000; Cadet et al. 2015). Lipid peroxides have subtly different properties from their native forms, decreasing bacterial membrane fluidity, altering membrane potential and causing a loss of anchoring for membrane-localised proteins (Anderson and Krinsky 1973; Cadet et al. 1992; Cabiscol et al. 2000; Alves et al. 2014). Ultimately, this results in the collapse of the bacterial membrane as a permeability barrier, causing leakage of cellular components, cellular lysis, and cell death (Anderson and Krinsky 1973; Cadet et al. 1992; Jori et al. 2006).

Given the variety of cellular damage types and targets under UV and PAR irradiation, the persistence of bacteria in regions of consistently high solar irradiation – such as deserts – relies

on the breadth of their strategies for protection from both direct DNA damage and oxidative stress. Consequently, bacterial communities from these regions are predominantly comprised of radiation tolerant organisms, which utilise a complex variety of physiological and behavioural solar tolerance systems.

1.3.3 Bacterial Tolerance to Solar Irradiation Stress

In environments where solar irradiation is both biologically stressful and stable, bacterial communities will reflect this through the predominance of radio-tolerant species, and community compositions robust to fluctuations in radiation intensity (Yuan et al. 2012; Hernández et al. 2016; Su et al. 2020). This acquired tolerance is determined by the stability of the community's solar exposure history (Paulino-Lima et al. 2013; Ruiz Gonzalez et al. 2013; Pérez et al. 2017). The longer a community's solar exposure history, the more stable and sophisticated in development the irradiation resistomes of its members will become (Paulino-Lima et al. 2013; Ruiz Gonzalez et al. 2013; Hernández et al. 2016; Reis-Mansur et al. 2019).

The high stability and intensity of solar irradiation in desert systems means that their bacterial communities possess prolonged solar exposure histories, and consequently present intricate and multifaceted irradiation-resistomes (Pointing and Belnap 2012; Paulino-Lima et al. 2013; Makhalanyane et al. 2015; Makhalanyane et al. 2017). Understanding the solar-tolerance mechanisms of desert organisms is thus valuable to our understanding of the complex tolerance systems used by bacteria subject to biologically extreme, long-term solar irradiation.

Bacteria persisting in environments of high solar insolation counteract radiation damage through irradiation-avoidance, DNA repair, or production of intracellular-protectants (Quesada and Vincent 1997; Albarracín et al. 2016). Desert systems demonstrate clear examples of organisms utilising each of these tolerance mechanisms for survival. The formation of endolithic/ hypolithic communities allows the persistence of bacteria in high irradiation environments through solar avoidance (Cowan et al. 2011). Here, radiation sensitive organisms colonise the interior or ventral surfaces of rocks as a method of shielding, reducing the incident radiation reaching cells to sub-lethal levels (Berner and Evenari 1978; Makhalanyane et al. 2015; Valverde et al. 2015). This radiation-avoidance is commonly observed in desert environments. Indeed, the Atacama, Gobi, Namib, Mojave, Kalahari and Negev Deserts all demonstrate substantial hypolithic community formation, colonising 21 – 100 % of the rock substrates within their intrinsic gravel/quartz plains (Berner and Evenari 1978; Cary et al. 2010; Azúa-

Bustos et al. 2011; Caruso et al. 2011; Chan et al. 2012; Stomeo et al. 2013; Wierzchos et al. 2015).

Edaphic organisms lack this external shielding, thus must rely on intrinsic tolerance systems to mitigate irradiation damage, including DNA repair mechanisms and ROS scavengers. The best-studied bacterial DNA repair systems are photo reactivation (PHR), base excision repair (BER), and nucleotide excision repair (NER) (Rastogi et al. 2010; Jones and Baxter 2017). In these systems, DNA adducts formed via ROS-oxidation or UV-absorption are enzymatically repaired or excised, preventing mutagenesis and lethality (Smith 1974; Goosen and Moolenaar 2008; Rastogi et al. 2010). While PHR employs targeted dimer-breakage by photolyase enzymes to restore original DNA structures, BER and NER are more severe, removing entire DNA bases or nucleotides respectively (Rettberg and Rothschild 2002; Rastogi et al. 2010; García-Gómez et al. 2012; Veen and Tang 2015). This allows BER/NER to remove more diverse classes of photoadducts, but necessitates subsequent action of DNA replication enzymes to restore the original DNA sequences (Friedberg 2003; Crowley et al. 2006; Stracy et al. 2016). The irradiation-tolerance of a variety of edaphic desert bacteria has been linked to the maintenance of these systems (Paulino-Lima et al. 2013; Hernández et al. 2016; Pavlopoulou et al. 2016). For example, *Deinococcus gobiensis* from sands of the Gobi desert presents a high UV tolerance, tightly linked to its well-regulated PHR system, and DNA repair genes are known to be maintained at a higher baseline expression in desert edaphic communities than those of temperate soils (Yuan et al. 2012; León-Sobrino et al. 2019).

Intrinsic protection from photodynamic stress relies on an organism's ability to prevent ROS-damage *in vivo* via use of ROS-removing scavengers, of which enzymes are a major contributor (Mattimore and Battista 1996; Cockell and Knowland 1999; Hernández et al. 2016). For example, superoxide dismutase (SOD) converts intracellular superoxide to H_2O_2, which undergoes further dismutation by catalase to yield water and oxygen (Whittaker 2003; Zamocky et al. 2008; Schatzman and Culotta 2018). Using catalase and SOD in tandem, bacteria are capable of removing both intracellular superoxide and hydrogen peroxide, mitigating formation of other ROS, and mediating cellular damage under UVA/PAR irradiation (Tyrrell and Keyse 1990; Chiang and Schellhorn 2012). This ability to remove intracellular ROS formed under irradiation is important to the intrinsic tolerance of organisms from regions of high solar insolation. Indeed, open soil bacteria of Antarctic and Gobi deserts commonly possess multiple copies of SOD/catalase genes, conducive to the maintenance of a tightly-controlled oxidative stress response (Yuan et al. 2012; Dsouza et al. 2015). Desert soil bacteria also show higher basal-expressions of these oxidative stress response genes than temperate communities, similar

in nature to the DNA repair systems previously described (León-Sobrino et al. 2019; Cowan et al. 2020).

Bacteria also use pigmentation, most prominently carotenoids, to protect themselves from radiation. Carotenoids provide bacteria protection from photodynamic damage through their capable ROS-quenching capacities (Britton 1995; Reis-Mansur et al. 2019; Sandmann 2019). Similar to enzymatic protectants, this allows carotenoids to remove intracellular ROS generated under irradiation before they cause cellular damage (Britton 1995).

Yellow to red coloured carotenoid pigments are frequently produced by radiation-resistant organisms from regions of high solar insolation (Paulino-Lima et al. 2013; Albarracín et al. 2016; Vila et al. 2019). For example, open desert soils such as in the Antarctic and Tunisian deserts demonstrate high abundances of carotenogenic bacteria (Chanal et al. 2006; Cary et al. 2010; Dieser et al. 2010; Paulino-Lima et al. 2013; Vila et al. 2019). The breadth of carotenoid production by organisms isolated from these environments suggests their importance to the multifaceted intrinsic irradiation-resistomes of edaphic desert bacteria (Dieser et al. 2010; Sandmann 2019; Vila et al. 2019). Indeed, previous research has specifically described carotenoid pigmentation as contributing to the UV-tolerance of open soil bacteria from Antarctic, Atacama and Gobi deserts (Zenoff et al. 2006; Dieser et al. 2010; Paulino-Lima et al. 2016; Pavlopoulou et al. 2016; Reis-Mansur et al. 2019; Silva et al. 2019; Flores et al. 2020). These types of explorations into organismal irradiation-tolerance systems meaningfully advances our knowledge of the complexity of bacterial irradiance-resistomes which develop under conditions of prolonged solar exposure (Pavlopoulou et al. 2016).

While carotenoid pigmentation contributes to bacterial irradiation-tolerance in other deserts, no work has yet examined this phenomenon in the Namib Desert. The Namib Desert is a valuable system for this type of characterisation, due to its high intensity and stability of irradiance (**Section 1.3.1.3)**. The solar irradiance of the Namib Desert demonstrably stimulates bacterial adaptation (Stomeo et al. 2013; Warren-Rhodes et al. 2013; León-Sobrino et al. 2019). Indeed, the Namib demonstrates a 95 % hypolithic community colonisation rate of quartz within its gravel plains, and metatranscriptomics studies have demonstrated its open-soil bacterial communities to present high expressions of genes involved in DNA repair pathways and enzymatic oxidative stress responses, both systems consistent with mechanisms aforedescribed in organismal adaptation to incident irradiation (Makhalanyane et al. 2015; Ramond et al. 2018; León-Sobrino et al. 2019; Ramond et al. 2019). The consistency of the Namib Desert's

atmospheric conditions further produces a uniquely stable surface irradiation (Cunningham 1998; Cunningham and Bodeker 2000; Kgabi et al. 2016). Consequently, the Namib Desert presents a prolonged, biologically stressful solar-exposure history for its soil organisms, necessitating development of complex and multi-faceted photo-protective mechanisms (Cunningham 1998; Cunningham and Bodeker 2000; Hernández et al. 2016). For such an important area to study, and given the well-characterised importance of carotenoids to bacterial resistomes in desert systems subject to analogous intensities of surface irradiation, the lack of study of organisms from the Namib Desert is surprising, and a gap in our understanding of irradiation-tolerance systems utilised by edaphic desert bacteria.

The contribution of carotenoids to bacterial irradiation-resistomes are largely attributed to their photoprotective capacities as intracellular antioxidants (Edge et al. 1997; Cockell and Knowland 1999). However, the nature of carotenoid protection from solar irradiance is complex, influenced by irradiation wavelengths, dosages and structures of the carotenoids themselves.

1.3.4 Carotenoids

1.3.4.1 Carotenoid Structures

Carotenoids are the most widespread class of natural pigments in nature, and serve a variety of biological roles (Britton 1993; Britton 2020). There are currently over 750 carotenoid pigments known across all domains of life, all based around the same poly-isoprenoid structure, and yielding yellow to red colourations (Britton 1995; Alcaíno et al. 2016; Britton 2020). Alterations in the base structure of carotenoids gives rise to molecules of widely differing colours and biological activities (Armstrong 1997; Llorente 2016).

Carotenoids are hydrophobic terpenoids, most commonly possessing a hydrocarbon skeleton of forty carbon atoms, with substantial methyl-branching (Córdova et al. 2018). A number of carotenoids show longer/shorter chain lengths, with extensions up to 50 carbon atoms (C_{50} carotenoids), or minimisations to C_{30} chains (Armstrong 1994; Pfander 1994; Armstrong 1997; Tao et al. 2005). The centre of the carotenoid molecule contains the functional feature of the carotenoid class; the chromophore (**Figure 1.3)** (Britton 1995). The chromophore is a long, conjugated polyene chain, comprising a series of alternating carbon-carbon single and double bonds (Britton 1995; Llorente 2016). The structure and length of the chromophore is

responsible for the colour, reactivity, and biological activity of the carotenoid (Mortensen and Skibsted 1997; Meléndez-Martínez et al. 2007). Longer chromophores possess higher numbers of conjugated double bonds (c.d.b.), increasing the delocalisation of pi-electrons across the chromophore length and thereby decreasing its triplet energy level (Britton 1995). This renders the carotenoid both more reactive and more easily elevated to its excited form with increasing chromophore lengths (Britton et al. 1995a; Tamura and Ishikita 2020).

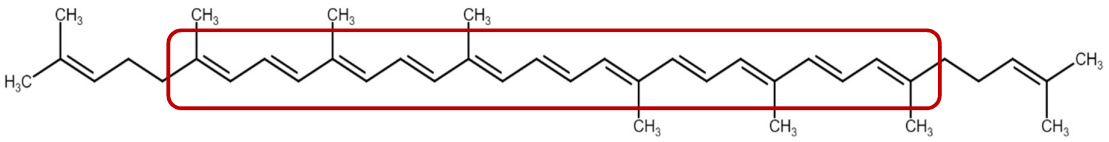

Figure 1.3: Skeletal structure of an acyclic, C_{40} carotenoid (lycopene). The region of the carotenoid constituting the chromophore is denoted by a red outline and represents a chromophore 11 c.d.b. in length.

Carotenoids may also differ structurally outside of the chromophore. The basic hydrocarbon skeleton may undergo cyclisation at one or both ends, or vary widely in desaturation and methyl-branching (Alcaíno et al. 2016; Córdova et al. 2018). Carotenoids may possess oxygen-containing functional groups, changing their classifications from anoxygenic 'carotenes' to oxygenic 'xanthophylls', both within the carotenoid class (Liang et al. 2018). These structural modifications all influence carotenoid energy levels, polarities, and biological functions.

While carotenoids are best characterised as serving in photosynthetic light-harvesting, their biological roles in bacteria extend considerably outside of this (Alcaíno et al. 2016). Carotenoids can aid membrane stabilisation, temperature adaptation and, as is the focus of this review, photoprotection from incident solar irradiation (Saito et al. 1994; Chattopadhyay and Jagannadham 2001; Young and Lowe 2001; Britton 2020).

1.3.5 Carotenoids in Photoprotection

The chromophore structure of carotenoids provides them high antioxidant capacity, allowing them to neutralise ROS or excited photosensitisers before they can induce cellular damage (Britton 1995; Ramel et al. 2012). The antioxidant capacity of carotenoids is significant, with *in vitro* studies demonstrating them as capable of antioxidant efficacies some 2 – 5 fold higher than other common intracellular antioxidants such as α-tocopherol and ascorbic acid (Mandelli et al. 2012; Squillaci et al. 2017; Sandmann 2019). Carotenoids thus contribute meaningfully to

the intracellular antioxidant capacities of bacteria, and provide ROS-protection via physical or chemical quenching, as outlined below.

1.3.5.1 Carotenoids as Antioxidants – Physical Quenching

In physical quenching, excess excitation energy is transferred from triplet photosensitisers or singlet oxygen to the ground-state carotenoid (Edge et al. 1997; Tamura and Ishikita 2020). As carotenoids have a triplet state energy below singlet oxygen, they are capable of draining its excitation energy directly, preventing it from stimulating cellular damage (Ramel et al. 2012). Furthermore, this low triplet energy means carotenoids will preferentially receive energy from photosensitisers over ground-state oxygen, actively preventing singlet-oxygen formation under irradiation (Frank and Cogdell 1993; Ramel et al. 2012; Sandmann 2019). Physical quenching by carotenoids is highly efficient, mediated at a nearly diffusion-controlled rate (Terao et al. 2011). Indeed, as much as 99.9 % of the triplet photosensitisers formed under irradiation in cyanobacteria are quenched by carotenoids prior to ROS generation (Krinsky 1978).

The energy-transfer reaction of physical quenching proceeds as demonstrated in **Figure 1.4**, yielding the ground state molecular oxygen or photosensitiser and triplet carotenoid (Edge et al. 1997; Ramel et al. 2012; Tamura and Ishikita 2020). The triplet state energy of the carotenoid is too low to form new ROS, and it instead dissipates its excess energy via rotational/vibrational interactions with surrounding solvents, losing small quantities of energy each time until it is returned to ground state (Krinsky 1978; Tamura and Ishikita 2020). As a result, excess excitation energy is dissipated without carotenoid destruction or ROS generation.

A:

B:

$$^{1}O_{2}^{*} + \text{Carotenoid} \longrightarrow O_{2} + {}^{3}\text{Carotenoid}^{*}$$

$$^{3}\text{Photosensitiser}^{*} + \text{Carotenoid} \longrightarrow \text{Photosensitiser} + {}^{3}\text{Carotenoid}^{*}$$

Figure 1.4: Schematic representation of carotenoid-mediated physical quenching of singlet oxygen (**A**) and excited photosensitisers (**B**) to generate the triplet excited state of the carotenoid molecule. Asterisks represent unpaired electrons, while superscript numbers denote the energy state (singlet/triplet) of the molecule.

The lower the carotenoid triplet state energy, the more efficiently its quenching reactions proceed (Tamura and Ishikita 2020). Consequently, carotenoid chromophore-length, being

inversely proportional to its triplet energy, is directly proportional to its physical quenching capacity (Wilkinson and Ho 1978; Conn et al. 1991; Tamura and Ishikita 2020). For example, the study of Di Mascio et al. (1989) demonstrated lycopene (11 c.d.b.) to possess a higher rate of singlet-oxygen quenching than lutein (10 c.d.b.), while Conn et al. (1991) reported that decapreno-β-carotene (15 c.d.b.) quenched singlet oxygen 1.5-fold more efficiently than β-carotene (11 c.d.b). While no clear consensus is maintained in the literature, most work places the minimum chromophore length for antioxidant capacity at 9 c.d.b. (Krinsky 1978; Britton 1995; Hashimoto et al. 2016).

1.3.5.2 Carotenoids as Antioxidants – Chemical Quenching

Carotenoid molecules may alternatively quench ROS through direct chemical reactions (Edge et al. 1997). Here, the electron-rich chromophore reacts directly with ROS, yielding a carotenoid radical (Britton 1995; Woodall, Britton, et al. 1997). These reactions proceed via either direct additions of ROS to the chromophore, or abstraction of hydrogen from the chromophore structure (Mortensen and Skibsted 1996; Woodall, Britton, et al. 1997). Unlike physical quenching, chemical quenching causes chromophore cleavage, and subsequent carotenoid decomposition (Liebler and McClure 1996; Young and Lowe 2001). While stimulating carotenoid destruction, this reaction pathway does mitigate ROS, further protecting organisms from photodynamic damage.

The chemical quenching efficacies of carotenoids are also positively related to their chromophore lengths (Young 1993; Mortensen and Skibsted 1996). Increasing chromophore lengths increases the delocalisation of electrons across the chromophore, rendering them more susceptible to electrophilic attack (Tamura and Ishikita 2020). For example, Yachai (2009) demonstrated lycopene (11 c.d.b.) to exhibit as much as two fold the efficacy in chemical quenching of lutein (10 c.d.b.), attributed to its greater chromophore length. Thus, in both chemical and physical quenching, increased chromophore lengths are conducive to an increased efficacy of antioxidant capacity.

Carotenoids are thus capable of removing intracellular ROS prior to their reactions with cell structures, preventing photodynamic damage (Sandmann 2019). This antioxidant capacity of carotenoids has been directly linked to the irradiation-resistomes of a variety of bacteria in *in vivo* studies.

1.3.5.3 Carotenoid Protection from UVA/PAR

Survival comparisons between pigmented and unpigmented cultures of the same organism are used to demonstrate the photoprotective functions of the organism's carotenoids (Jones and Baxter 2017; Sandmann 2019). Comparing cultures of the same species ensures consistency in other intrinsic-tolerance mechanisms which may influence UV-susceptibility, including DNA repair systems and enzymatic scavengers, focusing observed protective effects on carotenoids (Anderson and Krinsky 1973; Edge et al. 1997; Jones and Baxter 2017).

Carotenoids contribute to bacterial PAR and UVA tolerance. Both PAR and UVA rely on ROS-mediated photodynamic damage to stimulate cellular lethality (Girard et al. 2011). Through their antioxidant capacity, carotenoids quench intracellular ROS generated under irradiation, thereby preventing them from inflicting cellular damage (Ziegelhoffer and Donohue 2009). Indeed, studies with mutants of *Rhodobacter sphaeroides* have demonstrated that conversion of its wild-type carotenoids (11 c.d.b.) into shorter-conjugation predecessors decreases cellular survival under high intensity PAR, with complete loss of protection at phytoene (3 c.d.b.) (Glaeser and Klug 2005; Hashimoto et al. 2016). Indeed, while isolates retaining carotenoids of chromophores above 9 c.d.b. demonstrated 81 – 100 % survival rates (increasing with chromophore length), phytoene producing mutants had survival rates of just 3 % (Imhoff et al. 1984; Glaeser and Klug 2005). These findings support the PAR-protective capacity of carotenoids, as well as the correlation between photoprotective capacity, carotenoid antioxidant activity and chromophore lengths (Britton 1995; Hashimoto et al. 2016).

The presence of carotenoids is important in the photoprotection of non-phototrophic organisms (Krinsky 1978; Sandmann 2019). Studies in carotenoid-pigmented *Kocuria rosea* have demonstrated that lethality under high intensity PAR is exclusive to colourless cells, with death attributed to the loss of carotenoid antioxidant protection under the photodynamic stress this PAR exerts (Pezzoni et al. 2011). This has also been observed for non-phototrophic *Myxococcus xanthus, Mycobacterium marinum* and species of *Flavobacterium* (Mathews 1963; Burchard and Dworkin 1966; Weeks et al. 1973; Browning et al. 2003). These differences in lethality were further demonstrated to be oxygen-dependent, emphasising the photodynamic nature of PAR damage, and the protection offered by the carotenoid species as reliant on their antioxidant activity (Burchard and Dworkin 1966; Burchard and Hendricks 1969; Hodgson 1993).

Intracellular carotenoid concentrations also directly determine their contribution to cellular photoprotection (Mathews-Roth and Krinsky 1970). As antioxidant activity requires contact between carotenoids and photosensitisers/ROS, greater intracellular carotenoid concentrations increases the probability of this contact occurring (Manitto et al. 1987; Edge et al. 1997; Tamura and Ishikita 2020). Indeed, mutants of *Micrococcus luteus* producing a range of carotenoid concentrations have shown lethal sensitivities to PAR inversely proportional to these concentrations, and intracellular carotenoid concentrations serve as a significant predictor of PAR-tolerance in *R. sphaeroides* (Mathews-Roth and Krinsky 1970; Glaeser and Klug 2005).

Similar to PAR, bacterial UVA tolerance is directly dependent on the strength of their intracellular antioxidant activities, with intracellular ROS-concentrations both increasing linearly with UVA-dosages, and acting as the primary determinant of bacterial lethality (Tyrrell 1985; Eisenstark 1998; He and Häder 2002a; Khaengraeng and Reed 2005; Santos et al. 2013; Song et al. 2019). Consequently, the contribution of carotenoids to bacterial intracellular antioxidant capacities also provides UVA-protection. Carotenoid-pigmented, Antarctic desert soil organism *Microbacterium* sp. shows a two fold higher UVA tolerance than *Escherichia coli* isolates, attributed to the significantly higher intracellular antioxidant capacity provided by carotenoids of this pigmented organism (Reis-Mansur et al. 2019). The study of Tuveson et al. (1988) demonstrated that carotenoid-producing *E. coli* had significantly higher UVA tolerance compared to their non-pigmented equivalents. These differences were enhanced with additions of UVA photosensitisers, highlighting the importance of ROS-quenching in carotenoid-mediated UVA resistance. Furthermore, carotenoid chromophore lengths of greater than 9 c.d.b. have been found to be required for UVA protection – again linking back to the dependency of carotenoid antioxidant activity on chromophore length, and emphasising carotenoid UVA-tolerance as mediated by antioxidant activity (Blanc et al. 1976; Liebler and McClure 1996; Edge et al. 1997; Tamura and Ishikita 2020).

Carotenoids thus provide bacterial solar irradiation tolerance against the ROS damage generated by UVA and PAR wavebands. This protection is mediated through the antioxidant activity of carotenoids, and therein their ability to remove the ROS generated under irradiation prior to its ability to stimulate cellular damage.

1.3.5.4 Carotenoid Protection from UVB/UVC

Carotenoids are incapable of protecting against irradiation stimulating direct DNA damage (Edge et al. 1997; Cockell and Knowland 1999; Jones and Baxter 2017). Therefore, carotenoids typically provide no mitigation of damage or cell death arising from UVB or UVC irradiation. However, as cell death under lower dosages of UVB is influenced by ROS production, carotenoids do present limited contributions to bacterial UVB-resistomes (Wynn-Williams and Edwards 2002; Santos et al. 2012; Santos et al. 2013).

Carotenoids demonstrate protection against UVB dosages predominating in ROS-mediated damage. Survival of carotenogenic *E. coli* under low dose UVB irradiation is higher than the unpigmented wild-type (Sandmann et al. 1998). Observations that this protection was both dependent on carotenoid concentration, and only observed in carotenoids with chromophores above 9 c.d.b., links this protection to carotenoid antioxidant capacity (Sandmann et al. 1998; Tamura and Ishikita 2020). Furthermore, under both UVA and low dose UVB irradiation, carotenoid-deficient bacterial cells show severe cell membrane leakage consistent with photodynamic damage, lesions entirely absent from membranes of corresponding carotenogenic cells (Reis-Mansur et al. 2019).

However, above an organism-dependent dosage, ROS ceases to predominate as the cause of UVB lethality, as the accumulation of direct DNA damage becomes too stressful for the cell to survive (Santos et al. 2013; Song et al. 2019). Consequently, at UVB dosages where bacterial lethality predominates through DNA damage, carotenoid protection is lost. In carotenoid-pigmented cyanobacteria, the UVB tolerance observed at low dosages was rapidly lost at higher irradiance, a trend absent under UVA irradiance (Quesada et al. 1995). Similarly, the study of Tuveson et al. (1988) found that while carotenogenic *E. coli* was protected from UVA irradiation, pigmented and unpigmented organisms demonstrated identical inactivation kinetics under high-dose UVB. Similar results have been observed in studies of carotenogenic *Bacillus* spp. and a variety of marine bacteria, wherein carotenoids yield significant UVA-protection, but not UVB-tolerance (Eisenstark 1998; Wynn-Williams and Edwards 2002; Agogué et al. 2005; Moeller et al. 2005; Matallana-Surget and Wattiez 2013). As such, carotenogenic UVB-protection is considered restricted to those doses predominating in ROS damage.

Ultraviolet-C irradiation causes cell death through direct DNA damage (Rastogi et al. 2010; Anthis and Clore 2013; Santos et al. 2013). While some ROS generation occurs under UVC, it

is minor, and independent of lethality (Krisko and Radman 2010; Besaratinia et al. 2011; Schenk et al. 2011; Song et al. 2019). As a result, carotenoids are not expected to provide UVC tolerance. Indeed, while the pigmentation of *M. luteus* provides protection under photodynamic stress, pigmented and unpigmented cells are equally susceptible to UVC-killing (Mathews and Krinsky 1965). Similarly, studies of carotenogenic soil bacilli have concluded a complete lack of correlation between UVC survival and carotenoid production, while observing a substantially bolstered UVA tolerance in carotenogenic strains (Moeller et al. 2005; Khaneja et al. 2010). As such, UVC-lethality supersedes ROS-mediated damage, and is consequently insensitive to carotenoid production.

Carotenoids have been attributed some ability to protect cells from UVB/UVC-irradiation via direct irradiation screening, but this is contentious (Cockell and Knowland 1999; Dieser et al. 2010). Screening would allow carotenoids to directly absorb incident irradiation energy, and dissipate this energy prior to its ability to stimulate cellular damage (Cockell and Knowland 1999). While a number of carotenoids (such as β-carotene) do demonstrate absorbance in the UV spectral-region, there are few studies specifically examining carotenoid screening as a mechanism of cellular UV-protection (Cockell and Knowland 1999; Wynn-Williams and Edwards 2002; Solovchenko and Merzlyak 2008; Dieser et al. 2010; Stafsnes et al. 2010). The low intracellular concentrations of carotenoids, and their minor absorption intensities at UV-wavelengths relative to those of known screening compounds (i.e. scytonemins or mycosporine-like amino-acids) has stimulated doubt in carotenoid UV-screening capacities (Cockell and Knowland 1999). Echoing the sentiments of Cockell and Knowland (1999) and Solovchenko and Merzlyak (2008), UV-screening is an area of carotenoid work requiring a greater degree of exploration to better quantify its contribution to bacterial UV tolerance.

1.3.6 Photoprotection and Light-Induced Carotenogenesis

The induction of carotenoid production by non-phototrophic bacteria in response to light supports that their carotenoids are used in irradiation tolerance (Takano 2016; Henke et al. 2020). Studies of non-photosynthetic bacteria including *Deinococcus radiodurans, Corynebacterium glutamicum*, *M. xanthus, Flavobacterium* spp. and *Mycobacterium* spp. have all demonstrated PAR-inducibility of carotenoid production, and an accompanying reliance on carotenoid pigments for cellular survival under photodynamic stress (Rilling 1962; Mathews 1963; Howes and Batra 1970; Weeks et al. 1973; Koyama et al. 1974; Davis et al. 1999; Takano, Asker, et al. 2006; Heider et al. 2012; Takano 2016; Silva et al. 2019; Sumi et al. 2019). When grown under PAR illuminance, these organisms produce quantitatively greater

intracellular carotenoid concentrations, thereby conferring them greater photoprotective capacities (Davis et al. 1999; Glaeser and Klug 2005; Sumi et al. 2019). Light-induced carotenogenesis in non-phototrophic bacteria is thus considered an adaptive photoprotective response, used to counteract the photodynamic stress inflicted by irradiation (Eisenstark 1998; Takano, Asker, et al. 2006; Takano 2016). While this phenomenon is relatively rare in non-photosynthetic bacteria, it is thus physiologically relevant, and provides direct support for the photoprotective role of an organisms carotenoids (Takano, Asker, et al. 2006; Sumi et al. 2019).

As light-responsive carotenoid production is considered a physiological adaptation to irradiation, it is expected that carotenogenic organisms from regions subject to high solar irradiation would present this phenomenon more commonly (Takano et al. 2011; Takano et al. 2015; Takano 2016). This hypothesis is of growing interest, and has been examined in recent screening studies of sunlight-exposed soil bacteria such as those of Sumi et al. (2019) and Takano (2016). Such studies investigate the light-inducibility of carotenogenesis in non-phototrophic soil organisms at both phenotypic and genotypic levels. While phenotypic examinations rely solely on demonstrating quantitative increases in total cellular carotenoid content for cultures grown under illumination, genotypic investigations typically rely on *in-silico* exploration of bacterial genomes for homologues to known light-responsive carotenogenic regulators, demonstrating the capacity for light-inducible carotenogenesis within the organism (Takano 2016).

Knowledge of regulatory systems involved in light-responsive carotenogenesis of non-phototrophic bacteria is limited. The best understood systems are those reliant on the transcriptional repressor proteins CrtR (Carotenogenesis Regulator, as in *C. glutamicum*) and LitR (Light-Induced Transcription Regulator, as in *Streptomyces coelicolor*), which mediate light-responsive carotenogenesis within a variety of soil bacteria (Takano 2016; Sumi et al. 2019). These proteins bind the promoters of genes encoding enzymes for carotenoid biosynthesis to prevent their transcription under dark conditions (Takano et al. 2015; Henke et al. 2017; Sumi et al. 2019). Their DNA-binding capacity is lost under illumination, resulting from structural changes in the proteins stimulated by the absorption of visible light by their prosthetic, light-responsive ligands (Takano et al. 2015; Sumi et al. 2019). This results in the production of carotenoids exclusively under light conditions. While light-responsive carotenoid biosynthesis has been demonstrated in other non-phototrophic bacteria, including the bacteriophytochrome-mediated carotenogenesis of *D. radiodurans*, these lack specific demonstrations of their regulatory action (Davis et al. 1999). As a rapid method of denoting light-responsive carotenogenesis in a bacterium, the discovery of gene homologues to those

encoding CrtR or LitR within the genome has been used, and allows phenotypic observations of light-responsive carotenogenesis to be linked to genomic factors (Takano 2016; Sumi et al. 2019).

As stated above, it is suspected that bacteria from high-irradiance environments that utilise carotenoids as photoprotectants would present light-responsive carotenogenesis. However, in desert-isolated non-phototrophic bacteria, this phenomenon is entirely unexplored. Given the aforementioned high-irradiance and prevalence of bacteria utilising photoprotective carotenoids in desert environments, this lack of study is surprising. Further examination of desert bacteria through both these phenotypic and genotypic analyses may be valuable to develop our understanding of bacterial carotenogenesis as a photoresponse to high irradiation-stress.

1.3.7 Genus *Arthrobacter*

Arthrobacter is a genus within the family *Micrococcaceae,* and contains ubiquitous aerobic soil bacteria of global distribution (Jones and Keddie 2006; Sutthiwong, Fouillaud, et al. 2014). Most *Arthrobacter* are strictly aerobic, non-sporulating, respiratory chemorganotrophs that are extensively metabolically versatile (Jones and Keddie 2006; Busse et al. 2015; Busse 2016). At present, there are approximately 70 recognised species of *Arthrobacter*, demonstrating a high-level of physiological heterogeneity (Jones and Keddie 2006; Busse and Wieser 2014; Krishnan et al. 2016).

1.3.7.1 *Arthrobacter* in Desert Soils

Arthrobacter often constitutes the single most numerous culturable aerobic bacterium from a variety of soil types (Skyring and Quadling, 1969; Holm and Jensen, 1972; Lowe and Gray, 1972, Jones and Keddie 2006; Mongodin et al. 2006; Unell 2008). For example, the study of Crocker et al. (2000), found *Arthrobacter* to constitute approximately 24 % of the recoverable bacterial load from United States subsurface sediments, ranging from 21 to 83 % of isolates in other soil types. Holm and Jensen (1972) support this, finding *Arthrobacter* as 13 – 24 % of culturable bacteria from Danish beech forests, and the most prolific single genus overall. While dated, similar results were provided by studies including those of Skyring and Quadling (1969) and Lowe and Gray (1972), spanning wide geographic ranges.

Arthrobacter are also frequently isolated from desert soils, comprising major bacterial loads of soils from the Antarctic, Sonoran, Namib and Israeli deserts (Johnson and Cameron 1973; Arpin et al. 1975; Fong et al. 2001; Mongodin et al. 2006; Makhalanyane et al. 2015; Vikram et al. 2016; Ii et al. 2019; Silva et al. 2019). Indeed, as much as 14 – 22 % of culturable bacteria from Antarctic soils comprise species of *Arthrobacter*, with *Arthrobacter agilis*, *Arthrobacter glacialis,* and *Arthrobacter psychrochitiniphilus* all commonly recovered from Antarctic soils and surface waters (Arpin et al. 1975; Fong et al. 2001; Zdanowski et al. 2013; Pudasaini et al. 2017; Romaniuk et al. 2018; Silva et al. 2019). *Arthrobacter* is also a prominent genus in the Namib Desert, with consistent isolation from both refuge and open soil communities (Makhalanyane et al. 2015; Vikram et al. 2016). Inherent in its colonisation of desert soils, *Arthrobacter* possesses well-maintained systems for tolerance to xeric stress, oligotrophy and, most relevant to this literature review, solar-radiation (Zevenhuizen 1992; Potts 1994; Mongodin et al. 2006; Warren-Rhodes et al. 2013; Makhalanyane et al. 2015; Lebre et al. 2017; Solyanikova et al. 2017).

1.3.7.2 Irradiation-Tolerance of *Arthrobacter*

As irradiation is a significant selector in deserts, the prevalence of *Arthrobacter* suggests that they possess radiotolerance mechanisms consistent with those discussed for desert organisms (**Section 1.3.3**). In both Antarctic and Namib deserts, *Arthrobacter* constitute major components of endolithic and hypolithic communities, presenting irradiation tolerance through solar avoidance (Van Goethem et al. 2016; Vikram et al. 2016). The prominence of *Arthrobacter* in open soils further suggests systems of intrinsic tolerance. Extensive and complete DNA repair pathways (including PHR, BER and NER) have been repeatedly identified within genomes of *Arthrobacter* spp. isolated from open desert soils (Mongodin et al. 2006; Romaniuk et al. 2018; Ii et al. 2019; Buckley 2020). Furthermore, a variety of oxidative stress systems including SOD and catalase, and the regulatory pathways for these stress-responses have been demonstrated within *Arthrobacter* genomes (Mongodin et al. 2006; Dsouza et al. 2015; Luo et al. 2018). *Arthrobacter* spp. from desert systems thus present and maintain irradiation-protective mechanisms consistent with those expected of desert organisms.

1.3.7.3 Carotenoid Pigmentation of *Arthrobacter*

Desert-isolated *Arthrobacter* often also demonstrate carotenoid pigmentation (Fong et al. 2001; Dsouza et al. 2015; Ii et al. 2019; Silva et al. 2019). Carotenogenic isolates have been identified

from soils and surface waters of the Sonoran and Antarctic deserts (Fong et al. 2001; Reddy et al. 2002; Dsouza et al. 2015; Ii et al. 2019). Carotenoid pigmentation has further been speculated as a component of the UV-resistome in several *Arthrobacter* species by studies such as Ii et al. (2019), Dieser et al. (2010) and Silva et al. (2019). These pigments are expected to serve important physiological functions, as they are found in organisms frequently isolated from biologically-extreme environments.

Yellow carotenoids of *Arthrobacter* are typically attributed to the di-cyclic C_{50} xanthophyll decaprenoxanthin, with examples presented on **Table 1.1** (Arpin et al. 1975; Monnet et al. 2010; Heider et al. 2014; Sumi et al. 2019). While formally identified in some *Arthrobacter*, a number of yellow pigmented species have received no further attention past speculation of their pigmentation as carotenogenic, including *Arthrobacter monumenti, Arthrobacter tecti* and *Arthrobacter sulfureus* (Koyama et al. 1974; Arpin et al. 1975; Stackebrandt et al. 1983; Heyrman et al. 2005; Monnet et al. 2010; Kumar et al. 2016). Decaprenoxanthin-producing *Arthrobacter* have wide geographic spread, as demonstrated in isolates from Antarctica to Europe (Arpin et al. 1975; Dsouza et al. 2015).

Natural production of red/pink pigmentation by *Arthrobacter* is exclusively carotenogenic, and almost solely associated with production of the acyclic, C_{50} carotenoid bacterioruberin alongside a limited variety of its glycosylated/dehydrated carotenoid variants (**Table 1.1)** (Sutthiwong, Fouillaud, et al. 2014). The presence of bacterioruberin production by *Arthrobacter* appears globally distributed, having been reported from mesophilic areas such as Italy and Germany (Imperi et al. 2007; Tescari et al. 2018) to more extreme environments, such as Antarctic deserts (Arpin et al. 1975; Fong et al. 2001; Reddy et al. 2002). For example, *A. agilis* from Antarctic waters and sea-ice is known to produce complex combinations of bacterioruberin and its dehydrated/glycosidic variants (Fong et al. 2001). Indeed, the study of Fong et al. (2001) determined *A. agilis* strain MB813 to possess as many as seven detectable bacterioruberin pigment fractions, a finding similarly reported in Antarctic *A. agilis* by Silva et al. (2019).

The frequent isolation of carotenogenic *Arthrobacter* from regions of high solar-irradiance implies some photoprotective role for their carotenoid pigmentation (Dana et al. 1998; Margesin et al. 2004; Silva et al. 2019). However, these protective roles are rarely demonstrated in *Arthrobacter* directly, and are often instead inferred through reference to demonstrated functions of these carotenoids in other organisms.

Table 1.1: Carotenoid pigmentation produced by species of *Arthrobacter*, their identities, and the original site of isolation for biosynthetic organisms.

	Organism	Carotenoid(s)	Isolation Site	Reference
Yellow Pigmented	*Arthrobacter* sp. M3	Decaprenoxanthin	Unspecified	Arpin et al. (1972)
	Arthrobacter glacialis	Decaprenoxanthin, AG. 470	Glacial mud	Arpin et al. (1975)
	Arthrobacter flavus	Unidentified yellow carotenoid.	Antarctic pond	Reddy et al. (2000)
	Arthrobacter castelli	Decaprenoxanthin	Austrian Mural Painting	Dsouza et al. (2015)
	Arthrobacter phenanthrenivorans Sphe3	Decaprenoxanthin	Greek Soil	Dsouza et al. (2015)
	Arthrobacter isolate 35/47	Decaprenoxanthin	Antarctic soil	Dsouza et al. (2015)
	Arthrobacter isolate H20	Decaprenoxanthin	Antarctic soil	Dsouza et al. (2015)
	Arthrobacter psychrophenolicus	Unidentified yellow carotenoid.	Austrian Alpine Ice Cave	Margesin et al. (2004)
	Arthrobacter psychrochitiniphilus	Decaprenoxanthin	Antarctic defrost biofilm	Silva et al. (2019)
Red/Pink Pigmented	*Arthrobacter agilis*	Bacterioruberin, dehydrated derivatives, glycosidic derivatives	Italian patinas, Antarctic waters, Antarctic sea ice,	Fong et al. (2001); Dieser et al. (2010); Tescari et al. (2018); Silva et al. (2019)
	Arthrobacter roseus	Bacterioruberin	Antarctic cyanobacterial mat	Reddy et al. (2002)
	Arthrobacter bussei	Bacterioruberin, dehydrated derivatives, glycosidic derivatives	German Dairy Cheese	Flegler et al. (2020)
	Arthrobacter glacialis	Dehydrated bacterioruberin derivative	Morainic mud	Arpin et al. (1975)
	Unidentified *Arthrobacter* Species	Bacterioruberin	Pink Patina, Germany	Schabereiter-Gurtner et al. (2001)
	Arthrobacter sp. MN05-02	Unidentified red carotenoid.	Sonoran Desert	Ii et al. (2019)
	Unidentified *Arthrobacter* Species	Bacterioruberin	Pink Patina, Italy	Imperi et al. (2007)
	Arthrobacter sp. G20	Unidentified red carotenoid.	Surface waters of the Caspian Sea	Afra et al. (2017)

1.3.7.3.1 Function of Decaprenoxanthin in Photoprotection

The function of decaprenoxanthin lacks exploration in the literature due to its low biological yield (Fukuoka et al. 2004). However, prevalent decaprenoxanthin synthesis by *Arthrobacter* from a range of high-irradiance environments has been used to speculate its photoprotective utility (Dsouza et al. 2015; Sajjad et al. 2020). Decaprenoxanthin possesses structural features

that suggest its capacity for photoprotection via ROS-quenching, including a chromophore of 9 c.d.b. (Britton 1995; Edge et al. 1997; Woodall, Lee, et al. 1997; Yachai 2009; Silva et al. 2019). Indeed, decaprenoxanthin-producing *A. psychrochitiniphilus* has demonstrated a significantly higher survival under low dose UVB than unpigmented *E. coli*, potentially suggesting this pigment's capacity for protection from ROS (Cadet et al. 2015; Silva et al. 2019). While results such as this grant some support of Sajjad et al. (2020)'s assertion that decaprenoxanthin provides photoprotection in *Arthrobacter*, the lack of direct experimental demonstration of this function within *Arthrobacter* leaves this role as speculative.

1.3.7.3.2 Function of Bacterioruberin in Photoprotection

Bacterioruberin provides protection from PAR and UV irradiation in organisms outside of *Arthrobacter*, and these observations have been used to speculate similar roles within the genus (Saito et al. 1994; Dieser et al. 2010; Jones and Baxter 2017; Silva et al. 2019). Within *Arthrobacter*, the study of bacterioruberin's contribution to the UV-resistome is limited, and lacks the organism-level comparisons of pigmented and unpigmented cultures required to demonstrate specific pigment-conferred photoprotection (Dieser et al. 2010; Silva et al. 2019). To understand further the potential importance of this carotenoid in photoprotection of *Arthrobacter*, an exploration of the literature regarding its structural features and known contribution to the irradiation-resistomes of other organisms is required.

1.3.8 Bacterioruberin

As prior noted, bacterioruberin is an acyclic, C_{50} carotenoid possessing an extended chromophore thirteen conjugated double bonds in length, granting it a characteristic pink/red colouration (Schwieterman et al. 2015; Yang et al. 2015). Bacterioruberin is a xanthophyll, containing four terminal hydroxyl groups, which are symmetrically arranged either side of the central chromophore (**Figure 1.5)** (Jagannadham et al. 1996; Chattopadhyay et al. 1997).

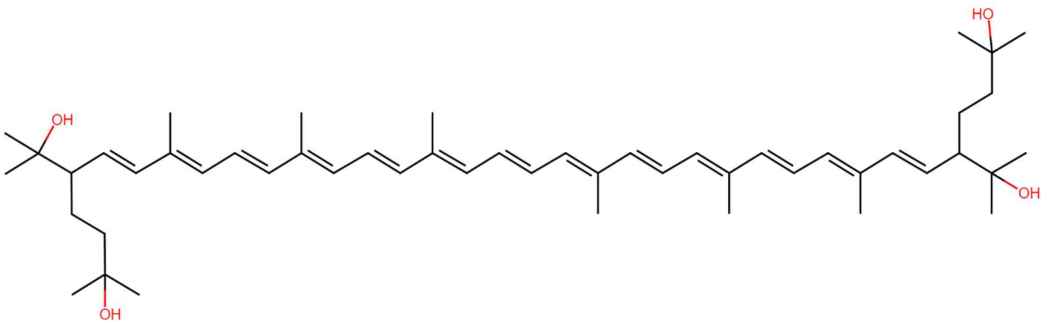

Figure 1.5: Skeletal chemical structure of bacterioruberin, with oxygen-containing functional groups highlighted in red.

Bacterioruberin is the major carotenoid of many halophilic archaea, particularly those of family *Halobacteriaceae* (Oren 2009; Yachai 2009; Dummer et al. 2011; Schwieterman et al. 2015). As many as 215/220 characterised *Halobacteria* contain the genes for bacterioruberin synthesis, including species such as *Haloferax volcanii*, *Halobacterium salinarium* and *Haloarcula japonica,* with bacterioruberin comprising 80 – 100 % of the carotenoid complements of these organisms (Ronnekleiv 1995; Mandelli et al. 2012; Yang et al. 2015; Peck et al. 2019). The bacteria *Rubrobacter radiotolerans* and *K. rosea* also produce both bacterioruberin and its dehydrated variants, comprising as much as 95 % of their carotenoid contents (Saito et al. 1994; Shahmohammadi et al. 1998).

1.3.8.1 Solar Irradiation Protection by Bacterioruberin

Studies investigating the photoprotective roles of bacterioruberin have focussed on this function in *Haloarchaea*. Bacterioruberin is considered a significant component of the irradiance resistome of *Haloarchaea*, enabling their persistence in the high-altitude saline lakes from which they are isolated (Mandelli et al. 2012; Jones and Baxter 2017). In these organisms, protective functions of bacterioruberin have only been explored under PAR and UVC irradiation, with these findings used to suggest similar functions within *Arthrobacter*.

1.3.8.1.1 Protection from PAR/UVA by Bacterioruberin

Bacterioruberin provides protection of *Haloarchaea* against PAR irradiation (Schwieterman et al. 2015; Calegari-Santos et al. 2016). The studies of Dundas and Larsen (1963), Brock and Petersen (1976) and Rodriguez-Valera et al. (1982) all demonstrated that loss of bacterioruberin

from *Haloarchaea* stimulated a lethal sensitivity to high-intensity PAR irradiation which was not observed for pigmented cells. This lethality was oxygen-dependent, highlighting the damage as photodynamic in nature, and reinforcing bacterioruberin's protective function as reliant on antioxidant action (Rodriguez-Valera et al. 1982).

It is unsurprising that bacterioruberin is able to provide protection against PAR as it has high antioxidant activity (Calegari-Santos et al. 2016). Bacterioruberin has a chromophore of 13 conjugated double bonds, meaning its triplet-state energy is low and it is rich in delocalised electrons, thus highly efficient in both physical and chemical quenching (Yachai 2009; Yatsunami et al. 2014). Indeed, Mandelli et al. (2012) demonstrated bacterioruberin to possess an ROS-scavenging efficacy some 1.7 – 5.3 fold higher than common cellular antioxidants (i.e. α-tocopherol, ascorbic acid), and a 2-fold higher efficacy than zeaxanthin (11 c.d.b.). Similarly, Yachai (2009) found bacterioruberin to consistently outperform two other common xanthophylls (astaxanthin, lutein) and carotenes (β-carotene, lycopene) in its ability to scavenge free radicals, quench singlet oxygen, and protect DNA from hydroxyl radical damage. These findings have consistently demonstrated bacterioruberin to have a high antioxidant activity, in substantial excess of other carotenoids and cellular antioxidants. Known connections between the antioxidant capacities of carotenoids and cellular PAR-tolerance supports bacterioruberin as a significant contributor to organismal PAR-resistomes, and strongly implies a similar protection under UVA which is thusfar unexplored (**Section 1.3.5.3**) (Mathews-Roth and Krinsky 1970; Tuveson et al. 1988; Hernández et al. 2016).

Photoprotective roles of bacterioruberin have been speculated in *Arthrobacter*, but lack direct demonstration. Silva et al. (2019) found the antioxidant capacity of bacterioruberin from Antarctic *A. agilis* to surpass that of decaprenoxanthin from *A. psychrochitiniphilus* and zeaxanthin from *Zobellia laminarie*. This finding indicated the high efficacy of bacterioruberin as an intracellular antioxidant in *Arthrobacter*, implying a similar photoprotective function to that observed in *Haloarchaea*. Furthermore, irradiation of a wide sample of Antarctic soil bacteria demonstrated bacterioruberin-producing *A. agilis* to present not only a substantially higher tolerance to broad spectrum solar irradiation than non-pigmented Antarctic soil isolates, but amongst the highest tolerance of the pigmented isolates (Dieser et al. 2010). While suggesting that bacterioruberin provides protection of *Arthrobacter* from solar-irradiance, the fact that unpigmented and pigmented isolates were of different species (with this *A. agilis* isolate being the only *Arthrobacter* examined) limits the findings of this study as specific evidence of pigment-mediated photoprotection. A variety of other factors (i.e. the presence/concentration of intracellular photosensitisers, maintenance of ROS-scavenging

systems) may have influenced organismal solar-susceptibility in this study, outside of the strict presence/absence of bacterioruberin pigmentation (Dieser et al. 2010).

As such, while bacterioruberin has demonstrated pronounced antioxidant activity in both *Haloarchaea* and *Arthrobacter*, evidence of its specific role in irradiation-protection from photodynamic damage within *Arthrobacter* remains insufficient. Furthermore, to this author's knowledge, no exploration of the protective role of bacterioruberin from UVA irradiation has been performed in *Haloarchaea* nor *Arthrobacter*, despite its comparable damage-mode to PAR. Given that PAR and UVA wavebands predominate the solar irradiance in environments from which bacterioruberin-producing *Arthrobacter* are commonly isolated (**Table 1.1)**, the lack of exploration of this photoprotective phenomenon is unexpected, and represents a gap in knowledge in characterising the irradiation-resistomes of these organisms (Girard et al. 2011; Kotilainen et al. 2020).

1.3.8.1.2 Protection from UVB/UVC by Bacterioruberin

Bacterioruberin contributes to the UVC-resistome of *Haloarchaea* (Saito et al. 1994; Saito et al. 1997; Jones and Baxter 2017). To this author's knowledge, no research has yet characterised the UVB-resistance conferred by bacterioruberin in *Haloarchaea* or otherwise. While bacterioruberin has no influence on UVC death curves of *Haloarchaea*, pigmented cells do have significantly higher recovery post irradiation under photoreactivation than their unpigmented equivalents (Hescox and Carlberg 1972; Sharma et al. 1984; Jones and Baxter 2017; Shahmohammadi et al. 1998). In strengthening photoreactivation, it has been speculated that bacterioruberin acts as a prosthetic chromophore for the photolyase enzyme, wherein it would absorb visible light for use by the enzyme as energy in dimer-repair (Hescox and Carlberg 1972; Sharma et al. 1984; Jones and Baxter 2017). However, this mechanism has not been demonstrated, and does not explain conflicting experimental observations such as those of Baxter et al. (2007), who found that bacterioruberin suppresses CPD formation under UVC even in conditions precluding photoreactivation, implying that the specific contributions of bacterioruberin to UVC tolerance still lack characterisation.

In *Arthrobacter*, some UVB/UVC protective role of bacterioruberin is inferred, but lacks specific investigation. Silva et al. (2019) demonstrated that *A. agilis* required approximately 1.5-fold higher UVB dosages to induce lethality than decaprenoxanthin-producing *A. psychrochitiniphilus*. As low-dose UVB predominately causes ROS-damage, this finding

implied *A. agilis* to possess a stronger antioxidant capacity than *A. psychrochitiniphilus*, a disparity potentially attributable to their differing carotenoids (Silva et al. 2019). This same study found equivalent UVC tolerance between these isolates, despite their differing carotenoids, implying a lack of protective function of bacterioruberin against UVC. This finding conflicts with the studies of *Haloarchaea* described above but does coincide with the lack of UVC-protection expected of carotenoids (Silva et al. 2019).

As such, the studies of the UVB/UVC tolerance afforded by bacterioruberin are restricted in scope and at times conflicting. Bacterioruberin appears to provide some protection from UVB-irradiation consistent with carotenoid-mediated ROS-quenching, though the nature of this protection is unclear, and literature is sparse. Protection by bacterioruberin under UVC irradiation is lacking sufficient mechanistic investigation to provide meaningful conclusions, but does appear consistent with the lack of protective capacity afforded by carotenoid species against direct DNA damage.

1.3.8.2 Summary of Bacterioruberin- and Carotenoid-Mediated Protection in *Arthrobacter*

The contribution of bacterioruberin, as other carotenoids, to the irradiation-resistome of *Arthrobacter* is poorly understood. While some protective function has been speculated from studies in *Haloarchaea*, there are a lack of appropriate species-level, pigment-deprivation studies within *Arthrobacter* sufficient to demonstrate these functions. Furthermore, current knowledge of bacterioruberin suffers from incomplete or conflicting information regarding its protective capacities under UVA, UVB, and UVC irradiation.

Given the substantial selection exerted by UV irradiation in the biologically-extreme regions from which carotenoid-producing *Arthrobacter* are commonly isolated (**Table 1.1)**, the lack of analysis of the contributions of carotenoid pigmentation to *Arthrobacter* irradiation resistomes is surprising, and represents a gap in our understanding of the systems used by this genus for persistence within desert systems (Dana et al. 1998; Silva et al. 2019). As carotenoid-pigmentation has been demonstrated as an important component of intrinsic UV tolerance in a variety of other bacteria, a similar role is implied within *Arthrobacter*, which is currently insufficiently explored (Dieser et al. 2010; Yuan et al. 2012; Pavlopoulou et al. 2016; Silva et al. 2019). One species of *Arthrobacter* that presents a potentially valuable model in which to

study this contribution of carotenoid pigmentation to the irradiation-resistome is *Arthrobacter* sp. NamB2.

1.3.9 *Arthrobacter* sp. NamB2

Arthrobacter sp. NamB2 is a novel isolate of *Arthrobacter* recovered from surface soils of the Namib Desert, and was the focus of a recent doctoral thesis characterising its mechanisms of intrinsic UV tolerance (Buckley 2020). As this organism was isolated from open soil of a desert subject to stable, biologically stressful solar irradiation (**Section 1.3.1.3)**, it likely presents a prolonged solar-exposure history, and therefore serves as a valuable model for characterising the breadth of intrinsic tolerance systems utilised by bacteria from regions of extreme irradiance (Pavlopoulou et al. 2016; Buckley et al. 2019; Buckley 2020).

Arthrobacter sp. NamB2 has demonstrated substantial UV tolerance relative even to other Namib Desert soil isolates (Buckley 2020). While a variety of the expected intrinsic irradiation protection mechanisms were characterised within the genome of *Arthrobacter* sp. NamB2 (i.e. maintenance of genes encoding PHR, BER and NER systems, catalases, SOD), of particular interest here was its production of a bright pink intracellular pigmentation (Buckley 2020). While no formal identification of this pigment has been performed, genus-contextual information led Buckley (2020) to speculate its identity as bacterioruberin, consistent with pink-pigmented *Arthrobacter* from other desert systems.

Investigations of the contribution of pigmentation in *Arthrobacter* sp. NamB2 to its UV irradiation resistome would serve several purposes. It would be the first characterisation of pigmentation as a photoprotectant in bacteria of the Namib Desert. This is an environment of demonstrably biologically-stressful irradiation which is as yet unstudied with respect to the role of pigmentation in intrinsic radiation tolerance of its indigenous bacteria. It would also serve as the first specific investigation characterising the contribution of pigmentation in *Arthrobacter* to its resistome, which has thusfar largely relied on inferred information.

In speculating the potential physiological roles of pigmentation in this organism, the identity of the pigment itself as a carotenoid would first require unambiguous determination, relying on common identification methods.

1.3.10 Carotenoid Identification

The unambiguous identification of carotenoids is based on three carotenoid-specific criteria (Britton et al. 2004):

1. Production of ultraviolet-visible (UV-visible) scanning spectra of the carotenoid, with characterisation of spectral fine structure.

2. Chromatographic properties of the carotenoid in at least two different chromatography systems, with co-elution of unknown carotenoids alongside an authentic standard.

3. A mass-spectrum of sufficient resolution to identify the molecular ion of the carotenoid and its distinctive fragmentation patterns.

1.3.10.1 Ultraviolet-Visible Spectroscopy

Carotenoids produce UV-visible spectra which are unique to the carotenoid pigment class and directly informative of their structure (Britton et al. 1995a). Due to their extended series of conjugated double bonds, carotenoids demonstrate strong absorbance within the 400 – 600 nm spectral range (Britton et al. 1995a). Within this range, carotenoids exhibit a characteristic, three-peaked absorbance response (exemplified in **Figure 1.6)**, with the central peak absorbing most strongly, denoted λ_{max} (Rodriguez-Amaya and Kimura 2004; Kopec et al. 2012). Demonstrating this unique spectral response in UV-visible scanning-spectra of bacterial pigment extracts is sufficient to classify pigment complements as carotenogenic in nature, and has been used in carotenoid screening studies from *Bacillus* to *Arthrobacter* (Dieser et al. 2010; El-Banna et al. 2012; Vila et al. 2019). The wavelengths of maximal absorbance in this three-peaked spectrum are reported in increasing wavelengths as peaks I, II (representing λ_{max}), and III respectively (Britton et al. 2004). Wavelength positions of these peaks are determined by the length of the carotenoid chromophore, and are thus uniform between carotenoids of equal conjugation (Britton et al. 1995a). Consequently, wavelength positions of these peaks may be used to determine the chromophore lengths of unknown carotenoids from UV-visible spectra alone.

The ratio in absorbance of peak III to peak II in the UV-visible spectrum of a purified carotenoid is reported as its 'spectral fine structure', and is theoretically carotenoid-unique,

though specificity in identification is limited (Britton and Young 1993; Britton et al. 2004; Kopec et al. 2012). For example, the spectral fine-structures of β-carotene, zeaxanthin and β-cryptoxanthin have all been reported as 25 % in petroleum ether, despite their differing structural properties (Rodriguez-Amaya and Kimura 2004). Appearance of minor 'cis-peaks' on UV-visible spectra of carotenoids,142 nm below peak III, demonstrates the presence of carotenoid cis-isomers (Britton et al. 1995a; Kopec et al. 2012). Cis-isomers of carotenoids are formed during extraction, and represent the isomerisation of the carotenoid around double bonds of the chromophore, with consequences on carotenoid polarities and the resolution of fine-structures (Britton et al. 1995b). Indeed, cis-isomers are known to confound the spectral-fine structures of carotenoids, and possess higher polarities than the trans form (Takaichi and Shimada 1992; Ladislav et al. 2004; Fanali et al. 2012). The presence of cis-isomers within a carotenoid mixture thus complicates carotenoid identifications, and should be minimised during extraction through protection of carotenoids from light and heat (Britton et al. 1995b).

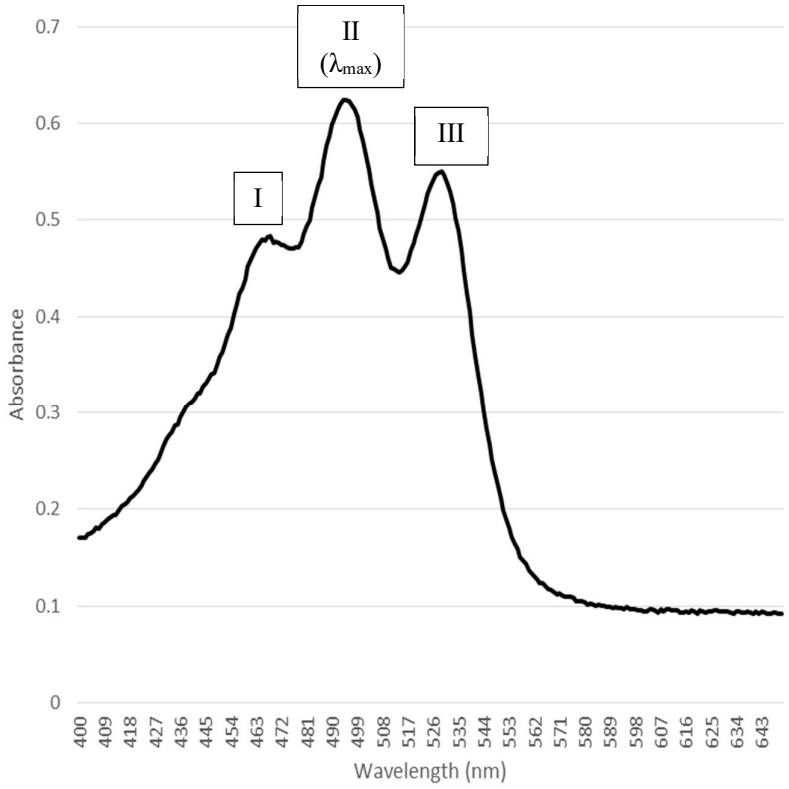

Figure 1.6: Example UV-visible scanning spectrum of a carotenoid. Maxima corresponding to peaks I, II and III of the three-peaked spectral response are denoted upon the spectrum.

Carotenoids obey the Beer-Lambert Law, thus their UV-visible spectra can be used for quantification (Britton et al. 1995b). The Beer-Lambert law dictates that the concentration of a wavelength-absorbing compound in solution is directly proportional to its absorbance

(Swinehart 1962; Parnis and Oldham 2013; Casasanta and Garra 2018). Consequently, the absorption intensity of carotenoids at λ_{max} is directly proportional to their concentration, and this forms the basis of quantitative carotenoid studies (Liaaen-Jensen and Jensen 1971; Yachai 2009; Kopec et al. 2012).

As such, UV-visible spectroscopy provides structural and quantitative information on carotenoids (Britton et al. 1995b; Amorim-Carrilho et al. 2014). The UV-visible spectra of purified carotenoids allows determination of carotenoid chromophore lengths from positions of absorption maxima, and carotenoid identity may be speculated from their calculated fine-structures. In quantitative studies, absorbance intensities of these spectra may be used to determine the concentrations of specific or total carotenoids within a pigment-extract (Liaaen-Jensen and Jensen 1971).

1.3.10.2 Chromatographic Separation

Intracellular carotenoids of bacteria and other organisms typically exist as pigment complements, comprising mixtures of carotenoids and their derivative compounds (Niessen 2006). For example, *Arthrobacter* pigment complements possess upwards of six – seven discrete carotenoids, while *Haloarchaea* have as many as 23 (Squillaci et al. 2017; Silva et al. 2019). Identification of individual carotenoids from biological samples thus first requires their purification, as achieved by chromatography (Takaichi 2014).

Chromatography separates heterogeneous mixtures between immiscible phases, a solid (stationary) phase and a liquid (mobile) phase, on the basis of polarity (Niessen 2006). As the mobile phase (containing the analyte mixture) flows over the stationary phase, molecules of the mixture bind to stationary phase particles with differing degrees of polarity, with a cycle of adsorption/desorption unique to each compound resulting in their eventual separation (Britton et al. 1995b; Fanali et al. 2012; Rivera and Canela-Garayoa 2012). In carotenoid analyses, chromatography is used to resolve the crude pigment complement into individual, polarity-distinct carotenoid fractions, allowing the estimation of each carotenoid's polarity from its chromatographic behaviour, and providing their purification for subsequent identification (Britton et al. 2004; Rodriguez-Amaya and Kimura 2004; Rivera and Canela-Garayoa 2012; Takaichi 2014). Carotenoid analyses typically use thin-layer chromatography (TLC) and liquid-chromatography (LC).

1.3.10.2.1 Thin-Layer Chromatography

In TLC, crude carotenoid mixtures (the solute) are carried across a plate coated in polar stationary phase particles via the capillary action of a non-polar mobile phase (the solvent), separating into pure fractions based on polar interactions between carotenoids and stationary phase particles (**Figure 1.7**) (Sherma and Fried 2003). Purified compounds of the mixture are visible on the TLC plate following development as independent spots or bands. The migration of each individual carotenoid band is modelled by retardation factors (Rf), values inversely proportional to their polarity, and determined from the migration of the carotenoid from origin relative to the total migration of the mobile phase (or solvent front) (Bidlingmeyer 1987; Britton et al. 1995b). Thin-layer chromatography thus grants information on both the total number of carotenoids within the pigment complement, alongside their relative polarities. The purified carotenoids may be scraped from the TLC plate and individually analysed via UV-visible spectroscopy for characterisation of their spectral fine-structures or conjugation lengths, or subject to higher-resolution structural elucidation under mass-spectrometry (Britton et al. 1995b; Poole 1999; Poole 2003).

The nature of the TLC analysis enables several samples to be run in tandem on the same plate, allowing co-analysis of unknown extracts alongside control carotenoids (Britton 2008). Similar Rf values demonstrate comparable polarities between carotenoids, thus similar structures and numbers of polar groups (Poole 2003). Consequently, presenting the co-elution and matching Rf of a carotenoid from an unknown sample alongside an authentic carotenoid standard is accepted information in the identification of unknown carotenoids (Fong et al. 2001; Sherma and Fried 2003; Britton 2008). Without *a priori* knowledge of identity, unknown carotenoid extracts may be run against carotenoid standards of known structures, with comparable migrations of these fractions demonstrating similar numbers of polar functional groups, and allowing some structural inference regarding structures of the unknown carotenoids (Hodisan et al. 1997; Sherma and Fried 2003; Takaichi 2014; Rodriguez-Amaya and Kimura 2004).

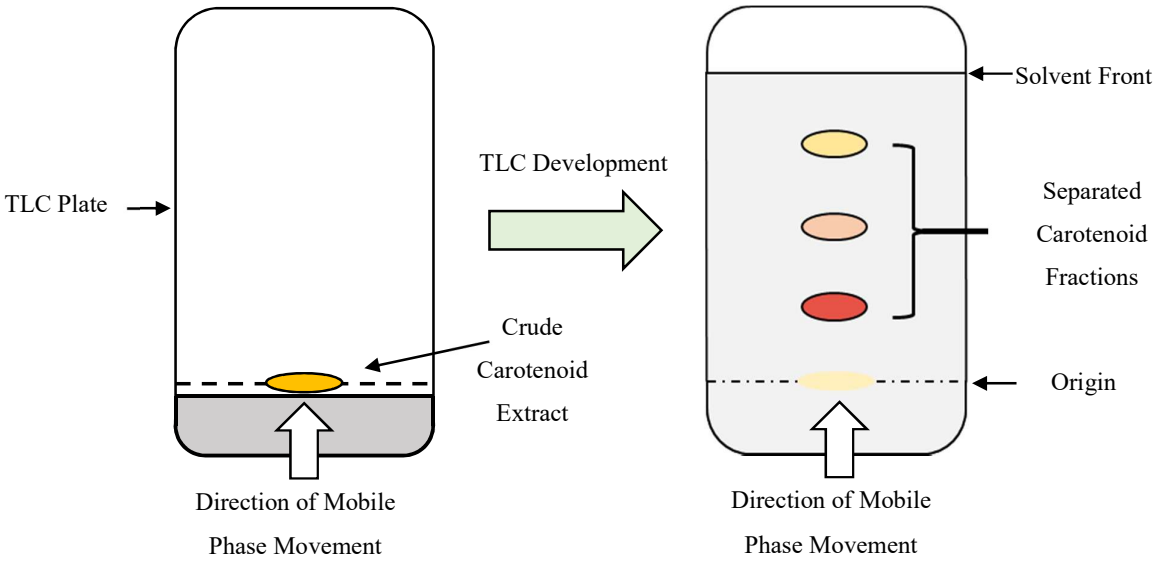

Figure 1.7: Schematic diagram of the process of TLC development. The left figure denotes the state of the TLC plate and crude carotenoid mixture at the beginning of the experiment – prior to movement of the mobile phase. The figure on the right displays the TLC plate following mobile phase development, including separation of the crude carotenoid mixture into a series of purified spots of different polarity. The solvent front denotes the total migration of the mobile phase.

1.3.10.2.2 Liquid Chromatography

In liquid chromatography (LC), a constant flow of polar mobile phase (the solvent) carries the carotenoid mixture (the solute) through a narrow, closed column coated with the non-polar stationary phase (Rivera and Canela-Garayoa 2012). Repeated adsorption/desorption with the stationary phase separates carotenoids over the length of the column, with purified carotenoids being detected via UV-visible spectroscopy as they elute from the column, and collected for further analysis (**Figure 1.8**) (Abate-Pella et al. 2017; Cortés-Herrera et al. 2019). The retention time of each carotenoid within the LC column is recorded as they elute, and directly reflects their polarity, with higher retention times within the non-polar column denoting lower polarity (Fanali et al. 2012). Similar to TLC, this chromatographic separation allows purification of individual carotenoids from the pigment complement, and speculation of their polarities from retention times in the LC system.

The efficacy of separation by LC is determined by the breadth of interactions between carotenoid molecules and stationary phase particles, which increases with increasing column

length and stationary phase density, as well as decreasing stationary phase particle size (Bijttebier et al. 2014). Different forms of LC, including high-performance liquid chromatography (HPLC) and ultra-HPLC (UHPLC) differ notably in these column features, resulting from their different system designs (Bijttebier et al. 2014). Consequently, their efficacies in carotenoid separation differ.

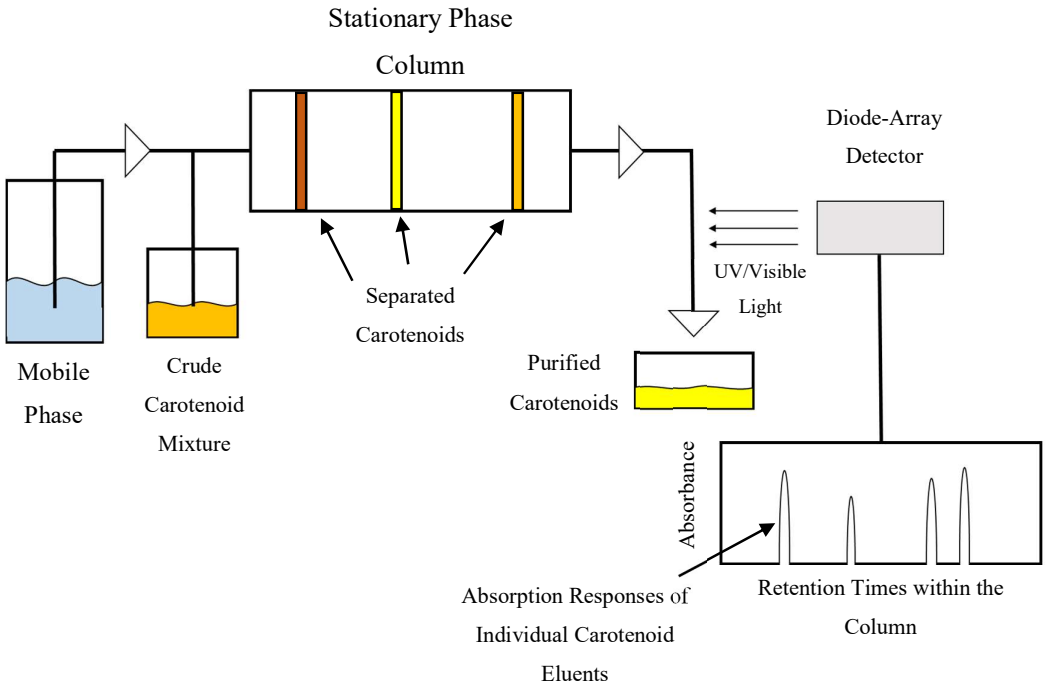

Figure 1.8: Schematic representation of the separation of crude carotenoid mixtures into purified fractions via LC. Separated carotenoids are detected via UV-visible spectroscopy as they exit the column, and their retention times are recorded.

1.3.10.2.3 High-Performance Liquid Chromatography

High-performance liquid chromatography is considered the gold standard for chromatographic separation of carotenoids, and is frequently used in carotenoid analyses within the literature (Britton et al. 1995b; Britton et al. 2004; Amorim-Carrilho et al. 2014; Takaichi 2014). Under HPLC, a high-pressure pump is used to drive the mobile phase (containing the carotenoid mixture) through the column (Rodriguez-Amaya and Kimura 2004; Barba et al. 2006; Corradini et al. 2011; Rivera and Canela-Garayoa 2012). This high pressure allows HPLC to use small stationary phase particle sizes (3 – 5 µm), long column lengths and high densities of stationary phase particle packing, granting it high resolution in carotenoid separation over the column length (Snyder et al. 1997; Doyle and Dorsey 1998; Corradini et al. 2011). Indeed, HPLC has

shown sufficient resolution to separate carotenoids from their geometrical isomers or derivatives which demonstrate only minor polarity distinctions (Mandelli et al. 2012; Bijttebier et al. 2014; Maurer et al. 2014). Application of HPLC utilising columns coated with octadecyl silane (C18) stationary phases are routine in carotenoid separation, while those using of triacontyl (C30) stationary phases provide even higher resolution, and are currently the gold standard for carotenoid purification (Fong et al. 2001; Mandelli et al. 2012; Rivera and Canela-Garayoa 2012; Bijttebier et al. 2014; Giuffrida et al. 2016).

1.3.10.2.4 Ultra-High Performance Liquid Chromatography

Ultra-high performance liquid chromatography is a recent development of HPLC utilising higher back-pressures to drive the mobile phase through the column (Rivera and Canela-Garayoa 2012; Fekete et al. 2014; Maurer et al. 2014; Walter and Andrews 2014). This UHPLC uses pressures two – three fold higher than standard HPLC, allowing it to utilise even smaller stationary phase particles (< 2 μm compared to the standard 5 μm of HPLC), and higher-density packing of these particles (Bohoyo-Gil et al. 2012; Rivera and Canela-Garayoa 2012; Bijttebier et al. 2014; Fekete et al. 2014; Maurer et al. 2014). These features have led to as high as two-fold higher resolutions in separation of carotenes and xanthophylls in UHPLC systems compared to standard HPLC (Chauveau-Duriot et al. 2010). In bacterial carotenoid analyses, this system has demonstrated the capacity to separate carotenoids from their geometrical isomers in extracts of *A. agilis, A. psychrochitiniphilus* and *Zobellia laminarie* (Silva et al. 2019). However, UHPLC columns have not yet received the same chemical optimisation for carotenoid analyses as demonstrated by C30 HPLC columns (Bijttebier et al. 2014). As a result, they are of lower specificity in separation of extracts containing widely varying polarities of carotenes/xanthophylls (Bijttebier et al. 2014).

1.3.10.3 Structural Identification – Mass Spectrometry

Carotenoids are identified post-purification through structural elucidation. Most typically, this is achieved through a combination of structural information from UV-visible spectroscopy (**Section 1.3.10.1**) and carotenoid fragmentation patterns generated under mass spectrometry (MS) (Britton et al. 2004; Takaichi 2014).

In MS, purified carotenoids of interest are ionised and fragmented, with the charged ions generated subsequently separated via their mass/charge ratios (m/z), and abundances determined (Dass 2007a; Hoffman and Stroobant 2007; Gross 2017a). The molecular ion is represented by the ion with the highest m/z value on the mass spectrum, and represents the mass of the intact, ionised analyte. From this mass-value, the molecular mass of the carotenoid may be determined and related to known structures for identification (Dass 2007b). Both the m/z of the molecular ion, and its fragmentation patterns, can be used for carotenoid identification (Britton et al. 2004).

Carotenoid MS typically uses a positive-mode atmospheric pressure chemical ionisation (APCI) ionisation source for fragmentation (Rivera and Canela-Garayoa 2012). This APCI provides low fragmentation intensity, thus clear resolution of molecular ions (denoted $[M+H]^+$ under positive-mode APCI), base peaks (the most abundant fragment ion of the spectrum) and fragmentation patterns (Breemen et al. 1996; van Breemen et al. 2012; Rivera et al. 2014). Carotenoid molecules produce replicable patterns of structural fragmentation under mass-spectrometry, easing identifications through comparisons to known mass spectra (Breemen et al. 1996; van Breemen et al. 2012). For example, fragment ions corresponding to m/z values of $[M+H - 92]^+$ (an m/z value 92 below the molecular ion) are common in carotenoid spectra, and result from the fragmentation of extended carotenoid chromophores (Rivera and Canela-Garayoa 2012). Fragmentation patterns of xanthophylls possessing hydroxyl groups are typified by ion peaks at sequential m/z values of $[M+H - 18]^+$, $[M+H - 18 - 18]^+$ etc., representing progressive losses of H_2O from the carotenoid structure, with base peaks often corresponding to the $[M+H - 18]^+$ ion (van Breemen et al. 2012; Kopec et al. 2012; Rivera et al. 2014). Mass spectra of carotenoids are thus structurally informative, replicable and distinct, and are consequently widely used in their unambiguous identification. An example carotenoid mass-spectrum, and how this spectrum can be structurally interpreted, is provided in **Figure 1.9**.

Tandem MS is a specific execution of MS which allows for the selection of an ion of a particular size from the sample prior to fragmentation, enabling exclusive production of its fragmentation pattern (Hoffman and Stroobant 2007; Gross 2017b). By selecting a molecular ion of a particular m/z prior to its fragmentation, tandem mass-spectrometry provides high selectivity to unambiguously demonstrate the occurrence of a specific carotenoid within a sample, as a mass-spectrum will only be produced if the selected molecular ion is present (Gross 2017b).

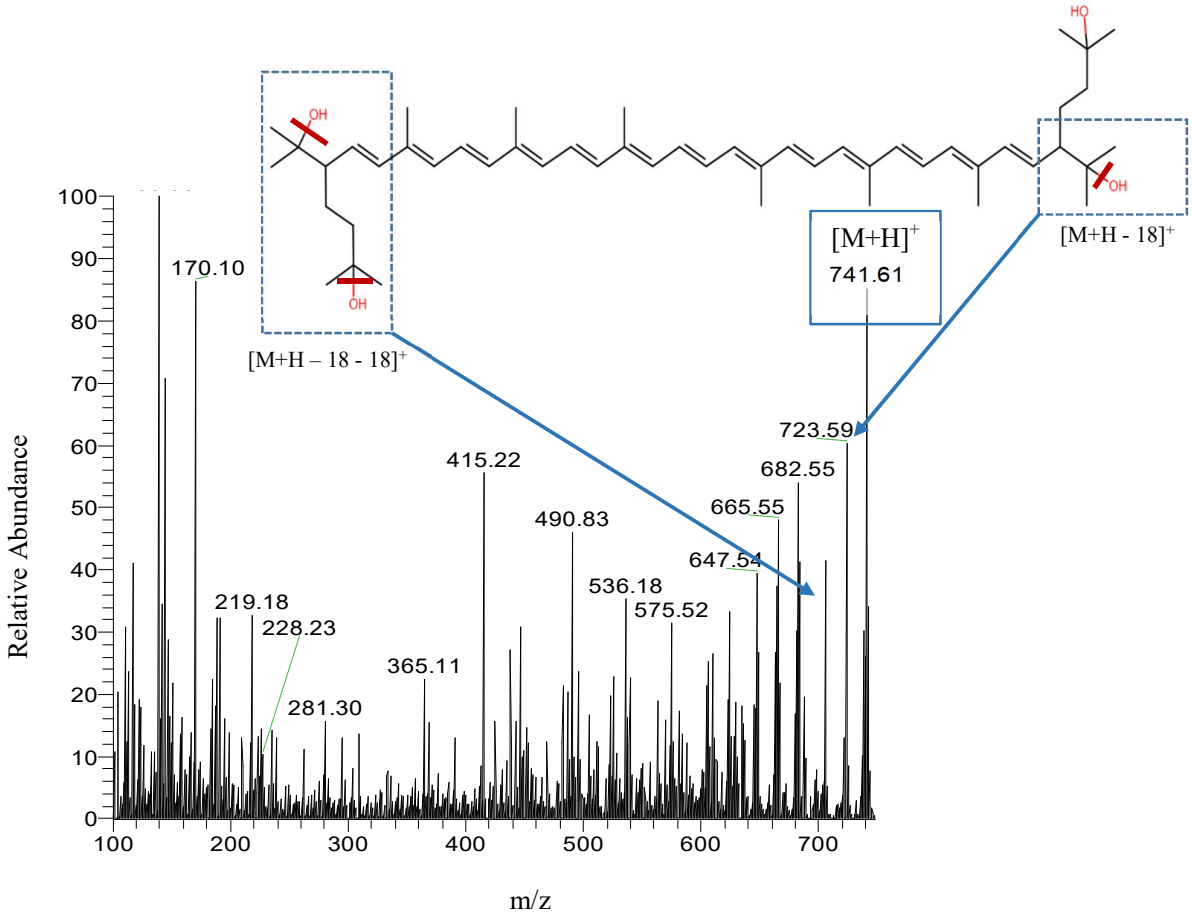

Figure 1.9: Example APCI mass spectrum produced from fragmentation of the carotenoid bacterioruberin. Peaks corresponding to the molecular ion of bacterioruberin (m/z 741) and ion peaks denoting fragments which have lost a single hydroxyl group ([M+H - 18]+) or two hydroxyl groups ([M+H – 18 - 18]+) are denoted on the figure. Breakages of hydroxyl group bonds are denoted by thick red lines on the carotenoid structure. The mass-spectrum analysed here was reproduced from the study of Flores et al. (2020).

1.3.11 Summary of the Literature Review

This literature review has discussed how solar irradiance acts as a selector for bacterial tolerance systems in regions where it reaches biologically stressful intensities. Of these tolerance systems, it has highlighted the contribution of carotenoid pigmentation towards the bacterial irradiation-resistome, and narrowed in scope to those pigments of genus *Arthrobacter*. The lack of adequate study of carotenoid photoprotection within *Arthrobacter* has been described, with the pink-pigmentation of *Arthrobacter* sp. NamB2 emphasised as a valuable model to examine this protective role.

Accepted methods of bacterial carotenoid identification have been outlined and will be

employed in initial identification of the pigmentation produced by *Arthrobacter* sp. NamB2 under Research Question One of this thesis (**Chapter 2**), allowing further speculation of its biological function. The connection between light-induced carotenoid production and cellular photoprotection has been described and will be explored here under Research Question Two (**Chapter 3**) for evidence of the photoprotective role of pigmentation in *Arthrobacter* sp. NamB2. Finally, the protection afforded to bacteria by carotenoids under differing UV wavelengths, and the requirement of specific, species-level pigment deprivation studies to demonstrate this, has been emphasised, and will be explored under Research Question Three (**Chapter 4**) to denote unambiguously the contribution of *Arthrobacter* sp. NamB2's pigmentation to its UV-resistome.

Chapter 2 Identification of the Pigment Complement of *Arthrobacter* sp. NamB2

2.1 Introduction

2.1.1 Pigment Identification and Biological Significance

Identifying the pigmentation produced by bacteria shapes our understanding of the physiological function which these pigments serve within the organism. The pigmentation of heterotrophic bacteria aids their survival via membrane-stabilisation, radiation screening or ROS-quenching (Büdel et al. 1997; Rajagopal et al. 1997; Chattopadhyay and Jagannadham 2001; Wynn-Williams and Edwards 2002; Selvameenal et al. 2009). Particular pigment classes correspond to different physiological functions, such as scytonemin and melanin providing UV-screening, and carotenoids serving photoprotection (Krinsky 1978; Garcia-Pichel and Castenholz 1993; Cockell and Knowland 1999; Alcaíno et al. 2016). As pigment production requires a substantial energy commitment, and desert environments are metabolically restricted, the maintenance of pigment production by desert heterotrophic bacteria suggests their pigments are physiologically important (Krinsky 1978; Büdel et al. 1997; Bay et al. 2018; Leung et al. 2020). Identification of these bacterial pigments is thus the first step towards understanding this import.

Arthrobacter sp. NamB2, isolated from Namib Desert soil, produces a pink pigmentation (Buckley 2020). As discussed in **Section 1.3.7.3**, pink pigmentation in *Arthrobacter* is associated with the production of carotenoids, particularly bacterioruberin (Fong et al. 2001; Dieser et al. 2010; Flegler et al. 2020). Bacterioruberin is an acyclic, C_{50} xanthophyll possessing an extended chromophore of thirteen c.b.d., yielding a pink colour (Schwieterman et al. 2015; Yang et al. 2015). This carotenoid is responsible for the pink colouration in a variety of *Arthrobacter* species, including *A. agilis* and *A. bussei* (Fong et al. 2001; Schabereiter-Gurtner et al. 2001; Dieser et al. 2010; Tescari et al. 2018; Flegler et al. 2020). Bacterioruberin-producing *Arthrobacter* are commonly isolated from high-irradiance desert environments, with their production of bacterioruberin thought to support their UV-irradiation resistomes (Fong et al. 2001; Dieser et al. 2010; Silva et al. 2019). Indeed, bacterioruberin is known to provide substantial PAR and UV tolerance to organisms outside of *Arthrobacter* **(Section 1.3.8.1)**, and identification of this pigment within the genus has been used to suggest a similar physiological

importance. As such, identifying whether the pigmentation of *Arthrobacter* sp. NamB2 is carotenogenic, and related to bacterioruberin, would serve as a strong first step in hypothesis formulation regarding its potential contribution to the irradiation-resistome of this organism.

2.1.2 Identification of Bacterial Pigment Complements

The identification of bacterial pigment complements within the literature follows a common workflow, a workflow similarly applied in prior investigations of *Arthrobacter* (Fong et al. 2001; Nugraheni et al. 2010; Sutthiwong, Caro, et al. 2014; Silva et al. 2019; Flegler et al. 2020). Treatment of bacteria with high-purity alcohols such as methanol is used to achieve total pigment extraction (Fong et al. 2001; Squillaci et al. 2017; Saini and Keum 2018). These crude pigment extracts are first screened for the presence of carotenoids via UV-visible spectroscopy, with the appearance of three-peaked carotenoid spectra used to confirm the pigmentation as carotenogenic, enabling subsequent directed pursuit of pigment identity using carotenoid-specific identification methods (Dieser et al. 2010; El-Banna et al. 2012; Vila et al. 2019). As bacterial pigment complements typically comprise complex mixtures of carotenoids, the purification of individual carotenoids from this mixture via chromatography is necessary for their identification (Niessen 2006; Rivera et al. 2011). Chromatographic separation of the complement via TLC and/or HPLC is thus used to purify individual carotenoids and provide information regarding their polarities (Poole 2003). Finally, the individual carotenoids separated by chromatography are identified using both their fine-structures under UV-visible spectroscopy, and structural information from mass-spectrometry (Britton et al. 1995b; Squillaci et al. 2017). The utility of each of these methods in carotenoid analyses has been discussed at length within **Section 1.3.10**.

Previously, such methods have demonstrated the pigment complements of pink/red *Arthrobacter* to comprise between five – seven polarity-distinct carotenoids of equal conjugation lengths, representing bacterioruberin and a limited diversity of its glycosylated/dehydrated variants (Fong et al. 2001; Silva et al. 2019; Flegler et al. 2020). The structures of these commonly isolated carotenoids are displayed in **Figure 2.1**. Bacterioruberin-producing *Arthrobacter* consistently demonstrate these low variety pigment complements, comprising only this limited pool of bacterioruberin-associated carotenoids (Mandelli et al. 2012; Squillaci et al. 2017; Flores et al. 2020). *Haloarchaea* – prominent producers of bacterioruberin – demonstrate this same trend, with pigment complements exclusively comprised of these molecules (Mandelli et al. 2012; Squillaci et al. 2017; Flores et al. 2020). Other carotenoids outside of those listed have not shown co-isolation from bacterioruberin-containing pigment complements of *Arthrobacter,* and are highly uncommon in complements of

other bacterioruberin-producing organisms (Fong et al. 2001; Silva et al. 2019; Flegler et al. 2020). The presence of bacterioruberin within the pigment-complement of an organism therefore strongly indicates the remainder of the complement will be comprised of these common glycosylated/dehydrated variants.

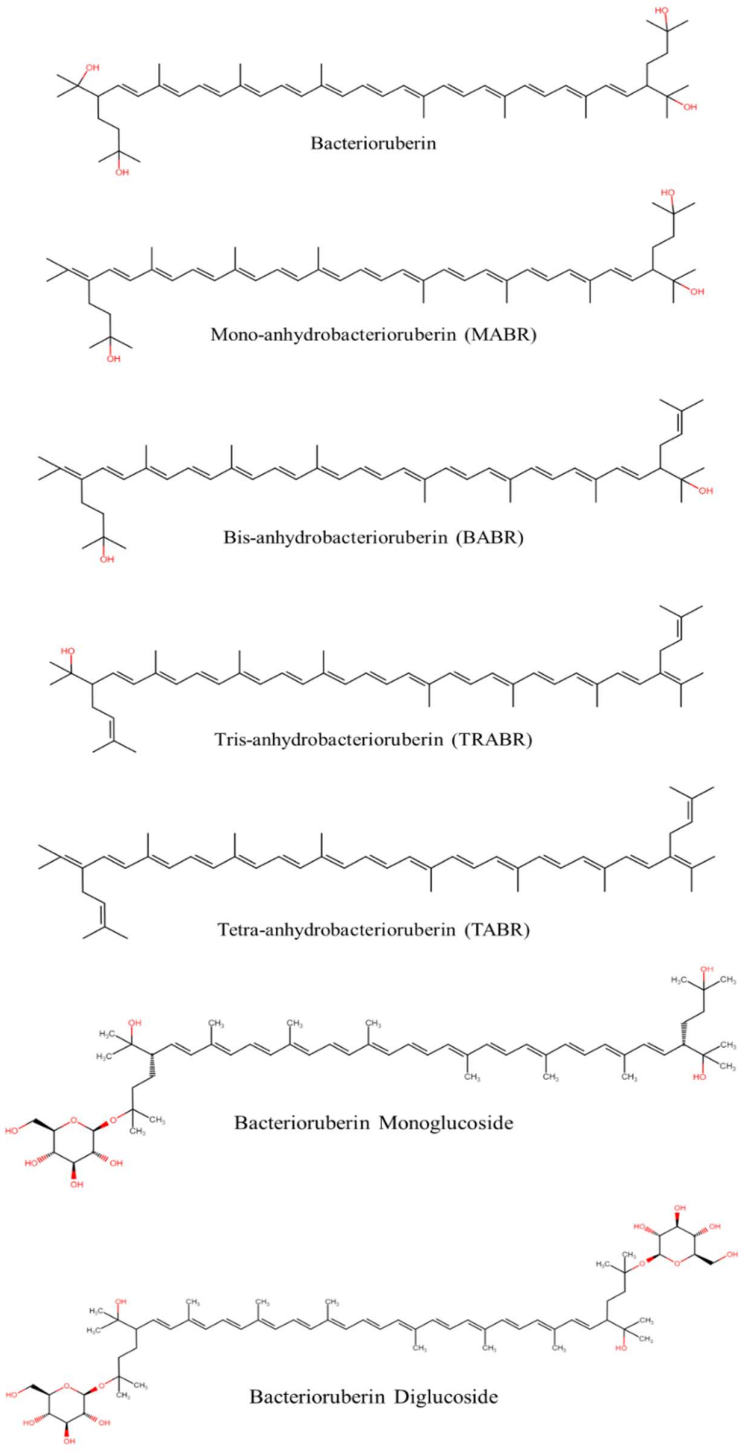

Figure 2.1: Chemical structures of bacterioruberin and its commonly co-isolated variants from bacterioruberin-producing organisms, with polar groups highlighted in red.

2.1.3 Pigment Identification in Namib Desert Organisms

While carotenoid pigment complements have been reported for heterotrophic bacteria from soils of the Atacama, Gobi and Antarctic deserts, and are well explored as adaptive strategies of these organisms to the high-irradiation stress of their environments, no study has yet been performed for bacteria of the Namib Desert (Dieser et al. 2010; Yuan et al. 2012; Buckley 2020; Cowan et al. 2020; Flores et al. 2020). This is a gap in our characterisation of the tolerance systems utilised by edaphic desert bacteria, as the Namib is subject to a demonstrably biologically-stressful intensity of irradiance analogous to these studied environments, and presents soil bacterial communities with clear maintenance of pigment production (Warren-Rhodes et al. 2013; León-Sobrino et al. 2019; Buckley 2020).

This chapter thus sought to determine the identity of the pink pigmentation produced by *Arthrobacter* sp. NamB2. It was hypothesised that this pigmentation was based around bacterioruberin – similarly to other *Arthrobacter* – thus would be comprised of the base bacterioruberin alongside a number of its dehydrated/glycosylated variants. **Figure 2.2** shows the workflow used to resolve the identity of pigmentation within this study. To characterise first whether the pigment complement was carotenogenic, pigmentation was extracted from *Arthrobacter* sp. NamB2 via treatment of cells with high-purity methanol, and subject to scanning UV-visible spectroscopy in examination for carotenoid three-peaked spectra (**Figure 2.2 – A**). Chromatography employing TLC and HPLC separation were used to denote the number and chromatographic properties of individual compounds comprising the pigment complement, and provide purification for their subsequent identification (**Figure 2.2 – B**). Purified pigments from the HPLC-analysis were identified via mass-spectrometry, while TLC-separated pigments were identified from comparisons of their pigment polarities to control carotenoids of known structure (**Figure 2.2 – C**).

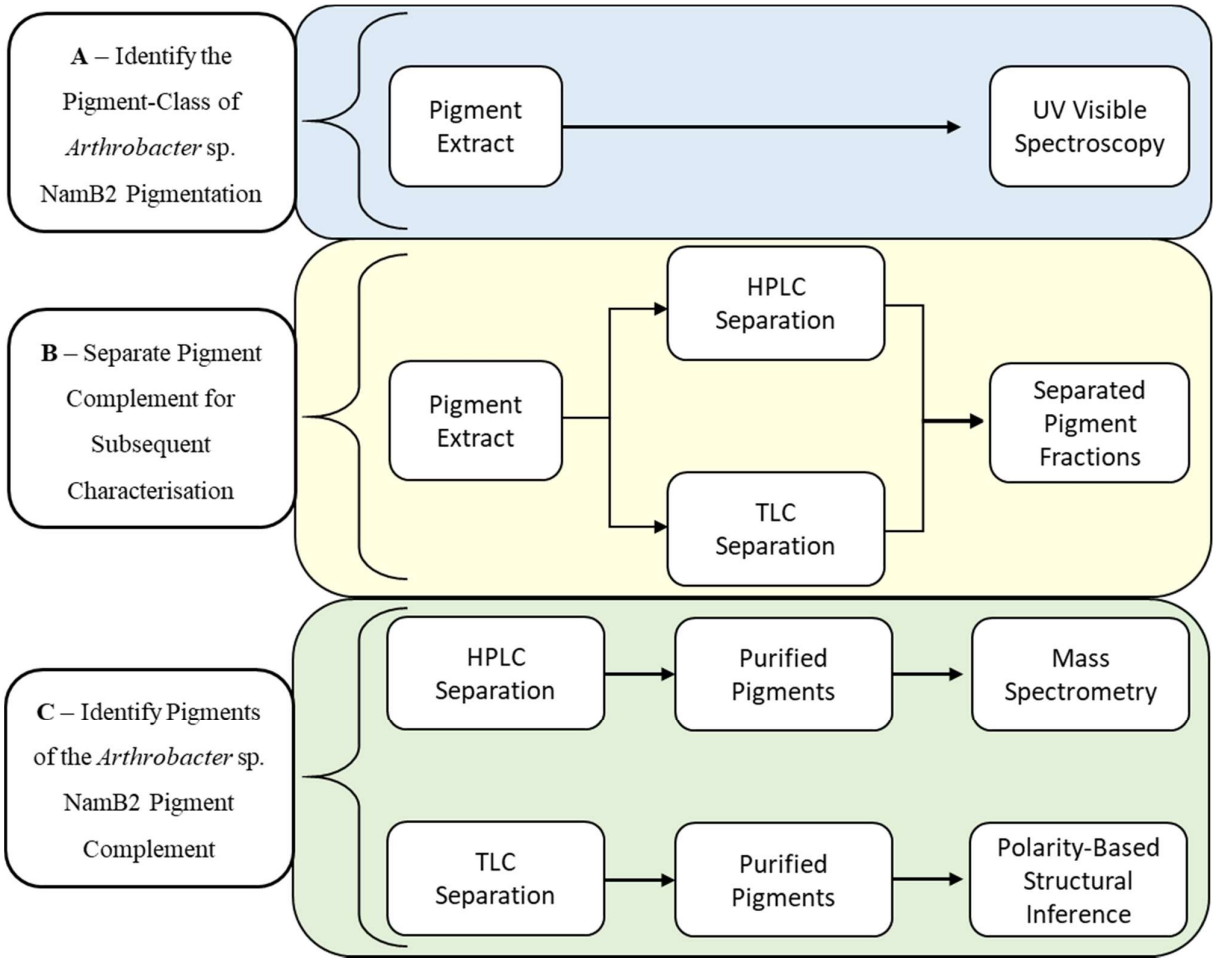

Figure 2.2: Schematic workflow of pigment-analysis performed within this chapter. 'Pigment extract' denotes the crude methanolic pigment extract from cells of *Arthrobacter* sp. NamB2.

2.2 Methods

A consistent protocol was used to cultivate and extract pigmentation from cultures of *Arthrobacter* sp. NamB2 before analysing these pigment extracts using UV-visible spectroscopy, TLC or HPLC/MS. This protocol followed a workflow of cell revival and growth, with subsequent cell harvest and pigment extraction.

2.2.1 Bacterial Cell Growth and Pigment Extraction

For cell revival, 300 µL of one glycerol stock of *Arthrobacter* sp. NamB2 was used to inoculate 5.0 mL of nutrient broth (Fort Richard Laboratories Ltd, New Zealand). This culture was grown at 20 ºC with 25 rpm agitation for 72 hours to achieve stationary phase at an optical density OD_{600} of approximately 0.5. This broth culture was used to inoculate triplicate nutrient agar plates (BD Difco, USA), by spread plating 100 µL onto each plate. These plates were subsequently incubated for 72 hours at 20 ºC to achieve sufficient cell growth for pigment extraction.

For cell harvest, colonies were reverse spread plated from each nutrient agar plate by adding 5.0 mL of nutrient broth to the plate and scraping the colonies from the agar's surface into the broth suspension using a plastic spreader. This broth suspension was collected via aspiration into a 50 mL centrifuge tube. The cell suspensions from all three plates were combined into the same centrifuge tube to increase cell density. The cell pellet was obtained via centrifugation at 7,745 x *g* for 15 minutes (4 ºC). The supernatant nutrient broth was discarded, the cell pellet was washed with 5.0 mL of distilled water, and re-pelleted via centrifugation (7,745 x *g*, 15 minutes, 4 ºC). Supernatant water was aspirated from around the cell pellet and discarded.

For pigment extraction, 7.5 mL of > 99.9 % HPLC-grade methanol was added to the cell pellet, with gentle physical agitation used to suspend the pellet within the methanol phase. All tubes and equipment from this stage were wrapped with two layers of aluminium foil to prevent light-mediated isomerisation or degradation of the pigment (Britton et al. 1995b). Gentle physical agitation of the cell pellet was used to facilitate pigment extraction via methanol. Following agitation, the cells were re-pelleted by centrifugation at 7,745 x *g* for 15 minutes (4 ºC). The pink methanolic supernatant (containing the pigment complement) was collected in a separate, aluminium foil-wrapped 50 mL centrifuge tube via aspiration. In cases where the pellet still

demonstrated a visible pink colour, further extractions were performed with 3.0 mL aliquots of > 99.9 % methanol until both pellet and supernatant (post-centrifugation) were colourless, to ensure total pigment extraction. The supernatant(s) from these further extractions were pooled with the supernatant from the original extraction.

The total pink methanolic pigment extract was dried to a solid via use of a rotary-evaporator (BUCHI Rotovapor® R-300, BUCHI Labortechnik AG, Switzerland) operated at 40 °C, and protected from light by wrapping the apparatus with aluminium foil. The dried pigment extract obtained from rotary evaporation was used as the starting material for the subsequent pigment analyses.

2.2.2 Ultraviolet-Visible Spectroscopy

To identify whether the pigment of *Arthrobacter* sp. NamB2 belonged to the carotenoid pigment class, a UV-visible scanning spectrum was produced for the crude pigment extract in methanol.

The dried pigment extract from *Arthrobacter* sp. NamB2 (prepared as described in **Section 2.2.1)** was redissolved in 2.0 mL of > 99.9 % HPLC-grade methanol. This concentrated extract was subject to a UV-visible scanning absorption spectrum from 350 – 800 nm using an Ultrospec 7000 UV-visible spectrophotometer (Cytiva, USA), with HPLC-grade methanol as a blank. This experimental process was repeated with three biological replicates to provide three independent UV-visible scanning-spectra of the pigment extract, to analyse the consistency of its spectral response.

The results of this analysis demonstrated the pigment complement of *Arthrobacter* sp. NamB2 was carotenogenic **(**outlined in **Section 2.3.1)**. Identification of the pigment complement was thus pursued in line with carotenoid-specific identification methods.

2.2.3 Thin-Layer Chromatography Analysis

Thin-layer chromatography was used to separate the pigment complement of *Arthrobacter* sp. NamB2 into its purified fractions. This separation allowed the enumeration of the number of

individual compounds comprising the pigment complement, and provided their purification for subsequent analysis of chromophore lengths and spectral fine structures via UV-visible spectroscopy. The migration of each fraction was compared to co-analysed spinach carotenoid controls of known structure to analyse their relative polarities, and draw structural inferences for the carotenoids of *Arthrobacter* sp. NamB2 from this.

2.2.3.1 Chromatographic Separation via TLC

The dried bacterial pigment extract (prepared as per **Section 2.2.1)** was re-dissolved in 1.0 mL of > 99.9 % HPLC-grade methanol. A control extract was prepared from fresh spinach leaves using the method of Sjursnes et al. (2015); with a mixture of hexane and acetone recovering both carotenoids and chlorophylls from the spinach. Each extract was carefully applied as a straight-streak 1.5 cm from the bottom of a commercial silica gel TLC plate (TLC Silica gel 60 F_{254}, Merck Millipore, USA) using a 0.2 mm capillary tube. Five layers of the concentrated pigment extract were applied to same streak, each layer being allowed to dry entirely between applications. The bacterial and spinach control extract were applied side by side, each taking up approximately half the plate. Simultaneous analysis of this spinach control alongside the bacterial extract enabled both the verification of successful TLC-separation, and allowed comparisons of polarities between pigments of *Arthrobacter* sp. NamB2 and spinach carotenoids of known structure.

Upright development of the TLC plate was carried out in an aluminium foil-wrapped 1.0 L beaker using a watch-glass as a lid, with the mobile phase filling approximately 1.0 cm of the beaker at TLC start-time. The mobile phase was a 7:3 mixture of hexane:acetone (Sjursnes et al. 2015). Development proceeded until the solvent front reached 1.0 cm from the top of the TLC plate. The TLC plate was subsequently removed from its chamber and kept in a minimal light environment while pigment spots were labelled and migrations of these spots from the origin recorded. Retardation factors (Rf) modelling the migrations of the spinach and *Arthrobacter* sp. NamB2 carotenoids were calculated for each individual pigment spot as per **Equation 2.1**.

Equation 2.1: Calculation of Retardation Factors (Rf) of Individual Pigment Spots as Separated via TLC

$$\text{Retardation Factor} = M_{(P)} / M_{(SF)}$$

Where:

$M_{(P)}$ = Migration distance of the pigment spot from the origin.

$M_{(SF)}$ = Migration distance of the solvent-front from origin.

2.2.3.2 Spectral Characterisation of TLC-Separated Pigments

Following development, the separated pigment fractions of the *Arthrobacter* sp. NamB2 pigment complement were individually scraped from the TLC plate, and dissolved in 1.0 mL of > 99.9 % HPLC-grade acetone within 1.5 mL microcentrifuge tubes. Gentle physical agitation allowed re-dissolution of carotenoids within the acetone. Tubes were centrifuged at 15,000 x *g* for 15 minutes (4 ºC) to separate purified pigments into the acetone layer from the silica gel. A scanning UV-visible absorption spectrum from 350 – 800 nm was recorded for each purified pigment fraction in acetone, using an Ultrospec 7000 UV-visible spectrophotometer (Cytiva, USA), and an HPLC-grade acetone blank.

Spectral fine structures of purified pigment fractions were determined from their UV-visible scanning spectra using the ratio calculation of Britton et al. (1995b) as presented in **Equation 2.2**. Cis-peak intensities of purified pigment spots were determined via the standard calculation of Britton et al. (1995b), as presented in **Equation 2.3**.

Equation 2.2: Calculation of the Spectral Fine Structure of Purified Carotenoids from their UV-Visible Spectra

$$\text{Spectral Fine Structure (\%)} = ((\text{Abs(III)} - \text{Abs(Trough)}) / (\text{Abs(II)} - \text{Abs(Trough)})) \times 100$$

Where:

Abs(III) = Absorbance of peak III

Abs(II) = Absorbance of peak II

Abs(Trough) = The lowest absorbance measurement between peaks II and III

Equation 2.3: Calculation of the Cis-Peak Intensity of Purified Carotenoids from their UV-Visible Spectra

$$\text{Intensity}_{(\text{Cis})}\ (\%) = (\text{Abs}_{(\text{Cis-peak})} \,/\, \text{Abs}_{(\lambda\text{max})})\ \text{x}\ 100$$

$$Where:$$

$$\text{Intensity}_{(\text{Cis})} = \text{Cis-peak intensity}$$

$$\text{Abs}_{(\text{Cis-peak})} = \text{Absorbance intensity of the highest-absorbance cis-peak}$$

$$\text{Abs}_{(\lambda\text{max})} = \text{Absorbance intensity of peak II}$$

2.2.4 High-Performance Liquid-Chromatography/Mass-Spectrometry Analyses

To provide a separate method of chromatographic separation and a higher-resolution identification of individual compounds comprising the pigment complement of *Arthrobacter* sp. NamB2, a coupled HPLC/MS analysis was performed. The HPLC analysis was used to separate the carotenoids of *Arthrobacter* sp. NamB2 into purified eluents on the basis of their polarity. Mass spectrometry of each purified HPLC-eluent was used to identify the individual pigments comprising the complement.

2.2.4.1 High-Performance Liquid-Chromatography Separation of Pigment Complement

The dried pigment extract of *Arthrobacter* sp. NamB2 (prepared as per **Section 2.2.1)** was redissolved in 2.0 mL of > 99.9 % HPLC-grade methanol, and transferred through a 0.2 μm filter (removing cellular impurities) to a foil-wrapped glass vial for HPLC analysis.

The HPLC analysis was carried out using an Agilent 1260 Infinity Quaternary HPLC System (Agilent, Santa Clara, USA) containing a 1260 quaternary pump, 1260 Infinity autosampler, and 1260 Infinity thermostatted column compartment. Detection of individual components as they eluted from the HPLC-column relied on their UV-visible absorption at specified wavelengths as measured via a 1260 Infinity diode array detector (DAD) (Agilent, Santa Clara, USA). Wavelengths of DAD detection were chosen based on prior UV-visible spectral responses from

purified TLC fractions, for the detection of compounds demonstrably relevant to the pigment complement. The UV-visible carotenoid spectra produced by individual TLC pigment fractions showed consistent peaks at approximately 460 (I), 494 (II), and 530 nm (III) (**Section 2.3.2.2)**. The DAD was thus first configured to detect eluents at a wavelength of 494 nm as they exited the HPLC column. The DAD detection was also calibrated for absorbance at 460 and 530 nm to demonstrate if eluents from the HPLC-column provided comparable absorption maxima to those characterised by TLC analyses.

High-performance liquid-chromatography used an XSelect charged surface hybrid C18 (2.1 x 100mm, 3µm) reverse-phase column (Waters™, Milford, USA). The flow rate of the mobile phase was calibrated to 0.4 mL/min, with a sample injection volume of 5 µL. Mobile phase A was composed of water containing 0.1% (v/v) formic acid, while mobile phase B was comprised of > 99.9 % HPLC-grade methanol. The initial gradient employed was a 20:80 mixture of mobile phase A:B, respectively. The proportion of mobile phase B was increased to 90 % from 2-6 minutes and held for 2 minutes, then increased to 100 % from 8-10 minutes and held for 3 minutes. From 13 – 14 minutes mobile phase B was decreased to 80 %, with the HPLC run concluding at 20 minutes.

2.2.4.2 Mass Spectrometry of the Separated Pigment Complement

Mass spectrometry of the purified HPLC eluents allowed the identification of individual compounds comprising the pigment complement. The HPLC system was connected to a 6420 triple quadrupole mass spectrometer (Agilent, Santa Clara, USA) containing a multimode ionisation source. Purified eluents from the HPLC analysis were thus directly injected into the mass spectrometer for production of mass fragmentation spectra corresponding to each. Positive mode APCI was used for molecular ionisation, with ionisation conditions employing a capillary voltage of 2 kV, drying gas temperature of 300 °C, drying gas flow of 5 L/min, vaporiser temperature of 250 °C, nebuliser pressure of 50 psi and a corona current of 4 µA. The positive ion scan for detection of fragment ions was performed with a scan range of m/z 100 – 1,000.

Contextual evidence and findings from analyses performed prior to this MS suggested that the pigment extract contained bacterioruberin. To unambiguously demonstrate the presence of bacterioruberin within the pigment complement, a product ion scan was performed on the most abundant HPLC-eluent (eluent IV **-** see **Section 2.3.3.1**) via tandem MS, selecting for a parent ion of m/z 741.5; the reported molecular ion mass of bacterioruberin (Fong et al. 2001). The

positive ion scan for detection of its fragmentation pattern was performed with a scan range of m/z 100 – 1,000.

2.3 Results

2.3.1 Carotenoid Screening via UV-Visible Spectroscopy

The pigment extract of *Arthrobacter* sp. NamB2 was screened for the presence of carotenoids via scanning UV-visible spectroscopy. Three independent analyses demonstrated that the pigment extract generated a characteristic three-peaked absorbance response consistent with carotenoids, with peaks of maximal absorbance at 466 (I), 493 (II, λ_{max}) and 526 nm (III) (**Figure 2.3**). Two additional peaks were observed at approximately 369 and 386 nm, likely corresponding to carotenoid cis peaks. No additional peaks of significant magnitude were observed on scanning spectra outside of these carotenoid-associated responses. These findings indicated that the pink pigment complement of *Arthrobacter* sp. NamB2 was carotenogenic. Consequently, the analysis of the pigment complement as a carotenoid was pursued.

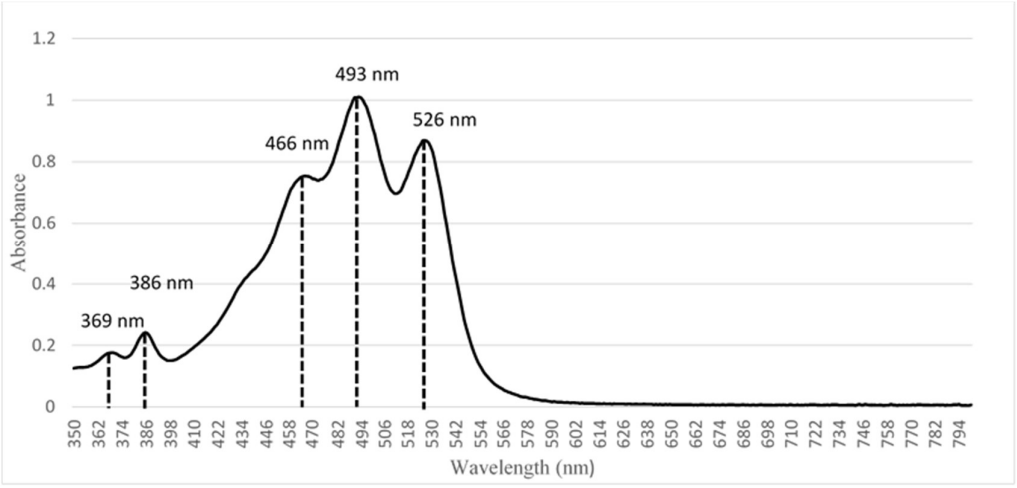

Figure 2.3: Example UV-Visible scanning spectrum of crude pigment extracts from *Arthrobacter* sp. NamB2 prepared in methanol. Wavelengths corresponding to peaks of the three peaked carotenoid spectrum are labelled, as are wavelengths corresponding to cis peaks.

2.3.2 Thin-Layer Chromatography of Crude Pigment Extracts

Thin-layer chromatography of the crude pigment extract from *Arthrobacter* sp. NamB2 was used to separate the individual carotenoids comprising the pigment complement. This allowed enumeration of the number of individual carotenoids comprising the complement, and purified each for subsequent structural characterisation via UV-visible spectroscopy. Structural information on TLC-separated carotenoids was further inferred by comparing their migrations (thus polarities) to those of the control spinach carotenoids.

2.3.2.1 Chromatographic Separation via TLC

Across duplicate successful TLC experiments, the crude pigment extract of *Arthrobacter* sp. NamB2 separated into six (TLC-2) or seven (TLC-1) pink-coloured fractions (**Figure 2.4**). Some fractions that were less abundant were observed immediately at the end of the experiment but degraded prior to photography. Spinach carotenoids were used as a control to verify TLC-separation, and confirmed the successful TLC-separation through the formation of four distinct bands (as expected) identified on the figure. Additional bands observed in the spinach control represented chlorophylls.

Similar Rf values denote comparable polarities between carotenoids, thus similar numbers of polar groups (Sherma and Fried 2003). Therefore, the TLC separation of spinach carotenoids of known structures alongside the unknown carotenoids of *Arthrobacter* sp. NamB2 was used to draw structural inferences regarding the number of polar groups within the individual carotenoids of the complement **(Figure 2.4**). The Rf values determined for each pigment fraction and spinach control carotenoid are presented in **Table 2.1**.

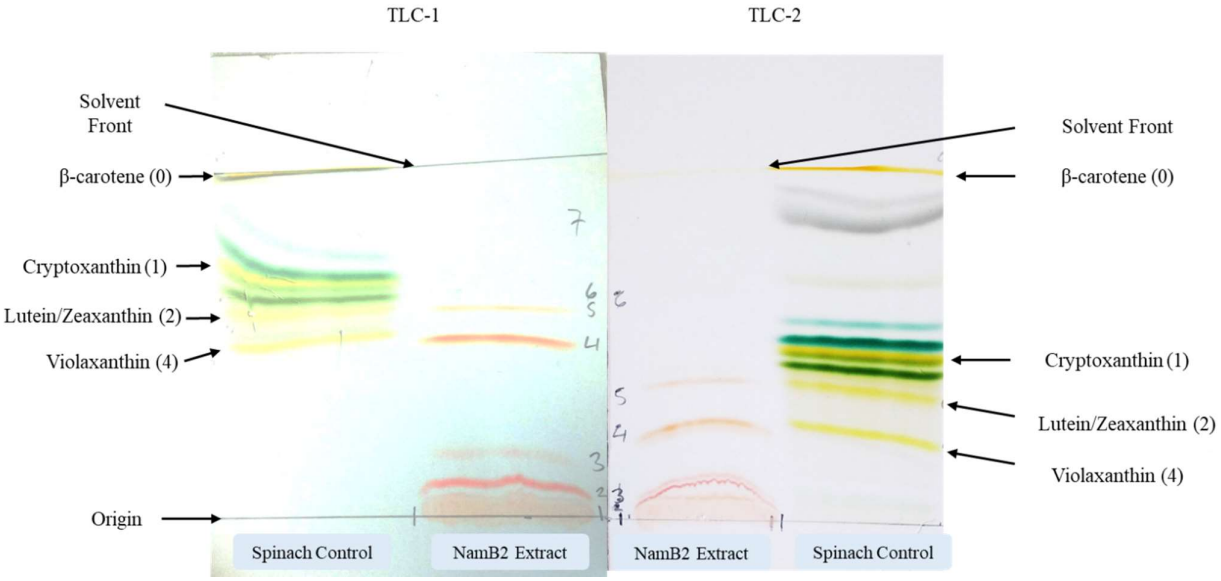

Figure 2.4: Overhead photographs of silica TLC plates following development with a mobile phase of 7:3 hexane:acetone. Development of plates occurred in a direction corresponding to an ascent of the page. Fractions labelled that are not visible within the photograph(s) were observed visually but degraded prior to photography. Identities of the spinach control carotenoids are denoted on the figure, with the number of polar groups within each control carotenoid reported in brackets.

Higher Rf values on silica-gel TLC plates denote decreasing polarities of the given carotenoid. Across both TLC analyses, fractions one, two and three of the *Arthrobacter* sp. NamB2 pigment complement had lower Rf values than any spinach carotenoid, implying they had higher polarities, and thus more than four polar groups (**Figure 2.4, Table 2.1**). Fractions four and five consistently co-migrated with spinach violaxanthin and lutein/zeaxanthin, suggesting that these have four and two polar functional groups, respectively (Sjursnes et al. 2015). Pigment fraction six was short-lived and unique to TLC-1, appearing as a faint band directly ahead of fraction five. Fraction seven of TLC-1 (corresponding to fraction six of TLC-2) demonstrated a migration and Rf higher than that of spinach's cryptoxanthin, but lower than β-carotene. This suggested that fraction seven possessed a higher number of polar groups than β-carotene (zero polar groups), but had a lower polarity than cryptoxanthin (one polar group), thus may be influenced by more subtle modifications in polarity. This fraction was also short-lived upon removal of the TLC plate from the developing chamber, and rapidly became colourless.

These analyses demonstrated *Arthrobacter* sp. NamB2's pigment complement possessed six – seven polarity-distinct pigment fractions. To determine whether each of these fractions was carotenogenic, and provide structural information on each from their spectral fine structures and chromophore lengths, each TLC-purified pigment fraction was recovered, and scanning UV-visible spectra prepared.

Table 2.1: Retardation factors, spectral fine structures, and cis-peak intensities determined for each TLC-separated pigment fraction. Retardation factors of spinach control carotenoids are listed below those of the *Arthrobacter* sp. NamB2 pigment fractions. N/A values denote those samples which failed in recovery/spectral response following TLC development. The value shown in red was considered an outlier.

TLC Pigment Fraction	Retardation Factor (Rf)		Spectral Fine Structure (%)		Cis-Peak Intensity (%)	
	TLC-1	TLC-2	TLC-1	TLC-2	TLC-1	TLC-2
One	0	0	52.9	55	131	35.71
Two	0.08	0.11	47	53	23.86	27.36
Three	0.18	0.13	50	53	52.94	27.36
Four	0.51	0.28	47.5	53.6	27.91	28.35
Five	0.59	0.39	48.46	N/A	43.9	N/A
Six	0.65	0.61	N/A	N/A	N/A	N/A
Seven	0.86	-	N/A	-	N/A	-
Violaxanthin	0.53	0.28				
Lutein/Zeaxanthin	0.61	0.37				
Cryptoxanthin	0.67	0.50				
β-carotene	1.00	1.00				

2.3.2.2 Spectral Characterisation of TLC-Separated Pigments

Several pigment fractions were not recovered from the TLC plates and therefore could receive spectral characterisation under UV-visible scanning spectrophotometry. Pigment fractions six and seven of TLC-1, and fraction six of TLC-2 degraded rapidly upon removal of TLC plates from the developing chamber, resulting in a loss of these fractions. Pigment fraction five of TLC-2 did not produce a UV-visible spectrum of sufficient absorbance or peak resolution for confident analysis.

All remaining fractions were recovered and produced three-peaked UV-visible scanning spectra consistent with the carotenoid class, with matching absorbance maxima at approximately 466 (I), 498 (II, λ_{max}), and 530 (III) nm. These spectra were consistent with findings from **Section 2.3.1**, and suggested that all recovered pigment fractions were carotenoids of uniform chromophore lengths. Examples of these spectra are shown in **Figure 2.5**. Wavelengths of absorption maxima were consistent between corresponding pigment fractions across the TLC replicates. The absorption intensities produced by pigment fraction two (TLC-1) and four (TLC-2) were the highest of the recovered fractions, followed by fraction four (TLC-1) and two (TLC-2), then fractions one, three and five (both TLC analyses). As the absorption intensities of carotenoids are directly proportional to their concentrations (**Section 1.3.10.1**), these intensities reflected the relative abundance of each of these carotenoid fractions within the pigment complement of *Arthrobacter* sp. NamB2. This suggested that fraction four and fraction two were the most abundant carotenoids within the pigment complement.

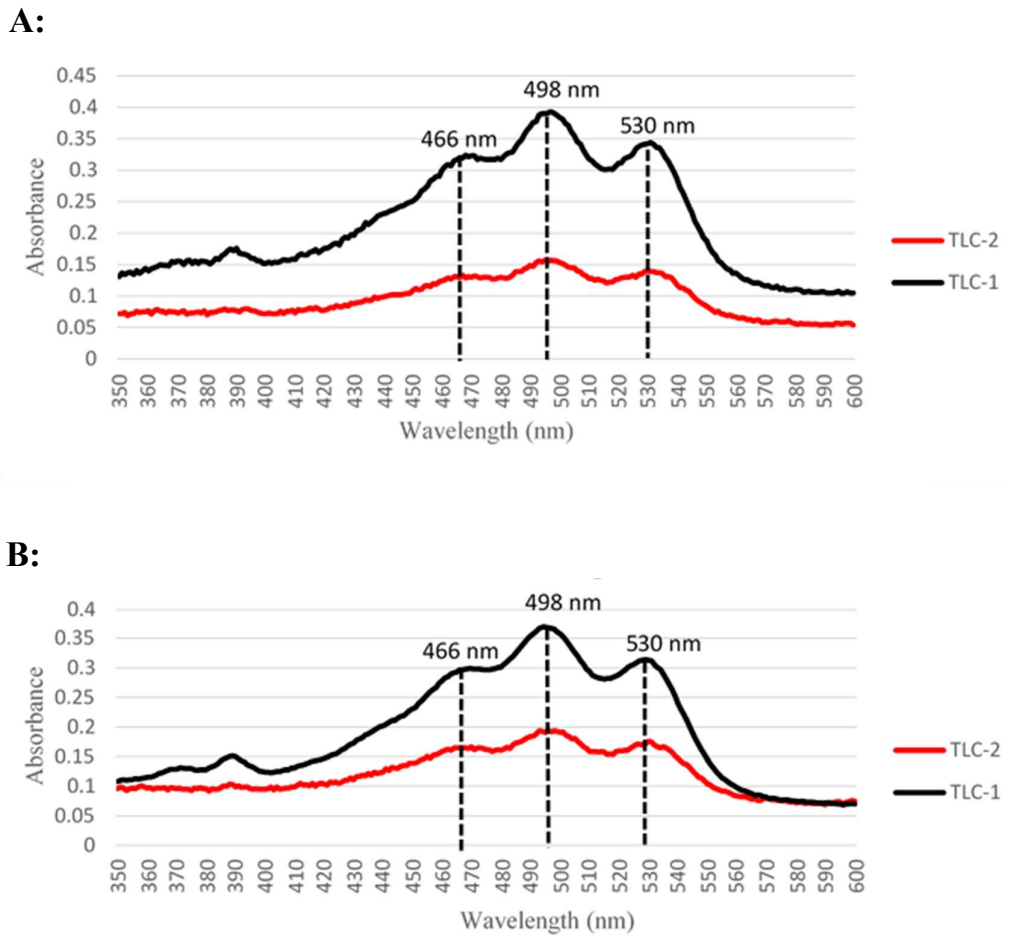

Figure 2.5: Scanning UV-visible absorbance spectra of TLC fraction two (**A**) and four (**B**) from the pigment complement of *Arthrobacter* sp. NamB2 in acetone. Wavelengths corresponding to the three-peaked carotenoid absorbance spectrum are indicated on each figure. The specific TLC experiment each spectrum is derived from is shown in black (TLC-1) or red (TLC-2).

Spectral fine structures of recovered pigment fractions are presented alongside their cis-peak intensities within **Table 2.1**. Fine structures of pigment fractions ranged between approximately 47 – 55 %, but were largely consistent between matching pigment fractions across TLC-replicates. A mixture of carotenoid cis-isomers was present within each TLC-fraction. This was concluded from the presence of cis-peaks occurring at 369 and 386 nm in the UV-visible spectrum of each recovered TLC-fraction (Tan and Soderstrom 1989; Britton et al. 1995a). The cis-peak intensities of individual carotenoids varied from 23 – 53 %, with some variability observed between matching pigment fractions of TLC replicates (i.e. TLC fraction three showing between 27 – 52 % cis-peak intensity). The extreme outlier of a cis-peak of intensity 131 % as reported by fraction one of TLC-1 was disregarded, as it was likely due to the high intensity background produced in the UV-visible spectrum of this pigment, as opposed to any

extreme isomerisation. The presence of cis-peaks indicated that a mixture of cis-isomers was present within each recovered TLC-fraction, which rendered their spectral fine structures unreliable for carotenoid identification. The spectral-fine structures of these carotenoids were thus not considered of sufficient resolution for identification here.

Chromatographic separation via TLC indicated that the pigment complement of *Arthrobacter* sp. NamB2 comprised six – seven polarity-discrete pigment fractions. Some fractions, for example fractions four and five, demonstrated polarities matching those of spinach carotenoids. Scanning UV-visible spectra of the recovered pigment fractions indicated they were carotenoids of uniform chromophore lengths. For separate validation of these structural and chromatographic features, HPLC/MS analysis of *Arthrobacter* sp. NamB2's pigment complement was applied.

2.3.3 Analysis of Crude Pigment Extract via HPLC/MS

An HPLC/MS analysis was used to separate the individual constituents of the pigment complement based on polarity (HPLC), and subsequently identify each HPLC-separated pigment fraction on the basis of their mass-fragmentation patterns (MS).

2.3.3.1 High-Performance Liquid-Chromatography Separation of Pigment Complement

The DAD responses for the HPLC analysis are presented in **Figure 2.6**, and demonstrate absorbance peaks corresponding to the retention times of each compound of the pigment complement within the HPLC-column. Higher retention times under reverse-phase HPLC analysis reflect a decreasing polarity of the analytes. The 494 nm response of the DAD indicated that HPLC-separation resolved eight distinct eluent peaks from the pigment complement (henceforth eluent peaks I – VIII) eluting at 9.41, 10.48, 11.76, 12.11, 12.56, 12.93 and 13.33 minutes respectively (**Figure 2.6-A**). These same elution times and number of peaks were obtained from the DAD operating at 460 and 530 nm (**Figure 2.6-B** and -**C** respectively), suggesting that each of these eight eluents absorbs strongly at 460, 494 and 530 nm. This absorbance pattern for each eluent was consistent with earlier-characterised carotenoid spectra from this pigment complement (**Figures 2.3, 2.5**). The number and spectral responses of the HPLC-eluent peaks thus implied the presence of at least eight compounds of distinct polarity

within the pigment complement, each absorbing strongly at 460, 494 and 530 nm, with absorbance at 494 nm consistently the highest.

The HPLC column retention times and DAD absorbance intensities revealed consistency in the chromatographic separation achieved from the HPLC and TLC. Similarly to the TLC analysis, three highly polar fractions (eluents I – III) of high absorbance, thus abundance, directly preceded the most abundant fraction of the pigment complement (eluent IV), which itself preceded four fractions of lower polarity and comparatively low abundance (eluents V – VIII). This consistency between the HPLC and TLC-mediated separation supported that the pigment complement of *Arthrobacter* sp. NamB2 contained between six – eight individual pigment fractions. There was notable peak overlap between eluent peaks IV, V and VI, indicating low-resolution separation of these compounds. Eluent IV consistently demonstrated the highest absorbance of the complement, followed by eluents II, VI, I, V, VII, VIII and III (**Figure 2.6-A**).

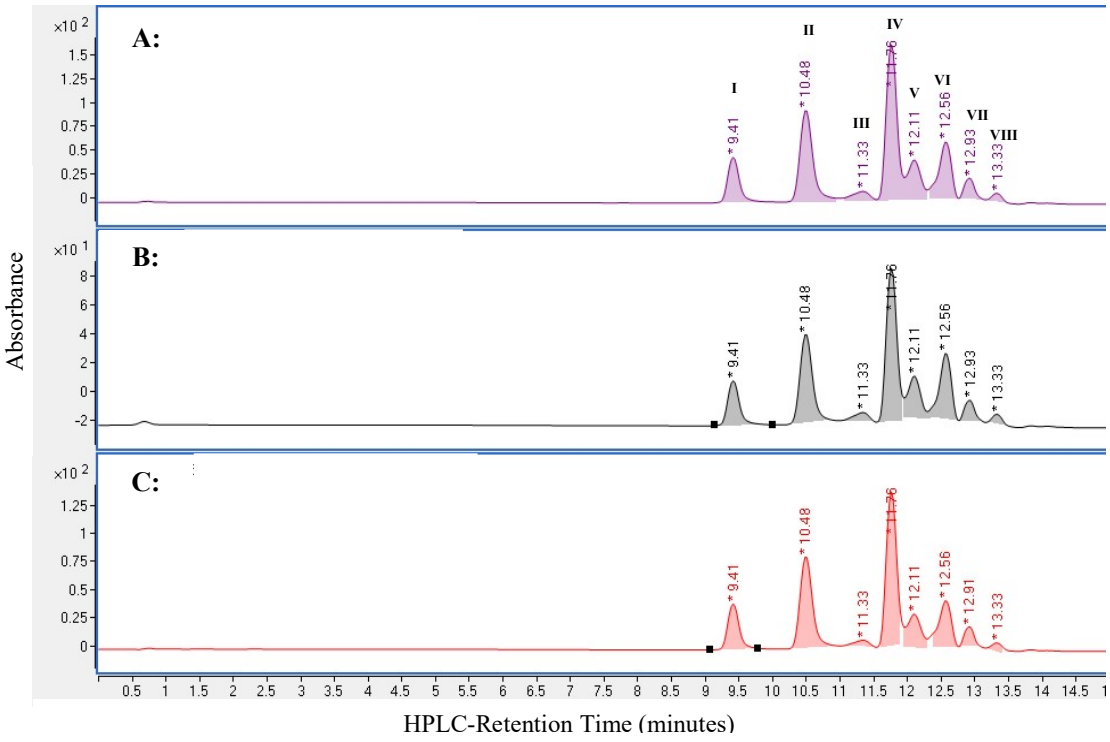

Figure 2.6: HPLC-DAD responses produced from carotenoid extracts of *Arthrobacter* sp. NamB2. Each figure denotes the intensity of the DAD-absorption response (y-axis) of each eluent compound as it eluted from the HPLC-column at each time-point (x-axis) given respective wavelengths of DAD acquisition. DAD-response of carotenoid eluents was calibrated at **A:** 494 nm. **B**: 460 nm. **C**: 530 nm.

2.3.3.2 Mass-Spectrometry Analysis of Pigment Complement

To identify the individual compounds comprising the pigment complement of *Arthrobacter* sp. NamB2, each HPLC-separated eluent was subject to positive-mode APCI-MS as they exited the HPLC column. This generated eight discrete mass-spectra, each corresponding to an individual HPLC-eluent. An example mass spectrum, corresponding to HPLC eluent IV, is provided in **Figure 2.7,** and all other MS scanning spectra produced are available in **Appendix 1; Supplementary Figures 1A – 1G**. Speculative molecular ion peaks and prominent peaks of the mass spectrum produced for each HPLC-eluent are presented in **Table 2.2**. Prominent ion peaks were identified as those demonstrating both notable abundance within the mass-spectrum, and possessing an m/z > 550, thus being potentially significant as carotenoid molecular ions or major fragmentation products (Rivera et al. 2014).

Common xanthophyll-fragmentation patterns (sequential m/z decreases of m/z 18 from the molecular ion (**Section 1.3.10.3**)) were observed in the mass-spectra of several eluents, suggesting fragmentations from molecular ions of m/z 741.5, 723.5 or 687.4 (i.e. HPLC-Eluents I-II, IV-VI). Several of these molecular ion masses and fragmentation patterns aligned with those known for bacterioruberin and its commonly co-isolated variants, including bacterioruberin monoglycoside (m/z 903.4 – Eluent III), MABR (m/z 723.5 – Eluent II)) and BABR (m/z 705.5) (Flores et al. 2020). Ion peaks corresponding to the molecular ion of bacterioruberin (m/z 741.5) and common fragment ions of its xanthophyll fragmentation pattern (i.e. m/z 723.5, 705.5, 687.5) were observed in the mass-spectra produced for HPLC-eluents IV, V and VI, strongly suggesting the presence of bacterioruberin within each of these eluents (van Breemen et al. 2012; Rivera et al. 2014; Silva et al. 2019).

Eluent III, consistent with its low DAD response, produced a mass-spectrum predominating in low-abundance ion peaks with poor peak resolution, and was likely not a major constituent of the pigment complement. Issues in peak resolution were observed for Eluents VII and VIII, with peaks such as m/z 685.4 (eluent VII) poorly separated from neighbouring peaks at 686.4 and 687.5. This poor peak resolution made the identification of molecular ion peaks within each of these spectra difficult.

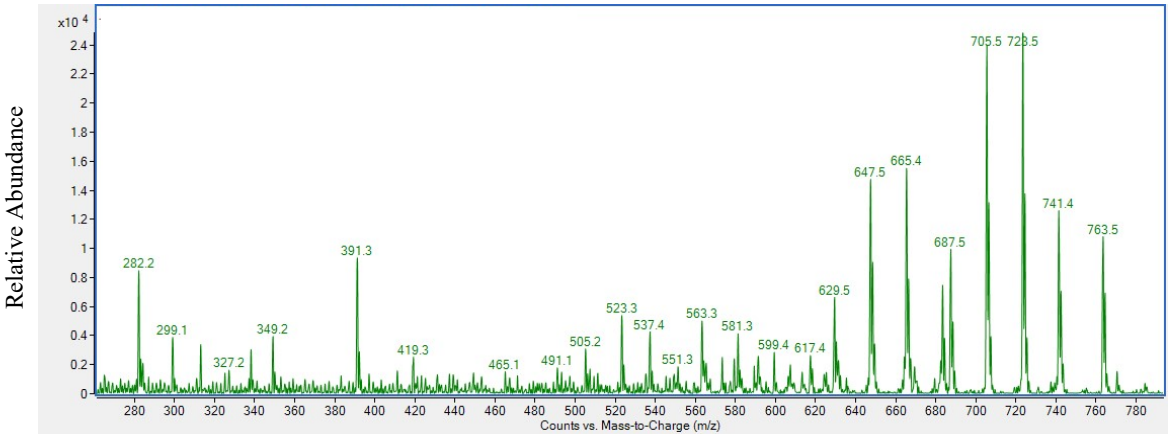

Figure 2.7: Positive mode APCI-MS scan of HPLC-eluent IV. The y-axis denotes ion abundance, and the x-axis the mass/charge ratio of each of the fragment ions. Truncation of the mass spectrum at m/z 780 is used to provide clarity of peaks, as additional fragment peaks were not evident above this m/z.

Table 2.2: Retention times of individual HPLC-eluents, and prominent fragment ions identified from mass-spectra of these HPLC-eluents. Putative molecular ions were identified from mass-peaks demonstrating maximal m/z values and high abundance on each mass-spectrum. Ion peaks corresponding to xanthophyll-related fragmentation ions are underlined.

HPLC-Eluent Peak	HPLC-Retention Time (minutes)	Putative Molecular Ion (m/z)	Prominent Ions (m/z)
Eluent I	9.41	809.2	687.4, 669.3, 629.4, 537.4
Eluent II	10.48	925.5	885.5, 867.4, 827.4, 723.4, 705.6, 687.5, 665.5, 647.5, 629.4
Eluent III	11.33	579.3	551.3, 537.4, 523.3
Eluent IV	11.76	763.5	741.4, 723.5, 705.5, 687.5, 665.4, 647.5
Eluent V	12.11	925.6	885.5, 827.4, 763.5, 741.5, 723.3, 705.4, 687.4, 647.4, 629.4
Eluent VI	12.56	885.4	763.4, 741.5, 723.5, 705.5, 683.4, 665.5, 647.4, 629.3
Eluent VII	12.93	887.5	847.4, 685.4, 649.4, 611.4
Eluent VIII	13.33	927.5	745.4, 725.5, 705.5, 687.4, 647.4, 629.5, 603.4, 563.4, 551.4

2.3.4 Tandem MS Analysis for Bacterioruberin

Previous evidence from pink-pigmented *Arthrobacter* suggested that the pigment complement responsible for the pink-pigmentation of *Arthrobacter* sp. NamB2 would be based around the carotenoid bacterioruberin. This hypothesis was supported by the presence of several mass-fragmentation patterns consistent with bacterioruberin as described under the previous section. To determine unambiguously whether the pigment complement of *Arthrobacter* sp. NamB2 contained bacterioruberin, a product ion scan was specifically performed examining the most abundant HPLC-eluent (eluent IV) via tandem MS, with transmission set to an m/z of 741.5; the reported molecular ion mass of bacterioruberin (Fong et al. 2001). The mass spectrum resulting from this scan is presented in **Figure 2.8.** This scan reported a mass spectrum in which a fragment of m/z 741.5 represented the molecular ion peak, with a smaller fragment observed most relevantly at m/z 723.2, representing the $[M+H - 18]^+$ ion. The occurrence of these peaks together is distinctive for bacterioruberin, unambiguously indicating its presence within eluent IV (Silva et al. 2019).

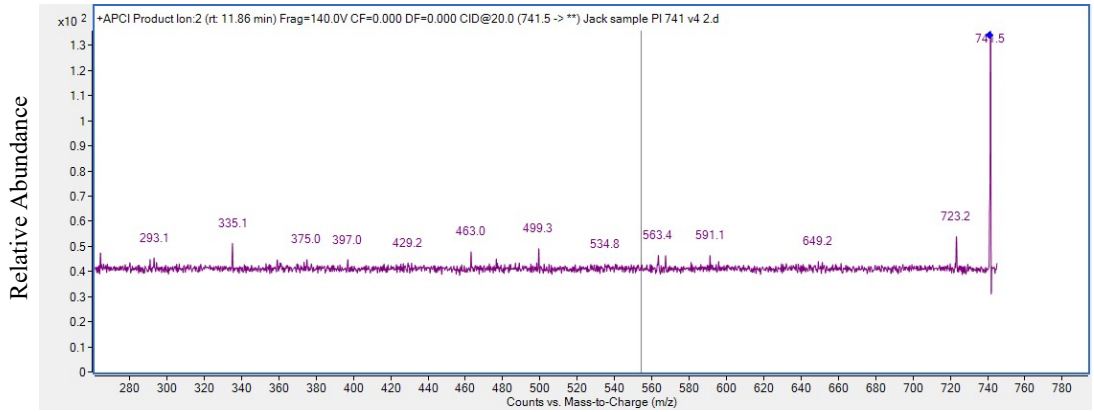

Figure 2.8: Tandem MS scan of HPLC-eluent IV, eluting at 11.76 minutes. The target molecular ion mass was 741.5 m/z, corresponding to the mass of bacterioruberin. The y-axis denotes the relative abundance of fragment ions, while the x-axis corresponds to the mass/charge ratio of these fragment ions.

2.4 Discussion

Carotenoid pigmentation of edaphic desert bacteria contributes to their irradiation resistomes, and has been characterised in this role in organisms from a variety of desert systems (Silva et al. 2019; Flores et al. 2020). The pigmentation of *Arthrobacter* sp. NamB2 was suspected to serve a similar function in irradiation-tolerance based on the isolation of this bacterium from Namib Desert soil, and prior conclusions on the utility of carotenoids within this genus (Ii et al. 2019; Silva et al. 2019). As the pigmentation of this organism is currently unexplored, its identification was thus the first step in speculating this physiological role. As such, this chapter sought to identify the pink pigmentation of *Arthrobacter* sp. NamB2, both in terms of its broad pigment class, as well as the specific characterisation of individual compounds comprising the pigment complement. It was hypothesised that this pigmentation was based around the production of the carotenoid bacterioruberin and its dehydrated/glycosylated variants, as is common within pink-pigmented *Arthrobacter*.

2.4.1 The Pigmentation of *Arthrobacter* sp. NamB2 is Carotenogenic

The pink-pigmentation of *Arthrobacter* sp. NamB2 is carotenogenic, as shown through its production of distinctive carotenoid spectra under UV-visible spectroscopy. Scanning UV-visible spectroscopy of crude pigment extracts from this organism consistently generated three-peaked absorbance responses with maxima at 466 (I), 493 (II, λ_{max}), and 526 (III) nm (+/-2 nm) (**Figure 2.3**). Production of three-peaked absorbance spectra between 400 – 600 nm is unique to the carotenoid pigment class, and thereby demonstrated that the pigment complement of *Arthrobacter* sp. NamB2 was carotenogenic (Britton et al. 2004; Kopec et al. 2012; Sutthiwong, Fouillaud, et al. 2014; Rodriguez-Amaya 2016). This spectral response further eliminated alternative photoprotective pigment classes commonly found in desert organisms such as scytonemins and mycosporine-like amino acids, as these would produce peaks at wavelengths within the 350 – 400 nm region (Garcia-Pichel et al. 1992; Abed et al. 2010; Pathak et al. 2015). These alternative pigments would have been extracted by the high-purity methanol treatment applied here, thus would have produced their spectral responses if present (Pathak et al. 2015). Therefore, it was concluded that the pink pigmentation of *Arthrobacter* sp. NamB2 belonged to the carotenoid class.

Pink/red pigmentation in the genus *Arthrobacter* is almost exclusively attributed to carotenoids, with no known exceptions under standard growth conditions (Reddy et al. 2002; Imperi et al.

2007; Dieser et al. 2010; Sutthiwong, Fouillaud, et al. 2014; Tescari et al. 2018; Flegler et al. 2020). Indeed, the pigment complements of pink-pigmented *A. agilis*, *A. bussei*, *A. roseus*, *Arthrobacter* sp. G20 and *Arthrobacter* MN05-02 have all been identified as carotenogenic (Fong et al. 2001; Reddy et al. 2002; Afra et al. 2017; Flegler et al. 2020). Consequently, the demonstration that the pink-pigmentation of *Arthrobacter* sp. NamB2 was a carotenoid was unsurprising, and consistent with other members of this genus.

2.4.2 The Pigment Complement of *Arthrobacter* sp. NamB2 Comprises Multiple Carotenoids

Through chromatographic separation, the pigment complement of *Arthrobacter* was found to comprise between six – eight polarity-distinct carotenoids. Both TLC and HPLC demonstrated a separation of the pigment complement wherein three highly polar fractions preceded the fraction of highest abundance (TLC-fraction four, HPLC eluent IV), which itself preceded between two – four compounds of lower polarity. These results indicated a consistency between the two chromatography systems, and a tacit reliability that the pigment complement of *Arthrobacter* sp. NamB2 comprises six – eight polarity-distinct compounds. The separation of pigment complements into multiple polarity-distinct fractions is typical of carotenogenic bacteria (Hodisan et al. 1997; Lysenko et al. 2011; Rezaeeyan et al. 2017). Indeed, other carotenogenic *Arthrobacter*, including *Arthrobacter psychrochitiniphilus, Arthrobacter* sp. M3 and *Glutamicibacter arilaitensis* (previously *Arthrobacter arilaitensis*) each contain five – six polarity-distinct carotenoids within their pigment complements (Arpin, Liaaen-Jensen, et al. 1972; Giuffrida et al. 2016; Silva et al. 2019). Bacterioruberin-based pigment complements from *Arthrobacter* and *Haloarchaea* have demonstrated similar chromatographic separations into six – twenty three polarity-distinct carotenoids (Arpin, Liaaen-Jensen, et al. 1972; Mandelli et al. 2012; Giuffrida et al. 2016; Squillaci et al. 2017; Silva et al. 2019). The separation of the pigment complement of *Arthrobacter* sp. NamB2 into six – eight constituents here was thus expected, and demonstrated the complement as comprised of a number of polarity-distinct compounds as opposed to a single carotenoid.

The compounds comprising the pigment complement of *Arthrobacter* sp. NamB2 were carotenoids of distinct polarity, but uniform chromophore lengths. Spectroscopic data from both the separated pigment spots of the TLC (UV-visible spectroscopy) and the HPLC eluents (DAD-detection maxima) confirmed that each constituent of the pigment complement produced a three-peaked UV-visible spectrum with absorption maxima at approximately 465 (I), 494 (II, λ_{max}), and 530 nm (III). The production of distinctive three-peaked UV-visible spectra

confirmed each of these constituents as carotenoids, while the consistent wavelength position of these absorption maxima indicated their uniform chromophore lengths (Britton et al. 1995a). Production of three-peaked spectra with absorbance maxima at approximately 460 (I), 492 (II) and 525 (III) nm corresponds to carotenoids containing chromophores of 13 conjugated double bonds (Takaichi and Shimada 1992; Britton et al. 1995a; Rodriguez-Amaya and Kimura 2004). The consistent spectral responses of the pigment fractions separated by TLC and HPLC, and the positions of absorption maxima within these spectral responses, demonstrated under two separate analyses that the pink-pigmentation of *Arthrobacter* sp. NamB2 was comprised exclusively of carotenoids containing a 13 c.d.b. chromophore, though each distinct in polarity.

Pigment complements comprised exclusively of polarity-distinct 13 c.d.b. carotenoids are consistent with prior studies of *Arthrobacter*, specifically those producing bacterioruberin. Pigment complements of pink-pigmented *A. agilis* and *A. bussei* consistently comprise five – seven polarity-distinct carotenoids, each being bacterioruberin or one of its dehydrated/glycosylated variants (Fong et al. 2001; Silva et al. 2019; Flegler et al. 2020). While each of these variants are polarity-distinct, thus separable via chromatography, their chromophores are of equal conjugation lengths, thus all produce UV-visible spectral responses consistent with 13 c.d.b. carotenoids, and identical to those observed in *Arthrobacter* sp. NamB2 (Fong et al. 2001; Silva et al. 2019; Flegler et al. 2020). Separation of the pigment complement of *Arthrobacter* sp. NamB2 into six – eight fractions all presenting as 13 c.d.b. carotenoids was thus consistent with other pink *Arthrobacter*, and reinforced that the pigment complement was comprised of carotenoids associated with bacterioruberin. This finding was thus consistent with the hypothesis set out by this chapter.

The diagnostic potential of UV-visible spectroscopy in carotenoid identification is limited, and it cannot be used in unambiguous identification as these spectra only reflect chromophore lengths. Other 13 c.d.b. carotenoids including spirilloxanthin, oscillaxanthin and rhodoxanthin are also pink in colouration, and produce UV-visible spectral responses identical to bacterioruberin, as their chromophores are of the same length (Lutnaes et al. 2002; Tao et al. 2005; Takaichi et al. 2009; Zhang et al. 2012; Tani et al. 2014; Niedzwiedzki et al. 2015). While these pigments have not been isolated from *Arthrobacter* or closely related genera, it is not possible to distinguish the carotenoids of *Arthrobacter* sp. NamB2 from these alternative carotenoids on spectral responses alone, necessitating the unambiguous identification provided by MS.

2.4.3 The Pigment Complement of *Arthrobacter* sp. NamB2 Contains Bacterioruberin

The pigment complement of *Arthrobacter* sp. NamB2 was unambiguously identified as containing bacterioruberin via product ion scan under tandem MS, supporting the hypothesis of this chapter. Tandem MS is highly specific and produces a mass spectrum only if the selected molecule of interest is present (Hoffman and Stroobant 2007; Gross 2017b). A product ion scan selecting for bacterioruberin within HPLC eluent IV produced a mass spectrum with a molecular ion peak at an m/z of 741.5, and a pronounced $[M+H - 18]^+$ fragment ion peak at m/z 723.2, both typical and distinctive of bacterioruberin (Squillaci et al. 2017; Silva et al. 2019; Flores et al. 2020). This unambiguously confirmed the production of bacterioruberin by *Arthrobacter* sp. NamB2, and its presence within eluent IV (Squillaci et al. 2017; Silva et al. 2019; Flores et al. 2020).

The identity of HPLC eluent IV as bacterioruberin was supported by the high abundance of this eluent, as it was the most abundant component of the pigment complement under the HPLC analysis (Casasanta and Garra 2018). This is a common observation, as bacterioruberin similarly represents the most abundant constituent in the bacterioruberin-based pigment complements of *K. rosea* (72 % of the pigment complement) *H. japonica* (68.1 %) and *H. volcanii* (81 %) (Jagannadham et al. 1991; Rønnekleiv and Liaaen-Jensen 1992; Ronnekleiv 1995; Chattopadhyay et al. 1997). While no such quantitative analysis has yet been performed in *Arthrobacter*, its predominance in the pigment complements of other bacterioruberin-producing organisms further supports the identification as eluent IV here.

As the separation of the pigment complement by HPLC and TLC appeared consistent (prior discussed), it was similarly supposed that TLC-fraction four also represented unmodified bacterioruberin. This was supported by the matching migration observed between TLC fraction four and violaxanthin, implying a matching polarity, and equal number of polar groups. Violaxanthin has four polar groups, as does unmodified bacterioruberin, the only carotenoid of common bacterioruberin-based pigment complements to have such (Britton et al. 2004; Yang et al. 2015). Furthermore, TLC-fraction four was consistently the highest or second highest abundance component of the complement, matching the aforementioned expectations of bacterioruberin (Casasanta and Garra 2018). The presence of bacterioruberin within the pigment complement was thus supported by the TLC-analysis, and was the likely identity of TLC-fraction four.

The knowledge that *Arthrobacter* sp. NamB2 produces bacterioruberin indicated its pigmentation as consistent with other characterised pink-*Arthrobacter* such as *A. bussei* and *A. agilis* (Fong et al. 2001; Flegler et al. 2020). Based on this information, the identity of remaining pigments of the complement were speculated from MS data, supported by knowledge of the limited diversity of carotenoids known to be co-isolated from bacterioruberin-producing organisms.

2.4.4 Identification of other Carotenoids within the Pigment Complement

As aforementioned, carotenoids comprising the pigment complement of bacterioruberin-producing organisms are limited to bacterioruberin itself and a restricted number of its glycosylated/dehydrated variants. *Arthrobacter* producing bacterioruberin consistently demonstrates pigment complements comprising only this carotenoid alongside a series of bacterioruberin glycosides, and (in order of decreasing polarity) the dehydrated variants of mono-anhydrobacterioruberin (MABR), bis-anhydrobacterioruberin (BABR) tris-anhydrobacterioruberin (TRABR) and tetra-anhydrobacterioruberin (TABR) (Fong et al. 2001; Silva et al. 2019; Flegler et al. 2020). Carotenoids outside of these listed have not been co-isolated from bacterioruberin-containing pigment complements of *Arthrobacter*.

As discussed, TLC and HPLC demonstrated the pigment complement of *Arthrobacter* sp. NamB2 comprised six – eight carotenoid fractions of distinct polarity, but all with chromophore lengths of 13 c.d.b., suggesting that they may represent these different modified forms of bacterioruberin. An effort was made to identify the compounds comprising the remainder of the pigment complement of *Arthrobacter* sp. NamB2, using the knowledge that as the pigment complement is based around bacterioruberin, it was likely consistent in composition with other bacterioruberin-producing *Arthrobacter.*

2.4.4.1 Glycosidic Forms of Bacterioruberin

Bacterioruberin glycosides can possess up to four glucose molecule additions to the base bacterioruberin structure (yielding bacterioruberin tetraglycoside), with the large number of polar groups conferred by additional glucose molecules resulting in a substantially higher polarity than the base bacterioruberin (Arpin, Fiasson, et al. 1972; Ertl et al. 2000; Fong et al.

2001; Johnsson et al. 2002; Caron and Ermondi 2016; Louie et al. 2020). It has also been reported that bacterioruberin glycosides are present in high concentrations within bacterioruberin-based pigment complements, comprising as much as 30 and 35 %, respectively, of pigment complements in studied bacteria (Arpin, Liaaen-Jensen, et al. 1972).

These features reflected key observations of TLC fractions one to three, and HPLC eluents I and II. These fractions/eluents showed high polarities; with TLC fractions one to three demonstrating low Rf values, suggesting higher polarities than any spinach carotenoid, or of fraction four (bacterioruberin) (Sherma and Fried 2003). Indeed, Rf values of 0.00 and 0.03 have previously been observed for bacterioruberin diglycoside and monoglycoside respectively on silica TLC, comparable to those observed here (**Table 2.1)** (Arpin, Liaaen-Jensen, et al. 1972). Similar observations were true for HPLC eluents I and II, which presented substantially higher polarity than the bacterioruberin component (eluent IV). Furthermore, these fractions/eluents were relatively high in concentration, presenting as the most abundant or second-most abundant components of the pigment complement, consistent with expectations of glycosides from bacterioruberin-producing bacteria (Arpin, Liaaen-Jensen, et al. 1972).

While the identity of the glycosides could not be determined confidently by TLC, MS did confirm the presence of the bacterioruberin-monoglycoside molecular ion (m/z 903.4) (in low abundance) and its common fragment ions (i.e. m/z 885.5, 867.4) in HPLC eluent II, but not eluent I (Silva et al. 2019). The presence of the bacterioruberin-diglycoside (m/z 1,066) or tetra-glycoside (m/z 1,386) within the pigment complement could not be confirmed as their molecular ions were outside of the MS instrument's scanning limit (1,000 m/z) (Fong et al. 2001; Silva et al. 2019). Conclusions regarding the presence/identity of glycosides within these eluents (in particular HPLC eluent I) would be substantially strengthened by a wider detection range for mass scanning (up to m/z 1,500) or specific product ion scans via tandem MS. Nevertheless, TLC fractions one to three and HPLC eluents I and II likely represented bacterioruberin glycosides. No characterisation of bacterioruberin-producing *Arthrobacter* has yet reported an absence of bacterioruberin glycosides, thus their presence was expected here (Fong et al. 2001; Silva et al. 2019; Flegler et al. 2020).

2.4.4.2 Dehydrated Bacterioruberin Variants

Dehydrated forms of bacterioruberin were also identified by TLC and HPLC/MS. Bacterioruberin is commonly co-isolated from bacteria with a series of intermediate carotenoids

of lower polarity, including MABR, BABR, TRABR and TABR (Mandelli et al. 2012; Squillaci et al. 2017; Flores et al. 2020). Both HPLC and TLC-separation demonstrated the presence of a series of carotenoid eluents/fractions of progressively lower polarity than bacterioruberin (TLC-fractions five – seven, HPLC-eluents V – VIII), but which maintained spectral responses indicating that they possessed the thirteen c.d.b. chromophore of bacterioruberin-associated carotenoids, reflecting common observations of these dehydrated variants (Mandelli et al. 2012; Squillaci et al. 2017; Flores et al. 2020).

On TLC, a number of these fractions showed migrations which matched spinach carotenoids, providing some indication of their number of polar groups and identities. TLC-fraction five aligned with lutein, suggesting it possessed two polar groups, thus was likely BABR (Fong et al. 2001). Given the position of TLC-fraction six (TLC-1), it was likely a di/poly-cis isomer of BABR (Britton et al. 1995b). In TLC analyses, di/poly-cis isomers of carotenoids are appear as faint, transient bands directly ahead of the predominant compound, hence its position just ahead of fraction five, and its rapid loss following the TLC-analysis (Britton et al. 1995b). Further, as carotenoid cis-isomers are considered artefacts of the extraction process, variable light/heat-stimulated isomerisation occurring between the preparation of the pigment complement for each TLC-analysis may explain its absence from TLC-2 (Rønnekleiv and Liaaen-Jensen 1992; Britton et al. 1995b; Alcaíno et al. 2016). Identification of BABR but not MABR within the pigment complement by TLC was unexpected, as MABR consistently comprises the higher abundance component of bacterioruberin-based pigment complements in studies examining *H. salinarium*, *H. japonica* and *K. rosea* (Kelly et al. 1970; Chattopadhyay et al. 1997; Yatsunami et al. 2014). While no quantitative studies have yet been performed in *Arthrobacter*, this unexpected finding may reflect the limitations of concluding carotenoid identity from TLC-based polarity-comparisons between carotenoids of differing structural features (as between bacterioruberins and spinach carotenoids), as further discussed in **Section 2.4.5.2.**

The TLC-fraction six (TLC-2) or seven (TLC-1) migrated to a point between cryptoxanthin (one polar group) and β-carotene (zero polar groups). Based on the number of polar groups alone, TRABR would be expected to co-migrate with cryptoxanthin while TABR would be expected to co-migrate with β-carotene. The intermediate polarity of this fraction is poorly explained by considering only functional group polarity, but did more strongly indicate the pigment as TABR, with subtle structural features which modify carotenoid polarity likely having an influence on this separation (Sherma and Fried 2003; Abdullah et al. 2019). Carotenoids containing cyclic end-groups (as in β-carotene) are less tightly adhered to polar stationary phases than are acyclic carotenoids (as in dehydrated bacterioruberins), thus will

migrate further (Sherma and Fried 2003; Barba et al. 2006; Daood et al. 2014; Haroon 2014). Furthermore, chromophores provide carotenoids with slight polarity, with longer chromophores providing a higher polarity (Lowry 1923; Hannay and Smyth 1946; Krinsky 1963; Kelly et al. 1970). The higher polarity of TABR relative to β-carotene would thus be provided via its longer chromophore conjugation (13 against 11 c.d.b.) and lack of ring-structures, but would be insufficient to match the polarity of cryptoxanthin as provided via its hydroxyl group (Ertl et al. 2000; Clark 2011; Daood et al. 2014; Haroon 2014; Abdullah et al. 2019). This conclusion is supported by the study of Kelly et al. (1970), who found that TABR never produced a matching Rf value with β-carotene (1.0) on silica TLC, instead ranging between 0.7 – 0.94, as observed here (0.86). This suggests the minor structural contributions outlined may be valid in explaining the lack of co-elution of TABR with β-carotene.

The HPLC/MS analysis supported the presence of dehydrated bacterioruberin variants within the pigment complement, but its conclusions were limited by issues with the resolution of the systems applied. The HPLC peaks of eluents V and VI overlapped with one another, and with eluent IV, implying poor chromatographic separation of these compounds. The carotenoids of eluents V and VI were considered most likely to be MABR and/or BABR, due to their lower polarity than bacterioruberin (eluent IV) (Fong et al. 2001; Squillaci et al. 2017). While the mass spectra produced from eluents V and VI did demonstrate peaks corresponding to the molecular ions of both MABR and BABR (m/z 723.5, 705.5, respectively), these peaks may have alternatively represented fragment ion peaks generated from unmodified bacterioruberin, whose molecular ion peak (m/z 741.5) was also present within mass spectra generated for these eluents (Fong et al. 2001; Squillaci et al. 2017). These mass spectra suggested that base bacterioruberin was present within these eluents, despite its specific assignment to eluent IV (Fong et al. 2001; Squillaci et al. 2017). This likely represented the presence of cis-geometrical isomers of bacterioruberin co-eluting within these eluents. Bacterioruberin cis-isomers demonstrate identical mass spectra to the natural trans-form, but show higher retention times under HPLC (Orset and Young 2000; Nguyen et al. 2001; Yachai 2009; Squillaci et al. 2017; Silva et al. 2019; Flores et al. 2020). Indeed, previous studies have reported co-elution of bacterioruberin cis-isomers with MABR and BABR under similar HPLC systems, and the formation of cis-isomers is known to have been pervasive within the analysis performed here (as discussed in **Section 2.4.5.1**) (Mandelli et al. 2012; Squillaci et al. 2017; Flores et al. 2020). Given that the masses of common fragment ions of bacterioruberin match those of the molecular ions of MABR and BABR (i.e. m/z 723.5, 705.5), and that low-resolution mass-spectrometry (as employed here) is not sensitive enough to unambiguously differentiate molecular and fragment ions, it was not possible to conclude on the identity of carotenoids comprising eluents V and VI (Hoffman and Stroobant 2007; Gross 2017c; Rochat 2018).

However, as these eluents did demonstrate fragmentation patterns consistent with bacterioruberin-based compounds, it is likely that they represented mixtures of bacterioruberin isomers and dehydrated bacterioruberin variants (Squillaci et al. 2017).

The presence of TRABR and TABR could not be identified with confidence by HPLC/MS. HPLC eluents VII and VIII demonstrated substantially lower polarities than other eluents, suggesting they may represent these dehydrated bacterioruberin variants. While the mass-spectrum of eluent VII indicated it was either TRABR or TABR, the low resolution of the mass-spectrum meant that it was unclear which of the four peaks (m/z 685.4, 687.5, 668.5, 667.5) represented the molecular ion, thus its identity could not be drawn clearly (Fong et al. 2001; Asker et al. 2002; Mandelli et al. 2012; Flores et al. 2020). The molecular ion (m/z 705.5) and fragmentation pattern of eluent VIII indicated this eluent was most likely BABR. However, the identification of prior eluents would suggest eluent VIII to possess a lower polarity than TRABR/TABR, which was inconsistent with expectations of BABR and chromatographic theory. Fong et al. (2001) demonstrated that violations of chromatographic theory can occur when analysing bacterioruberin pigment-fractions of low concentration. The low absorbance of eluent VIII in DAD-responses demonstrated that this eluent was of low concentration, suggesting it may confound chromatographic separation similarly, and provides some justification for its identification as BABR.

The possibility that the 13 c.d.b. carotenoids produced by *Arthrobacter* sp. NamB2 were carotenoids unrelated to bacterioruberin was dismissed via mass-spectrometry. The molecular ion peaks of spirilloxanthin and oscillaxanthin (m/z 597.48 and 996 respectively) were not detected in the mass-spectra generated from any HPLC eluent or in total ion scans, confirming their absence from the complement (Hertzberg and Liaaen-Jensen 1969; Aakermann et al. 1992; Britton et al. 2004; Chi et al. 2015). Other 13 c.d.b. carotenoids including rhodoxanthin, 3,4-dehydrolycopene, and di-demethylspirilloxanthin were similarly discounted from a lack of molecular/fragment ion peaks (Britton et al. 1977; Cyronak et al. 1977; Jansen et al. 1995; Britton et al. 2004; Hudon et al. 2007; Takaichi et al. 2009). Mass-spectrometry thus dismissed the presence of alternative 13 c.d.b. carotenoids, reinforcing bacterioruberin as responsible for the pink-pigmentation of *Arthrobacter* sp. NamB2.

A summary of the identification of each TLC fraction and HPLC eluent is given in **Table 2.3**. Both methods agreed on the presence of bacterioruberin glycosides and highlighted a carotenoid of consistent chromatographic, absorption and mass-spectral properties with unmodified

bacterioruberin. While both methods demonstrated fractions of consistent chromatographic or MS properties to dehydrated bacterioruberin variants, their specific identifications were contentious, or lacked the resolution required for definitive characterisation.

The pink pigmentation of *Arthrobacter* sp. NamB2 was thus carotenogenic, and specifically based around the carotenoid bacterioruberin and a series of its dehydrated/glycosylated variants. The identity of this pigment complement was consistent with other desert-isolated *Arthrobacter*, including *A. agilis* from soils and surface waters of Antarctic desert systems (Fong et al. 2001; Dieser et al. 2010; Silva et al. 2019). This pigmentation has been further isolated from *Haloarchaea* of other deserts such as the Atacama, and regions of comparable irradiation (Baxter et al. 2007; Imperi et al. 2007; Flores et al. 2020). As bacterioruberin has demonstrated protection of *Haloarchaea* from UV/PAR-irradiation mediated lethality, it is thus speculated that bacterioruberin in *Arthrobacter* sp. NamB2 serves a similar protective role against the irradiance of the Namib Desert (Dieser et al. 2010; Jones and Baxter 2017).

Table 2.3: Summary of speculative identities for individual pigment fractions comprising the pigment complement of *Arthrobacter* sp. NamB2 as determined via HPLC/MS and TLC analyses.

HPLC Eluent	Speculated Identity	TLC Fraction (TLC-1 Numbering)	Speculated Identity
Eluent I	Bacterioruberin glycoside	**Fraction One**	Bacterioruberin glycoside
Eluent II	Bacterioruberin mono-glycoside	**Fraction Two**	Bacterioruberin glycoside
Eluent III	Fragmentation product of Eluent II	**Fraction Three**	Bacterioruberin glycoside
Eluent IV	Bacterioruberin	**Fraction Four**	Bacterioruberin
Eluent V	Bacterioruberin Geometrical isomers, potential MABR/BABR	**Fraction Five**	BABR
Eluent VI	Bacterioruberin Geometrical isomers, potential MABR/BABR	**Fraction Six**	Geometrical isomer of BABR
Eluent VII	TRABR/TABR	**Fraction Seven**	TABR
Eluent VIII	BABR		

2.4.5 Limitations of this Analysis

2.4.5.1 Carotenoid Degradation and Isomerisation

Carotenoids are highly fragile to oxygen, heat and light, and their identification can therefore be complicated by their degradation or isomerisation during extraction and analysis (Britton et al. 1995b). Carotenoids are highly sensitive to oxygen, and are rapidly destroyed on exposure (Britton and Young 1993). A consequence of this could be seen here in the disparity between the number of fractions resolved under HPLC and TLC – likely resulting from the differing oxygen exposure of the carotenoids under each method. Carotenoids separated on TLC plates are highly susceptible to oxygen, being directly exposed to open air on the plate's surface (Bidlingmeyer 1987; Britton and Young 1993). Given that ambient air exposure can yield losses of as much as 10 % of total carotenoids during analysis, and that individual carotenoids within the pigment complement may represent only 2 – 5 % of this complement, losses of entire pigment fractions are a known risk under TLC-separation, as was the case here (Chattopadhyay et al. 1997; Cernelic et al. 2013). The closed column system and comparatively high speed of HPLC analysis means that samples have lower oxygen exposure during separation, reducing degradation and more readily allowing the detection of low-abundance carotenoids (Kopec et al. 2012; Amorim-Carrilho et al. 2014; Butnariu 2016). Degradation of pigment fractions via oxygen exposure was thus likely responsible for the different conclusions under HPLC and TLC analyses regarding the number of compounds comprising the pigment complement.

Oxygen exposure during pigment extraction and sample preparation may have resulted in the partial degradation of carotenoids in a manner confounding their identification. For example, HPLC eluent III likely represents the result of carotenoid degradation as opposed to a distinct constituent of the complement. The existence of eluent III as a low abundance, broad trailing peak from eluent II in the HPLC suggested it was instead a series of degradation products from eluent II, as opposed to a distinct carotenoid (Niessen 2006; Flores et al. 2020). To minimise carotenoid degradation via oxygen during extraction and analysis, some carotenoid studies perform all stages of analysis under inert gaseous atmospheres such as argon or nitrogen (Britton et al. 1995a; Jagannadham et al. 2000; Britton 2008; Mandelli et al. 2012; Rodriguez-Amaya and Kimura 2004). While exceeding the resources of the current study, this may be employed in future analyses into this pigment complement to maximise the accuracy of its identification.

Carotenoids are easily isomerised into their cis-forms, which can further confound their identification. Cis-isomers are formed as artefacts of extraction – from the exposure of carotenoids to light or heat (Britton et al. 1995). Due to their low excitation energies, carotenoids are highly sensitive to heat/light-stimulated isomerisation, making the formation of cis-isomers unsurprising and difficult to control throughout carotenoid extraction and analysis (Sherma and Fried 2003; Britton 2008). Such geometric isomerisation can confound interpretation of a carotenoid's spectral-fine structure (Takaichi and Shimada 1992; Ladislav et al. 2004; Fanali et al. 2012). Indeed, base bacterioruberin can demonstrate fine structures from 33.0 – 65.0 % based on its geometric isomerisation, with a similar range reported for MABR (34.5 – 54.0 %) (Rønnekleiv and Liaaen-Jensen 1992; Ronnekleiv 1995; Mandelli et al. 2012; Squillaci et al. 2017). These spectral fine structures overlap those of other 13 c.d.b. carotenoids including oscillaxanthin (40 %) and spirilloxanthin (65 %), demonstrating the lack of specificity these fine-structures provide for identification when cis-isomers are present (Britton et al. 2004).

Cis-peaks in carotenoid UV-visible scanning spectra denote the presence of carotenoid cis-isomers, and were observed in the UV-visible spectra produced for all recovered TLC-fractions here (Tan and Soderstrom 1989; Britton et al. 1995a). The presence of these peaks implied that geometrical isomerisation had occurred during sample preparation or execution of the TLC analysis, causing mixtures of geometrical isomers to be present within each TLC-fraction. As the extent of the influence exerted by geometric isomerisation on the fine structures of each of these pigment fractions was unknown, these fine structures could not be used for identification of the TLC fractions. In this study, efforts were made to minimise carotenoid isomerisation in line with well-established recommendations of Britton et al. (1995a), via minimisation of light-exposure of the crude pigment extract at all stages and maintenance of temperatures below 40^{o}C (Rodriguez-Amaya 2016). However, the prevalence and mixtures of cis-isomers observed within the TLC spectra implies a breakdown in this process (Ladislav et al. 2004; Meinhardt-Wollweber et al. 2018).

2.4.5.2 Limitations of the TLC analysis

In formal carotenoid identification, TLC chromatographic properties of unknown carotenoids of suspected identity are typically demonstrated alongside authentic carotenoid standards to confirm their shared identities (Britton et al. 2004; Takaichi 2014). These comparisons avoid influences on polarity caused by differing structural features between carotenoids and standards. This formal identification was not employed here due to the lack of commercially available authentic bacterioruberin standard, and the unknown identity of the pigment at the beginning of

this analysis. The validity of polarity comparisons between the pigments of *Arthrobacter* sp. NamB2 and spinach control carotenoids under TLC was imperfect here due to differences in their structural features (Poole 2003). As chromophore extension and cyclisation can influence carotenoid polarities, comparisons between carotenoids of differing conjugation lengths or cyclic classes are cautioned (Krinsky 1963; Kelly et al. 1970; Poole 2003; Sherma and Fried 2003). Furthermore, the polarity conferred by a given functional group can be influenced by its specific molecular environment, with allylic hydroxyls (as in lutein) providing lower polarity than non-allylic hydroxyls (as in bacterioruberin) (Krinsky 1963; Sherma and Fried 2003; Caron and Ermondi 2016). As such, the migration of the control carotenoids here (cyclic carotenoids, 11 c.d.b.) and bacterioruberins of *Arthrobacter* sp. NamB2 (acyclic carotenoids, 13 c.d.b.) were potentially modulated by their differing structural features outside of the polarity strictly provided by their functional groups (Ertl et al. 2000; Britton 2008; Caron and Ermondi 2016). Consequently, simplifications of polarity to numeric comparisons of functional groups was unlikely to accurately compare samples, and may have contributed to unexpected findings, such as in conclusion of presence of BABR as opposed to MABR within the pigment complement (Ertl et al. 2000; Britton 2008; Caron and Ermondi 2016). To develop this analysis further, the crude pigment of *Arthrobacter* NamB2 should be run via TLC against the pigment extracts of a known bacterioruberin producer, such as *A. bussei* or *A. agilis*, as has been employed previously (Fong et al. 2001; Flegler et al. 2020).

2.4.5.3 Limitations of the HPLC/MS Analysis

The lower resolution of HPLC analysis employed here hindered the specificity of subsequent MS identification for a number of eluents. Indeed, the confounded mass spectra and inconclusive identities of eluents V and VI were attributed to the co-elution of bacterioruberin isomers with dehydrated variants of bacterioruberin within each of these eluents. Use of HPLC-columns with a triacontyl (C30) stationary phase is considered the gold-standard for carotenoid separation, and these columns have consistently outperformed octadecyl silane (C18) columns (as applied here) in carotenoid resolution (Sander et al. 1994; Sander et al. 2000; Kopec et al. 2012; Bijttebier et al. 2014). This higher resolution is attributed to column features including ligand length and the specific stationary phase chemistry of C30 chains, and these have previously demonstrated the specificity necessary for clear separation of carotenoid geometrical isomers (Sander et al. 1994; Sander et al. 2000; Rivera and Canela-Garayoa 2012; Bijttebier et al. 2014). Furthermore, C30 HPLC columns have been applied in recent studies successfully resolving bacterioruberin-based complements of *A. bussei* and *H. salinarium* (Mandelli et al. 2012; Flegler et al. 2020). A C18 column was applied here due to its common application in general bacterial carotenoid separation, but is of lower resolution, and does match stationary-

phases employed in some recent studies which have suffered from co-elution of bacterioruberins (Fong et al. 2001; Squillaci et al. 2017; Flores et al. 2020). The chromatographic separation of the *Arthrobacter* sp. NamB2 pigment complement may thus be improved by application of an HPLC column of higher resolution.

Stepwise chromatographic separation of the pigment complement may also have improved pigment resolution. Squillaci et al. (2017) and Flores et al. (2020) were able to separate bacterioruberin-based carotenoid complements of *Haloarchaea* – including geometrical isomers – into 17 – 23 distinct fractions at high resolution. Both achieved this through their use of multiple stages of chromatographic separations of increasing resolution, such as in the progression from HPLC separation to UHPLC separation of co-eluted HPLC-eluents as described in Flores et al. (2020). Similar stepwise chromatography would improve separation of the pigments comprising the complement of *Arthrobacter* sp. NamB2 for subsequent identification (Britton et al. 1995b; Takaichi 2014; Squillaci et al. 2017; Flores et al. 2020).

The low-resolution MS employed here further limited pigment identification. The resolution of a mass spectrometer denotes the minimal mass difference by which peaks of the mass spectrum may be distinguished, with heightened accuracy at increasing resolutions (Gross 2017c; Louie et al. 2020). Low-resolution MS struggles to distinguish fragment peaks of similar masses, as was observed in the mass spectrum of eluent VII (Lebedev and Cabrol-Bass 1998; Gross 2017c; Rochat 2018). Issues with peak resolution were worsened here by the aforementioned HPLC co-elution of bacterioruberin and its dehydrated derivatives as in eluent V and VI (Britton et al. 2004; Squillaci et al. 2017). High resolution MS is commonly applied in identifications of carotenoid complements, including those of *Arthrobacter* and *Haloarchaea*, and would be capable of distinguishing fragment peaks from molecular-ion peaks with a high level of accuracy (Fong et al. 2001; Mandelli et al. 2012; Squillaci et al. 2017; Rochat 2018; Reis-Mansur et al. 2019; Silva et al. 2019; Flores et al. 2020). Application of high-resolution mass-spectrometry would have more clearly delineated fragment and molecular-ion peaks for individual eluents here, and significantly enhanced the reliability of the MS-conclusions drawn.

Overall, while limited, the application of TLC and HPLC/MS did enable identification of the pigment complement of *Arthrobacter* sp. NamB2 as bacterioruberin and its glycosylated/dehydrated variants. These findings were consistent with common pigment complements characterised within *Arthrobacter* and other bacterioruberin-producing organisms (Fong et al. 2001; Mandelli et al. 2012; Squillaci et al. 2017; Flegler et al. 2020). Application of

higher-resolution chromatographic separations of the pigment complement, followed by high-resolution mass spectrometry, would provide a more robust characterisation of the pigment complement of *Arthrobacter* sp. NamB2.

2.5 Conclusions and Next Steps

Identifying the pigmentation of heterotrophic bacteria provides information on the physiological role(s) that these pigments are likely to serve the organism (Bay et al. 2018; Leung et al. 2020). *Arthrobacter* sp. NamB2 had been identified previously as highly UV resistant, and it is speculated that its pink pigmentation has a role in this phenotype (Buckley 2020). As the first step in determining the physiological utility this pigmentation may provide *Arthrobacter* sp. NamB2, this chapter explored the identity of its pigment complement.

The pigment was identified as carotenogenic, and comprised of a mixture of the carotenoid bacterioruberin and its dehydrated/glycosylated variants common within bacterioruberin-based pigment complements. The carotenogenic nature of the pigment was concluded from its production of distinctive three-peaked carotenoid UV-visible spectra upon extraction (Britton et al. 2004). Separate TLC/HPLC analyses indicated the presence of at least six – eight discrete carotenoid compounds with chromophore lengths of thirteen c.b.d within the pigment complement, which mass spectrometry further identified as bacterioruberin and a series of its glycosylated/dehydrated variants. While high confidence in the presence of bacterioruberin is emphasised, the specific identities of other carotenoids within the complement are more ambiguous, due to limited resolution of the methods employed. Further analysis of this pigment complement with higher-resolution instrumentation or multiple rounds of chromatography would be necessary to confirm pigment identity consistent with the standards as set out by Britton et al. (2004) and Takaichi (2014).

The production of carotenoid pigmentation, and in-particular bacterioruberin, by *Arthrobacter* sp. NamB2 was consistent with *Arthrobacter* isolated from other desert systems (Fong et al. 2001; Dieser et al. 2010; Silva et al. 2019). The established role of carotenoid production by desert bacteria as providing intrinsic irradiation-tolerance suggests a similar importance within *Arthrobacter* sp. NamB2. These speculations were supported by the known contribution of bacterioruberin to the UV-resistome of *Haloarchaea* (Jones and Baxter 2017). Consequently, it was hypothesised that the pink, carotenoid pigmentation of *Arthrobacter* sp. NamB2 serves a protective role against the substantial irradiance of the Namib Desert, and contributes

meaningfully to its irradiation-resistome. Investigation of the photoprotective role conferred by pigmentation of *Arthrobacter* sp. NamB2 was thus further explored via evidence of its photoinducibility (**Chapter 3**) and specific contributions to its UV-resistome (**Chapter 4**).

Chapter 3 Light Inducibility of Pigmentation in *Arthrobacter* sp. NamB2

3.1 Introduction

3.1.1 Light-Responsive Carotenogenesis in Photoprotection

A variety of non-phototrophic bacteria which use carotenoids for photoprotection demonstrate light-responsive carotenoid production (Purcell and Crosson 2008). As carotenoid biosynthesis is a substantial energy commitment, the induction of carotenogenesis as a response to light stress allows production only when this commitment is strictly required (Young 1993; Tisch and Schmoll 2010; Llorente 2016). While relatively rare, examples of this phenomenon exist in organisms including *Deinococcus radiodurans, Myxococcus xanthus, Flavobacterium, Mycobacterium*, *Streptomyces* and *Corynebacterium glutamicum*, all of which demonstrate both a reliance on carotenoids for photoprotection, and a coinciding light-inducibility of their carotenogenesis (Rilling 1962; Mathews 1963; Burchard and Dworkin 1966; Howes and Batra 1970; Weeks et al. 1973; Koyama et al. 1974; Browning et al. 2003; Takano, Asker, et al. 2006; Heider et al. 2012; Takano 2016; Silva et al. 2019; Sumi et al. 2019). Connections between carotenoid photoprotection in non-phototrophic bacteria and light-induced carotenogenesis means that demonstrating light-responsive carotenoid production acts as evidence for the bacterial employ of carotenoids for irradiation-tolerance (Takano 2016).

It was of interest to determine whether *Arthrobacter* sp. NamB2 undergoes light-responsive carotenogenesis. *Arthrobacter* sp. NamB2 has been found within this thesis to produce carotenoid pigmentation based around the carotenoid bacterioruberin (**Chapter 2)**. Given the irradiation-tolerance conferred by carotenoid pigments in other desert bacteria, and the previous demonstration of photoprotection by bacterioruberin in *Haloarchaea*, a similar photoprotective role of the carotenoids in *Arthrobacter* sp. NamB2 is suspected (Jones and Baxter 2017). This role of pigmentation is speculative, and demonstration of light-responsive carotenogenesis by *Arthrobacter* sp. NamB2 would thus serve as strong evidence of the function of its pigmentation in irradiation-protection.

3.1.2 Investigations of Light-Induced Carotenogenesis

Studies examining light-induced carotenogenesis quantify and compare the total carotenoid content of organisms grown under differing light intensities (Burchard and Hendricks 1969; Sumi et al. 2019). Cultures are typically grown at a range of static PAR intensities, with extraction, quantification and comparisons of total carotenoid content between cultures at the end of growth cycles used to determine whether total organismal pigment production is significantly influenced by light-exposure (Rilling 1962; Mathews 1963; Burchard and Hendricks 1969; Sumi et al. 2019). In broth cultures, PAR intensities used to examine light-inducibility of non-phototrophic bacteria extend up to 200 µmol m^{-2} s^{-1}, while solid-media experiments tend towards lower exposures of 2.0 – 50 µmol m^{-2} s^{-1} (Davis et al. 1999; Takano et al. 2005; Ortiz-Guerrero et al. 2011; Takano et al. 2015; Sumi et al. 2019).

Quantitative carotenoid analyses rely on the Beer-Lambert law (Kopec et al. 2012; Rodriguez-Amaya and Kimura 2004). This law dictates that the concentration of a wavelength-absorbing species in solution is directly proportional to its absorbance as light passes through a one-centimetre pathlength of the solution (Swinehart 1962; Parnis and Oldham 2013; Casasanta and Garra 2018). As carotenoids in solution obey the Beer-Lambert Law, their concentrations are directly proportional to their absorbance at λ_{max}, and can thus be determined simply from UV-visible scanning spectra (Liaaen-Jensen and Jensen 1971; Britton et al. 1995a; Britton et al. 2004; Machmudah and Goto 2013). Application of a standard calculation using the λ_{max} absorbance of crude bacterial pigment extracts and a generalised molar extinction coefficient can thus be used to quantify the total carotenoid content within these extracts as a value in milligrams, with standardisation to cell dry-weights enabling the comparison of pigment contents between cultures (Young and Britton 1993; Britton et al. 1995a; Lichtenthaler and Buschmann 2001; Rodriguez-Amaya and Kimura 2004; Rodriguez-Amaya 2016).

3.1.3 Regulators Controlling Light-Responsive Carotenogenesis

Exploration of bacterial genomes for homologues to known regulators controlling light-responsive carotenoid production is a valid *in silico* method for speculating light-induced carotenogenesis (Takano et al. 2005; Takano et al. 2015; Sumi et al. 2019). These *in silico* analyses enable phenotypic demonstrations of light-responsive carotenogenesis to be related to an organism's genotype, and have been used in a number of recent screening studies (Takano 2016; Sumi et al. 2019).

Knowledge of the regulators involved in light-responsive carotenogenesis of non-phototrophic bacteria is limited. The best understood molecular mechanisms controlling carotenoid biosynthesis are those using transcriptional repressor proteins CrtR and LitR (Takano 2016; Sumi et al. 2019). The CrtR regulator is a member of the multiple antibiotic resistance regulator (MarR) family of transcriptional repressors, while LitR is a mercuric resistance (MerR) family repressor, with specific regulatory activities as described prior (**Section 1.3.6).** These proteins repress carotenoid production under dark conditions, but lose their ability to bind to DNA when exposed to light, allowing transcription of genes involved in carotenoid biosynthesis (Takano et al. 2015; Sumi et al. 2019). Other light-responsive carotenoid regulators have been identified in non-phototrophic bacteria, such as the bacteriophytochrome of *D. radiodurans*, but lack functional characterisation (Davis et al. 1999). Discovery of genes homologous to *litR* and *crtR* in bacterial genomes has been used to support conclusions regarding light-responsive carotenogenesis (Takano 2016; Sumi et al. 2019). Genomic context of these genes is also an important criterion, as close proximity between the *litR* and *crtR* genes to their regulated carotenoid genes is required for regulatory action, and must also be observed for their regulation of carotenogenesis to be considered likely (Takano 2016; Sumi et al. 2019; Henke et al. 2020). The availability of the *Arthrobacter* sp. NamB2 genome provides an opportunity to identify *litR* and *crtR* homologues, and to explore possible mechanisms for light induced bacterioruberin production (Buckley et al. 2019).

3.1.4 Light-Induced Carotenogenesis in *Arthrobacter* and close relatives

Carotenogenesis in some *Arthrobacter* is environmentally-responsive and connected to physiological adaptation (Fong et al. 2001; Dieser et al. 2010). For example, bacterioruberin production in *A. agilis* is temperature-responsive, with lower growth temperatures increasing the total bacterioruberin synthesis in service of membrane stabilisation (Chattopadhyay and Jagannadham 2001; Fong et al. 2001).

While light-responsive carotenogenesis has been demonstrated in many close relatives of *Arthrobacter* within *Micrococcaceae,* studies within the genus itself are limited (Sumi et al. 2019). Studies reporting that *A. agilis*, *Arthrobacter* sp. 21022 and *Arthrobacter* sp. PAMC 25486 lack light-induced carotenogenesis have failed to provide formal quantifications of pigment content, light exposure conditions, light sources or irradiation times, information considered important for complete characterisations of photoresponses (Björn 2008a; Björn

2008b; Tescari et al. 2018; Sumi et al. 2019). The limitations of these prior studies suggests that light-responsive carotenogenesis in *Arthrobacter* is currently underexplored, and worthy of investigation in a manner addressing these limitations.

Surprisingly, light-induced carotenogenesis has not been studied in desert bacteria. This is unexpected as there is increasing evidence of the connections between the photoprotective function of carotenoids in bacteria and their light-responsive production (Takano 2016; Sumi et al. 2019). Articles such as Takano (2016) stress the importance of maintaining light-inducible carotenogenic systems as a component of the photoprotective machinery within bacteria subject to prevalent irradiation exposure. As edaphic desert organisms frequently produce carotenoids as photoprotectants, and are exposed to constant stress from high light, the maintenance of light-responsive carotenogenesis would, therefore, be expected, and is worthy of study (Dieser et al. 2010; Wierzchos et al. 2015; Silva et al. 2019; Flores et al. 2020).

The intent of this chapter was therefore to determine whether *Arthrobacter* sp. NamB2 demonstrated light-responsive carotenogenesis, consistent with the suspected function of its bacterioruberin pigment in photoprotection. The first aim of this study was to test the light-inducibility of bacterioruberin production. Light-inducibility assays were performed by comparing the total carotenoid content produced by cultures of *Arthrobacter* sp. NamB2 grown under a series of PAR-light intensities known to stimulate light-responsive carotenogenesis in other non-phototrophic bacteria. The light intensities selected focussed first upon low-intensity PAR in line with those demonstrated to induce carotenogenesis in *Micrococcales* and *Actinobacteria*, and were increased in intensity in an attempt to reach carotenogenesis saturation (Davis et al. 1999; Takano et al. 2005; Ortiz-Guerrero et al. 2011; Sumi et al. 2019). The second aim of this chapter was to explore the *Arthrobacter* sp. NamB2 genome for the presence of homologous sequences to known regulators controlling light-responsive carotenoid production in non-phototrophic bacteria. This was done to identify possible mechanisms by which the light-induction may be occurring, and validate conclusions drawn from the light-inducibility assays.

3.2 Methods

3.2.1 Light-Inducibility of Carotenoid Pigmentation in *Arthrobacter* sp. NamB2

The light-inducibility of pigmentation in *Arthrobacter* sp. NamB2 was tested by growing cultures at a range of static PAR intensities shown to induce carotenogenesis in recent investigations of non-phototrophic bacteria (Davis et al. 1999; Takano et al. 2005; Ortiz-Guerrero et al. 2011; Sumi et al. 2019). The total pigment content produced by each of these cultures was quantified and compared for evidence of differences attributable to light-responsive carotenoid production.

3.2.1.1 Cell Revival and Light-Exposure

Figure 3.1 shows the workflow used for the growth of *Arthrobacter* sp. NamB2 cultures in different light intensities. For cell revival, 200 µL of one glycerol stock of *Arthrobacter* sp. NamB2 was inoculated onto nutrient agar via spread plate and grown at 20 °C for 72 hours. Following growth, the bacterial lawn was reverse spread plated from the nutrient agar by adding 5.0 mL nutrient broth to the plate, and scraping the colonies from the agar's surface into the broth suspension using a plastic spreader. This broth culture was subsequently recovered, adjusted to an OD_{600} of 0.5 using nutrient broth, and used to inoculate a total of nine nutrient agar plates via spread plate (100 µL per plate). These plates were incubated under illuminance from a 36 watt white light-emitting diode (LED) bulb (OSRAM, Munich, Germany) with three plates each receiving white light at their relevant intensities over the entire period of incubation, as outlined below.

The light-exposure experiment was performed twice, once comparing cultures grown under incident PAR intensities of 0, 5 and 10 µmol m^{-2} s^{-1}, and once comparing 0, 50 and 100 µmol m^{-2} s^{-1}. The execution of two separate experiments was necessitated by limited incubator space disallowing simultaneous examination of all light-intensities. The 0 µmol m^{-2} s^{-1} light exposure condition was provided by wrapping the nutrient agar plates in two layers of aluminium foil to prevent light penetration. Incident light upon the surface of the agar plates was controlled by changing the distance between the bulb and plates. Incident light intensities were verified at the surface of the agar plates using a PASCO PS-3213 wireless light sensor (PASCO Scientific, Roseville, USA). Each culture was grown at its respective light-intensity at 20 °C for 72 hours prior to cell harvest for pigment extraction. Temperature effects of the lamp upon irradiated

cultures were not considered significant, as the LED bulb was found to impart minimal heat on the plate's surface relative to the holding temperature of the incubator (as examined via preliminary studies).

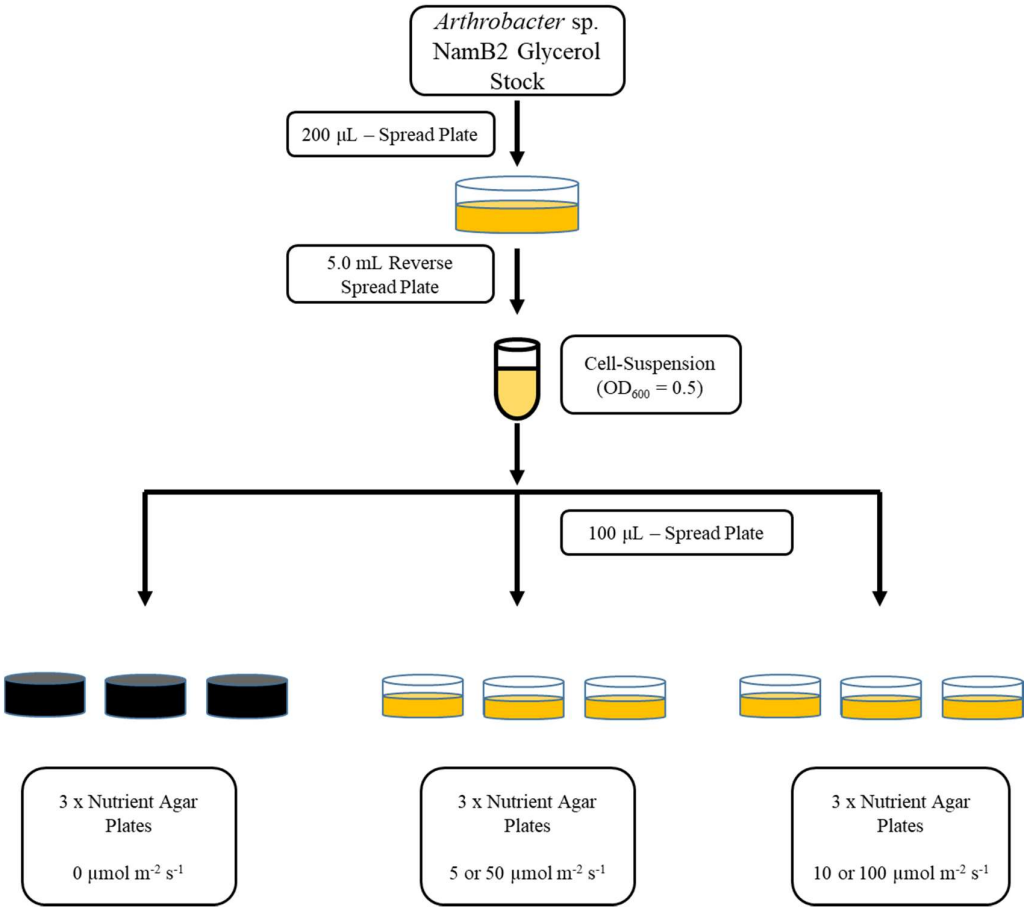

Figure 3.1: Schematic representation of the light-inducibility experiments performed. Light conditions compared were analysed in two separate executions of the experiment (once comparing cultures grown at 0, 5 and 10 µmol m^{-2} s^{-1} and once comparing 0, 50 and 100 µmol m^{-2} s^{-1}).

Following 72 hours of growth at their given light intensities, cultures were harvested from each nutrient agar plate through addition of 5.0 mL nutrient broth to the plate, and scraping the colonies from the agar's surface into the broth suspension using a plastic spreader. Each broth suspension was aspirated and collected in pre-weighed, separate 50 mL centrifuge tubes. Cells were pelleted via centrifugation at 7,745 x *g* for 15 minutes (4 °C). The supernatant was discarded from the cell pellet, which was subsequently washed with 5.0 mL of distilled water, and re-pelleted via centrifugation (7,745 x *g*, 15 minutes, 4 °C). Water was carefully removed from the area around the pellet via aspiration, and centrifuge tubes containing the cell pellets

were placed in a drying oven at 60 ºC for 24 hours to dry the pellet to a constant mass. Following the drying period, cell dry mass was measured, and pellets re-hydrated with 2.0 mL of distilled water to ease subsequent pigment extraction. Cells were re-pelleted via centrifugation (7,745 x *g*, 15 minutes, 4 ºC), with the re-hydrating supernatant water carefully removed via aspiration.

3.2.1.2 Pigment Extraction and Carotenoid Quantification

To quantify the pigment content of cultures grown under different light-conditions, total pigment extractions were performed on the cell pellets obtained from each culture grown under each PAR-intensity. Each of these pigment extracts were subsequently examined via UV-visible spectroscopy to quantify the total carotenoid production by each culture.

For pigment extraction, 3.0 mL of > 99.9 % HPLC-grade methanol was added to each rehydrated cell pellet, with gentle physical agitation used to suspend the pellet within the methanol phase. The pigment extraction method described in Section **2.2.1** was then followed, but extracting with 3.0 mL aliquots of methanol, and without final rotary evaporation of the pigment extracts. Extraction was continued until both pellet and supernatant (post-centrifugation) lacked visible pink colour. Pigment extracts were subject to a final centrifugation at 7,745 x *g* for 15 minutes (4 ºC) to remove remaining cellular particulates from the suspension prior to UV-visible absorption readings.

A scanning UV-visible spectrum from 350 – 800 nm was generated for the total pigment extract recovered from each culture grown at each light-intensity. These UV-visible spectra were generated using an Ultrospec 7000 UV-visible spectrophotometer (Cytiva, USA), with HPLC-grade methanol used as the blank. The wavelength of absorption corresponding to $\lambda_{max,}$ and absorbance reading at this λ_{max} wavelength was recorded for each extract for subsequent pigment-quantification. To maintain accuracy of the instrument, samples were diluted where appropriate with HPLC-grade methanol to ensure final absorbances at λ_{max} were between 0.2 and 1.0.

The carotenoid content (mg) of each replicate culture grown under each light-intensity was calculated from the absorbance values of their pigment extract at λ_{max} using the standard calculation for total carotenoid content as displayed in **Equation 3.1.** An average extinction

coefficient of 2,500 $M^{-1}cm^{-1}$ was used, as is standard for total carotenoid mixtures (Liaaen-Jensen and Jensen 1971; Flores et al. 2020). Using the dry-weight of cell pellets from which the pigment was extracted, the total pigment content of each culture in milligrams of carotenoid per gram of cell dry mass (mg/g) was determined.

Equation 3.1: Calculation of Carotenoid Content in Pigment Extracts from UV-visible Absorbance Intensities (Liaaen-Jensen and Jensen 1971)

$$\text{Carotenoid Content}_{(mg)} = A_{\lambda max} \text{ x Vol x Df x } (10/2500)$$

Where:

$A_{\lambda max} = \text{Absorbance of the carotenoid extract at } \lambda_{max}$

$\text{Vol} = \text{Volume of methanolic carotenoid extract (mL)}$

$\text{Df} = \text{Dilution factor}$

3.2.1.3 Statistical Analysis

The total pigment content of cultures grown under each intensity of PAR-irradiance was compared to determine whether growth under differing illumination conditions stimulated a significant difference in total carotenoid production.

Milligrams of carotenoid pigment per gram of cell dry mass (henceforth 'pigment content') was calculated for each plate (of triplicate) grown under each light condition. For statistical analyses, the total pigment content of cultures from both experimental executions (Comparing 0, 5, 10 µmol m^{-2} s^{-1} and 0, 50, 100 µmol m^{-2} s^{-1} conditions) were examined together, giving five experimental conditions total. The 0 µmol m^{-2} s^{-1} condition thus possessed six replicate pigment content readings, while each other condition possessed three.

Evidence of a statistically-significant difference (p value < 0.05) in mean pigment content between cultures grown under different light intensities was examined using analysis of variance (ANOVA) testing. Post-hoc analysis via Tukey's honest significant difference (Tukey's HSD) testing was used to determine whether the total pigment content was significantly different between any two light conditions (p value < 0.05). The assumption of

homoscedasticity was verified via Bartlett's testing of input data. Normality in distribution of pigment contents of cultures grown under each light intensity was verified using Shapiro-Wilks normality testing in R (R Core Team 2020). The appropriateness of the ANOVA model was examined via the generation of standard diagnostic plots for the model in R (R Core Team 2020).

3.2.2 Identification of Candidate Light-Responsive Carotenogenesis Regulators in *Arthrobacter* sp. NamB2

To determine if there was a genetic basis for light-induced carotenogenesis in *Arthrobacter* sp. NamB2, and to relate observations from light-inducibility experiments to genomic features, the available genome assembly of *Arthrobacter* sp. NamB2 (GenBank; GCA_005281365.1) was explored for the presence and genomic context of sequences encoding proteins similar to the light responsive carotenogenesis regulators CrtR, LitR and *D. radiodurans* bacteriophytochrome (Davis et al. 1999; Takano et al. 2005; Sumi et al. 2019). This analysis was limited to the examination of known light-responsive carotenoid regulators of non-phototrophic bacteria, as carotenoid regulatory systems in photoautotrophs are typically coupled to assemblages of the photosynthetic apparatus, systems not applicable in non-photosynthetic *Arthrobacter* (van der Horst et al. 2007; Auldridge and Forest 2011; Llorente 2016).

Protein sequences corresponding to CrtR, LitR and the *D. radiodurans* bacteriophytochrome were acquired from the GenBank protein database (www.ncbi.nlm.nih.gov/protein, **Table 3.1**). These protein sequences were used as query terms to search against the complete protein transcript of *Arthrobacter* sp. NamB2 via use of the National Centre for Biotechnology Information's (NCBI) Basic Local Alignment Search Tool (BLAST) BLASTp algorithm (www.ncbi.nlm.nih.gov) (Expect threshold = 0.05, Word Size = 3). *Arthrobacter* sp. NamB2 proteins demonstrating sequence similarities with these regulator proteins below 30 % were discarded from the analysis to prevent the retrieval of proteins likely differing in function from these regulators (Wass and Sternberg 2008; Gong et al. 2016; Makrodimitris et al. 2019). Candidate proteins from *Arthrobacter* sp. NamB2 which were above this similarity cutoff were aligned against the corresponding query regulator protein sequences using the MEGAX software v10.0.5 (Kumar et al. 2018). These protein alignments were manually examined to identify regions of high sequence similarity and conserved protein motifs (with reference to literature) to aide identification of potential shared-functions between the candidate homologue proteins of *Arthrobacter* sp. NamB2 and known carotenogenesis regulators.

Table 3.1: Sources of the CrtR, LitR and bacteriophytochrome sequences used in this study.

Regulator Protein	Source Organism	GenBank Accession Number	Reference
CrtR	*Corynebacterium glutamicum* AJ1511	BAV22458	Sumi et al. (2019)
LitR	*Streptomyces coelicolor* A3(2)	QFI40492	Takano et al. (2005)
	Thermus thermophilus HB27	AAS82386	Takano et al. (2011)
	Thermus thermophilus HB8	BAD71896	Ortiz-Guerrero et al. (2011)
	Bacillus megaterium QMB1551	ADE71366	Takano et al. (2015)
	Bacillus megaterium DSM319	ADF41172	Takano et al. (2015)
Bacteriophytochrome	*Deinococcus radiodurans*	AAF12261	Davis et al. (1999)

As the genes encoding CrtR and LitR must cluster closely to their regulated genes upon the genome (within 1,000 – 10,000 base pairs (bp)) to exert regulatory control, the genomic positions of *Arthrobacter* sp. NamB2 genes encoding candidate protein homologues to the CrtR and LitR regulators were identified, and a genomic region some 10,000 base-pairs either side of each of these genes was examined for the presence of putative carotenogenesis genes (Takano 2016; Sumi et al. 2019). Given that this proximity to carotenoid genes is required for regulatory control by CrtR and LitR, this analysis was used to scrutinise whether the identified homologues in *Arthrobacter* sp. NamB2 were likely to have a similar regulatory role in carotenogenesis (Brown et al. 2003; Takano 2016; Deochand and Grove 2017; Sumi et al. 2019). This investigation was not extended to those genes encoding candidate bacteriophytochromes, as the proximity of bacteriophytochrome genes to their regulons is not generally considered relevant to regulation (Bhoo et al. 2001; Auldridge and Forest 2011). This analysis required the identification of the genomic location of carotenoid genes in *Arthrobacter* sp. NamB2.

The genomic location of the gene cluster likely responsible for carotenogenesis in *Arthrobacter* sp. NamB2 was identified through genetic similarity to carotenoid biosynthesis genes phytoene synthase (locus tag RY94_RS00755) and phytoene desaturase (RY94_RS00760) as identified in the genome of closely related *Arthrobacter agilis* strain L77 (GenBank assembly accession number GCA_000816565) by Ii et al. (2019). The nucleotide sequences of these carotenogenesis genes from *A. agilis* strain L77 were used as query terms and searched against the whole genome of *Arthrobacter* sp. NamB2 via use of the NCBI BLASTn algorithm (www.ncbi.nlm.nih.gov) (Expect threshold = 0.05, Word Size = 28). The top-scoring gene

matches in the genome of *Arthrobacter* sp. NamB2 were considered to represent the equivalent carotenogenesis genes within this organism.

3.3 Results

3.3.1 Light Inducibility of Carotenoid Pigmentation

Light-inducibility of carotenogenesis in *Arthrobacter* sp. NamB2 was examined by comparing the total pigment content produced by cultures grown under a series of PAR-light intensities. Total pigment extraction and carotenoid quantification via UV-visible spectroscopy was used to determine the total pigment production by each culture grown under each light intensity. These pigment contents were subsequently compared for evidence of statistically-significant differences in total carotenoid production arising from illumination.

The UV-visible scanning spectra of pigment extracts from cultures grown under each light-intensity demonstrated absorption responses consistent with the findings of **Chapter 2**, in the production of three-peaked carotenoid spectra with prominent peaks at 464 (I), 491 (II) (λ_{max}) and 525 (III) nm (+/- 2 nm) in methanol (**Figure 3.2**). No major differences were observed in wavelength-positions of the three-peaked spectra between cultures grown under different light-intensities, suggesting a broad consistency in the identity of carotenoids produced under all light-conditions.

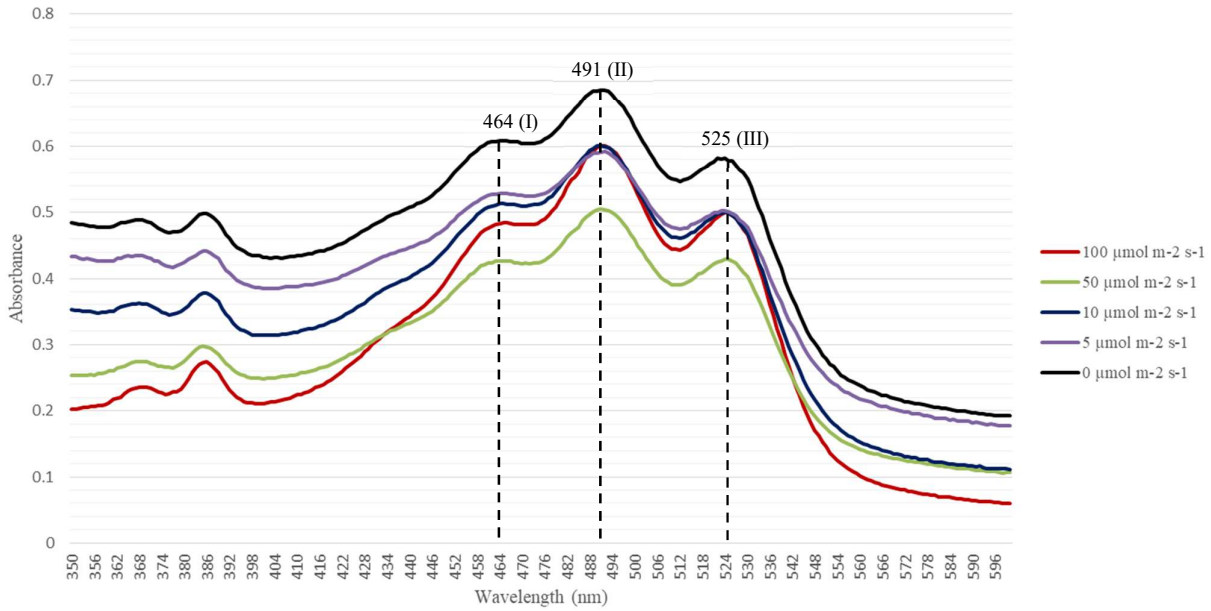

Figure 3.2: Example UV-visible scanning spectra of pigment extracts from *Arthrobacter* sp. NamB2 cultures grown under each light-intensity. Wavelength positions corresponding to peaks I, II and III within the three-peaked carotenoid response are denoted on the figure. Truncation at 600 nm is used to emphasise the three-peaked carotenoid response, as no further peaks were observed beyond 600 nm.

Comparisons of the pigment content of cultures grown under each light intensity is presented in **Figure 3.3**. This figure demonstrates a substantial overlap in the pigment content produced by cultures grown under all differing light-conditions, with no clear trends in pigment content reflecting incident light intensity. Tukey's HSD analysis reported no significant differences between the total pigment content of cultures from any two light conditions, nor between light and dark grown cultures. These findings were supported by the ANOVA model (**Table 3.2**), which reported a p-value of 0.16, above the threshold of significance ($p > 0.05$), thereby concluding that there was no significant difference between the mean pigment content of cultures grown at differing light intensities. Both of these analyses demonstrated light intensity to have no significant influence on the total pigment content of *Arthrobacter* sp. NamB2. Consequently, the production of pigmentation by *Arthrobacter* sp. NamB2 was concluded to be not light-responsive.

Note that separate ANOVA analyses comparing pigment contents within each experimental execution (i.e. comparing pigment content of cultures grown at 0, 5 and 10 µmol m^{-2} s^{-1} and pigment content of cultures grown at 0, 50 and 100 µmol m^{-2} s^{-1}) concluded identically to the above analysis. These findings similarly denoted a lack of significant differences between the pigment content of cells grown under differing light-intensities.

The appropriateness of these statistical conclusions was examined through testing of the ANOVA model to ensure adherence to model assumptions. Appropriate ANOVA models require homogeneity of residuals variance (homoscedasticity), normality of residuals and absence of outliers, examined here through the generation of standard diagnostic plots (**Figure 3.4**) (Kozak and Piepho 2018). Diagnostic plots demonstrated all assumptions were fulfilled here. The residuals demonstrated homoscedasticity and linearity in residuals vs fitted and scale-location plots (via production of horizontal trendlines), normality in distribution via Normal Q-Q plots (via adherence to the trendline), and a lack of highly influential outliers in the residuals vs leverage plot (via homogenous clustering of points). The ANOVA assumptions were thus well supported in this model, and conclusions drawn from the model considered valid.

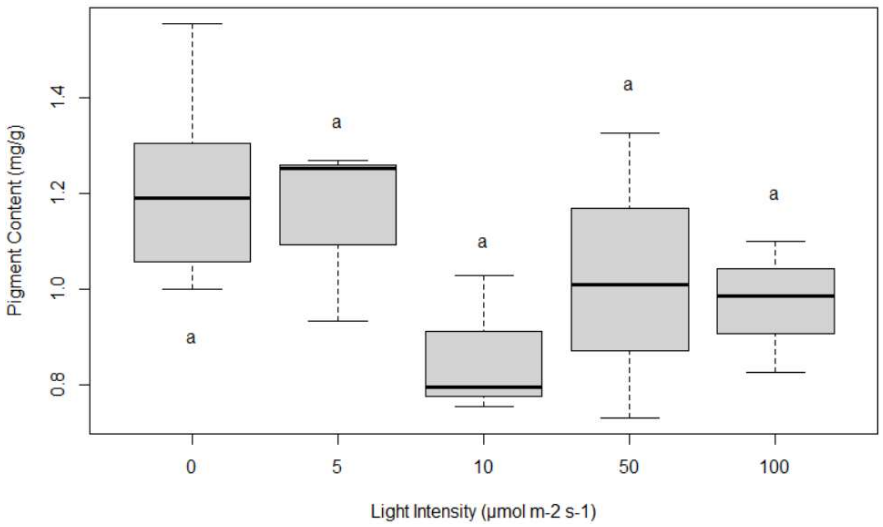

Figure 3.3: Tukey's boxplots demonstrating variability of pigment content produced by cultures of *Arthrobacter* sp. NamB2 grown at differing light intensities. Bold lines represent the median pigment content of each group. Letters denote the compact-letter display of significance groupings as determined via Tukey's HSD analysis. Boxplots annotated with the same letters are not statistically-significantly different from one another, while those of differing letters demonstrate significant differences ($p < 0.05$).

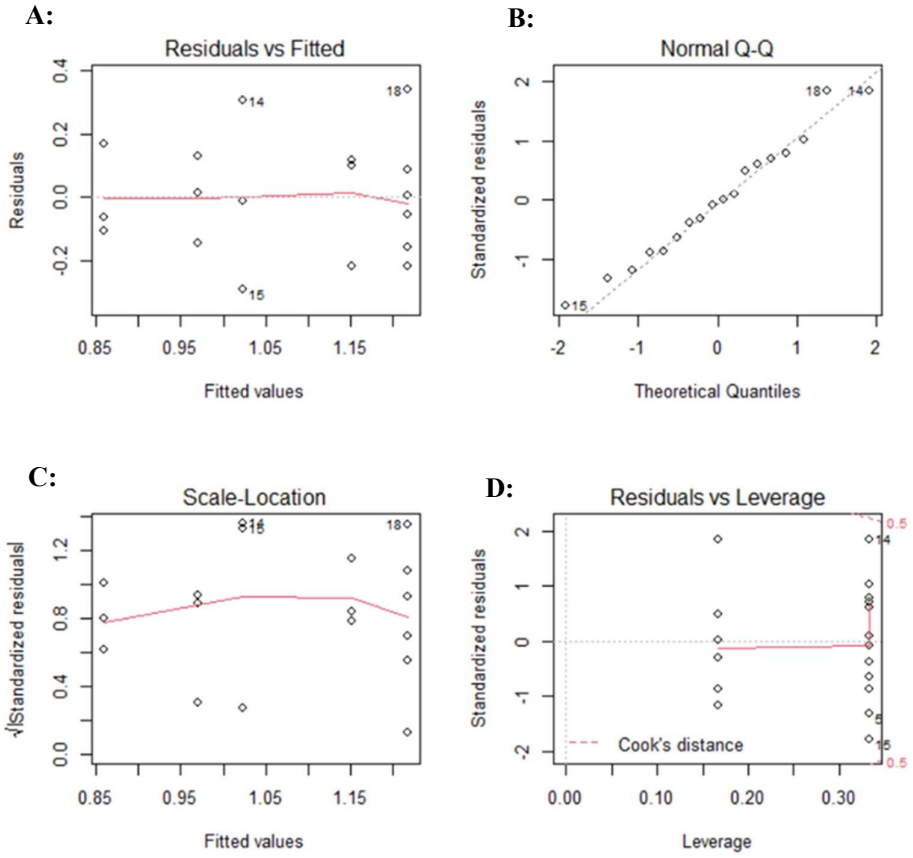

Figure 3.4: Diagnostic plots produced for the ANOVA model comparing total pigment content of *Arthrobacter* sp. NamB2 cultures grown at differing PAR light-intensities. **A:** Residuals vs Fitted diagnostic plot of residual's linearity and homoscedasticity. **B:** Normal Q-Q plot of residual's normality. **C:** Scale location plot regarding homoscedasticity of residuals. **D:** Residuals vs Leverage plot denoting the presence of highly influential values.

Table 3.2: Results of the ANOVA model examining the differences in mean pigment content produced by cultures grown under differing illumination conditions, as computed via R (R Core Team 2020).

	Degrees Of Freedom	Sum Of Squares	Mean (Sum Of Squares)	F-Value	P-Value
Sample	4	0.3194	0.07984	1.96	**0.16**
Residuals	13	0.5296	0.04074	-	-

3.3.2 Presence of Candidate Light-Responsive Carotenoid Regulators in *Arthrobacter* sp. NamB2

To examine if there was a genetic basis for light-responsive carotenogenesis in *Arthrobacter* sp. NamB2, its genome assembly was investigated for sequences encoding proteins similar to the known light-responsive regulator proteins CrtR, LitR, and *D. radiodurans'* bacteriophytochrome.

3.3.2.1 Identification of Candidate CrtR Sequences in *Arthrobacter* sp. NamB2

BLASTp of CrtR from *C. glutamicum* AJ1511 against the *Arthrobacter* sp. NamB2 protein transcript identified a series of sixteen hits. Of these, only three proteins of *Arthrobacter* sp. NamB2 presented protein sequence similarities to the CrtR regulator above 30 %. These sequences (TKV29755, TKV25909 and TKV29754) had all been annotated as 'MarR family transcriptional regulators'. Details of the BLASTp output scores of these three proteins against the CrtR of *C. glutamicum* AJ1511 is presented in **Table 3.3**.

Protein alignments between the three candidate CrtR proteins of *Arthrobacter* sp. NamB2 and the CrtR of *C. glutamicum* demonstrated that the greatest protein similarity occurred across amino acids 78 – 166 (*C. glutamicum* CrtR numbering, **Figure 3.5**). This region corresponds to the known DNA-binding winged helix-turn-helix (wHTH) domain which is conserved within regulators of the MarR family, and is responsible for their ability to bind DNA and exert transcriptional repression (Wilkinson and Grove 2006). This alignment further highlighted the almost uniform presence of invariant functional motifs of this wHTH domain within these candidate proteins, including $Lx_3Gx(V/I)xR$, DxR and L(T/S), denoted as green boxes within **Figure 3.5** (Perera and Grove 2010; Deochand and Grove 2017). This suggested that the CrtR

candidate proteins identified in *Arthrobacter* sp. NamB2 possessed the DNA-binding and regulatory activity of the general MarR regulatory family, and were therefore likely transcriptional regulators of this family (Perera and Grove 2010; Deochand and Grove 2017). Protein similarities between CrtR and these candidate proteins outside of the wHTH region was weaker, particularly over the first 60 amino acids. As the ligand-binding domain of CrtR is currently unknown, no specific comment may be made on its alignment here.

Table 3.3: Details of the BLASTp alignment scores of CrtR from *C. glutamicum* AJ1511 (BAV22458) (query sequence) against identified CrtR candidate proteins of *Arthrobacter* sp. NamB2 (subject sequences). Data for proteins where the similarity to CrtR was below 30 % are not presented. Candidate proteins from *Arthrobacter* sp. NamB2 are presented as their GenBank protein accession numbers.

***Arthrobacter* sp. NamB2 Candidate Protein**	**Alignment Score**	**Query Cover (%)**	**Similarity (%)**	**E Value**
TKV29755	68.2	72.0	33.10	2e-15
TKV25909	55.5	62.0	32.23	4e-11
TKV29754	52.0	76.0	32.89	1e-09

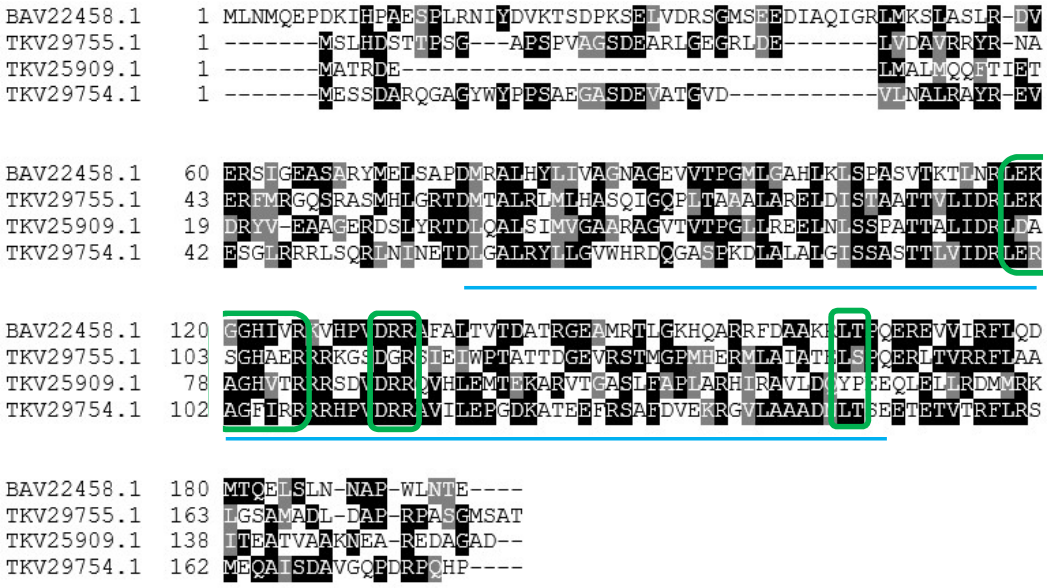

Figure 3.5*:* Protein sequence alignment of CrtR of *C. glutamicum* AJ1511 (GenBank; BAV22458) against the candidate CrtR protein sequences identified from *Arthrobacter* sp. NamB2 as denoted in **Table 3.3**. The protein region corresponding to the DNA-binding wHTH fold of MarR-type regulators is underlined in blue. Highly conserved motifs of the MarR family $Lx_3Gx(V/I)xR$, DxR, and L(T/S) within the wHTH fold are highlighted via green-boxes (Wilkinson and Grove 2006).

3.3.2.2 Genome Positions of CrtR Candidate Sequences

As the gene encoding CrtR must cluster closely with its regulated carotenoid-biosynthesis genes to exert regulatory control, a genome region some 10,000 base-pairs surrounding each gene encoding the identified CrtR candidate proteins (**Table 3.3**) upon the genome of *Arthrobacter* sp. NamB2 was examined for the presence of carotenoid genes. The proximity of candidate CrtR protein coding genes to carotenoid biosynthesis genes on the genome of *Arthrobacter* sp. NamB2 would provide supporting evidence of a functional role of these candidate proteins in the regulation of carotenoid biosynthesis.

BLASTn analyses using the carotenoid genes of *A. agilis* strain L77 characterised by Ii et al. (2019) as query sequences against the genome of *Arthrobacter* sp. NamB2 allowed the identification of the putative carotenoid gene cluster of *Arthrobacter* sp. NamB2. These BLASTn searches returned only a single hit each between the phytoene synthase and phytoene desaturase genes of *A. agilis* strain L77 and the genome of *Arthrobacter* sp. NamB2, identifying genes which were already annotated as encoding phytoene synthase and phytoene desaturase enzymes (locus tags FDK12_00535, FDK12_00540 respectively). The BLASTn scores were high for each of these alignments (gene sequence identities > 84 %, gene query covers > 95 %, E-values 0.0), granting high confidence in their shared identities. This analysis assigned the putative carotenogenesis gene cluster of *Arthrobacter* sp. NamB2 on contig one (GenBank: SZWI01000001) of its genome assembly, clustering between nucleotides 104,083 - 109,708 of this 795,432 nucleotide contig.

The genomic positions of genes encoding the candidate *Arthrobacter* sp. NamB2 CrtR proteins are given in **Table 3.4**. While genes encoding TKV29754 and TKV29755 were on the same contig as the putative carotenogenesis gene cluster, none of the three genes occurred within 10,000 bp of these carotenoid genes, instead consistently appearing greater than 100,000 bp distant. The candidate *ctrR* genes clustered instead with *Arthrobacter* sp. NamB2 sequences annotated as encoding ATP-binding cassette (ABC) transporter proteins (genes encoding TKV29754 and TKV29755) or mycobacterial membrane large (MMPL) family transport proteins (gene encoding TKV25909) on highly disparate regions of the genome. This lack of proximity to carotenoid genes indicated a lack of connection between the regulons of the identified CrtR candidates in *Arthrobacter* sp. NamB2 and the carotenoid-biosynthesis of this organism. This supported the earlier finding that pigment production is not light-responsive within *Arthrobacter* sp. NamB2.

Table 3.4: Genomic positions of genes encoding candidate *Arthrobacter* sp. NamB2 CrtR proteins. Protein accession numbers of candidate CrtR proteins correspond to those identified in **Table 3.3**.

***Arthrobacter* sp. NamB2 Protein Candidate**	**Locus Tag of Encoding Gene**	***Arthrobacter* sp. NamB2 Contig Containing the Encoding Gene**	**Contig Position of Gene (Nucleotides)**
TKV29755	FDK12_02285	Contig One (SZWI01000001)	500,202 – 499,654
TKV25909	FDK12_14640	Contig Ten (SZWI01000010)	29,821 – 30,291
TKV29754	FDK12_02280	Contig One (SZWI01000001)	499,580 – 499,041

3.3.2.3 Identification of LitR Candidates in *Arthrobacter* sp. NamB2

BLASTp analyses of the LitR regulators considered in **Table 3.1** against the protein transcript of *Arthrobacter* sp. NamB2 yielded only weak alignments, which were consistently below 30 % protein query coverage and 40 % protein sequence similarity. The LitR protein of *S. coelicolor* A3(2) failed to produce any significant alignment with proteins of *Arthrobacter* sp. NamB2. Only three proteins of *Arthrobacter* sp. NamB2 were identified with greater than 30 % protein similarity to the LitR regulators. These proteins; TKV25896, TKV30076 and TKV28253, have all been annotated as 'MerR-family transcriptional regulators', and were identified using the LitR protein sequence of *T. thermophilus* HB27 and HB8. Only TKV30076 was also identified using the LitR of *B. megaterium* as a query sequence. Details of the BLASTp outputs for the top scoring protein sequences identified in *Arthrobacter* sp. NamB2 when using the LitR protein sequence of *T. thermophilus* HB27 as the query are presented in **Table 3.5**.

The protein alignment of these candidate Lit sequences from *Arthrobacter* sp. NamB2 against the LitR protein sequence of *T. thermophilus* HB27 is shown in **Figure 3.6**. This alignment confirmed the poor similarity between the *Arthrobacter* sp. NamB2 sequences and the LitR of *T. thermophilus* HB27. The greatest similarity between protein sequences appeared over the first 100 amino-acids (*T. thermophilus* HB27 numbering), which corresponds to the helix-turn-helix (HTH) domain common to proteins of the MerR regulatory family, a domain required by regulators of this family to bind DNA and exert transcriptional repression (Brown et al. 2003). Minimal alignment with the candidate proteins occurred over the known light-responsive LitR

adenosylcobalamin (AdoB12) substrate-binding domain, and multiple conserved motifs of this domain were absent from all *Arthrobacter* sp. NamB2 protein candidates. These absent motifs included the AdoB12-binding motifs (M/L)xxVG, (D/E)xHExG and VxLSxV (**Figure 3.6**), indicating that the candidate proteins identified likely lacked the AdoB12 binding capacity of LitR (Ortiz-Guerrero et al. 2011; Takano et al. 2016). These alignments suggested that while these *Arthrobacter* sp. NamB2 candidate proteins were likely members of the MerR family, and are capable of DNA-binding and transcriptional repression consistent with members of this family, they lack the substrate binding domain of LitR regulators, and are incapable of binding AdoB12.

Table 3.5: Details of the BLASTp alignment of LitR from *T. thermophilus* HB27 (AAS82386) (query sequence) against identified LitR candidate proteins of *Arthrobacter* sp. NamB2 (subject sequences). Data for proteins where the similarity to LitR was below 30 % are not presented. Candidate proteins from *Arthrobacter* sp. NamB2 are presented as their GenBank protein accession numbers.

***Arthrobacter* sp. NamB2 Candidate Protein**	**Alignment Score**	**Query Cover (%)**	**Similarity (%)**	**E-Value**
TKV25896	43.5	29.0	33.33	1e-06
TKV30076	37.4	17.0	40.00	1e-04
TKV28253	35.0	24.0	31.58	0.003

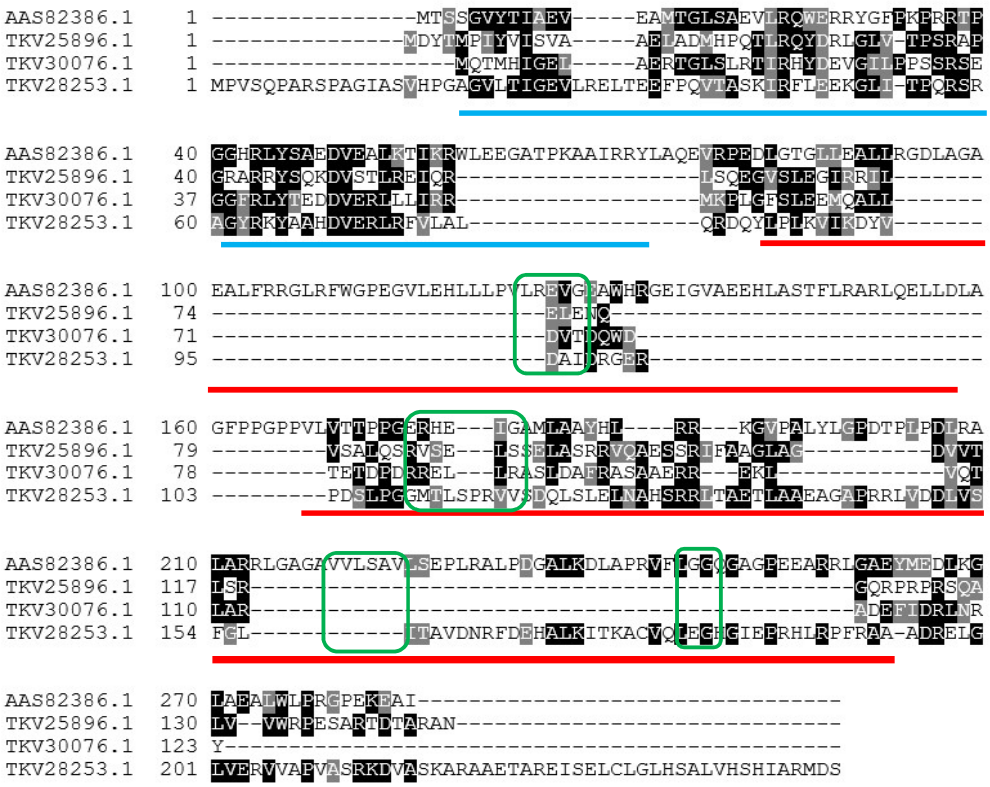

Figure 3.6: Protein sequence alignment of LitR from *T. thermophilus* HB27 (GenBank; AAS82386) with candidate LitR sequences identified from *Arthrobacter* sp. NamB2 as denoted in **Table 3.5**. Protein regions corresponding to the MerR-family HTH DNA-binding domain and the LitR ligand-binding, light-responsive domain are underlined in blue and red respectively. Conserved motifs with function in AdoB12 ligand binding within LitR are outlined in green, and are (in order) (M/L)xxVG, (D/E)xHExG, VxLSxV, and GG (Ortiz-Guerrero et al. 2011).

3.3.2.4 Genome Positions of LitR Candidate Sequences

Similar to *ctrR*, genes encoding *litR* regulators occur within 10,000 base-pairs of the carotenoid genes they control (Takano, Beppu, et al. 2006; Ortiz-Guerrero et al. 2011; Takano 2016; Sumi et al. 2020). As such, a genomic region some 10,000 base-pairs surrounding each gene encoding the candidate LitR proteins on the *Arthrobacter* sp. NamB2 genome was examined for the presence of carotenoid genes, to determine whether these identified homologues were likely to exert regulation on carotenogenesis. The contig-positions of genes encoding these identified LitR candidate proteins within *Arthrobacter* sp. NamB2 are given in **Table 3.6**. While the gene encoding TKV30076 was on the same contig as the putative carotenoid genes, none of the genes encoding LitR candidates were present within 10,000 bp of the carotenogenic gene cluster of *Arthrobacter* sp. NamB2. The genes encoding candidate LitR proteins instead clustered with genes annotated as encoding short-chain dehydrogenase family oxidoreductases (TKV30076), heat shock proteins (TKV25896) or nucleases (TKV28253). These findings were similar to

those of CtrR, and suggested that while these candidate proteins are likely MerR-family regulators, their regulons are likely unlinked to carotenogenesis. This further supported the lack of light-responsive carotenoid biosynthesis in *Arthrobacter* sp. NamB2.

Table 3.6: Genomic positions of genes encoding candidate *Arthrobacter* sp. NamB2 LitR proteins. Protein accession numbers of candidate LitR proteins correspond to those identified in **Table 3.5.**

***Arthrobacter* sp. NamB2 Candidate Protein**	**Locus Tag of Encoding Gene**	***Arthrobacter sp. NamB2* Contig Containing the Encoding Gene**	**Contig Position of Gene (Nucleotides)**
TKV25896	FDK12_14575	Contig Ten (SZWI01000010)	15,824 – 15,384
TKV30076	FDK12_03555	Contig One (SZWI01000001)	722,309 – 772,680
TKV28253	FDK12_09855	Contig Four (SZWI01000004)	261,622 – 260,873

3.3.2.5 Identification of Bacteriophytochrome Candidates in *Arthrobacter* sp. NamB2

Only a single bacteriophytochrome has been highlighted in relation to light-responsive carotenoid biosynthesis, being that of *D. radiodurans* (Davis et al. 1999). BLASTp of this bacteriophytochrome protein (AAF12261) against the *Arthrobacter* sp. NamB2 protein transcript identified 14 protein hits, but only two with greater than 30 % protein similarity. These proteins (TKV27492 and TKV29091) were both annotated as histidine kinase (HK)-domain containing sensor proteins. Protein similarities and query coverages were poor between the bacteriophytochrome of *D. radiodurans* and candidate sequences of *Arthrobacter* sp. NamB2, as presented in the BLASTp alignment output of **Table 3.7**.

Protein alignments between these *Arthrobacter* sp. NamB2 candidate proteins and the *D. radiodurans* bacteriophytochrome are presented in **Figure 3.7**, and demonstrate that protein similarity between these sequences was restricted to the C-terminal region of the bacteriophytochrome. Strong alignments between the candidate proteins and the bacteriophytochrome consistently started at amino acid 530 of the 755 amino acid *D. radiodurans* bacteriophytochrome, with only minor similarity observed prior to this region. Protein sequences corresponding to functionally-important phytochrome domains within the bacteriophytochrome of *D. radiodurans* demonstrated weak alignment with protein homologues

of *Arthrobacter* sp. NamB2. This alignment suggested that the similarity between the bacteriophytochrome and these candidate sequences was exclusive to the histidine kinase domain, and that none of the functional phytochrome domains of the *D. radiodurans* bacteriophytochrome were present within the candidate proteins of *Arthrobacter* sp. NamB2 (Davis et al. 1999). As the phytochrome domains of bacteriophytochromes are highly conserved, and required for light-responsive activity of the regulator, their absence from the candidate proteins of *Arthrobacter* sp. NamB2 indicated that these proteins were not bacteriophytochromes, and were thus unlikely to possess light-responsive activity (Bhoo et al. 2001; Wagner et al. 2008). This supported the lack of light-responsive carotenogenesis in *Arthrobacter* sp. NamB2.

Table 3.7: Details of the BLASTp alignment of the bacteriophytochrome of *D. radiodurans* (AAF12261) (query sequence) against bacteriophytochrome candidate proteins of *Arthrobacter* sp. NamB2 (subject sequences). Data for proteins where the similarity to the bacteriophytochrome was below 30 % are not presented. Candidate proteins from *Arthrobacter* sp. NamB2 are presented as their GenBank protein accession numbers

***Arthrobacter* sp. NamB2 Candidate Protein**	**Alignment Score**	**Query Cover (%)**	**Similarity (%)**	**E Value**
TKV27492	93.2	32.0	30.04	3e-21
TKV29091	89.4	40.0	31.30	7e-20

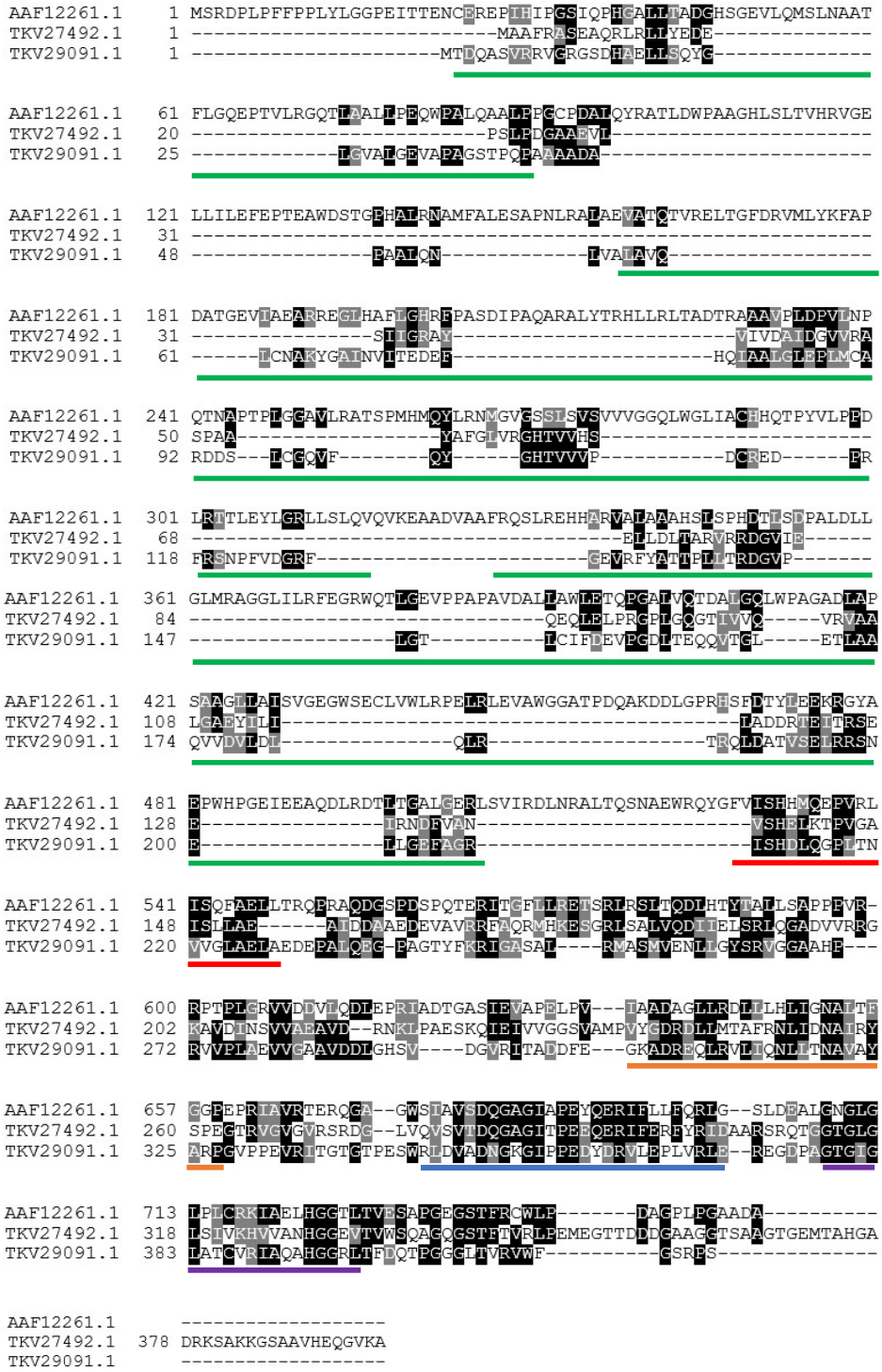

Figure 3.7: Protein sequence alignment of the bacteriophytochrome of *D. radiodurans* (GenBank; AAF12261) with candidate bacteriophytochrome sequences from *Arthrobacter* sp. NamB2 as denoted in **Table 3.7**. Protein regions corresponding to the conserved domains of the phytochrome-photosensory core of the *D. radiodurans* bacteriophytochrome are underlined in green, while the conserved H- N- D/F- and G-boxes of histidine kinase proteins are underlined in red, brown, blue and purple, respectively (Davis et al. 1999).

3.4 Discussion

Light-responsive carotenoid production in non-phototrophic bacteria suggests a photoprotective function for their carotenoids (Takano, Asker, et al. 2006; Takano 2016). Given the previous demonstration of environmentally-responsive carotenogenesis by *Arthrobacter* in the literature, and the suspected contribution of *Arthrobacter* sp. NamB2's bacterioruberin pigment to its irradiation resistome, the light-inducibility of pigmentation in this organism was investigated to examine its speculative function in photoprotection. This chapter thus quantified and compared the total pigment content of *Arthrobacter* sp. NamB2 cultures grown under differing light intensities to determine whether carotenoid production was demonstrably light-responsive. To relate these results to genomic observations, the genome of *Arthrobacter* sp. NamB2 was examined to identify sequences encoding candidate light-responsive regulator proteins as a means to determine a possible mechanism by which light-inducibility might occur.

3.4.1 Light Inducibility Assays of Pigmentation in *Arthrobacter* sp. NamB2

Pigment production in *Arthrobacter* sp. NamB2 does not appear to be light-inducible. Cultures grown under a range of different PAR intensities showed no significant differences in total pigment content from one another, nor from dark-grown cultures. These results demonstrated that the production of carotenoid pigmentation by *Arthrobacter* sp. NamB2 was not light-responsive at the PAR intensities investigated. Previous studies demonstrating light-inducibility of pigmentation in non-phototrophic bacteria have observed statistically significant differences in the pigment content of cells grown at the light-intensities examined here (Sutthiwong and Dufossé 2014). Indeed, significantly higher carotenoid content occurred in *M. xanthus* and *T. thermophilus* grown at 4.0 and 45.7 μmol m^{-2} s^{-1} (respectively) compared to dark-grown cells, while *D. radiodurans* has demonstrated linear increases in carotenoid content at increasing PAR intensities up to 100 μmol m^{-2} s^{-1} (Burchard and Hendricks 1969; Davis et al. 1999; Ortiz-Guerrero et al. 2011). For many soil organisms, pigmentation is exclusive to cultures irradiated at 2.4 μmol m^{-2} s^{-1} PAR or higher (Takano et al. 2005; Takano et al. 2011; Takano et al. 2015; Sumi et al. 2019). While the inducibility of pigmentation at higher light intensities cannot be excluded, its absence at light intensities routinely described in the literature and demonstrated to induce pigmentation in other bacteria strongly suggests that pigment production in *Arthrobacter* sp. NamB2 is not light-inducible.

Quantitative differences in pigment content observed between differently-illuminated cultures of *Arthrobacter* sp. NamB2 were also notably below those magnitudes expected for induced carotenogenesis. Organisms presenting light-induced carotenogenesis often demonstrate increases in carotenoid content under light-irradiation of magnitudes three – five-fold compared to dark-grown cultures (Burchard and Dworkin 1966; Howes and Batra 1970; Bhosale 2004; Vega et al. 2016). For example, in the closely related *Glutamicibacter arilaitensis* (previously *Arthrobacter arilaitensis*), light irradiation causes four-fold increases in mean carotenoid content (0.2 – 0.8 mg/g), while the temperature-induced carotenogenesis of *A. agilis* observes a seven-fold increase in mean carotenoid content (0.17 – 1.2 mg/g) (Fong et al. 2001; Sutthiwong and Dufossé 2014). In the current analysis, no irradiated culture presented carotenoid content significantly different from dark grown cultures. Furthermore, the minor differences in mean carotenoid content between dark grown cultures and those grown under irradiation (below 0.36 mg/g in all comparisons) were notably below literature expectations of light-induction, and reflected the lack of significant light-responsive carotenogenesis in *Arthrobacter* sp. NamB2.

The lack of light-responsive carotenogenesis in *Arthrobacter* sp. NamB2 is not unexpected, as this phenomenon is relatively uncommon in non-phototrophic bacteria (van der Horst et al. 2007). Indeed, of the 1,100 soil isolates screened by Sumi et al. (2019), only 24 exhibited light-responsive carotenoid production. Similarly, only 70/375 species of *Streptomyces* demonstrated light-responsive pigmentation (Kato et al. 1995). Furthermore, while close relatives of *Arthrobacter* are capable of light-responsive carotenogenesis, including *Paenarthrobacter aurescens* (previously *Arthrobacter aurescens*), *G. arilaitensis* (previously *Arthrobacter arilaitensis*), *Paenarthrobacter ureafaciens* (previously *Arthrobacter ureafaciens*) and *Pimelobacter simplex* (previously *Arthrobacter simplex*), no examined species of genus *Arthrobacter* (*A. agilis*, *Arthrobacter* sp. 21022 and *Arthrobacter* sp. PAMC 25486) retains this phenomenon (Koyama et al. 1974; Sutthiwong and Dufossé 2014; Busse 2016; Tescari et al. 2018; Sumi et al. 2019). The sparse distribution of light-inducible carotenogenesis in non-phototrophic bacteria, combined with the lack of prior evidence of light-inducibility within the *Arthrobacter* genus, makes the lack of light-responsive carotenoid production by *Arthrobacter* sp. NamB2 unsurprising, if a contribution to our understanding of light-responsive pigmentation in this genus.

The lack of light-inducibility of pigmentation in *Arthrobacter* sp. NamB2 does not discount its potential photoprotective role. A variety of organisms demonstrate the use of carotenoids for photoprotection, but lack light-inducibility in biosynthesis. For example, *Haloarchaea* use bacterioruberin as a protective carotenoid against PAR and UV-irradiation, but light-responsive

carotenogenesis within this genus is rare (Rodriguez-Valera et al. 1982; Calegari-Santos et al. 2016; Vega et al. 2016). The fellow *Micrococcaceae K. rosea* similarly relies on its carotenoid pigmentation for protection from broad-spectrum solar irradiation, but lacks light-inducibility (Pezzoni et al. 2011; Vinay Kumar et al. 2015; Sumi et al. 2019). Further examples exist in organisms including *Rhodobacter sphaeroides*, and various species of *Flavobacterium* (Weeks et al. 1973; Koyama et al. 1974; Glaeser and Klug 2005). Lack of light-inducibility therefore does not rule out the photoprotective function of the carotenoids within *Arthrobacter* sp. NamB2 (Eisenstark 1998; Matallana-Surget and Wattiez 2013).

3.4.1.1 Limitations of the Light Inducibility Investigation

3.4.1.1.1 Light Emission Spectra

Irradiation wavelengths used in studies of light-inducibility are important to consider, as light-responsive regulators often display exclusive activities within specific wavelength ranges (Nitzan and Kauffman 1999; Björn 2015b; Protti et al. 2019; Kotilainen et al. 2020). For example, both LitR and CrtR regulators are responsive to blue light (400 – 460 nm) but not red light (600 – 700 nm) (Takano et al. 2005; Takano et al. 2015; Sumi et al. 2019). Conversely, the bacteriophytochrome of *D. radiodurans* relies on red light for its induction of carotenoid synthesis (Davis et al. 1999; Wagner et al. 2008; Kaminski et al. 2009; Battocchio et al. 2020). To ensure light inducibility is detected, a broad wavelength light source should thus be used to ensure regulator stimulation.

Here, a white LED bulb was used for irradiation. While the emission spectrum of this bulb was not measured, analogous OSRAM white LED bulbs are known to produce emission spectra with responses peaking at 450 nm, but maintaining a high intensity across the entire visible region (Abdel-Rahman et al. 2017; Kim et al. 2018; Tosini et al. 2016). Successful light-inducibility studies with LitR and CrtR consistently use low-intensity light from fluorescent bulbs, which produce unequal emission spectra with strong responses at 400 – 500 nm, followed by a series of discrete, high intensity peaks at 550 and 630 nm, and minimal emission towards 700 nm (Takano et al. 2005; Chignell et al. 2008; Takano et al. 2011; Takano et al. 2015; Abdel-Rahman et al. 2017; Retzlaff et al. 2017; Sumi et al. 2019; Tosini et al. 2016). The restricted nature of the emission spectra from fluorescent bulbs, combined with their tacit suitability for stimulation of light-responses in recently published papers, suggests that the stronger and wider spectral emission as provided by the LED bulb employed in this study

should be sufficient to stimulate responses reliant on visible-spectrum wavelengths. Direct measurement of the spectral emission of the lamp used here at the level of the cells via spectrometer would ensure the wavelength ranges to which the cells are exposed are correct, as opposed to the reliance on secondary sources (Chignell et al. 2008; Abdel-Rahman et al. 2017). Furthermore, the use of known light-inducible carotenogenic organisms as controls (i.e. *C. glutamicum* AJ1511 or *S. coelicolor* A3(2)) grown under the same conditions as *Arthrobacter* sp. NamB2 would have confirmed the emission spectra here as valid in light-inducible regulator stimulatory capacity (Takano 2016).

3.4.2 Presence of Candidate Light-Responsive Carotenoid Regulators in *Arthrobacter* sp. NamB2

Arthrobacter sp. NamB2's genome assembly was investigated for the presence of genes encoding proteins similar to CrtR, LitR and the *D. radiodurans* bacteriophytochrome – known light-responsive carotenogenesis regulators from non-phototrophic bacteria. This was used to determine whether there was any genetic basis for light-responsive carotenogenesis within *Arthrobacter* sp. NamB2. While a number of proteins producing significant alignments with these known regulators were identified via BLASTp analyses, protein similarities were generally low (30 – 40 %), and genomic context of their encoding genes relative to the putative carotenoid genes of *Arthrobacter* sp. NamB2 did not support their role in the regulation of carotenogenesis (Takano, Beppu, et al. 2006; van der Horst et al. 2007). Furthermore, specific protein alignments demonstrated several of the candidate proteins lacked important conserved domains of the light-responsive carotenoid regulators, suggesting they differ in function or regulons.

3.4.2.1 Dismissal of Candidate Regulator Proteins

The CtrR candidate proteins identified within *Arthrobacter* sp. NamB2 appeared to belong to the MarR family of regulators, the same regulatory protein family containing CrtR (Sumi et al. 2019). This was concluded from the uniform conservation of the MarR-family DNA-binding wHTH fold within these candidate proteins, suggesting that these proteins were capable of transcriptional regulation consistent with the MarR-family (Deochand and Grove 2017). As proteins of the MarR regulatory family are known to control a variety of stress responses, their presence did not imply that these candidate genes were related to the control of carotenoid biosynthesis (Panina et al. 2003; Guerra et al. 2011; Deochand and Grove 2017). MarR-family

regulators are known to exclusively regulate genes within the immediate proximity of their encoding genes (Alekshun et al. 2001; Wilkinson and Grove 2006; Perera and Grove 2010; Deochand and Grove 2017). The genes encoding the candidate CrtR homologs were not proximal to the putative carotenoid biosynthesis genes of *Arthrobacter* sp. NamB2 on the genome, but instead clustered with genes well-characterised as being under MarR regulation in bacterial stress response pathways unrelated to carotenogenesis, such as those encoding ABC-transporters and MMPL-fold proteins (Panina et al. 2003; Ballal and Manna 2010; Guerra et al. 2011; Hillion and Antelmann 2015; Deochand and Grove 2017; Colson et al. 2020). Therefore, the candidate proteins identified were likely MarR-family regulators controlling the expression of these latter genes, and were thus unrelated to light-inducibility of carotenoid biosynthesis (Panina et al. 2003; Ballal and Manna 2010; Guerra et al. 2011; Hillion and Antelmann 2015; Deochand and Grove 2017; Colson et al. 2020).

Consequently, the CrtR candidate proteins of *Arthrobacter* sp. NamB2 were likely identified as CrtR homologs on the basis of the common presence of the MarR-family DNA-binding domain. Genome positions of genes encoding these homologues suggested their regulons as unrelated to those involved in carotenoid biosynthesis. These proteins were thus dismissed from relevance to light-responsive carotenoid production in *Arthrobacter* sp. NamB2.

The LitR candidate proteins of *Arthrobacter* sp. NamB2 are likely members of the MerR family of transcriptional regulators, the same regulator-protein family as LitR (Takano 2016). MerR-family regulators all possess a highly conserved N-terminal helix-turn-helix (HTH) domain which is used to facilitate DNA-binding, a domain which was similarly identified in the candidate LitR proteins of *Arthrobacter* sp. NamB2 (Brown et al. 2003; Hobman 2007; Ortiz-Guerrero et al. 2011). However, the alignment between the candidate LitR protein sequences of *Arthrobacter* sp. NamB2 and the substrate/AdoB12-binding domain of LitR was weak (**Figure 3.6**) and *Arthrobacter* sp. NamB2 homologues further lacked a number of conserved motifs known to be required for AdoB12-binding (Takano et al. 2016). As it is the C-terminal, AdoB12-binding domain which is distinctive of LitR regulators, and is required for LitR to exert a light-response, its absence from the *Arthrobacter* sp. NamB2 candidate proteins indicates they lack light-responsive activity, and are thus likely unrelated to LitR (Takano, Beppu, et al. 2006; Sjuts et al. 2013; Takano 2016; Takano et al. 2016). Further, the genes encoding these candidate proteins did not cluster with carotenoid genes (as required for MerR regulatory action), and instead clustered with carboxylase and heat-shock protein genes, genes that are known to be under MerR-regulation in other bacterial stress-response pathways (Yura et

al. 1993; Baranova et al. 1999; Brown et al. 2003; Harrison 2003; Maleki et al. 2016; Roncarati and Scarlato 2017; Sumi et al. 2018).

As such, the LitR-homologues identified within *Arthrobacter* sp. NamB2 were likely MerR regulators unrelated to light-mediated regulation of carotenoid genes. This was concluded on the basis of their poor-alignment with LitR's light-responsive substrate-binding domain, and absence of genomic clustering with suspected carotenoid genes, as is required for LitR regulators (Takano 2016).

Bacteriophytochrome proteins all possess an N-terminal photosensory core, containing multiple conserved regions required to bind the light-responsive chromophore and confer light-responsive activity (Bhoo et al. 2001). For signal transmission following light-absorption, bacteriophytochrome proteins utilise a C-terminal, two-component histidine-kinase (HK) system (Bhoo et al. 2001; Wagner et al. 2008; Cheung and Hendrickson 2010; Björling et al. 2016; Battocchio et al. 2020). The *D. radiodurans* bacteriophytochrome adheres to this structure, containing a series of light-responsive conserved domains within its N-terminal photosensory core, and a C-terminal HK domain (Wagner et al. 2008; Burgie et al. 2016; Multamäki et al. 2020). Alignments between the *D. radiodurans* bacteriophytochrome and *Arthrobacter* sp. NamB2 candidate proteins almost exclusively occurred over the C-terminal region, and corresponded only to the HK domain of the bacteriophytochrome (Davis et al. 1999; Yoon et al. 2008). These candidate proteins of *Arthrobacter* sp. NamB2 were thus likely identified as homologues of the *D. radiodurans* bacteriophytochrome on account of their HK domain. However, as they evidently lack the photosensory domains of bacteriophytochromes, they are incapable of similar light-responsive activity. This suggests that these proteins were not bacteriophytochromes, but simply other HK-utilising proteins (Bhoo et al. 2001; Cheung and Hendrickson 2010; Auldridge and Forest 2011). Histidine kinase domains are common within bacterial proteins involved in cellular signalling, including proteins which mediate chemotaxis, temperature responses and redox-sensors, of which bacteriophytochromes are only a subclass (Albanesi et al. 2009; Bogel et al. 2009; Kirby 2009; Cheung and Hendrickson 2010).

As such, *Arthrobacter* sp. NamB2 does not appear to produce a bacteriophytochrome, thus consequently lacks a comparable light-responsive carotenogenesis system to that of *D. radiodurans*.

3.4.2.2 *Arthrobacter* sp. NamB2 Lacks Known Light-Induced Carotenoid Regulators

Arthrobacter sp. NamB2 did not possess relevant homologues to known light-responsive carotenogenesis regulators from other non-phototrophic bacteria. These findings reinforced the negative conclusions of the light-inducibility assays, and were unsurprising given the rarity of these regulatory systems in non-phototrophic soil bacteria (Takano, Asker, et al. 2006; Takano 2016).

Most soil bacteria produce carotenoids constitutively (Takano, Asker, et al. 2006). This is attributed to the instability of transcriptional regulators of carotenogenesis within bacteria (Krügel et al. 1999; Lee et al. 2001; Takano 2016). The loss of carotenoid regulatory genes is well-reported, particularly in regards to light-inducible carotenogenesis regulators. In *Actinobacteria*, light-responsive carotenogenesis is unstable, with organisms such as *Streptomyces* losing these regulatory systems at high frequencies (Kato et al. 1995; Krügel et al. 1999; Takano 2016). This loss has been attributed to the localisation of carotenoid-regulatory genes in low-conservation regions of the genome (Lee et al. 2001). Indeed, the study of Phadwal (2005), modelling the evolution and conservation of carotenoid genes, demonstrated that carotenoid regulatory genes (including those mediating light-responses) present poor conservation, and high rates of non-synonymous mutation. This poor conservation, combined with the frequent disruptive horizontal-transfer of carotenoid genes occurring throughout their dissemination and evolution, means the loss of light-responsive carotenoid regulators is a relatively unsurprising phenomenon (Phadwal 2005; Klassen 2010; Takano 2016).

As such, the lack of light-responsive carotenoid regulators within the genome of *Arthrobacter* sp. NamB2 was not unexpected here, considering the low prevalence of these systems within characterised bacteria, and their instability in genomic maintenance. These findings supported those of the light-inducibility assays, and further reinforced the lack of light-responsive carotenogenesis within *Arthrobacter* sp. NamB2.

3.4.3 Limitations of Genetic Analysis

3.4.3.1 The Carotenogenesis Gene Cluster is Unproven

Dismissal of the candidate regulator proteins for LitR and CrtR in this analysis was based partially on the lack of proximity between their encoding genes and the carotenoid biosynthesis gene cluster of *Arthrobacter* sp. NamB2. However, this carotenoid gene cluster has not been functionally demonstrated, but was rather inferred based on comparisons to the gene cluster of *A. agilis* strain L77, which itself is unproven, and was in turn identified on the basis of gene orthology to *Micrococcus luteus* (Ii et al. 2019). Until the location and function of the carotenogenesis genes within *Arthrobacter* sp. NamB2 are confirmed, these candidate carotenoid regulators cannot be completely dismissed, as their proximity to the carotenogenesis genes is uncertain certain. Confirmation of this gene cluster in *Arthrobacter* sp. NamB2 as carotenogenic would require functional demonstrations of the role of each individual gene in carotenoid biosynthesis. This could be achieved similarly to prior studies demonstrating carotenogenic pathways through individual gene knockouts, followed by subsequent biochemical characterisations of changes in the overall carotenoid complement (Krubasik et al. 2001; Yang et al. 2015). Demonstrating the position of carotenoid genes within *Arthrobacter* sp. NamB2 would strengthen the conclusions drawn here regarding their proximity to regulatory genes.

3.4.4 Future Directions of Study

3.4.4.1 Transcriptional Analyses

This chapter concluded on the nature of light-responsive carotenogenesis in *Arthrobacter* sp. NamB2 by examining evidence of the expected end-product of this phenomenon (quantitative shifts in total pigment content) as opposed to its specific mechanism. As light-responsive carotenogenesis is a transcriptional response, this study may have been made more comprehensive through examining changes in the expression of carotenoid biosynthetic genes following light-exposure (Takano et al. 2015; Sumi et al. 2019). Quantitative reverse transcription polymerase chain reaction (RT-qPCR) could be used to examine the upregulation of carotenoid genes upon exposure of *Arthrobacter* sp. NamB2 to irradiation, as has been performed by other studies within the field (Takano et al. 2005; Takano et al. 2011; Sumi et al.

2018). Such analyses would be constrained by lack of specific knowledge of carotenoid genes in *Arthrobacter* sp. NamB2 as outlined above since genes mediating carotenogenesis have not been explicitly demonstrated within *Arthrobacter*. Examinations using RT-qPCR would thus either require the assumption that the carotenogenesis gene cluster identified here is correct or would necessitate functional demonstrations (as per **Section 3.4.3.1)** prior to transcriptional analyses of this nature.

Phytoene desaturase would be of particular interest in transcriptional analyses here. Phytoene desaturase (encoded by the gene *crtI*), catalyses the conversion of phytoene to lycopene, the first committed step of bacterial carotenogenesis (Moise et al. 2014). The importance of this gene in carotenoid biosynthesis means it is tightly regulated, and thus a common target of light-inducible repressors (Moise et al. 2014; Llorente 2016). Indeed, the light-responsive regulatory systems of organisms such as *C. glutamicum* and *B. megaterium* act directly upon the *crtI* promoter, with 5 – 45 fold increases in *crtI* expression occurring upon exposure of these organisms to light (Sandmann 1995; Takano et al. 2015; Avalos et al. 2017; Sumi et al. 2019; Marente et al. 2020). Consequently, *crtI* would serve as an important starting point in the examination of *Arthrobacter* sp. NamB2's potential genetic light inducibility.

3.4.4.2 Light-Responsive Shifts in Pigment Composition

The analysis of light-responsive carotenogenesis presented here was limited to comparisons of the total pigment content produced by cultures irradiated at differing PAR intensities, consistent with recent studies within this field. However, further physiological information may have been provided by examining the specific pigment complements of these cultures.

Environmentally responsive carotenogenesis occurs as an adaptation to physiological stress, and can involve shifts in pigment composition as opposed to quantitative changes in total carotenoid content (Chattopadhyay and Jagannadham 2001). For example, the pigment complement of *K. rosea* shifts to favour higher proportions of glycosidic bacterioruberins when moved from growth at 20 to 5 ℃, while *Sphingobacterium antarcticus* shifts from production of a diverse pigment complement to almost exclusively zeaxanthin under the same conditions, both phenomena being linked to the strong membrane-stabilising capacity of the carotenoids induced under these reduced temperatures (Jagannadham et al. 1991; Chattopadhyay et al. 1997; Jagannadham et al. 2000). While light-responsive shifts in carotenoid compositions are lacking study, there is some precedence, with *Dunaliella bardawil* producing a carotenoid composition

when exposed to UVA/visible light irradiation different from those of dark grown cells, and which possesses a stronger absorbance within the 350 – 400 nm wavelength region (Jahnke 1999; Battocchio et al. 2020). This response is attributed to the UVA screening potential of these induced carotenoids, and is considered a direct physiological adaptation to irradiation (Jahnke 1999; Battocchio et al. 2020). Modelling these shifts in carotenoid composition can thus be informative to physiological adaptive roles of carotenoids.

The limited resolution of UV-visible spectroscopy applied here was insufficient to draw conclusions regarding shifts in carotenoid compositions which may have accompanied the growth of *Arthrobacter* sp. NamB2 under differing light conditions (Britton et al. 1995b; Kopec et al. 2012). While outside of the scope of the current study, it may be physiologically informative to examine any shift in the composition of the carotenoid complement of *Arthrobacter* sp. NamB2 induced by variable light conditions. Such analyses would explore physiologically-relevant light-responsive carotenoid biosynthesis outside of quantitative shifts in total carotenoid content. Similarly to **Chapter 2**, these analyses would require the directed separation/analysis of the pigment complement of *Arthrobacter* sp. NamB2 grown under differing illuminance conditions via the employ of HPLC, with subsequent structural elucidation of carotenoid identities through mass-spectrometry, alongside quantifications of the abundance of each individual carotenoid species as a proportion of the overall complement (Kopec et al. 2012).

3.4.4.3 Photoprotective Capacity and UV

Protective roles of pigments against irradiation at a particular wavelength may be partially supported through biosynthetic inducibility at that wavelength (Cockell and Knowland 1999). As the pigmentation of *Arthrobacter* sp. NamB2 is speculated elsewhere in this thesis to provide protection from UV-irradiation, investigations of its UV-inducibility may be valuable to support this protective function. Prior studies have demonstrated carotenoid production in direct response to UV-irradiation in algae and archaea, with *D. bardawil* known to accumulate higher concentrations of carotenoids under UVA, and *Sulfolobus solfataricus* and *Sulfolobus acidocaldarius* demonstrating short-term, two-fold upregulation of carotenoid genes in response to UVC (Grogan 1989; Jahnke 1999; Götz et al. 2007; Lao et al. 2011). Specific UV investigations here were precluded by the lack of availability of closed-growth vessels allowing full UV-spectrum penetration over accepted multi-day periods of carotenogenesis induction, without stimulating contamination (Jahnke 1999; Libkind et al. 2004). Examining the potential

for induction of carotenogenesis by wavelengths below 400 nm in *Arthrobacter* sp. NamB2 may further aide in understanding the photoprotective inducibility of its pigmentation.

3.5 Conclusions and Next Steps

Photoinducibility of carotenogenesis suggests the use of carotenoids as photoprotectants in non-phototrophic bacteria (Browning et al. 2003; Purcell and Crosson 2008). To investigate the hypothesised photoprotective function of carotenoids in *Arthrobacter* sp. NamB2, this chapter examined evidence of photoinducibility in the biosynthesis of its carotenoid pigmentation.

The results presented within this chapter indicate that carotenogenesis is not light-induced within *Arthrobacter* sp. NamB2 at the light intensities examined. This was determined through the lack of significant differences observed between the total carotenoid content produced by *Arthrobacter* sp. NamB2 cultures grown under light conditions known to induce carotenogenesis in related organisms. Genomic investigations of *Arthrobacter* sp. NamB2 further concluded it lacked equivalent regulators to those known in other organisms to control light-responsive carotenogenesis, reinforcing the absence of light-inducible pigmentation observed. These findings were unsurprising given comparisons to other studies within the genus, and the overall prevalence of light-responsive carotenogenesis in soil bacteria (van der Horst et al. 2007; Takano et al. 2016; Tescari et al. 2018; Sumi et al. 2019). As discussed, light-responsive carotenogenesis is poorly explored within both the genus *Arthrobacter* and within edaphic desert bacteria, and this study thus provides novel contributions to our understanding of this phenomenon within these organisms. While this study also represents (to the author's knowledge) the first characterisation of light-inducibility of carotenoid production in a non-phototrophic desert organism, it was insufficient in scope to constitute a meaningful analysis of the prevalence of this phenomenon within the desert environment.

While light-responsive carotenogenesis does support the photoprotective function of carotenoids, its absence does not rule out this as a function of *Arthrobacter* sp. NamB2's pigmentation. As noted, a variety of organisms which utilise carotenoids as PAR or UV protectants (including those specifically reliant on bacterioruberin) produce carotenoids constitutively. As such, the contribution of pigmentation in *Arthrobacter* sp. NamB2 to its irradiance-resistome is still worthy of investigation. The protective function of this pigmentation against UV-irradiation is examined further in **Chapter 4.**

Chapter 4 Contribution of Pigmentation to the Ultraviolet-Resistome of *Arthrobacter* sp. NamB2

4.1 Introduction

4.1.1 Desert Solar Irradiation and Carotenoid Protection

As deserts are subject to biologically stressful irradiance, the persistence of their indigenous bacteria is strongly determined by their ability to avoid or mitigate radiation damage (Cary et al. 2010; Cowan et al. 2011; Chan et al. 2012; Meslier et al. 2018). Consequently, solar irradiation significantly influences the composition and distribution of desert edaphic bacterial communities (Cary et al. 2010; Cowan et al. 2011; Di Capua et al. 2011; Chan et al. 2012; Fernández-Zenoff et al. 2014). Furthermore, the UV-tolerance and complexity of irradiation resistomes is consistently greater in bacteria isolated from desert environments than those of more temperate conditions, resulting from the selection exerted by solar-irradiation for the development of such robust survival systems (Dsouza et al. 2015; Albarracín et al. 2016; Pavlopoulou et al. 2016). Amongst the solar-protective mechanisms of these irradiated organisms, carotenoid pigments are frequently emphasised (Albarracín et al. 2016; Pavlopoulou et al. 2016).

Carotenoid pigmentation contributes significantly to the irradiation-resistomes of bacteria from regions of high solar insolation. These include the pigment complements of bacteria from high-altitude Andean lakes, and soils of the Gobi, Antarctic and Atacama Deserts (Dieser et al. 2010; Yuan et al. 2012; Paulino-Lima et al. 2013; Fernández-Zenoff et al. 2014; Reis-Mansur et al. 2019; Silva et al. 2019; Flores et al. 2020). As discussed in **Section 1.3.5**, carotenoid-mediated protection from irradiation largely relies on their ability to quench the intracellular ROS generated by particular irradiation wavelengths through their antioxidant activity (Sandmann 2019). However, despite the widely reported importance of carotenoids to the irradiation resistomes of desert bacteria, there are limited studies which specifically demonstrate the protective roles carotenoids serve in these bacteria through comparisons of pigmented and unpigmented cultures. Specific demonstrations of carotenoid photoprotection are thus needed to better understand the multifaceted resistomes these organisms use to persist in regions of biologically extreme solar irradiation (Pavlopoulou et al. 2016).

Given its isolation from high-irradiance Namib Desert soils and production of carotenoid pigmentation (**Chapter 2**), *Arthrobacter* sp. NamB2 presents a valuable model in which to study the specific contributions of carotenoids to the irradiation-resistomes of desert bacteria. *Arthrobacter* sp. NamB2 presents a well-developed and multifaceted UV-resistome, and a high tolerance to UV-irradiation (**Section 1.3.9)** (Buckley 2020). The pigmentation of this organism has only been casually connected to its UV-tolerance previously, in line with findings from limited studies of other pink pigmented *Arthrobacter* (Buckley 2020). Exploring the specific contribution of carotenoid pigmentation to the UV-tolerance of *Arthrobacter* sp. NamB2 is thus valuable both to further characterise the multifaceted systems of UV-tolerance employed by this organism, and to support carotenoids as important to the resistomes of edaphic desert bacteria.

4.1.2 Investigations of Carotenoid Photoprotection

Survival comparisons between pigmented and unpigmented cultures of the same organism is the accepted method of demonstrating photoprotective functions of an organism's carotenoids (Tian et al. 2007; Tian et al. 2009; Pezzoni et al. 2011). Indeed, survival comparisons between pigmented and unpigmented *Mycobacterium* spp.*, K. rosea*, *Haloarchaea* spp. and *D. radiodurans* under irradiation have been used to conclude on the specific protective roles of their pigments (Dundas and Larsen 1963; Burchard and Dworkin 1966; Mathews-Roth and Krinsky 1970; Mattimore and Battista 1996; Shahmohammadi et al. 1997; Tian et al. 2007; Pezzoni et al. 2011). Comparisons between cultures of the same species provides consistency in organismal DNA repair pathways and irradiation-susceptibilities, allowing differences in survival to be specifically attributed to the presence of carotenoids (Sandmann 2019).

To obtain unpigmented cultures of a carotenogenic organism for these survival comparisons, the production of carotenoids must be prevented. While carotenoid deprivation can be achieved through gene knockouts or random mutation, application of the carotenogenesis inhibitor diphenylamine (DPA) is more common (Shahmohammadi et al. 1997; Tian et al. 2007). Diphenylamine is a competitive inhibitor of the bacterial phytoene desaturase enzyme (CrtI), the enzyme responsible for introduction of double bonds into colourless phytoene (3 c.d.b) to generate the first coloured carotenoid, lycopene (11 c.d.b) (Raisig and Sandmann 2001; Tang et al. 2019). As lycopene is the precursor for most bacterial carotenoid biosynthetic pathways, CrtI inhibition typically prevents the biosynthesis of coloured carotenoids (Moise et al. 2014; Liang et al. 2018; Tang et al. 2019). Growth of bacteria in the presence of DPA has thus been widely used to generate unpigmented cultures for survival comparisons with pigmented cultures under

irradiation (Mathews 1963; Burchard and Dworkin 1966; Hescox and Carlberg 1972; Pezzoni et al. 2011).

As discussed in **Section 1.3.5**, carotenoids exert cellular irradiation protection through ROS-quenching, providing no protection from irradiation which stimulates direct DNA or protein damage (Goosen and Moolenaar 2008; Jones and Baxter 2017; Sandmann 2019). However, some carotenoids have been attributed the ability to directly screen UV, absorbing and dissipating incident energy which may otherwise stimulate cell damage (Krinsky 1978; Cockell and Knowland 1999; Stafsnes et al. 2010). This would allow these carotenoids to exert a protective effect independent of antioxidant action, and may allow them confer cellular protection from the direct DNA damage of UVB or UVC. While this role is speculated for a number of bacterial carotenoids, specific demonstrations of protective UV-screening by carotenoids is rare (Cockell and Knowland 1999; Dieser et al. 2010; Stafsnes et al. 2010; Perez-Fons et al. 2011; Mohana et al. 2013). Demonstrating a pigment as capable of UV-screening relies on a number of criteria, most importantly its high absorbance at relevant screening wavelengths (Cockell and Knowland 1999). This property may be identified via examination of the UV-visible scanning spectra of the pigment for the presence of pronounced, high-intensity absorbance peaks at the speculated screening wavelengths (Cockell and Knowland 1999; Solovchenko and Merzlyak 2008; Stafsnes et al. 2010). Screening of incident UV-irradiation by carotenoids would contribute to the bacterial UV-resistome, thus is worthy of investigation.

4.1.3 Carotenoid Photoprotection in *Arthrobacter*

Carotenoid pigmentation in *Arthrobacter* has previously been speculated to provide UV-tolerance, but lacks demonstration (**Section 1.3.8.2**). Carotenogenic *Arthrobacter* are commonly recovered from high-irradiance environments including Sonoran and Antarctic Desert soils, and have demonstrated notable UV-resistance compared to co-isolated, unpigmented bacteria of different species (Fong et al. 2001; Reddy et al. 2002; Dieser et al. 2010; Ii et al. 2019; Silva et al. 2019; Sajjad et al. 2020). While carotenoids are commonly speculated as a component of *Arthrobacter's* UV-resistome, no study has yet presented comparisons of UV-tolerance between pigmented and unpigmented cultures of the same species, as is required to demonstrate this function.

Carotenoid pigmentation is considered significant to the irradiation resistomes of edaphic bacteria from deserts of analogous irradiation-intensity to the Namib, and the production of the

carotenoid bacterioruberin by *Arthrobacter* sp. NamB2 suggests a similar importance of carotenoids to its UV-resistance (Dieser et al. 2010; Yuan et al. 2012; Paulino-Lima et al. 2013; Fernández-Zenoff et al. 2014; Reis-Mansur et al. 2019; Silva et al. 2019; Flores et al. 2020). Furthermore, bacterioruberin has previously demonstrated protection of *Haloarchaea* from both PAR-stimulated ROS damage alongside UVC-mediated DNA damage, conflicting known limitations of carotenoid-mediated photoprotection, and suggesting its production by *Arthrobacter* sp. NamB2 may a present a significant UV-protective capacity (Shahmohammadi et al. 1997; Shahmohammadi et al. 1998; Jones and Baxter 2017).

As such, this chapter sought to characterise the contribution of the carotenoid pigmentation of *Arthrobacter* sp. NamB2 to its UV-resistome. The capacity of the pigment to provide protective screening against UV was investigated by examining its absorbance within the UV-region of the spectrum for the presence of pigment-specific, high-intensity absorption peaks conducive to screening. To determine within which waveband(s) the pigment was capable of providing a protective effect, the survival of pigmented and unpigmented cultures of *Arthrobacter* sp. NamB2 were compared under UVA (365 nm), UVB (302 nm) and UVC (254 nm) irradiation. Irradiation with UVA was used to examine the protective capacity of the pigment against photodynamic damage, in line with known functions of carotenoids. Irradiation with UVB was tested at a range of dosages to examine the protection provided by the pigment against the dosage dependent UVB-stimulated ROS and DNA damage. Irradiation with UVC was used to examine whether the pigment was capable of mitigating direct DNA damage, as reported by some prior studies of bacterioruberin (Jones and Baxter 2017).

4.2 Methods

4.2.1 Diphenylamine Treatment and Pigment Inhibition

Survival comparisons between pigmented and unpigmented cultures of *Arthrobacter* sp. NamB2 under UV-irradiation required the generation of unpigmented cultures. To obtain unpigmented cultures, *Arthrobacter* sp. NamB2 was grown in the presence of the carotenogenesis inhibitor DPA.

Preliminary experiments were performed to verify the ability of DPA to inhibit pigment production in *Arthrobacter* sp. NamB2 without influencing cell growth. Pigment inhibition was explored by comparing the total pigment content of cultures grown in the presence of DPA to those of control cultures. Furthermore, as DPA-treatment in excess concentrations inhibits cell growth, and inhibition of cell growth in unpigmented cultures would confound fair comparisons to pigmented cultures under subsequent irradiation-survival assays, DPA-mediated influences upon cell growth were examined by comparing the cell dry mass of DPA-treated and untreated cultures. Comparisons of cell dry mass is a quantification commonly applied in the study of DPA-mediated cellular inhibition (Fan et al. 1995; Chumpolkulwong et al. 1997; Perez-Fons et al. 2011; Wang et al. 2016).

4.2.1.1 Cell Growth and Preparation of the Diphenylamine Inhibitor

For cell revival, 200 µL of one glycerol stock of *Arthrobacter* sp. NamB2 was inoculated onto nutrient agar via spread plate and grown at 20 °C for 72 hours. Following growth, the bacterial lawn was reverse spread plated from the nutrient agar plate through addition of 5.0 mL of nutrient broth to the plate, and scraping colonies from the agar's surface into the broth suspension using a plastic spreader. This broth culture was recovered, adjusted to an OD_{600} of 0.5 using nutrient broth, and used to inoculate a total of nine customised nutrient agar plates via spread plate (100 µL per plate) for examinations of DPA-inhibition.

Three of these nine plates were prepared from 20 mL of nutrient agar with 143 µL added DPA solution (in ethanol (EtOH) solvent). A 0.0143 M DPA solution was prepared via dissolution of 0.005 g of solid DPA in 2.0 mL of > 99.9 % EtOH, and filter sterilised by passing the solution through a 0.20 µm filter before addition to the cooling nutrient agar, to yield a final

concentration of 100 µM within the nutrient agar. Three plates were prepared with 20 mL each of standard nutrient agar without modification, and three plates were prepared through addition of 143 µL of > 99.9 % EtOH to 20 mL aliquots of nutrient agar prior to pouring, These latter control plates were employed to rule out influences of the EtOH solvent, used in preparation of the DPA solution, on cellular pigmentation or growth. Following inoculation, these plates were incubated at 20 ^{o}C for 72 hours prior to pigment extraction and determination of cell dry mass.

4.2.1.2 Pigmentation and Cell Mass Quantification

To investigate the influence of DPA treatment on pigment production by *Arthrobacter* sp. NamB2, the total pigment content of cultures grown on unmodified nutrient agar plates (Control), and those with added DPA solution (+DPA) or EtOH (+EtOH) was quantified and compared. The cell dry mass recovered from each of these cultures was similarly recorded and compared to detect cellular inhibition arising from DPA-treatment.

Following 72 hours of growth, the bacterial cultures were harvested from each of the nine plates and their dry cell masses determined using the harvesting method for dry cell pellets as described in **Section 3.2.1.1.** The total carotenoid pigmentation was extracted from these cell pellets using the method described in **Section 3.2.1.2**. For pigment quantification, UV-visible spectra were prepared for each pigment extract as outlined under **Section 3.2.1.2.**

The carotenoid content (mg) of each replicate culture grown in each condition (Control, +EtOH, +DPA) was calculated from their absorbance values at λ_{max} using the standard calculation for total carotenoid content as displayed in **Equation 3.1** of **Chapter 3,** with an extinction coefficient of 2,500 $M^{-1}cm^{-1}$ for total carotenoid mixtures (Liaaen-Jensen and Jensen 1971; Flores et al. 2020). Using the dry weight of cells from which the pigment was extracted, the total pigment content of each culture in milligrams of carotenoids per gram of cell dry mass (henceforth 'pigment content') was determined, to ease comparisons of total carotenoid production between cultures.

4.2.1.3 Statistical Analysis

To examine if the DPA treatment significantly influenced carotenoid production, the total pigment content of cultures grown on control, +EtOH and +DPA plates were compared for evidence of a statistically-meaningful difference.

The pigment content of +DPA cultures could not be calculated as their methanolic extracts did not produce carotenoid absorption spectra – indicating a total loss of carotenoid production by DPA-treated cells (see **Results Section 4.3.1**). As such, only the pigment content of +EtOH and control cultures could be calculated and compared here. This comparison was used to rule out any inhibition of pigment production in +DPA cultures which was attributable to the EtOH solvent used in preparation of DPA solutions. Evidence of a significant differences in the mean pigment content of control and +EtOH cultures was examined via a two-sided, two-sample Student's t-test. The normality of pigment content distributions from cultures grown under each condition was verified using Shapiro-Wilks testing in R (R Core Team 2020).

The impact of DPA treatment on cellular growth was analysed by comparing the mean differences in cell pellet dry weights of control, +DPA and +EtOH cultures using ANOVA with subsequent Tukey's-HSD post-hoc analysis. The normality in distributions of cell pellet dry mass obtained from cultures within each condition were verified using Shapiro-Wilks testing in R (R Core Team 2020).

As presented later in this chapter, these preliminary studies concluded that DPA inhibited pigment production in *Arthrobacter* sp. NamB2 without influencing cell growth **(Section 4.3.1)**. Treatment with the DPA-inhibitor was thus suitable for generation of unpigmented cultures for subsequent investigations of pigment-mediated UV-protection in *Arthrobacter* sp. NamB2.

4.2.2 Examination of Pigment UV-Screening

To characterise the contribution of pigmentation to *Arthrobacter* sp. NamB2's UV resistance, the pigment's capacity to screen UV-irradiation (particularly at wavelengths tested in subsequent UV-survival assays) was first investigated. Examination of the UV-visible spectrum of the pigment across the 200 – 800 nm waveband was used to determine if the pigment was capable of UV screening. The spectra produced by the pink methanolic pigment extracts of

pigmented cells were compared to those produced from unpigmented cultures for evidence of pigment-specific UV-absorption.

Triplicate pigmented and unpigmented cultures of *Arthrobacter* sp. NamB2 were prepared for subsequent pigment extraction and UV-visible spectroscopy. Revival of *Arthrobacter* sp. NamB2 from glycerol stock, and adjustment of the revival culture to an OD_{600} of 0.5 was carried out as described in **Section 4.2.1.1**. Aliquots of 100 µL of this revival culture were used to spread inoculate (in triplicate) unmodified nutrient agar plates, or those possessing DPA at a concentration of 100 µM, prepared as described under **Section 4.2.1.1**. Cells were grown on these plates at 20 ^{o}C for 72 hours prior to pigment-extraction. Pigment extraction from these cultures was performed as per the method described in **Section 4.2.1.2**.

Confounding cellular particulates were removed from the methanolic extracts of pigmented and unpigmented cultures by passing these extracts through a 0.20 µm filter. Each purified extract was aliquoted directly into a quartz cuvette (Starna Scientific, Illford, England) for full UV-spectrum penetration. A UV-visible scanning spectrum was produced for each extract in methanol from 200 – 800 nm using an Ultrospec 7000 UV-visible spectrophotometer (Cytiva, USA), with > 99.9 % HPLC-grade methanol (also prepared within a quartz cuvette) as a blank.

4.2.3 Survival Assays under Ultraviolet-Irradiation

To determine whether the pigmentation of *Arthrobacter* sp. NamB2 provided protection of the cells against UV-irradiation, and within which wavebands, the survival of pigmented and unpigmented cultures was compared under irradiation with UVA, UVB and UVC. Differences in survival between pigmented and unpigmented UV-exposed cultures was used to characterise the contribution of the pigment to the UV-resistome of *Arthrobacter* sp. NamB2.

Pigmented and unpigmented cultures of *Arthrobacter* sp. NamB2 were prepared for comparison under subsequent UV-survival assays. Revival of *Arthrobacter* sp. NamB2 from glycerol stock, and adjustment of the revival culture to an OD_{600} of 0.5 was carried out as described in **Section 4.2.1.1.** . Aliquots of 100 µL from this culture were used to spread inoculate (in triplicate) unmodified nutrient agar plates, or those possessing DPA at a concentration of 100 µM, prepared as described under **Section 4.2.1.1**. Cells were grown on these plates at 20 ^{o}C for 72 hours prior to harvest for UVA, UVB or UVC exposure.

Cultures grown on unmodified nutrient agar plates (pigmented), or those plates containing DPA (unpigmented), were harvested via reverse spread plating through addition of 5.0 mL nutrient broth to the plate, and scraping the colonies from the agar's surface into the broth suspension using a plastic spreader. Each broth culture was subsequently recovered and adjusted to an OD_{600} of 0.5 using nutrient broth. This produced triplicate, OD_{600} 0.5 suspensions of pigmented and unpigmented *Arthrobacter* sp. NamB2, each of which was serially diluted (1:9) in diluents of 9.0 mL peptone water (Difco, USA) up to the 1 x 10^{-5} dilution. Each 10 mL 1 x 10^{-5} peptone solution was thoroughly mixed via vortex, and separated into two 5.0 mL aliquots, with one aliquot placed into each half of an empty 90 mm split petri dish (Techno Plas, St Marys, South Australia, Australia). One half of this plate was covered with a cardboard barrier during irradiation to prevent UV exposure (henceforth, unexposed sample), while one half was left open to the UV lamp, thus was UV-exposed (henceforth, exposed sample). This gave both an exposed condition and unexposed control condition for each of triplicate cultures of pigmented and unpigmented cells. The experimental setup of this irradiation is demonstrated on **Figure 4.1**.

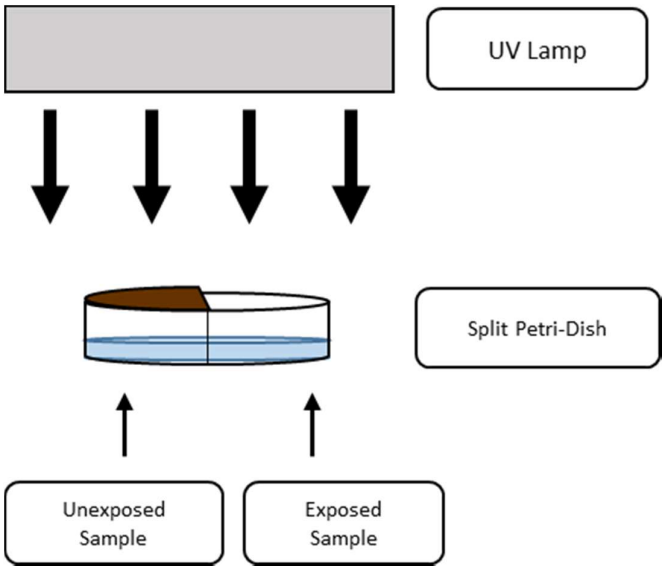

Figure 4.1: Experimental setup for UV-irradiation assays. Both UV-exposed and unexposed samples were contained within an empty 90 mm split petri dish. The half of the dish containing the UV-unexposed sample was protected from irradiation using a cardboard barrier, while the UV-exposed sample was left open to irradiation.

Irradiation with UVA (365 nm) at an intensity of 30 W/m^2, UVB (302 nm) at intensities of 6 W/m^2 or 11 W/m^2, or UVC (254 nm) at an intensity of 1 W/m^2 was provided using an 8.0 W UVP 3UV™ Lamp (Analytik Jena, Upland, CA, USA) maintained at 3 cm (UVA), 12/15 cm (for 6/11 W/m^2 UVB, respectively), or 43 cm (UVC) above the surface of the split petri dish.

Intensity of UV at the plate's surface was verified using a Solarmeter® UVA Meter Model 4.0, UVB Meter Model 6.0, or UVC Meter Model 8.0 (Solarlight Company, Glenside, PA, USA) for UVA, UVB and UVC, respectively. During irradiation, agitation was provided to the exposed sample using a magnetic stirrer bar operated at 350 rpm.

Cell counts were recorded for both the UV-exposed and unexposed sides of each culture throughout the irradiation period to examine cell survival. For UVA, irradiation proceeded for a total of 60 minutes for each sample, with survival counts performed at 0, 30, and 60 minutes. For UVB, irradiation proceeded for a total of 5 minutes for each sample, with survival counts performed at 0, 2.5 and 5 minutes. For UVC, irradiation proceeded for a total of 10 minutes for each sample, with survival counts performed at 0, 5 and 10 minutes. The total UV-dosages to which each culture was exposed under each of these irradiation times and intensities are presented on **Table 4.1**, as determined through the equations of Kvam and Benner (2020) and Silva et al. (2019).

Survival counts were performed by sampling 100 µL aliquots of the peptone solution from each side (exposed/unexposed) of the split plate, consistently 1.5 cm in distance from the edge of the plate, and spread plating these separately upon nutrient agar for subsequent cell counts. Each side of the culture plate was thoroughly mixed via aspiration prior to sampling. Plates for survival counts were incubated at 20 ºC for 72 hours prior to counting. For UVC, plates were held at ambient light (4.0 µmol m^{-2} s^{-1}) for one hour prior to illuminated incubation to allow photoreactivation pathways to engage.

Table 4.1: Total UV-dosages applied to exposed cultures of *Arthrobacter* sp. NamB2 under each irradiance wavelength and time of irradiation.

Irradiation Intensity	Irradiation Time (Minutes)	Dosage (J/m^2)
UVA	0	0
30 W/m^2	30	54,000
	60	108,000
UVB	0	0
6 W/m^2	2.5	900
	5	1,800
UVB	0	0
11 W/m^2	2.5	1,650
	5	3,300
UVC	0	0
1 W/m^2	5	300
	10	600

4.2.3.1 Statistical Analysis

To examine evidence of pigment-mediated UV-protection, the survival of pigmented and unpigmented cultures of *Arthrobacter* sp. NamB2 under each UV wavelength was compared, with the unexposed samples of each used as controls. The sampling performed gave triplicate cell counts (converted into colony forming units per millilitre (cfu/mL)) for each exposure condition prepared (pigmented exposed, pigmented unexposed, unpigmented exposed and unpigmented unexposed) at each time-point of UV-irradiation. Survival counts in cfu/mL for each exposure condition at each time-point were converted into $\log_{10}$ cfu/mL values for subsequent statistical analyses. These $\log_{10}$ cfu/mL values were plotted as survival curves to examine broad trends in lethality between exposure conditions under each wavelength of UV-irradiation.

Changes in $\log_{10}$ cfu/mL between each time point of UV-irradiation for each exposure condition were calculated and compared. These changes in $\log_{10}$ cfu/mL directly reflected the lethality exerted by UV-irradiation on each culture, thus allowed comparisons of the extent of UV-mediated lethality between exposure conditions. These changes in $\log_{10}$ cfu/mL between individual time points were compared via ANOVA and subsequent Tukey's HSD analysis to examine evidence of significant differences in survival between different exposure conditions under UV-irradiation. Normality of these changes in $\log_{10}$ cfu/mL within each exposure condition was verified using Shapiro-Wilks testing in R to ensure applicability for ANOVA comparisons (R Core Team 2020).

4.3 Results

4.3.1 Effects of Diphenylamine Inhibition

Arthrobacter sp. NamB2 was treated with the carotenogenesis inhibitor DPA to generate unpigmented cultures. Cells were grown on nutrient agar containing DPA at a final concentration of 100 µM (+DPA), unmodified nutrient agar plates (Control), or on plates containing a controlled quantity of the EtOH solvent used in preparation of the DPA solution (+EtOH). To verify DPA-mediated pigment inhibition, the total pigment content produced by cultures grown in each condition was quantified via UV-visible spectroscopy and compared.

Growth in the presence of diphenylamine prevented carotenoid production by *Arthrobacter* sp. NamB2. Visually, cells grown on control and +EtOH plates presented with the expected pink pigmentation, while those grown upon +DPA plates were entirely white, suggesting total inhibition of pigmentation. Subsequent UV-visible spectroscopy of pigment extracts from these cultures demonstrated that those treated with DPA had lost the characteristic three-peaked carotenoid spectrum previously associated with bacterioruberin (**Figure 4.2**). This indicated a total loss of carotenoid production from DPA-treated cultures. Bacterioruberin-associated carotenoid spectra were maintained in extracts from control and +EtOH cultures, indicating that carotenoid synthesis was retained under these conditions. This demonstrated that DPA was capable of inhibiting carotenoid production in *Arthrobacter* sp. NamB2.

Inhibition of pigment production was due to the DPA itself and not to the ethanol solvent in which it was prepared. As the +DPA cultures did not produce carotenoid spectra, total carotenoid quantification and comparisons from UV-visible spectroscopy could only be performed on control and +EtOH cultures. The total pigment content determined for these +EtOH and control cultures demonstrated a substantial overlap (**Figure 4.3**). Student's t-testing did not detect any significant differences in the mean pigment content of these treatments ($p = 0.7679$), indicating ethanol had no influence on pigment production by *Arthrobacter* sp. NamB2. Pigment deprivation observed in DPA-treated cultures was thus specifically attributable to the action of the DPA inhibitor itself.

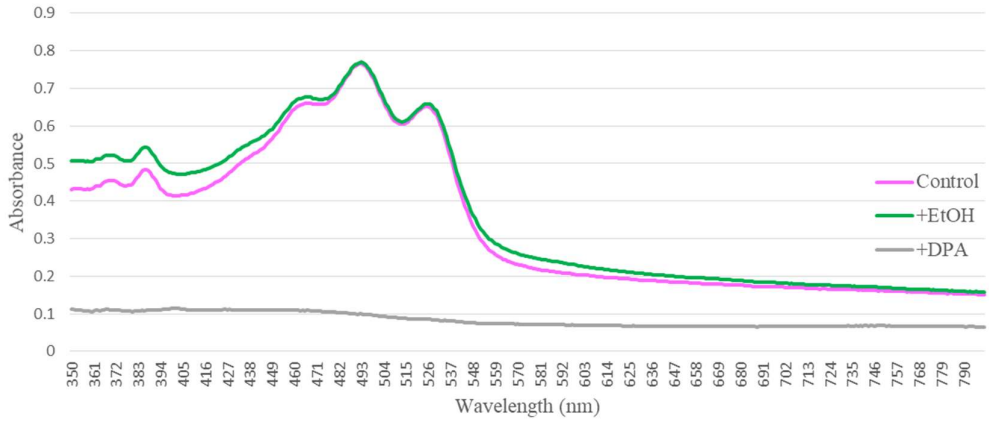

Figure 4.2: Average absorbances of triplicate UV-visible scanning spectra (350 – 800 nm) of methanolic pigment extracts from *Arthrobacter* sp. NamB2 grown on unmodified nutrient agar (Control), nutrient agar with added EtOH (+EtOH) or nutrient agar with added DPA (100 µM) in EtOH (+DPA).

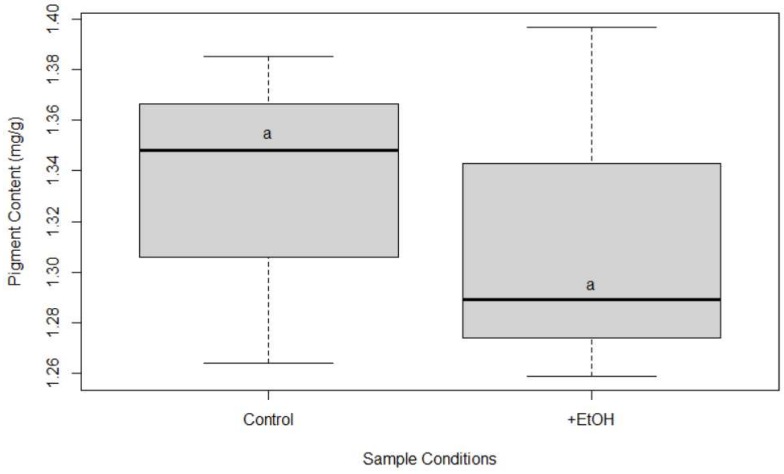

Figure 4.3: Tukey's boxplots demonstrating the variance in pigment content between triplicate cultures of *Arthrobacter* sp. NamB2 grown on unmodified nutrient agar (Control), or nutrient agar with added EtOH (+EtOH). Letters denote compact letter display of the result of the two-sample Student's t-test. Boxplots annotated with the same letters are not statistically-significantly different from one another, while those of differing letters do demonstrate significant differences ($p < 0.05$).

Diphenylamine can inhibit cell growth at excessive concentrations, which could negatively influence the comparison of unpigmented to pigmented cells in subsequent UV-survival assays. Evidence of growth inhibition arising from DPA-treatment was examined by comparing the cell masses of DPA-treated and control cultures.

Cell pellet dry masses obtained from triplicate cultures grown under each condition (Control, +EtOH, +DPA) are presented on **Figure 4.4**, with results of Tukey-HSD analyses examining evidence of significant differences between these pellet masses reported upon the figure. Both +EtOH and +DPA cultures presented cell pellet dry-masses overlapping those of the control, and Tukey-HSD post-hoc testing similarly confirmed no growth condition to produce pellet-weights significantly different from any other, nor from control cultures. These results confirmed that neither DPA nor EtOH treatments significantly influenced cell mass relative to untreated control cultures at the concentrations applied. As such, DPA-treatment did not negatively influence cell growth of *Arthrobacter* sp. NamB2 at the concentrations required for pigment-deprivation.

Consequently, DPA-treatment successfully inhibited pigment production by *Arthrobacter* sp. NamB2, without influencing cell growth. This DPA-treatment was thus deemed suitable in production of unpigmented cultures for subsequent UV-survival assays.

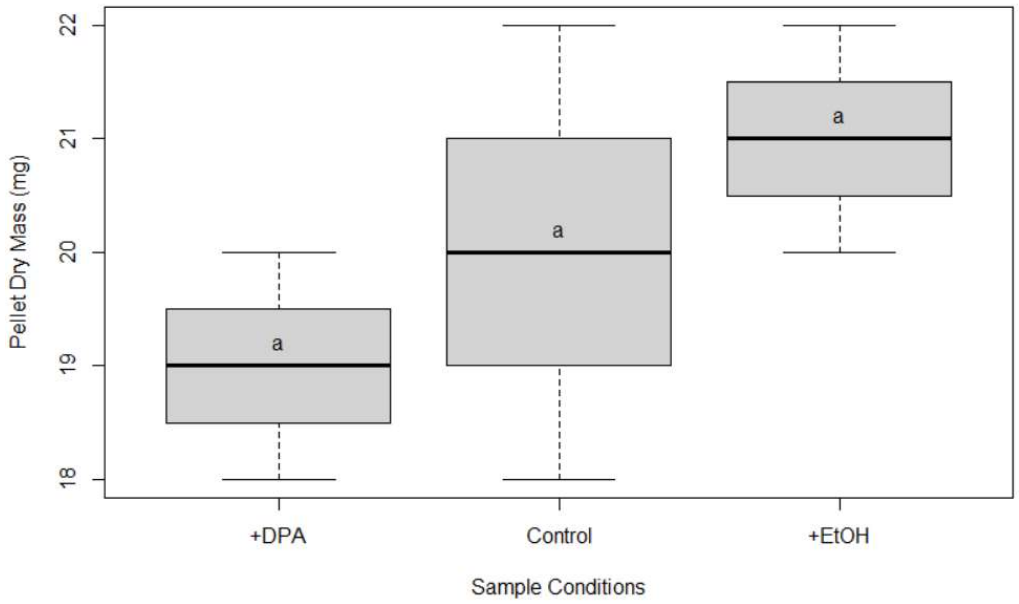

Figure 4.4: Tukey's boxplots demonstrating the variance in cell dry mass between triplicate cultures of *Arthrobacter* sp. NamB2 cells grown on unmodified nutrient agar (Control), nutrient agar with added EtOH (+EtOH), or nutrient agar with 100 μM DPA in ethanol solvent (+DPA). Bold lines denote the median cell dry mass of each condition. Letters denote compact-letter display of significance groupings as determined via Tukey's HSD analysis. Boxplots annotated with the same letters are not statistically-significantly different from one another, while those of differing letters demonstrate significant differences ($p < 0.05$).

4.3.2 Examination of Pigment UV-Screening Capacity

Strong absorbance in the UV region may indicate screening as a mechanism by which a pigment provides protection against UV-irradiation. To examine whether the pigmentation of *Arthrobacter* sp. NamB2 was likely to be capable of direct UV-screening, the absorbance of the pigment within the UV-wavelength region was investigated. To achieve this, 200 – 800 nm UV-visible scanning spectra were prepared for the methanolic extracts from pigmented and unpigmented cultures of *Arthrobacter* sp. NamB2. Wavelengths of UV-irradiation employed in UV-survival assays were examined within these spectra for evidence of pigment-specific absorbance peaks of intensities that may indicate screening.

Average UV-visible scanning spectra produced from triplicate methanolic extracts of pigmented and unpigmented cultures are presented on **Figure 4.5**. High-intensity absorption peaks conducive to screening effects of the pigment were not observed in the UV-region of the spectrum, nor at the UV-wavelengths examined in subsequent survival assays. As expected, the carotenoid three-peaked absorption spectrum within the range of 430 – 600 nm was absent from the spectra of unpigmented cells, as were the carotenoid cis-peaks at 369 and 386 nm.

Subtracting the average absorbance values of unpigmented cells at each wavelength from those of pigmented cells emphasised the spectral features specific to the pigment, as presented in **Figure 4.6A,** with this figure truncated to emphasise the UV-spectral region in **Figure 4.6B**. While the extracts from pigmented cultures demonstrated higher average absorbances at UV wavelengths used in the subsequent survival assays (0.122 higher at 254 nm; 0.022 at 302 nm; 0.067 at 365 nm), these absorbances were minor, and no major disparities in spectral features (i.e. pronounced absorbance peaks) were observed between pigmented/unpigmented cells at these wavelengths. From this, it was concluded that the pigment of *Arthrobacter* sp. NamB2 lacked pronounced screening capacity at these irradiance wavelengths, and thus likely did not present a protective screening effect against incident UV-irradiation.

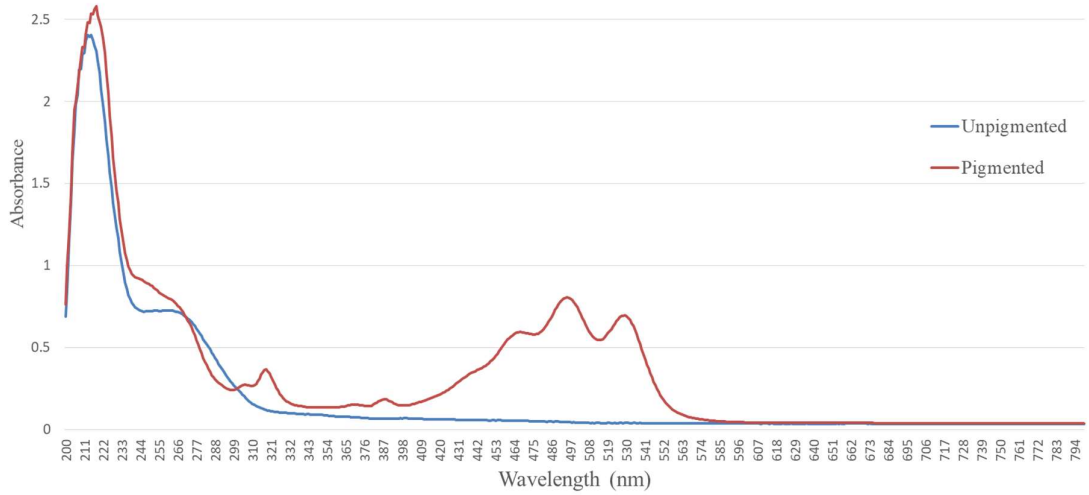

Figure 4.5: Average UV-visible scanning spectra (200 – 800 nm) of methanolic extracts from triplicate pigmented and unpigmented cultures of *Arthrobacter* sp. NamB2.

A:

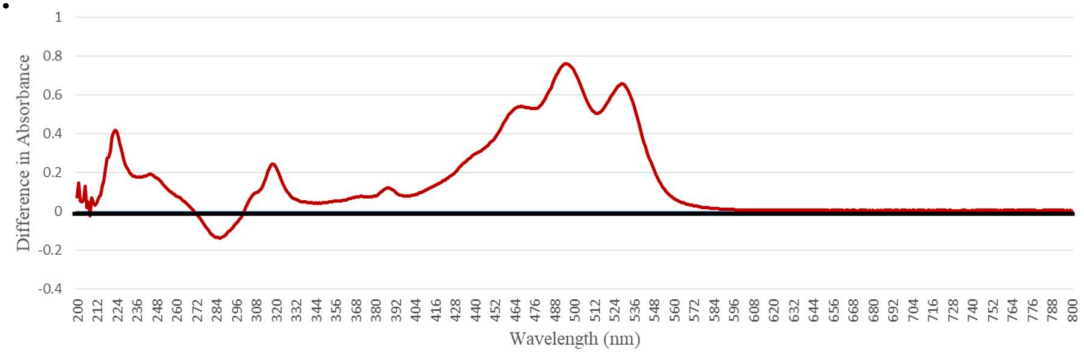

B:

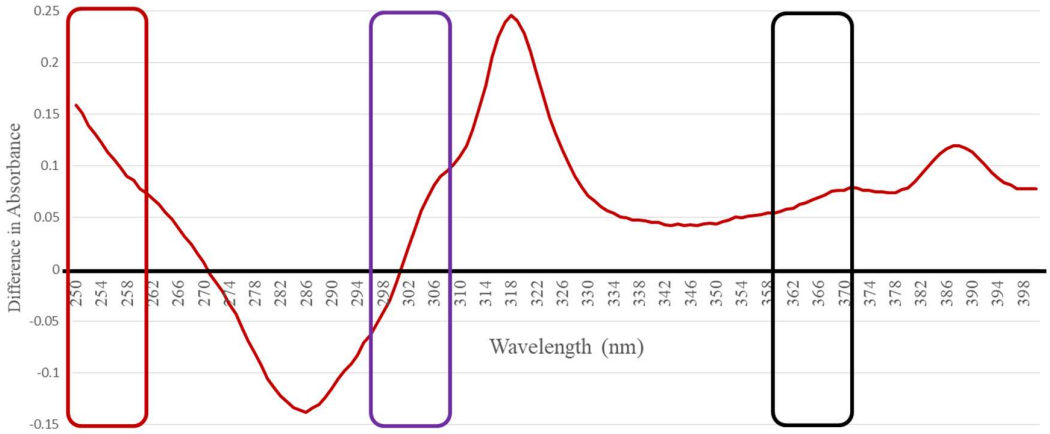

Figure 4.6: Difference in the average absorbance of methanolic extracts from triplicate pigmented and unpigmented cultures. The absorbance spectrum is presented across **A:** The full 200 – 800 nm scanning range **B:** The 250 – 400 nm UV region. Coloured boxes denote UV-wavelengths of interest used in subsequent irradiation assays, with UVA (black) highlighted at 365 nm, UVB (purple) highlighted at 302 nm, and UVC (red) highlighted at 254 nm.

4.3.3 Ultraviolet Irradiation Survival-Assays

To determine the contribution of carotenoid pigmentation to the UV-resistance of *Arthrobacter* sp. NamB2, the survival of pigmented and unpigmented cultures under UVA, UVB and UVC irradiation was compared. These bacterial cultures were irradiated at a series of set intensities, with their survival counts at specific time points **(Table 4.1**) determined. Four exposure conditions were prepared (each in triplicate) for comparison under each wavelength of UV-irradiation; pigmented cells exposed to UV irradiation (Pigmented Exposed) pigmented cells unexposed to UV irradiation (Pigmented Unexposed) unpigmented cells exposed to UV irradiation (Unpigmented Exposed) and unpigmented cells unexposed to UV irradiation (Unpigmented Unexposed). Unexposed samples were those shielded via a cardboard barrier during the irradiation period, and served as controls for each exposed condition, in which minimal changes in cell counts (thus minimal lethality) was expected.

4.3.3.1 Ultraviolet-A Survival Assay

The pigment of *Arthrobacter* sp. NamB2 provided protection against UVA. The $\log_{10}$ cfu/mL values determined from survival counts at each time-point for each exposure condition under UVA are plotted as survival curves in **Figure 4.7**. Minimal changes in $\log_{10}$ cfu/mL survival counts (below ± 0.03 $\log_{10}$ cfu/mL) were observed for the unexposed samples over the course of the 60-minute UVA-irradiation. These changes were expected, and comparable to those negligible changes observed for the UVA-exposed pigmented cells (0.018 $\log_{10}$ cfu/mL). In contrast, the survival of unpigmented UVA-exposed cells declined with each time point to a total decrease of over 0.5 $\log_{10}$ cfu/mL over the 60-minute exposure period. Lethality under UVA-exposure was thus uniquely observed in the unpigmented, UVA-exposed cultures, and was absent from those retaining pigmentation.

Cellular lethality of pigmented and unpigmented cultures was analysed by comparing the changes in $\log_{10}$ cfu/mL for each exposure condition over 60 minutes of UVA irradiation. These comparisons are reported in **Figure 4.8** as boxplots with Tukey's-HSD comparisons between conditions. No significant differences were observed between the unexposed control samples, nor between the unexposed samples and the exposed, pigmented sample. This indicated that UVA lacked lethal effects on pigmented cultures in a comparable nature to those entirely unexposed to UVA. However, the unpigmented cultures demonstrated a significantly larger

decrease in $\log_{10}$ cfu/mL compared to all other samples ($p < 0.05$) under UVA-irradiation. These results demonstrated that UVA-lethality was exclusive to those UVA-exposed cultures lacking carotenoid pigmentation, and was significantly greater than that of pigmented, UVA-exposed cultures.

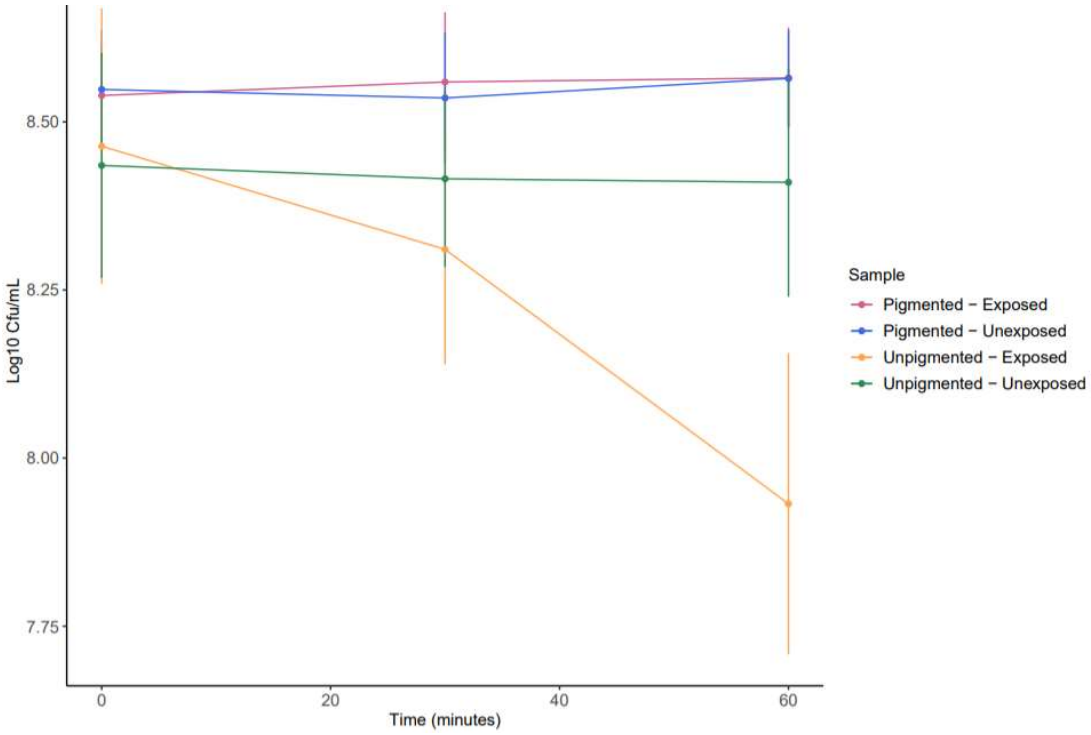

Figure 4.7: Survival curves demonstrating the $\log_{10}$ cfu/mL counts (y axis) obtained for each exposure condition of *Arthrobacter* sp. NamB2 with increasing time of UVA-irradiation (x axis). Error bars were calculated from the standard deviation of the $\log_{10}$ cfu/mL from triplicate samples at each time-point.

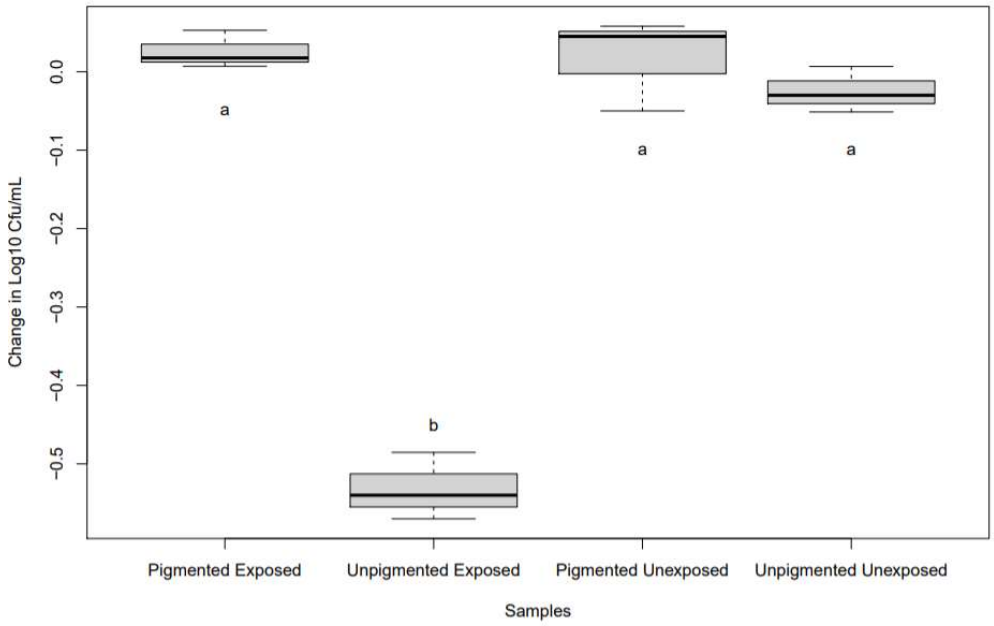

Figure 4.8: Boxplots denoting changes in $\log_{10}$ cfu/mL for each exposure condition of *Arthrobacter* sp. NamB2 between 0 – 60 minutes of UVA exposure. Bold lines denote the median of each group. Letters denote compact-letter display of significance groupings as determined via ANOVA analysis followed by Tukey's HSD-post-hoc testing. Boxplots annotated with the same letters are not statistically-significantly different from one another, while those of differing letters demonstrate statistically significant differences ($p < 0.05$).

4.3.3.2 Ultraviolet-B Survival Assay

The carotenoid pigmentation of *Arthrobacter* sp. NamB2 afforded protection against UVB-irradiation. Survival curves prepared for each exposure condition under 6.0 W/m^2 and 11 W/m^2 UVB irradiation are presented in **Figures 4.9A** and **B** respectively. Unexposed cultures demonstrated negligible changes in cell counts under each UVB intensity (below 0.05 $\log_{10}$ cfu/mL), while exposed cultures demonstrated more dramatic variability. For both irradiation intensities and at all time points, unpigmented UVB-exposed cultures demonstrated greater decreases in $\log_{10}$ cfu/mL than did those retaining pigmentation. Indeed, pigmented and unpigmented UVB-exposed cultures decreased by an average of 0.4 and 1.42 $\log_{10}$ cfu/mL respectively over the 5 minutes of 6 W/m^2 UVB, compared to 0.48 and 1.08 $\log_{10}$ cfu/mL respectively over 5 minutes of 11 W/m^2 UVB. These results indicated that while both pigmented and unpigmented cultures were susceptible to lethality under UVB-irradiation, unpigmented cultures required a lower dosage, thus presented a higher sensitivity to UVB-lethality.

Boxplots comparing changes in $\log_{10}$ cfu/mL for each exposure condition between 0 – 2.5 minutes and 2.5 – 5 minutes of UVB-exposure are presented in **Figure 4.10A** and **B** for 6.0 and 11 W/m^2 UVB irradiation, respectively. Specific examination of changes between each time-point are presented here to analyse the differing dynamics in lethality observed as total UVB-dosages increased. Under both 6.0 and 11 W/m^2 irradiation, between 0 – 2.5 minutes (representing dosages up to 1,650 J/m^2 as per **Table 4.1**), only the unpigmented, exposed cultures demonstrated significantly greater decreases in $\log_{10}$ cfu/mL relative to the unexposed controls, indicating UVB-mediated lethality. However, between 2.5 – 5 minutes of irradiation at each UVB intensity (total UVB dosages of 1,800 – 3,300 J/m^2), both pigmented and unpigmented cultures demonstrated decreases in $\log_{10}$ cfu/mL which were significantly greater than the unexposed controls, indicating mutual UVB-mediated lethality. At these UVB intensities which were mutually lethal, the $\log_{10}$ cfu/mL decreases of pigmented and unpigmented cultures were still significantly different from one another, with unpigmented cultures exhibiting significantly greater lethality than those of pigmented cultures.

Unpigmented cultures thus demonstrated lethal sensitivity to UVB at all dosages (900 – 3,300 J/m^2), while pigmented cultures only presented lethal sensitivity to UVB at higher dosages (1,800 – 3,300 J/m^2). The UVB sensitivity of unpigmented cells was consistently significantly higher than pigmented cells, even at dosages stimulating lethality in both.

A:

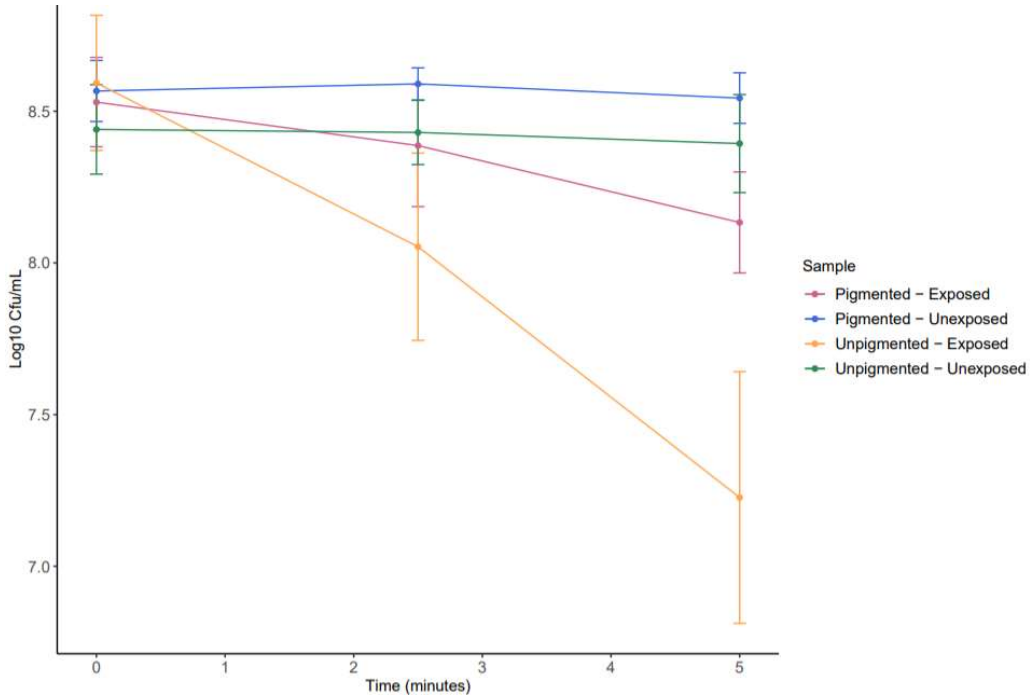

B:

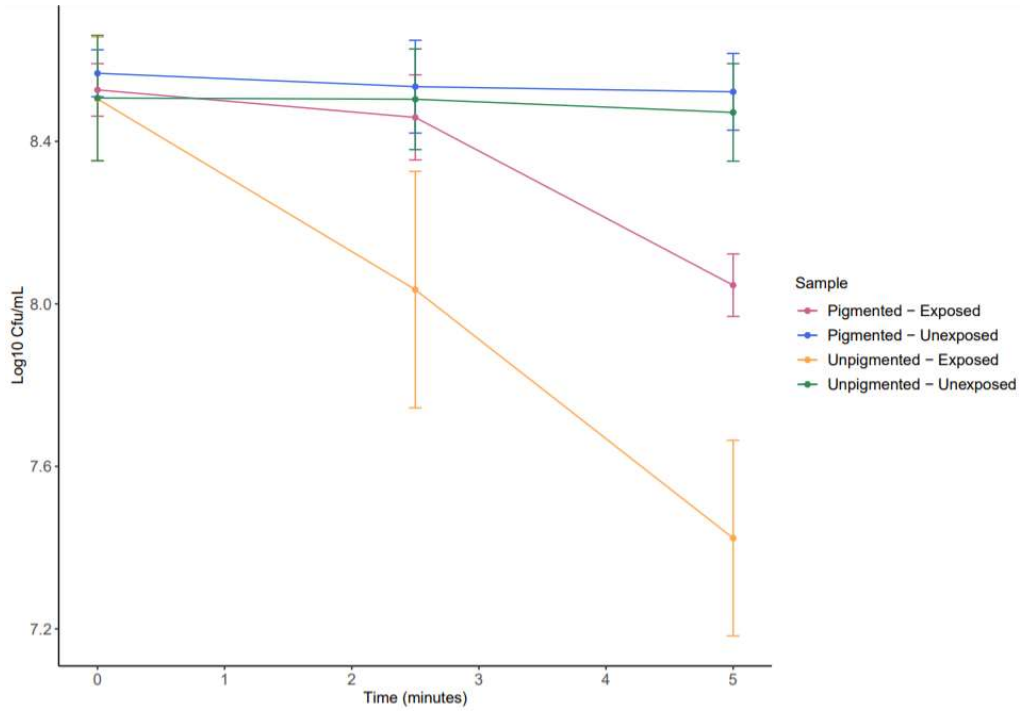

Figure 4.9: Survival curves presenting the $\log_{10}$ cfu/mL counts (y axis) obtained for each exposure condition of *Arthrobacter* sp. NamB2 with increasing time (x axis) of UVB irradiation at **A)** 6.0 W/m^2 and **B)** 11 W/m^2. Error bars were calculated from standard deviation of $\log_{10}$ cfu/mL from triplicate samples at each time point.

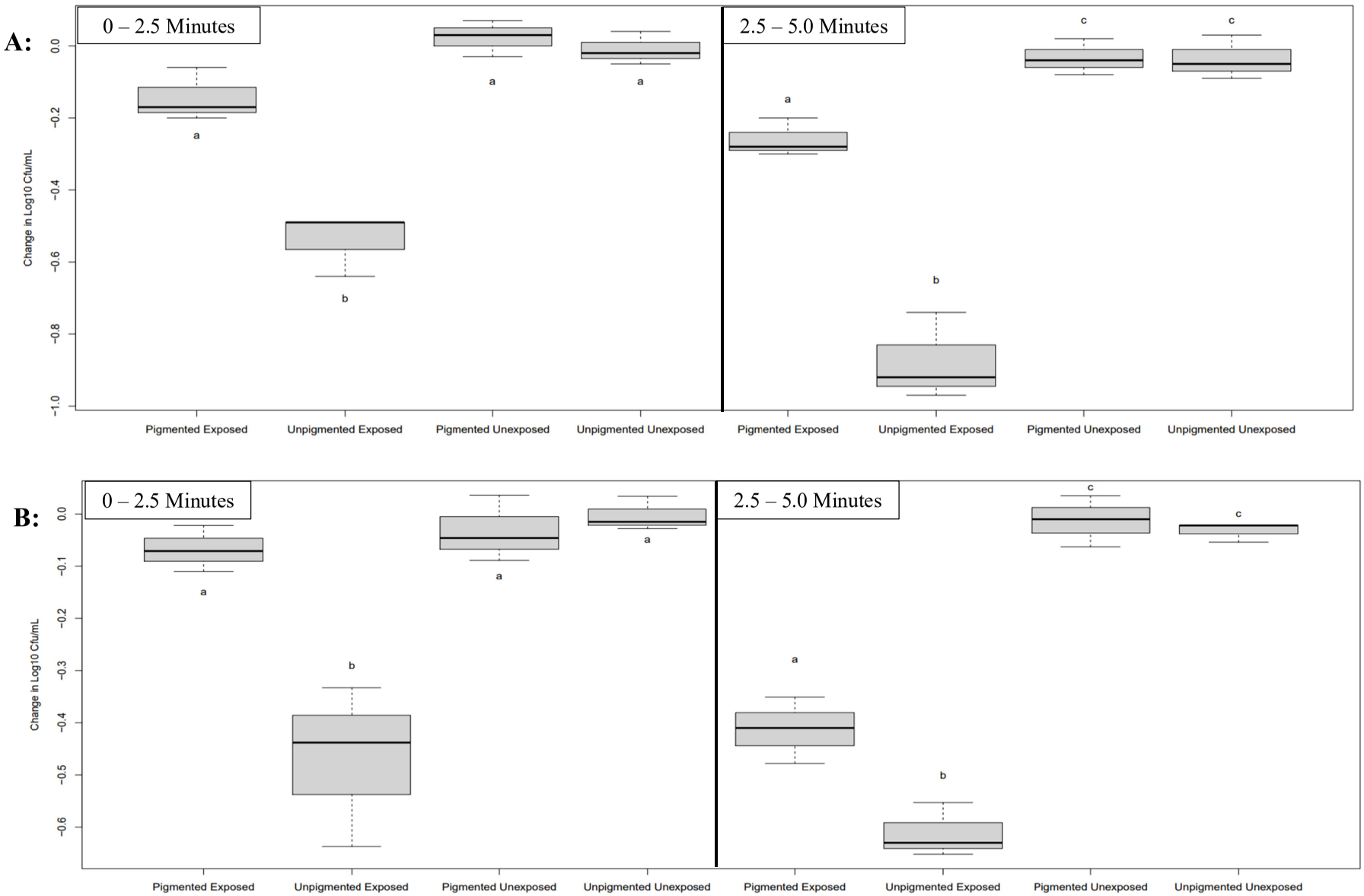

Figure 4.10: Boxplots denoting changes in $\log_{10}$ cfu/mL for *Arthrobacter* sp. NamB2 of each exposure condition between 0 – 2.5 (left) and 2.5 – 5 minutes (right) of **A)** 6 W/m^2 or **B)** 11 W/m^2 UVB irradiation. Letters denote compact-letter display of significance groupings as determined via ANOVA analysis followed by Tukey's HSD post-hoc testing. Boxplots annotated with the same letters are not statistically-significantly different from one another, while those of differing letters demonstrate significant difference ($p < 0.05$).

4.3.3.3 Ultraviolet-C Survival Assay

Bacterioruberin does not appear to protect *Arthrobacter* sp. NamB2 from UVC irradiation. The survival curves for each exposure condition under UVC irradiation are plotted in **Figure 4.11**. Unexposed control samples showed minimal changes in $\log_{10}$ cfu/mL over the course of the experiment (below 0.03 $\log_{10}$ cfu/mL), while both pigmented and unpigmented cells exposed to UVC demonstrated severe declines in survival. Over the ten-minute exposure, $\log_{10}$ cfu/mL counts of UVC-exposed pigmented and unpigmented cultures decreased by an average of 1.74 and 2.06, respectively, with no evident differences between the responses of these exposed cultures. These survival curves suggested comparable susceptibility of cultures to UVC-lethality irrespective of pigmentation.

Changes in $\log_{10}$ cfu/mL counts determined for each exposure condition over the course of the 10-minute UVC exposure are compared in **Figure 4.12**. While significant differences were observed between exposed and unexposed cultures ($p < 0.05$), no difference in survival was observed between the exposed cultures regardless of their pigmentation. These results suggested that while UVC-exposure imparted significant lethality on *Arthrobacter* sp. NamB2, the presence/absence of cellular pigmentation did not influence this lethality.

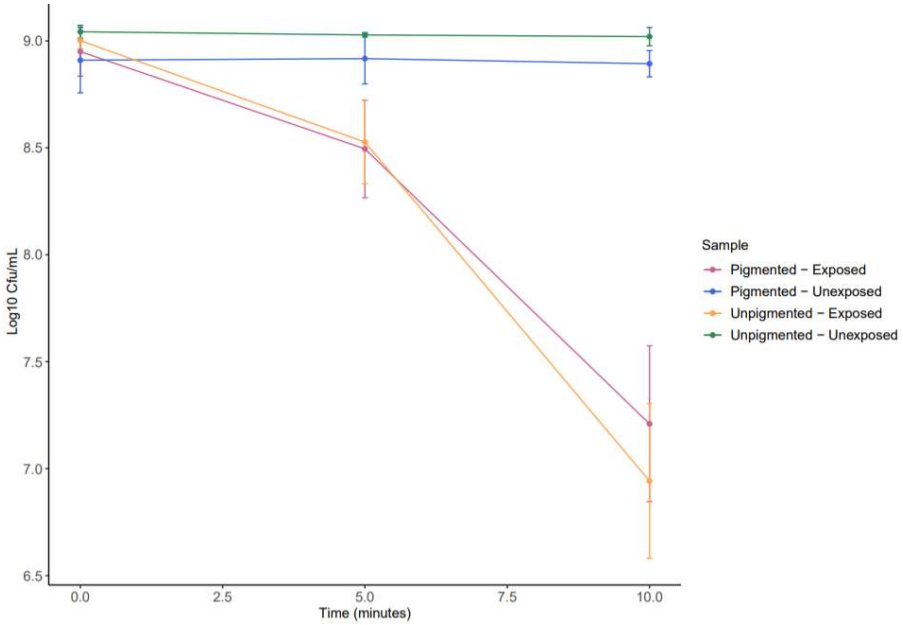

Figure 4.11: Line-graph demonstrating the $\log_{10}$ cfu/mL counts (y-axis) obtained for each exposure condition of *Arthrobacter* sp. NamB2 with increasing time of UVC-irradiation (x-axis). Error bars were calculated from standard deviation of triplicate samples at each time-point.

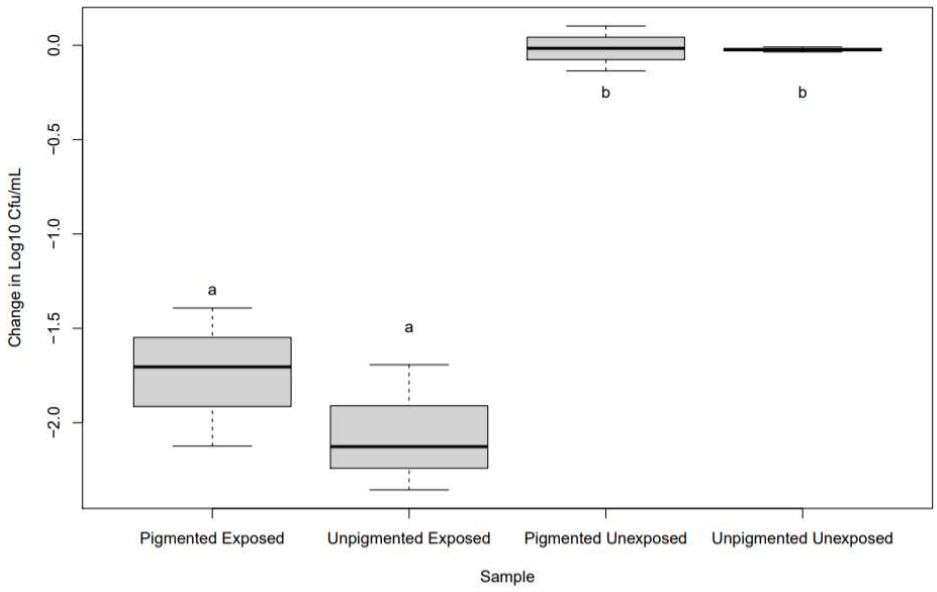

Figure 4.12: Boxplots denoting changes in $\log_{10}$ cfu/mL for *Arthrobacter* sp. NamB2 of each for exposure condition between 0 – 10 minutes of UVC exposure. Letters denote compact-letter display of significance groupings as determined via ANOVA analysis followed by Tukey's HSD-post hoc testing. Boxplots annotated with the same letters are not statistically-significantly different from one another, while those of differing letters demonstrate significant difference ($p < 0.05$).

4.4 Discussion

Carotenoid pigmentation contributes to the irradiation-resistomes of desert organisms (Cowan et al. 2011; Flores et al. 2020). Given the isolation of *Arthrobacter* sp. NamB2 from high-irradiance Namib Desert soil, its substantial tolerance to UV-irradiation, and previous identification of its pink-pigmentation as a carotenoid within this thesis (**Chapter 2**), a similar protective function of pigmentation was suspected within this organism. Therefore, this chapter sought to characterise the specific contribution of carotenoid pigmentation to the UV-resistome of *Arthrobacter* sp. NamB2.

4.4.1 Diphenylamine-Mediated Inhibition of *Arthrobacter* sp. NamB2

Generation of unpigmented cultures of *Arthrobacter* sp. NamB2 for survival comparisons to pigmented cultures under UV-irradiation was successfully achieved through growth of cells in the presence of the carotenogenesis inhibitor DPA. Growth of *Arthrobacter* sp. NamB2 on nutrient agar containing the DPA inhibitor at a final concentration of 100 μM successfully deprived cells of their carotenoid pigmentation. This was observed through both the loss of visible cellular colour from these cultures, and the total loss of carotenoid-associated absorption peaks in UV-visible spectra prepared from their methanolic extracts. Losses of carotenoid absorption spectra resulting from DPA-treatment have been observed previously in bacteria, and are used to demonstrate successful pigment deprivation, indicating similarly that the inhibition of carotenogenesis in *Arthrobacter* sp. NamB2 was successful here (Hammond and White 1970; Hescox and Carlberg 1972; Brausemann et al. 2017). The lack of influence from the ethanol solvent alone on pigment production by *Arthrobacter* sp. NamB2 (**Figure 4.3**) confirmed that it was the action of the DPA specifically that was responsible for pigment deprivation.

Diphenylamine is a specific, competitive inhibitor of the bacterial CrtI-type phytoene desaturase enzyme, and has no influence on non-carotenogenic or non-bacterial carotenogenic pathways (Sandmann and Fraser 1993; Sandmann 1994; Breitenbach et al. 2013; Brausemann et al. 2017). The loss of pigmentation from *Arthrobacter* sp. NamB2 resulting from DPA treatment therefore supported the identity of its pigment complement as exclusively carotenogenic (as discussed in **Chapter 2**), and indicated that biosynthesis of its carotenoids was reliant on a CrtI-type phytoene desaturase. This was expected as the CrtI-enzyme is required for lycopene synthesis, the precursor compound for almost all bacterial carotenoid biosynthetic pathways (Liang et al.

2018). Indeed, the bacterioruberin biosynthetic pathway utilises lycopene as an intermediate carotenoid, and is reliant on a CrtI-phytoene desaturase enzyme for its production (Yang et al. 2015). The implied reliance on a CrtI-type phytoene desaturase by *Arthrobacter* sp. NamB2 for bacterioruberin biosynthesis thus provides a likely mechanism through which DPA exerted pigment-inhibition in this study. In **Section 3.4.4.1**, it was suggested that expression of the phytoene desaturase gene might be an appropriate candidate for studying the light-inducibility of bacterioruberin production. The DPA-mediated pigment inhibition demonstrated here supports the presence and activity of this key carotenogenesis enzyme within *Arthrobacter* sp. NamB2, and would support the intended study of **Section 3.4.4.1**.

Diphenylamine treatment at excessive concentrations is known to inhibit cell growth (Squina and Mercadante 2005). As growth inhibition resulting from DPA treatment would confound subsequent UV-survival assays as an unfair predisposition to UV-damage in unpigmented cells, evidence of this growth inhibition was investigated. No significant differences in cell dry mass were detected between DPA and control cultures of *Arthrobacter* sp. NamB2, indicating a lack of cellular-inhibition resulting from DPA-treatment. These results were expected given the conservative concentration of DPA applied here. Indeed, growth in DPA at a final concentration of 100 μM has previously been shown as capable of inhibiting carotenogenesis in other *Micrococcaceae* without damaging cell growth, with growth inhibition by DPA requiring high concentrations some 1.6 – 2.0 fold greater than those required for inhibition of CrtI (Sanpietro and Kula 1998; Squina and Mercadante 2005; Pezzoni et al. 2011). At concentrations not influencing cell mass, the effects of DPA are limited to inhibition of the carotenogenesis pathway, with no further influences on cellular physiology such as membrane compositions, membrane masses or fatty acid profiles (Salton and Ehtisham-ud-Din 1965; Hammond and White 1970; Fan et al. 1995; Sharp et al. 1999; Doddaiah et al. 2013). Therefore, it is unlikely that the DPA treatment used here modified the sensitivity of the unpigmented cells to UV-irradiation outside of pigment-deprivation, and thus that UV sensitivity of these cells was due solely to the loss of pigmentation.

4.4.2 Potential UV-Screening of Pigmentation

The potential UV-screening role of pigmentation in the protection of *Arthrobacter* sp. NamB2 from irradiation was explored through examination of the pigment's UV-visible scanning spectrum for pronounced absorption peaks conducive to screening. Scanning UV-visible spectra produced from cultures of pigmented *Arthrobacter* sp. NamB2 did not produce substantial absorption peaks at UV-wavelengths examined in subsequent UV-survival assays (**Figure**

4.6B). While extracts from pigmented cells did demonstrate higher absorbances at these wavelengths than those lacking pigmentation, these differences were minor, and lacked the intensities expected of screening compounds (Solovchenko and Merzlyak 2008).

Compounds capable of radiation screening readily absorb incident light at their screening wavelengths (Cockell and Knowland 1999; Solovchenko and Merzlyak 2008). This screening generates absorbance peaks of substantial intensity at these screening wavelengths in UV-visible spectra of these compounds, such as in the spectrum-dominating UV-screening peaks of scytonemin and mycosporine-like amino acids (Llewellyn and Mantoura 1997; Cockell and Knowland 1999; Squier et al. 2004; Solovchenko and Merzlyak 2008). As the pigment of *Arthrobacter* sp. NamB2 did not produce demonstrably exclusive, pronounced absorbance in the UV range, UV-screening as a protective mechanism of carotenoid pigmentation in *Arthrobacter* sp. NamB2 was dismissed (Cockell and Knowland 1999; Solovchenko and Merzlyak 2008).

This finding was unsurprising as carotenoids are not generally considered capable of UV-screening (Cockell and Knowland 1999; Solovchenko and Merzlyak 2008), Carotenoid UV-absorption intensities are typically low, with their structures favouring absorbance within the visible region (Cockell and Knowland 1999; Jahnke 1999; Solovchenko and Merzlyak 2008; Mohana et al. 2013). Where carotenoids are capable of UV-absorbance, their low intracellular concentrations limit their functional screening capacities (Cockell and Knowland 1999). Consequently, this lack of screening capacity by the pigmentation of *Arthrobacter* sp. NamB2 was anticipated.

4.4.3 Pigment-Mediated UV Protection

4.4.3.1 Protection from UVA Irradiation

The pigmentation of *Arthrobacter* sp. NamB2 significantly contributes to its UVA-tolerance. Significant differences in survival were observed between pigmented and unpigmented cultures exposed to UVA irradiation, with lethality exclusively observed in unpigmented cells (**Figures 4.7, 4.8**). These results indicated that loss of pigmentation was directly connected to the development of lethal UVA-sensitivity. As UVA lethality predominates through the generation of intracellular ROS, the pigmentation of *Arthrobacter* sp. NamB2 likely provides UVA-

protection through the action of its carotenoids as antioxidants, an antioxidant capacity lost under pigment-deprivation.

An organism's UVA tolerance is determined by the strength of its intracellular antioxidant activity (Khaengraeng and Reed 2005; Cadet et al. 2015). Intracellular ROS concentrations increase linearly with UVA dosages, and bacterial death due to UVA exposure is directly proportional to accumulation of ROS damage (Tyrrell 1985; Eisenstark 1998; He and Häder 2002a; Khaengraeng and Reed 2005; Santos et al. 2013; Song et al. 2019). Adding high concentrations of antioxidants to UVA-exposed bacterial cultures is known to mitigate UVA-lethality, highlighting the importance of cellular antioxidants to bacterial UVA-tolerance (Tyrrell 1985; He and Häder 2002a; Khaengraeng and Reed 2005).

Carotenoids are strong intracellular antioxidants, and provide substantial UVA protection consistent with this (Krinsky 1978; Eisenstark 1998; Stahl and Sies 2002). Deprivation of carotenoid pigmentation from bacteria increases their UVA sensitivity by 1.2 – 2.3 fold, while adding carotenoid extracts to unpigmented organisms substantially improves UVA tolerance (Ehling-Schulz and Scherer 1999; Pezzoni et al. 2011; Vinay Kumar et al. 2015; Rezaeeyan et al. 2017; Reis-Mansur et al. 2019). This tolerance is attributed to the antioxidant activities of carotenoids in mitigating UVA-induced ROS-damage, with carotenoids of greater antioxidant capacity providing stronger UVA-protective effects (Sies and Stahl 2004; Mohana et al. 2013). Bacterioruberin is known to be an excellent antioxidant as described prior (**Section 1.3.8.1.1)**. Therefore, the production of bacterioruberin by *Arthrobacter* sp. NamB2 likely substantially enhances its intracellular antioxidant capacity, particularly when considering its high efficacy as an antioxidant (Yachai 2009; Mandelli et al. 2012). This would provide pigmented *Arthrobacter* sp. NamB2 intracellular protection from UVA-stimulated ROS damage, thus lethality, which was absent from unpigmented cells. The carotenoid pigmentation of *Arthrobacter* sp. NamB2 thus significantly contributes to its UVA-resistome, likely through its antioxidant activity in quenching UVA-generated ROS.

Carotenoid pigmentation as a component of the UVA-resistome has been previously speculated in desert bacteria. For example, the prevalence of carotenoids in Antarctic bacteria is considered an adaptation of these organisms to the intense UVA-irradiation of their environment, while UVA-tolerance of desert-isolated *D. radiodurans* and *D. gobiensis* is at least partially attributed to the ROS-scavenging capacity of the carotenoid deinoxanthin (Carbonneau et al. 1989; Tian et al. 2009; Dieser et al. 2010; Yuan et al. 2012). Connections between bacterial UVA-tolerance

and carotenoid pigmentation in desert environments are thus consistent with prior findings, though novel here in study of the Namib Desert, and in the specific survival comparisons between pigmented and unpigmented cultures (Cowan et al. 2020; Flores et al. 2020).

4.4.3.2 Protection from UVB Irradiation

The pigmentation of *Arthrobacter* sp. NamB2 significantly contributes to its UVB-tolerance. Pigmented cultures were insensitive to UVB-lethality at dosages below 1,800 J/m^2, doses exerting significant lethality on unpigmented cells **(Figures 4.9 – 4.10)**. Above 1,800 J/m^2, both pigmented and unpigmented cultures showed UVB-lethality, though still of significantly greater intensity in unpigmented cultures. As the type of cellular damage predominating under UVB irradiation is dose-dependent, these findings suggested pigmentation to be limited in protection of *Arthrobacter* sp. NamB2 to the photodynamic damage inflicted by UVB, consistent with the known limitations of protection afforded by carotenoids.

Cellular damage inflicted by UVB irradiation is dose dependent. The main determinant of cellular damage at lower UVB doses is oxidative stress – resulting from the generation of intracellular ROS by UVB-responsive photosensitisers (Santos et al. 2012; Santos et al. 2013; Knak et al. 2014). Indeed, ROS-mediated damage is the main determinant of lethality under lower dosages of UVB irradiation (Santos et al. 2012; Santos et al. 2013). While DNA damage does occur, the formation of DNA photoadducts is relatively infrequent under low dose UVB, and is ameliorable by the cellular DNA repair machinery (Santos et al. 2012; Santos et al. 2013). However, as total UVB dosages increase, DNA damage accumulates and eventually overwhelms the DNA repair systems, and while ROS generation is still inflicting cellular damage, this direct DNA damage becomes the primary determinant of cellular inactivation (He and Häder 2002b; He and Häder 2002c; Qiu et al. 2005; Santos et al. 2012; Santos et al. 2013). Consequently, the antioxidant capacities of bacterial cultures are only effective in mitigating the damaging effects of low dose UVB, and eventually lose efficacy as DNA damage takes precedence as the determinant of cellular inactivation (Sandmann et al. 1998; He and Häder 2002b; He and Häder 2002c; Santos et al. 2012; Santos et al. 2013). As carotenoids exert protective effects predominantly through their antioxidant activity, a similar loss of protective efficacy reflecting these shifts in UVB damage modes would be expected.

The pigment-mediated UVB-protection observed in *Arthrobacter* sp. NamB2 appeared to match these shifting dynamics of UVB-damage. The insensitivity of pigmented cultures to lower UVB

doses (below 1,800 J/m^2) compared to unpigmented cultures may be attributed to antioxidant activity of bacterioruberin in mitigation of UVB-mediated ROS damage, similar to that suggested for UVA. As total UVB-doses increased past 1,800 J/m^2, pigmented cultures developed lethal UVB sensitivity, though still significantly below that of unpigmented cells. This development of lethality in pigmented cells may demonstrate the shift to DNA damage as the determinant of cellular inactivation, which bacterioruberin would be unable to mitigate. Carotenoids are considered unable to ameliorate direct DNA damage outside of their screening roles, and direct UVB-screening by the pigmentation of *Arthrobacter* sp. NamB2 has already been dismissed within this chapter (**Section 4.4.2**) (Cockell and Knowland 1999; Cockell et al. 2003). The significantly higher survival of pigmented cells, even at high UVB dosages, suggests that ROS generation was still occurring and stimulating intracellular damage (Santos et al. 2012). Indeed, ROS damage to membrane structures and proteins under UVB irradiation is known to weaken the ability of organisms to generate energy to sustain DNA repair pathways, compounding the impact of UVB irradiation (Qiu et al. 2005; Santos et al. 2013). The significantly higher lethality of unpigmented cultures at these high UVB-dosages therefore likely reflected their continued inability to mitigate UVB-stimulated ROS to the same capacity as pigmented cells, compounding the lethality of direct DNA damage with additional ROS-damage and the susceptibility this inflicts. The carotenoid pigmentation of *Arthrobacter* sp. NamB2 thus contributes significantly to its UVB-irradiation resistome. From the known damage modes of UVB, this protection likely represented the mitigation of UVB-induced ROS-damage by the pigment, providing no protection against the direct DNA damage predominating at higher UVB dosages.

Carotenoid pigmentation has been attributed roles in the UVB-resistome of other desert bacteria. The UVB tolerance of *Microbacterium* from Antarctic soils is partially connected to ROS-quenching provided by its carotenoid pigmentation, with unpigmented *E. coli* supplemented by its pigment extract showing a 2-fold increase in UVB-resistance (Reis-Mansur et al. 2019). Bacterioruberin-producing Antarctic *A. agilis* has demonstrated significantly higher survival under UVB-irradiation than decaprenoxanthin-producing *A. psychrochitiniphilus*, a difference potentially attributable to the heightened efficacy of bacterioruberin in quenching UVB-stimulated ROS (Silva et al. 2019). Again, this chapter demonstrates novelty in its specific characterisation of pigment-mediated UVB-protection in *Arthrobacter* sp. NamB2 through comparisons of pigmented and unpigmented cultures, and its exploration of this phenomenon within the Namib Desert.

4.4.3.3 Protection from UVC Irradiation

The pigmentation of *Arthrobacter* sp. NamB2 had no contribution to its UVC resistance. No significant differences in survival were observed at any time-point between pigmented and unpigmented cells of *Arthrobacter* sp. NamB2 under UVC irradiation. This was expected as cellular lethality inflicted by UVC is through direct DNA/protein damage as opposed to the production of damaging intermediates such as ROS (Taylor 2005; Santos et al. 2013). Bacterial DNA absorbs UVC directly, producing mutagenic/lethal adducts (Kuluncsics et al. 1999; Yoon et al. 2000; Besaratinia et al. 2011). Indeed, bacterial lethality under UVC is directly proportional to the accumulation of direct DNA damage markers and mutagenic photoadducts (Rastogi et al. 2010; Besaratinia et al. 2011; Santos et al. 2013). As the protective effects of carotenoids are predominantly associated with their antioxidant capacity, and ROS-generation is negligible under UVC-irradiation, carotenoid protection from UVC is unexpected, and would be reliant on screening effects (Cockell and Knowland 1999). As the pigmentation of *Arthrobacter* sp. NamB2 has been shown to lack notable absorbance in the UVC-region, and thereby lacks UVC-screening effects (**Section 4.4.2**), it was not expected to contribute to the UVC-tolerance of this organism, as was observed here.

Without screening effects, UVC-survival of pigmented and unpigmented cells would be determined instead by their DNA repair pathways, which would be unaffected by carotenoid deprivation (Rastogi et al. 2010; Pavlopoulou et al. 2016; Jones and Baxter 2017; Buckley 2020). As pigmented and unpigmented cells are expected to possess the same DNA damage responses, their ability to mediate UVC damage is equivalent, as was demonstrated here through their comparability in UVC-lethality (Britton 1995; Pavlopoulou et al. 2016; Jones and Baxter 2017). Consistent with expectations of carotenoids, the pigmentation of *Arthrobacter* sp. NamB2 did not contribute to its UVC-resistome.

Carotenoid pigments of desert organisms are rarely considered a component of their resistome against irradiation stimulating direct DNA damage (Paulino-Lima et al. 2013; Albarracín et al. 2016; Pavlopoulou et al. 2016). Deinoxanthin in *D. gobiensis and D. radiodurans* provides no protection from UVC-irradiance, with their tolerance instead connected to the action of photolyase genes and DNA repair proteins (Mattimore and Battista 1996; Tanaka et al. 2004; Tian et al. 2007; Yuan et al. 2012; Pavlopoulou et al. 2016). Carotenoids with dramatically differing biological and antioxidant capacities provide no differences in UVC-tolerance, suggesting an insensitivity of UVC damage to carotenoid biological activities (Dundas and Larsen 1963; Sharma et al. 1984; Silva et al. 2019). While the production of carotenoid

pigmentation correlates well with UVC-tolerance in desert organisms, this likely corresponds less to the action of these carotenoids in UVC-protection, and more towards organismal adaptation to the accompanying photodynamic stress other wavelengths of solar irradiation exert in these extreme environments, as UVC is screened quantitatively by atmospheric effects (Bowker et al. 2002; Abed et al. 2010; Girard et al. 2011; Paulino-Lima et al. 2013).

Bacterioruberin has been linked to UVC-tolerance in *Haloarchaea*. While bacterioruberin does not influence UVC-death curves, pigmented cells do demonstrate significantly higher recovery from UVC-irradiation under subsequent photoreactivation (Hescox and Carlberg 1972; Sharma et al. 1984; Shahmohammadi et al. 1998; Jones and Baxter 2017). This is possibly through the action of bacterioruberin as a chromophore for the photoreactivation system, providing energy to the photolyase enzyme for DNA repair, although this lacks direct demonstration, and is contentious in mechanism (Hescox and Carlberg 1972; Sharma et al. 1984; Jones and Baxter 2017). *Arthrobacter* sp. NamB2 is known to encode a complete photoreactivation system, and the intentional incubation of cells in light conditions post-UVC irradiation as employed here should have engaged this system (Oguma et al. 2002; Quek and Hu 2008; Buckley 2020). However, disparities in UVC-recovery between pigmented and unpigmented bacteria were not observed here. Thus, the protective mechanism of bacterioruberin in *Haloarchaea* does not appear to occur in *Arthrobacter* sp. NamB2. As such a mechanism would rely on interactions between bacterioruberin and photolyase enzymes, and photolyase enzymes are known to be highly variable in sequence and structure between bacteria and archaea, the differences between the photolyase enzymes of *Arthrobacter* and *Haloarchaea* may potentially be attributable to the absence of this phenomenon here (Mei and Dvornyk 2015). Regardless, the lack of protection provided by pigmentation of *Arthrobacter* sp. NamB2 against UVC irradiation was largely expected, and was consistent with known limitations of carotenoid UV-protective capacities and conclusions from other desert organisms.

The pigmentation of *Arthrobacter* sp. NamB2 thus contributed significantly to its UVA and UVB irradiation resistome, with no contribution to its UVC-tolerance. In the Namib Desert, ground-level UV-irradiation is constrained to the UVA and UVB wavebands, with UVC being quantitatively screened by atmospheric ozone (Cunningham 1998; Beckmann et al. 2014; Cordero et al. 2014). While specific dosages of irradiation cannot be compared to findings here due to the substantially longer irradiation-cycles of the Namib Desert and variable influences of soil UV-screening, the significant contribution of pigmentation to the survival of *Arthrobacter* sp. NamB2 under these irradiation wavebands does indicate the pigment to provide a physiologically-relevant protective function to this organism against a pronounced stressor of its

natural environment (Zhang et al. 2010; Warren-Rhodes et al. 2013; León-Sobrino et al. 2019). The pigmentation of *Arthrobacter* sp. NamB2 thus contributes meaningfully to its multifaceted UV-resistome, and presents protection against irradiation-stresses directly relevant to the desert environment from which it was isolated.

4.4.3.4 Limitations of the UV Irradiation Analysis

4.4.3.4.1 The Mechanisms of UV-Damage were Inferred

The protective mechanisms of carotenoid pigmentation in *Arthrobacter* sp. NamB2 under UVA, UVB and UVC irradiation were concluded from known damage modes of these different UV wavelengths as opposed to being specifically demonstrated. Directly demonstrating the nature of cell damage occurring under each UV-wavelength, and connecting these to the corresponding protection afforded by bacterioruberin, would strengthen conclusions regarding the mechanism by which pigmentation contributes to the UV-resistome.

The antioxidant protection attributed to the pigment against UVA and low-dose UVB may have been demonstrated by proving the photodynamic nature of cellular-damage occurring under these irradiation wavelengths, and connecting this to the resistance of pigmented cells. Photodynamic reactions which generate ROS rely on the presence of light, an endogenous photosensitiser and oxygen (Ziegelhoffer and Donohue 2009; Alves et al. 2014). If cellular lethality was dependent on photodynamic damage, then prevention of ROS generation under UVA/UVB irradiation would be expected to reduce the cell death in unpigmented cells to the same level as in pigmented cells. This could be achieved through replacement of oxygen in the exposure system with an inert gas such as nitrogen, to observe whether the same dynamics of lethality occur (Dundas and Larsen 1963; Krinsky 1978; Rodriguez-Valera et al. 1982). Exclusive lethality of oxygen-exposed irradiated cells would demonstrate the photodynamic nature of the damage occurring, and lack thereof in pigmented cells could be more strongly connected to the function of carotenoids as antioxidants (Rodriguez-Valera et al. 1982). Demonstration of ROS-mediated UV stress may also be explored through examination of cell markers indicative of oxidative damage, including modelling lipid peroxidation and/or protein oxidation (Santos et al. 2012; Santos et al. 2013). Given that both UVA and UVB are capable of inflicting direct DNA damage in addition to photodynamic effects, demonstrating that lethality here was photodynamic would have strengthened the conclusions drawn that the antioxidant

effects of the carotenoid were specifically attributable to the protective actions observed (Santos et al. 2013).

Under high-dose UVB and UVC, DNA damage was presumed to be the primary cause of cellular-lethality. Demonstrations of irradiation-stimulated DNA damage in literature typically quantify common DNA damage markers occurring under irradiation, such as the formation of CPD's, thymine dimers, or double stranded breakages of the DNA (Baxter et al. 2007; Santos et al. 2012; Santos et al. 2013). Quantifying these markers of DNA damage under UVB and UVC irradiation, and comparing their formation in pigmented and unpigmented organisms, would more directly demonstrate both the nature of damage inflicted by these wavebands, and the efficacy of the pigment in protection from this damage.

4.4.3.4.2 The Photosensitiser of *Arthrobacter* sp. NamB2 is Unknown

It was inferred here that UVA and low-dose UVB stimulated damage in *Arthrobacter* sp. NamB2 via photodynamic action, reliant on endogenous photosensitisers (Ziegelhoffer and Donohue 2009; Alves et al. 2014). Specific identification of these photosensitisers would support these inferred mechanisms of damage, and develop our understanding of the manner by which solar irradiation exerts lethality upon *Arthrobacter* sp. NamB2 (Hessling et al. 2017). Such an analysis might focus on porphyrins, which act as endogenous UVA photosensitisers in a variety of bacteria (Burchard and Dworkin 1966; Tyrrell and Keyse 1990; Nitzan and Kauffman 1999; Baier et al. 2006; Hope et al. 2016; Brem et al. 2017; Shleeva et al. 2019) and which are produced by *Arthrobacter* spp. (Kortstee 1969; Kortstee 1970; Kajiwara et al. 1994; Kajiwara et al. 1995; Yang and Hoober 1995; Sutthiwong, Fouillaud, et al. 2014). Indeed, genes for the complete porphyrin biosynthetic pathway are conserved within the *Arthrobacter* sp. NamB2 genome, suggesting its capacity for the biosynthesis of a variety of photosensitising porphyrins including uroporphyrin II, coproporphyrin III, and protoporphyrin IX. Riboflavin is also capable of acting as a photosensitiser under UVA and UVB irradiation (Heck et al. 2003; Baier et al. 2006; Knak et al. 2014; Brem et al. 2017; Vollmerhausen et al. 2017). *Arthrobacter* spp. are known to produce and accumulate riboflavin (Yamane et al. 1993; Yamane et al. 1995; Sutthiwong, Fouillaud, et al. 2014) and *Arthrobacter* sp. NamB2 appears to retain genes for the standard bacterial riboflavin biosynthetic pathway – suggesting a possible role for this as a photosensitiser (Vitreschak et al. 2002; Thakur et al. 2017). Characterisation of the specific photosensitiser(s) of *Arthrobacter* sp. NamB2 would strengthen conclusions regarding mechanisms of photodynamic damage occurring here, and more clearly characterise its irradiance-susceptibility.

4.5 Conclusions

Carotenoids are considered significant contributors to irradiation resistomes of edaphic bacteria from a variety of desert systems (Dieser et al. 2010; Yuan et al. 2012; Reis-Mansur et al. 2019). As *Arthrobacter* sp. NamB2 presents substantial UV tolerance, and has been demonstrated within this thesis to produce carotenoid pigmentation, this chapter sought to examine the contribution of the carotenoid pigmentation of *Arthrobacter* sp. NamB2 to its UV-resistome.

Carotenoid pigmentation was found to significantly enhance the survival of *Arthrobacter* sp. NamB2 under UVA and UVB irradiation, with no protection under UVC. Pigment-mediated UV-screening was dismissed from contributing to UV-tolerance here, due to the pigment's lack of strong absorbance at relevant irradiation wavelengths used in the UV-survival assays. Consequently, this protection was inferred to be exerted through amelioration of ROS generated by incident irradiation through the antioxidant activity of bacterioruberin. Direct DNA damage resulting from high-dose UVB and UVC was not expected to be mitigated by carotenoid pigmentation, and findings here were consistent with these expectations. The carotenoid pigmentation of *Arthrobacter* sp. NamB2 was thus concluded to contribute significantly to its UVA and UVB resistome, but not its UVC resistome. Direct demonstration of the pigment's specific protective mechanisms under these irradiation conditions would strengthen these inferred conclusions.

As UV-irradiation in the Namib Desert predominates in the UVA and UVB wavebands, this pigmentation likely confers a tangible physiological advantage to *Arthrobacter* sp. NamB2 within its natural environment (Cunningham 1998; Beckmann et al. 2014; Cordero et al. 2014). The contribution of carotenoids to irradiation resistomes of edaphic desert bacteria and organisms within the genus *Arthrobacter* have been widely purported, but are rarely specifically demonstrated (Tian et al. 2009; Dieser et al. 2010; Pavlopoulou et al. 2016; Silva et al. 2019). This research thus presents a novel contribution to several foci of study. This is the first study to specifically demonstrate UV-protective functions of carotenoids in *Arthrobacter* through organism-level comparison of pigmented and unpigmented cultures. It is also (to this author's knowledge), the first analysis of this nature examining the protective roles of bacterioruberin against UVA and UVB irradiation. This study also joins the limited scope of literature specifically demonstrating carotenoid-mediated UV-protection of desert bacteria, and represents the first characterisation of carotenoid pigmentation as a photoprotectant in bacteria of the Namib Desert, a yet unstudied model for pigment-mediated bacterial protection.

Chapter 5 Final Discussion

Deserts are subject to biologically stressful intensities of irradiation which significantly influence bacterial community compositions and distributions within these environments (Cary et al. 2010; Cordero et al. 2018; Cowan et al. 2020). Prolonged solar irradiation is further known to stimulate the development of complex, multifaceted irradiation-resistomes within desert bacteria in tolerance of this stress (Albarracín et al. 2016; Pavlopoulou et al. 2016). Characterising the specific tolerance mechanisms utilised by bacteria within desert systems thus strengthens our understanding of the complexity of resistome-features which enable bacterial persistence under prolonged solar irradiation (Pavlopoulou et al. 2016).

This thesis investigated the role of intracellular pigmentation in the irradiation-resistance of the highly UV-tolerant, novel edaphic bacterium *Arthrobacter* sp. NamB2, recently identified from soils of the Namib Desert (Buckley 2020). Intracellular carotenoid pigmentation is considered a significant component of the irradiation-resistome in edaphic bacteria from a variety of desert systems, and a similar function was suspected for the pink pigment produced by this novel organism (Yuan et al. 2012; Reis-Mansur et al. 2019; Silva et al. 2019; Flores et al. 2020).

The overarching objective of this research was thus to determine the contribution of pigmentation to the irradiation-resistome of *Arthrobacter* sp. NamB2. To achieve this, the pigmentation was first identified, its light-inducibility was explored to examine evidence of its role in photoprotection, and its protective capacity under different wavelengths of UV-irradiation was determined.

5.1 Research Question 1: What is the likely identity of the pink-pigmentation produced by *Arthrobacter* sp. NamB2?

The pigment complement of *Arthrobacter* sp. NamB2 was extracted and subject to established protocols for pigment identification (Britton and Young 1993; Britton et al. 1995b). Total pigment extraction and analysis via UV-visible spectrophotometry demonstrated the pigmentation to belong to the carotenoid class through its production of characteristic carotenoid three-peaked spectral responses. Subsequent TLC and HPLC analyses supplemented by UV-visible spectrophotometry determined that the pigment complement comprised six – eight carotenoids of distinct polarity, all with chromophores thirteen conjugated double-bonds

in length. Finally, MS specifically demonstrated the presence of the carotenoid bacterioruberin within the pigment complement, and strongly supported the remaining carotenoids as being glycosylated/dehydrated bacterioruberin variants commonly co-isolated alongside bacterioruberin. These results were supported by polarity-based identifications provided from TLC analyses. While the limited resolution of the methods applied precluded definitive identification of each individual carotenoid, the conclusion that *Arthrobacter* sp. NamB2 produces a carotenoid pigment complement comprising bacterioruberin and its common variants was consistent with findings from other pink, desert-isolated *Arthrobacter* (Fong et al. 2001; Silva et al. 2019). As carotenoid pigmentation from desert bacteria is typically associated with roles in irradiation-tolerance, this potential function of pigmentation within *Arthrobacter* sp. NamB2 was further explored.

5.2 Research Question 2: Is production of the pink-pigmentation of *Arthrobacter* sp. NamB2 light-induced?

As light-responsive carotenoid production by bacteria indicates their use of carotenoids in photoprotection, evidence of light-induced carotenogenesis was explored in *Arthrobacter* sp. NamB2 to support the photoprotective roles speculated for its pigment (Takano 2016). Growth of *Arthrobacter* sp. NamB2 cultures at a range of different light intensities concluded a lack of light-responsive carotenogenesis by the organism. This was supported by the absence of relevant homologues to known regulator proteins which would confer this function within its genome. This finding was unsurprising due to the scarcity of light-responsive pigmentation in soil bacteria, and the poor genomic maintenance of these regulators. Nevertheless, these findings contributed novel information to the yet uncharacterised prevalence of light-responsive pigmentation in desert bacteria, and to its limited study within the genus *Arthrobacter*. Furthermore, these findings did not discredit the potential photoprotective role of pigmentation in *Arthrobacter* sp. NamB2, only supporting that its production does not occur specifically as a photoresponse.

5.3 Research Question 3: What contribution does pigmentation provide the ultraviolet irradiation resistome of *Arthrobacter* sp. NamB2?

Finally, to characterise the specific contribution of pigmentation to the UV-resistome of *Arthrobacter* sp. NamB2, the survival of pigmented and unpigmented cultures exposed to UV-irradiation was compared. Pigmented and unpigmented *Arthrobacter* sp. NamB2 were irradiated with UVA, UVB and UVC to determine within which irradiance wavelength(s) the pigment was capable of providing protection, and in doing so, speculate on its protective mechanism. These investigations demonstrated the pigmentation of *Arthrobacter* sp. NamB2 to confer protection to UVA and low dose UVB, with limited protection under higher dosages of UVB, and a complete loss under UVC. These findings were consistent with protective capacities expected of carotenoid pigments, and suggested that the pigmentation provided UV-protection through ROS-quenching, and was incapable of preventing direct DNA/protein damage. The pigmentation was further concluded as lacking protective UV-screening due to its low-intensity absorbance within the UV waveband, as observed from scanning UV-visible absorbance spectra. While consistent with theoretical expectations, this analysis would benefit from specific demonstrations of the antioxidant nature of protection attributed to the pigment, as this protective mechanism is currently speculative. In the Namib Desert, this pigmentation is thus expected to provide cellular protection from irradiation-stimulated photodynamic damage from UVA and low-intensity UVB, which comprises the majority of ground-level UV-irradiation to which edaphic bacteria are subject.

5.4 Future Directions

Throughout this thesis, a number of areas for further development of the study were identified:

- **Formal pigment identification.** While the methods employed here confirmed the presence of bacterioruberin within *Arthrobacter* sp. NamB2, they did not meet the standards required for formal identification of the pigment complement (Britton et al. 2004; Takaichi 2014). Higher-resolution chromatographic analysis of the pigment complement run alongside known bacterioruberin standards, and a greater specificity in structural elucidation through high-resolution MS would have been required to

strengthen identification here to a level consistent with formal expectations, and to resolve ambiguities regarding the identity of several pigment fractions.

- **Transcriptomics analysis of light-inducibility.** This thesis concluded a lack of light-responsive carotenogenesis in *Arthrobacter* sp. NamB2 from total carotenoid quantifications of cultures grown under differing intensities of light. While this end-product quantification is accepted in demonstrations of carotenoid light-inducibility, specific examinations of *Arthrobacter* sp. NamB2 carotenoid gene-activity via RT-qPCR under differing conditions of irradiation would demonstrate more directly whether carotenogenesis was responsive to visible light.
- **Broader inducibility wavelengths.** This study examined light-responsive carotenogenesis through irradiation of *Arthrobacter* sp. NamB2 with light in the PAR range. Carotenoid inducibility has previously been demonstrated to extend into the UV-waveband, and UV-inducibility can provide specific information regarding the protective roles of carotenoid pigments. Investigating inducibility of *Arthrobacter* sp. NamB2 carotenoids at UV-wavelengths employed here in survivability studies (i.e. within UVA, UVB and UVC wavebands) could provide novel information regarding the UV-protective role of pigmentation.
- **Light-induced shifts in pigment composition.** Some studies monitoring environmentally-responsive carotenoid production have detected physiologically relevant changes in the proportions of individual carotenoids comprising the pigment complement, which would not have been detected here. It may be of interest to investigate light-responsive shifts in the proportions of individual carotenoid components comprising the pigment complement of *Arthrobacter* sp. NamB2, to characterise any physiologically relevant carotenoid light-responses which were undetected via the methods employed.
- **Specific demonstrations of pigment protective mechanisms.** The nature of the protection provided by pigmentation in *Arthrobacter* sp. NamB2 under irradiation was inferred here from established information regarding the damage modes of different UV-wavelengths. Antioxidant protection of pigmentation under UVA and low-dose UVB irradiation may have been demonstrated directly by investigating the importance of oxygen to the irradiation-mediated lethality of unpigmented cells. Equally, the DNA-mediated damage of high dose UVB and UVC may have been demonstrated via quantification of common DNA damage markers such as CPD's or double stranded breaks, as performed in studies such as Baxter et al. (2007). These demonstrations would aide specific conclusions regarding the pigment's contribution to the UV-resistome, which are at present inferred.
- **Demonstration of photosensitisers.** Specific identification of the intracellular photosensitiser(s) of *Arthrobacter* sp. NamB2 which stimulated the speculated ROS-

generation under UVA and UVB irradiation would strengthen the inferred antioxidant role attributed to the pigment, and would provide clearer indication of the wavebands capable of stimulating photodynamic damage within this organism.

5.5 Conclusions

This study presents the first characterisation of carotenoid pigmentation from edaphic bacteria of the Namib Desert, and its protective function against irradiation. Within this research, both the identity and UV-resistome contributions of the pink pigmentation from novel bacterium *Arthrobacter* sp. NamB2 have been investigated.

Common methods of identification demonstrated the pink pigmentation of *Arthrobacter* sp. NamB2 as carotenogenic, and specifically comprised of the carotenoid bacterioruberin and its commonly co-isolated carotenoid variants. This pigment complement was consistent with those from other desert-isolated *Arthrobacter* with speculated photoprotective functions, and suggested a similar role in the protection of *Arthrobacter* sp. NamB2 from irradiation. Both phenotypic and genomic investigations of carotenogenic light-inducibility concluded a lack of light-responsive carotenoid biosynthesis, demonstrating that *Arthrobacter* sp. NamB2 does not produce its pigment specifically as a photoprotective response. This was unsurprising due to the scarcity of light-responsive pigmentation in soil bacteria, and the poor genomic-maintenance of these regulators, and did not rule out the potential irradiation-protection afforded by this pigment. Finally, investigations of the contribution of pink pigmentation to the UV-resistome of *Arthrobacter* sp. NamB2 demonstrated pigmentation to confer protection from UVA and low dose UVB, with limited protection under higher dosages of UVB, and a complete loss under UVC. These findings followed the protective capacities expected of carotenoid pigments, and suggested pigmentation to provide UV-protection via ROS-quenching, with an inability to prevent direct DNA/protein damage. In the Namib Desert, this pigmentation is thus expected to provide *Arthrobacter* sp. NamB2 with protection from UVA and UVB-stimulated photodynamic damage, wavebands which comprise the majority of the surface irradiation of this environment. The pink-pigmentation of *Arthrobacter* sp. NamB2 thus contributes meaningfully to its multifaceted UV-resistome.

Demonstrating the bacterioruberin pigment of *Arthrobacter* sp. NamB2 as contributing to its UV-resistome is novel in several ways. It is the first specific demonstration of carotenoid-mediated irradiation protection within genus *Arthrobacter*, in which photoprotective roles of

pigmentation have thusfar only been speculated – despite the wide distribution of pigmented isolates in high-irradiance environments. Similarly, it is the first demonstration of the contribution of bacterioruberin to UVA and UVB tolerance. Finally, it is the first study examining bacterial carotenoid pigmentation – and its contribution to intrinsic irradiation-tolerance – in the Namib Desert, and adds to a limited breadth of literature specifically demonstrating the importance of carotenoids to the irradiance-survival of desert bacteria. Consequently, this study contributes meaningfully to our understanding of the mechanisms of irradiation-tolerance used by extremophilic organisms from environments of biologically stressful irradiation.

References

Aakermann T, Skulberg OM, Liaaen-Jensen S. 1992. A comparison of the carotenoids of strains of *Oscillatoria* and *Spirulina* (cyanobacteria). Biochem Syst Ecol. 20(8):761–769. doi:10.1016/0305-1978(92)90035-C.

Abate-Pella D, Freund DM, Slovin JP, Hegeman AD, Cohen JD. 2017. An improved method for fast and selective separation of carotenoids by LC–MS. J Chromatogr B. 1067:34–37. doi:10.1016/j.jchromb.2017.09.039.

Abdel-Rahman F, Okeremgbo B, Alhamadah F, Jamadar S, Anthony K, Saleh MA. 2017. *Caenorhabditis elegans* as a model to study the impact of exposure to light emitting diode (LED) domestic lighting. J Environ Sci Health A Tox Hazard Subst Environ Eng. 52(5):433–439. doi:10.1080/10934529.2016.1270676.

Abdullah MA, Dajah SA, Murad AA, El-Salem AM, El-Salem AM. 2019. Extraction, purification, and characterization of lycopene from Jordanian vine tomato cultivar, and study of its potential natural antioxidant effect on Samen Baladi. Curr Res Nutr Food Sci. 7(2):532–546. doi:10.12944/CRNFSJ.7.2.22

Abed RMM, Al Kharusi S, Schramm A, Robinson MD. 2010. Bacterial diversity, pigments and nitrogen fixation of biological desert crusts from the Sultanate of Oman. FEMS Microbiol Ecol. 72(3):418–428. doi:10.1111/j.1574-6941.2010.00854.x.

Adesina JA, Piketh SJ, Formenti P, Maggs-Kölling G, Holben BN, Sorokin MG. 2019. Aerosol optical properties and direct radiative effect over Gobabeb, Namibia. Clean Air Journal. 29(2):1–11. doi:10.17159/caj/2019/29/2.7518.

Afra S, Makhdoumi A, Matin MM, Feizy J. 2017. A novel red pigment from marine *Arthrobacter* sp. G20 with specific anticancer activity. J Appl Microbiol. 123(5):1228–1236. doi:10.1111/jam.13576.

Agogué H, Joux F, Obernosterer I, Lebaron P. 2005. Resistance of marine bacterioneuston to solar radiation. Appl Environ Microbiol. 71(9):5282–5289. doi:10.1128/AEM.71.9.5282-5289.2005.

Albanesi D, Martín M, Trajtenberg F, Mansilla MC, Haouz A, Alzari PM, de Mendoza D, Buschiazzo A. 2009. Structural plasticity and catalysis regulation of a thermosensor histidine kinase. Proc Natl Acad Sci USA. 106(38):16185–16190. doi:10.1073/pnas.0906699106.

Albarracín VH, Gärtner W, Farias ME. 2016. Forged under the sun: life and art of extremophiles from Andean lakes. Photochem Photobiol. 92(1):14–28. doi: doi.org/10.1111/php.12555.

Alcaíno J, Baeza M, Cifuentes V. 2016. Carotenoid distribution in nature. In: Stange C, editor. Carotenoids in nature: biosynthesis, regulation and function. Cham (Switzerland): Springer International Publishing. p. 3–33.; [accessed 2020 Sep 19]. https://doi.org/10.1007/978-3-319-39126-7_1.

Alekshun MN, Levy SB, Mealy TR, Seaton BA, Head JF. 2001. The crystal structure of MarR, a regulator of multiple antibiotic resistance, at 2.3 Å resolution. Nat Struct Mol Biol. 8(8):710–714. doi:10.1038/90429.

Alves E, Faustino MA, Neves MG, Cunha A, Tome J, Almeida A. 2014. An insight on bacterial cellular targets of photodynamic inactivation. Future Med Chem. 6(2):141–164. doi:10.4155/fmc.13.211.

Amagasa J. 1981. Dye binding and photodynamic action. Photochem Photobiol. 33(6):947–955. doi:10.1111/j.1751-1097.1981.tb05519.x.

Amorim-Carrilho KT, Cepeda A, Fente C, Regal P. 2014. Review of methods for analysis of carotenoids. Trends Anal Chem. 56:49–73. doi:10.1016/j.trac.2013.12.011.

Andersen H, Cermak J. 2018. First fully diurnal fog and low cloud satellite detection reveals life cycle in the Namib. Atmos Meas Tech. 11(10):5461–5470. doi:10.5194/amt-11-5461-2018.

Andersen H, Cermak J, Fuchs J, Knippertz P, Gaetani M, Quinting J, Sippel S, Vogt R. 2020. Synoptic-scale controls of fog and low-cloud variability in the Namib Desert. Atmos Chem Phys. 20(6):3415–3438. doi:10.5194/acp-20-3415-2020.

Andersen H, Cermak J, Solodovnik I, Lelli L, Vogt R. 2019. Spatiotemporal dynamics of fog and low clouds in the Namib unveiled with ground- and space-based observations. Atmos Chem Phys. 19(7):4383–4392. doi:10.5194/acp-19-4383-2019.

Anderson SM, Krinsky NI. 1973. Protective action of carotenoid pigments against photodynamic damage to liposomes. Photochem Photobiol. 18(5):403–408. doi:10.1111/j.1751-1097.1973.tb06440.x.

Andrew DR, Fitak RR, Munguia-Vega A, Racolta A, Martinson VG, Dontsova K. 2012. Abiotic factors shape microbial diversity in Sonoran Desert soils. Appl Environ Microbiol. 78(21):7527–7537. doi:10.1128/AEM.01459-12.

Anthis NJ, Clore GM. 2013. Sequence-specific determination of protein and peptide concentrations by absorbance at 205 nm. Protein Sci. 22(6):851–858. doi:10.1002/pro.2253.

Armstrong GA. 1994. Eubacteria show their true colors: genetics of carotenoid pigment biosynthesis from microbes to plants. J Bacteriol. 176(16):4795–4802. doi:10.1128/jb.176.16.4795-4802.1994

Armstrong GA. 1997. Genetics of Eubacterial carotenoid biosynthesis: a colorful tale. Annu Rev Microbiol. 51(1):629–659. doi:10.1146/annurev.micro.51.1.629.

Arpin N, Fiasson JL, Liaaen-Jensen A. 1972. Bacterial carotenoids. XXXIX. C_{50}-carotenoids. 10. Bacterioruberin mono- and diglucoside. Acta Chem Scand. 26(6):2526–2528. doi:10.3891/acta.chem.scand.26-2526.

Arpin N, Fiasson J-L, Norgård S, Borch G, Liaaen-Jensen S. 1975. Bacterial carotenoids. XLVI. C_{50}-carotenoids. 14. C_{50}-carotenoids from *Arthrobacter* glacialis. Acta Chem Scand. 29:921–926. doi:10.3891/acta.chem.scand.29b-0921.

Arpin N, Liaaen-Jensen S, Trouilloud M, Watson KJ, Svensson S. 1972. Bacterial carotenoids. XXXVIII. C_{50}-carotenoids. 9. Isolation of decaprenoxanthin mono- and diglucoside from an *Arthrobacter* sp. Acta Chem Scand. 26:2524–2526. doi:10.3891/acta.chem.scand.26-2524.

Asker D, Awad T, Ohta Y. 2002. Lipids of *Haloferax alexandrinus* strain TMT: an extremely halophilic canthaxanthin-producing archaeon. J Biosci Bioeng. 93(1):37–43. doi:10.1016/S1389-1723(02)80051-2.

Auldridge ME, Forest KT. 2011. Bacterial phytochromes: more than meets the light. Crit Rev Biochem Mol Biol. 46(1):67–88. doi:10.3109/10409238.2010.546389.

Avalos J, Pardo-Medina J, Parra-Rivero O, Ruger-Herreros M, Rodríguez-Ortiz R, Hornero-Méndez D, Limón MC. 2017. Carotenoid biosynthesis in *Fusarium*. J Fungi. 3(3):39. doi:10.3390/jof3030039.

Azúa-Bustos A, González-Silva C, Mancilla RA, Salas L, Gómez-Silva B, McKay CP, Vicuña R. 2011. Hypolithic cyanobacteria supported mainly by fog in the coastal range of the Atacama Desert. Microb Ecol. 61(3):568–581. doi:10.1007/s00248-010-9784-5.

Baier J, Maisch T, Maier M, Engel E, Landthaler M, Bäumler W. 2006. Singlet oxygen generation by UVA light exposure of endogenous photosensitizers. Biophys J. 91(4):1452–1459. doi:10.1529/biophysj.106.082388.

Baliga NS, Bjork SJ, Bonneau R, Pan M, Iloanusi C, Kottemann MCH, Hood L, DiRuggiero J. 2004. Systems level insights into the stress response to UV radiation in the halophilic archaeon *Halobacterium* NRC-1. Genome Res. 14(6):1025. doi:10.1101/gr.1993504.

Ballal A, Manna AC. 2010. Control of thioredoxin reductase gene (*trxB*) transcription by SarA in *Staphylococcus aureus*. J Bacteriol. 192(1):336–345. doi:10.1128/JB.01202-09.

Baptista M da S, Cadet J, Di Mascio P, Ghogare AA, Greer A, Hamblin MR, Lorente C, Nunez SC, Ribeiro MS, Thomas AH, et al. 2017. Type I and II photosensitized oxidation reactions: guidelines and mechanistic pathways. Photochem Photobiol. 93(4):912–919. doi:10.1111/php.12716.

Baranova NN, Danchin A, Neyfakh AA. 1999. Mta, a global MerR-type regulator of the *Bacillus subtilis* multidrug-efflux transporters. Mol Microbiol. 31(5):1549–1559. doi:10.1046/j.1365-2958.1999.01301.x.

Barba AIO, Hurtado MC, Mata MCS, Ruiz VF, Tejada MLS de. 2006. Application of a UV–vis detection-HPLC method for a rapid determination of lycopene and β-carotene in vegetables. Food Chem. 95(2):328–336. doi:10.1016/j.foodchem.2005.02.028.

Battocchio G, González R, Rao AG, Schapiro I, Mroginski MA. 2020. Dynamic properties of the photosensory domain of *Deinococcus radiodurans* bacteriophytochrome. J Phys Chem B. 124(9):1740–1750. doi:10.1021/acs.jpcb.0c00612.

Baxter BK, Eddington B, Riddle MR, Webster TN, Avery BJ. 2007. Great Salt Lake halophilic microorganisms as models for astrobiology: evidence for desiccation tolerance and ultraviolet irradiation resistance. In: Hoover RB, Levin GV, Rozanov AY, Davies PCW, editors. Instruments, methods, and missions for astrobiology X. 6694:669415. Bellingham (WA): SPIE.; [accessed 2020 Aug 31]. https://www-spiedigitallibrary-org/conference-proceedings-of-spie/6694/669415/Great-Salt-Lake-halophilic-microorganisms-as-models-for-astrobiology/10.1117/12.732621.short.

Bay S, Ferrari B, Greening C. 2018. Life without water: How do bacteria generate biomass in desert ecosystems? Microbiol Aust. 39(1):28–32. doi:10.1071/MA18008.

Beckmann M, Václavík T, Manceur AM, Šprtová L, Wehrden H von, Welk E, Cord AF. 2014. glUV: a global UV-B radiation data set for macroecological studies. Methods Ecol Evol. 5(4):372–383. doi: doi.org/10.1111/2041-210X.12168.

Ben-Amotz A, Shaish A, Avron M. 1989. Mode of action of the massively accumulated β-carotene of *Dunaliella bardawil* in protecting the alga against damage by excess irradiation. Plant Physiol. 91(3):1040–1043. doi:10.1104/pp.91.3.1040

Berner T, Evenari M. 1978. The influence of temperature and light penetration on the abundance of the hypolithic algae in the Negev desert of Israel. Oecologia. 33(2):255–260. doi:10.1007/BF00344852.

Besaratinia A, Yoon J, Schroeder C, Bradforth SE, Cockburn M, Pfeifer GP. 2011. Wavelength dependence of ultraviolet radiation-induced DNA damage as determined by laser irradiation suggests that cyclobutane pyrimidine dimers are the principal DNA lesions produced by terrestrial sunlight. FASEB J. 25(9):3079–3091. doi:10.1096/fj.11-187336.

Bhoo SH, Davis SJ, Walker J, Karniol B, Vierstra RD. 2001. Bacteriophytochromes are photochromic histidine kinases using a biliverdin chromophore. Nature. 414(6865):776–779. doi:10.1038/414776a.

Bhosale P. 2004. Environmental and cultural stimulants in the production of carotenoids from microorganisms. Appl Microbiol Biotechnol. 63(4):351–361. doi:10.1007/s00253-003-1441-1.

Bidlingmeyer BA. 1987. Preparative Liquid Chromatography. New York (NY): Elsevier.

Bijttebier S, D'Hondt E, Noten B, Hermans N, Apers S, Voorspoels S. 2014. Ultra high performance liquid chromatography versus high performance liquid chromatography: stationary phase selectivity for generic carotenoid screening. J Chromatogr A. 1332:46–56. doi:10.1016/j.chroma.2014.01.042.

Biswas J, Haque FN, Paul AK. 2016. Carotenogenesis in *Haloferax* sp. strain BKW301, a halophilic archaeon from Indian Solar Saltarns. J Adv Microbiol. 1(3):1–11. doi:10.9734/JAMB/2016/31559.

Björling A, Berntsson O, Lehtivuori H, Takala H, Hughes AJ, Panman M, Hoernke M, Niebling S, Henry L, Henning R, et al. 2016. Structural photoactivation of a full-length bacterial phytochrome. Sci Adv. 2(8):e1600920. doi:10.1126/sciadv.1600920.

Björn LO. 2008a. Light as a tool for biologists: recent developments. In: Björn LO, editor. Photobiology: the science of life and light. New York (NY): Springer. p. 93–122.; [accessed 2021 Apr 11]. https://doi.org/10.1007/978-0-387-72655-7_5.

Björn LO. 2008b. Principles and nomenclature for the quantification of light. In: Björn LO, editor. Photobiology: the science of life and light. New York (NY): Springer. p. 41–49.; [accessed 2021 Apr 11]. https://doi.org/10.1007/978-0-387-72655-7_2.

Björn LO. 2015a. Terrestrial daylight. In: Björn LO, editor. Photobiology: the science of life and light. New York (NY): Springer. p. 71–75.; [accessed 2021 Jan 9]. https://doi.org/10.1007/978-1-4939-1468-5_6.

Björn LO. 2015b. Photoactive proteins. In: Björn LO, editor. Photobiology: the science of life and light. New York (NY): Springer. p. 139–150.; [accessed 2021 Jan 9]. https://doi.org/10.1007/978-1-4939-1468-5_11.

Björn LO, Huovinen P. 2015. Phototoxicity. In: Björn LO, editor. Photobiology: the science of life and light. New York (NY): Springer. p. 335–345.; [accessed 2021 Jan 9]. https://doi.org/10.1007/978-1-4939-1468-5_21.

Blanc PL, Tuveson RW, Sargent ML. 1976. Inactivation of carotenoid-producing and albino strains of *Neurospora crassa* by visible light, blacklight, and ultraviolet radiation. J Bacteriol. 125(2):616–625. doi:10.1128/JB.125.2.616-625.1976.

Bliss S. 2018. Landscapes and landforms: Deserts: Namib desert. Geography Bulletin. 50(1):37.

Bogel G, Schrempf H, Ortiz de Orué Lucana D. 2009. The heme-binding protein HbpS regulates the activity of the *Streptomyces reticuli* iron-sensing histidine kinase SenS in a redox-dependent manner. Amino Acids. 37(4):681–691. doi:10.1007/s00726-008-0188-5.

Bohoyo-Gil D, Dominguez-Valhondo D, García-Parra JJ, González-Gómez D. 2012. UHPLC as a suitable methodology for the analysis of carotenoids in food matrix. Eur Food Res Technol. 235(6):1055–1061. doi:10.1007/s00217-012-1838-0.

Bowker MA, Reed SC, Belnap J, Phillips SL. 2002. Temporal variation in community composition, pigmentation, and fv/fm of desert cyanobacterial soil crusts. Microb Ecol. 43(1):13–25. doi:10.1007/s00248-001-1013-9

Brausemann A, Gemmecker S, Koschmieder J, Ghisla S, Beyer P, Einsle O. 2017. Structure of phytoene desaturase provides insights into herbicide binding and reaction mechanisms involved in carotene desaturation. Structure. 25(8):1222-1232.e3. doi:10.1016/j.str.2017.06.002.

van Breemen RB, Dong L, Pajkovic ND. 2012. Atmospheric pressure chemical ionization tandem mass spectrometry of carotenoids. Int J Mass Spectrom. 312:163–172. doi:10.1016/j.ijms.2011.07.030.

van Breemen RB, Huang C-R, Tan Y, Sander LC, Schilling AB. 1996. Liquid chromatography/mass spectrometry of carotenoids using atmospheric pressure chemical ionization. J Mass Spectrom. 31(9):975–981. doi:10.1002/(SICI)1096-9888(199609)31:9<975::AID-JMS380>3.0.CO;2-S.

Breitenbach J, Gerjets T, Sandmann G. 2013. Catalytic properties and reaction mechanism of the CrtO carotenoid ketolase from the cyanobacterium *Synechocystis* sp. PCC 6803. Arch Biochem Biophys. 529(2):86–91. doi:10.1016/j.abb.2012.11.003.

Brem R, Guven M, Karran P. 2017. Oxidatively-generated damage to DNA and proteins mediated by photosensitized UVA. Free Radic Biol Med. 107:101–109. doi:10.1016/j.freeradbiomed.2016.10.488.

Britton G. 1993. Structure and nomenclature of carotenoids. In: Young AJ, Britton G, editors. Carotenoids in photosynthesis. Dordrecht: Springer Netherlands. p. 1–15.; [accessed 2021 Jan 9]. https://doi.org/10.1007/978-94-011-2124-8_1.

Britton G. 1995. Structure and properties of carotenoids in relation to function. FASEB J. 9(15):1551–1558. doi:10.1096/fasebj.9.15.8529834.

Britton G. 2008. TLC of carotenoids. In: Waksmundzka-Hajnos M, Sherma J, Kowalska T, editors. Thin layer chromatography in phytochemistry. Florida (FL): CRC Press. p. 543–575.

Britton G. 2020. Carotenoid research: history and new perspectives for chemistry in biological systems. Biochim Biophys Acta Mol Cell Biol Lipids. 1865(11):158699. doi:10.1016/j.bbalip.2020.158699.

Britton G, Goodwin TW, Harriman GE, Lockley WJS. 1977. Carotenoids of the ladybird beetle, *Coccinella septempunctata*. Insect Biochem. 7(4):337–345. doi:10.1016/0020-1790(77)90035-X.

Britton G, Liaaen-Jensen S, Pfander H. 1995a. Carotenoids, volume 1B: spectroscopy. Basel, Switzerland: Birkhauser Verlag AG.

Britton G, Liaaen-Jensen S, Pfander H, editors. 1995b. Carotenoids, volume 1A: isolation and analysis. Basel, Switzerland: Birkhäuser Basel.

Britton G, Liaaen-Jensen S, Pfander H, editors. 2004. Carotenoids: handbook. Basel, Switzerland: Birkhäuser Basel. [accessed 2020 Dec 5]. https://www.springer.com/gp/book/9783764361808.

Britton G, Young AJ. 1993. Methods for the isolation and analysis of carotenoids. In: Young AJ, Britton G, editors. Carotenoids in photosynthesis. Dordrecht, Netherlands: Springer Netherlands. p. 409–457.; [accessed 2020 Dec 29]. https://doi.org/10.1007/978-94-011-2124-8_10.

Brock TD, Petersen S. 1976. Some effects of light on the viability of rhodopsin-containing halobacteria. Arch Microbiol. 109(1):199–200. doi:10.1007/BF00425136.

Brown NL, Stoyanov JV, Kidd SP, Hobman JL. 2003. The MerR family of transcriptional regulators. FEMS Microbiol Rev. 27(2–3):145–163. doi:10.1016/S0168-6445(03)00051-2.

Browning DF, Whitworth DE, Hodgson DA. 2003. Light-induced carotenogenesis in *Myxococcus xanthus*: functional characterization of the ECF sigma factor CarQ and antisigma factor CarR. Mol Microbiol. 48(1):237–251. doi:10.1046/j.1365-2958.2003.03431.x.

Buckley E. 2020. Phenotypic and genomic insights into ultraviolet resistance of *Arthrobacter* and *Pseudarthrobacter* isolated from desert soil [dissertation]. Auckland, New Zealand: Auckland University of Technology.

Buckley E, Lee KC, Higgins CM, Seale B. 2019. Whole-genome sequences of one *Arthrobacter* strain and three *Pseudarthrobacter* strains isolated from the Namib Desert. Microbiol Resour Announc. 8(43). doi:10.1128/MRA.00885-19

Büdel B, Karsten U, Garcia-Pichel F. 1997. Ultraviolet-absorbing scytonemin and mycosporine-like amino acid derivatives in exposed, rock-inhabiting cyanobacterial lichens. Oecologia. 112(2):165–172. doi:10.1007/s004420050296.

Burchard RP, Dworkin M. 1966. Light-induced lysis and carotenogenesis in *Myxococcus xanthus*. J Bacteriol. 91(2):535–545. doi:10.1128/JB.91.2.535-545.1966.

Burchard RP, Hendricks SB. 1969. Action spectrum for carotenogenesis in *Myxococcus xanthus*. J Bacteriol. 97(3):1165–1168.

Burgie ES, Zhang J, Vierstra RD. 2016. Crystal structure of *Deinococcus* phytochrome in the photoactivated state reveals a cascade of structural rearrangements during photoconversion. Structure. 24(3):448–457. doi:10.1016/j.str.2016.01.001.

Busse H-J. 2016. Review of the taxonomy of the genus *Arthrobacter*, emendation of the genus *Arthrobacter* sensu lato, proposal to reclassify selected species of the genus *Arthrobacter* in the novel genera *Glutamicibacter* gen. nov., *Paeniglutamicibacter* gen. nov., *Pseudoglutamicibacter* gen. nov., *Paenarthrobacter* gen. nov. and *Pseudarthrobacter* gen. nov., and emended description of *Arthrobacter roseus*. Int J Syst Evol. 66(1):9–37. doi:10.1099/ijsem.0.000702.

Busse H-J, Wieser M. 2014. The genus *Arthrobacter*. In: Rosenberg E, DeLong EF, Lory S, Stackebrandt E, Thompson F, editors. The Prokaryotes: *Actinobacteria*. Berlin, Heidelberg: Springer. p. 105–132.; [accessed 2020 Nov 21]. https://doi.org/10.1007/978-3-642-30138-4_204.

Busse H-J, Wieser M, Buczolits S. 2015. *Arthrobacter*. In: Bergey's manual of systematics of archaea and bacteria. New Jersey (NJ): John Wiley & Sons, Inc. p. 1–70.; [accessed 2020 Nov 21]. https://onlinelibrary.wiley.com/doi/abs/10.1002/9781118960608.gbm00118.

Butnariu M. 2016. Methods of analysis (extraction, separation, identification and quantification) of carotenoids from natural products. J Ecosyst Ecogr. 6(2):2–19. doi:10.4172/2157-7625.1000193

Cabiscol E, Tamarit J, Ros J. 2000. Oxidative stress in bacteria and protein damage by reactive oxygen species. Int Microbiol. 3(1):3–8. doi: 10.1038/nrmicro.2017.26

Cadet J, Anselmino C, Douki T, Voituriez L. 1992. New trends in photobiology: photochemistry of nucleic acids in cells. J Photochem Photobiol B, Biol. 15(4):277–298. doi:10.1016/1011-1344(92)85135-H.

Cadet J, Douki T, Ravanat J-L. 2015. Oxidatively generated damage to cellular DNA by UVB and UVA radiation. Photochem Photobiol. 91(1):140–155. doi:10.1111/php.12368.

Calegari-Santos R, Diogo RA, Fontana JD, Bonfim TMB. 2016. Carotenoid production by halophilic archaea under different culture conditions. Curr Microbiol. 72(5):641–651. doi:10.1007/s00284-015-0974-8.

Carbonneau MA, Melin AM, Perromat A, Clerc M. 1989. The action of free radicals on *Deinococcus radiodurans* carotenoids. Arch Biochem Biophys. 275(1):244–251. doi:10.1016/0003-9861(89)90370-6.

Caron G, Ermondi G. 2016. Molecular descriptors for polarity: the need for going beyond polar surface area. Future Med Chem. 8(17):2013–2016. doi:10.4155/fmc-2016-0165.

Caruso T, Chan Y, Lacap DC, Lau MCY, McKay CP, Pointing SB. 2011. Stochastic and deterministic processes interact in the assembly of desert microbial communities on a global scale. ISME J. 5(9):1406–1413. doi:10.1038/ismej.2011.21.

Cary SC, McDonald IR, Barrett JE, Cowan DA. 2010. On the rocks: the microbiology of Antarctic Dry Valley soils. Nat Rev Microbiol. 8(2):129–138. doi:10.1038/nrmicro2281.

Casasanta G, Garra R. 2018. Towards a generalized Beer-Lambert Law. Fractal Fract. 2(1):8. doi:10.3390/fractalfract2010008.

Cernelic K, Prosek M, Golc-Wondra A, Rodic Z, Simonovska B, Puklavec M. 2013. Influence of synthetic antioxidants on extraction of all-trans-lutein from spinach under air and nitrogen atmosphere. Food Nutr Sci. 4(2):195–200. doi:10.4236/fns.2013.42027.

Chan Y, Lacap DC, Lau MCY, Ha KY, Warren-Rhodes KA, Cockell CS, Cowan DA, McKay CP, Pointing SB. 2012. Hypolithic microbial communities: between a rock and a hard place. Environ Microbiol. 14(9):2272–2282. doi:10.1111/j.1462-2920.2012.02821.x.

Chanal A, Chapon V, Benzerara K, Barakat M, Christen R, Achouak W, Barras F, Heulin T. 2006. The desert of Tataouine: an extreme environment that hosts a wide diversity of microorganisms and radiotolerant bacteria. Environ Microbiol. 8(3):514–525. doi:10.1111/j.1462-2920.2005.00921.x.

Chattopadhyay MK, Jagannadham MV. 2001. Maintenance of membrane fluidity in Antarctic bacteria. Polar Biol. 24(5):386–388. doi:10.1007/s003000100232.

Chattopadhyay MK, Jagannadham MV, Vairamani M, Shivaji S. 1997. Carotenoid pigments of an Antarctic psychrotrophic bacterium *Micrococcus roseus*: temperature dependent biosynthesis, structure, and interaction with synthetic membranes. Biochem Biophys Res Commun. 239(1):85–90. doi:10.1006/bbrc.1997.7433.

Chauveau-Duriot B, Doreau M, Nozière P, Graulet B. 2010. Simultaneous quantification of carotenoids, retinol, and tocopherols in forages, bovine plasma, and milk: validation of a novel UPLC method. Anal Bioanal Chem. 397(2):777–790. doi:10.1007/s00216-010-3594-y.

Cheung J, Hendrickson WA. 2010. Sensor domains of two-component regulatory systems. Curr Opin Microbiol. 13(2):116–123. doi:10.1016/j.mib.2010.01.016.

Chi SC, Mothersole DJ, Dilbeck P, Niedzwiedzki DM, Zhang H, Qian P, Vasilev C, Grayson KJ, Jackson PJ, Martin EC, et al. 2015. Assembly of functional photosystem complexes in *Rhodobacter sphaeroides* incorporating carotenoids from the spirilloxanthin pathway. Biochim Biophys Acta - Bioenerg. 1847(2):189–201. doi:10.1016/j.bbabio.2014.10.004.

Chiang SM, Schellhorn H. 2012. Regulators of oxidative stress response genes *in Escherichia coli* and their functional conservation in bacteria. Arch Biochem Biophys. doi:10.1016/j.abb.2012.02.007.

Chignell CF, Sik RH, Bilski PJ. 2008. The photosensitizing potential of compact fluorescent vs incandescent light bulbs. Photochem Photobiol. 84(5):1291–1293. doi:10.1111/j.1751-1097.2008.00366.x.

Chumpolkulwong N (Hiroshima U (Japan) F of E, Kakizono T, Nagai S, Nishio N. 1997. Increased astaxanthin production by *Phaffia rhodozyma* mutants isolated as resistant to diphenylamine. J Ferment Bioeng. 83(5):429–434. doi:10.1016/S0922-338X(97)82996-0

Clark DE. 2011. What has polar surface area ever done for drug discovery? Future Med Chem. 3(4):469–484. doi:10.4155/fmc.11.1.

Cockell C, Rettberg P, Horneck G, Scherer K, Stokes DM. 2003. Measurements of microbial protection from ultraviolet radiation in polar terrestrial microhabitats. Polar Biol. 26(1):62–69. doi:10.1007/s00300-002-0438-z.

Cockell CS, Knowland J. 1999. Ultraviolet radiation screening compounds. Biol Rev. 74(3):311–345. doi:10.1111/j.1469-185X.1999.tb00189.x.

Colson P, Pinault L, Azza S, Armstrong N, Chabriere E, La Scola B, Pontarotti P, Raoult D. 2020. A protein of the metallo-hydrolase/oxidoreductase superfamily with both beta-lactamase and ribonuclease activity is linked with translation in giant viruses. Sci Rep. 10(1):21685. doi:10.1038/s41598-020-78658-8.

Conn PF, Schalch W, Truscott TG. 1991. The singlet oxygen and carotenoid interaction. J Photochem Photobiol B, Biol. 11(1):41–47. doi:10.1016/1011-1344(91)80266-K.

Cordero RR, Damiani A, Jorquera J, Sepúlveda E, Caballero M, Fernandez S, Feron S, Llanillo PJ, Carrasco J, Laroze D, et al. 2018. Ultraviolet radiation in the Atacama Desert. Antonie van Leeuwenhoek. 111(8):1301–1313. doi:10.1007/s10482-018-1075-z.

Cordero RR, Damiani A, Seckmeyer G, Jorquera J, Caballero M, Rowe P, Ferrer J, Mubarak R, Carrasco J, Rondanelli R, et al. 2016. The solar spectrum in the Atacama Desert. Sci Rep. 6(1):22457. doi:10.1038/srep22457.

Cordero RR, Seckmeyer G, Damiani A, Riechelmann S, Rayas J, Labbe F, Laroze D. 2014. The world's highest levels of surface UV. Photochem Photobiol Sci. 13(1):70–81. doi:10.1039/c3pp50221j.

Córdova P, Baeza M, Cifuentes V, Alcaíno J. 2018. Microbiological synthesis of carotenoids: pathways and regulation. Progress in Carotenoid Research. doi:10.5772/intechopen.78343. [accessed 2021 Jan 23]. https://www.intechopen.com/books/progress-in-carotenoid-research/microbiological-synthesis-of-carotenoids-pathways-and-regulation.

Corradini D, Eksteen E, Eksteen R, Schoenmakers P, Miller N, editors. 2011. Handbook of HPLC. Florida (FL): CRC Press.

Cortés-Herrera C, Chacón A, Artavia G, Granados-Chinchilla F. 2019. Simultaneous LC/MS analysis of carotenoids and fat-soluble vitamins in Costa Rican avocados (*Persea americana* Mill.). Molecules. 24(24):4517. doi:10.3390/molecules24244517.

Cowan DA, Hopkins DW, Jones BE, Maggs-Kölling G, Majewska R, Ramond J-B. 2020. Microbiomics of Namib Desert habitats. Extremophiles. 24(1):17–29. doi:10.1007/s00792-019-01122-7.

Cowan DA, Pointing SB, Stevens MI, Craig Cary S, Stomeo F, Tuffin IM. 2011. Distribution and abiotic influences on hypolithic microbial communities in an Antarctic Dry Valley. Polar Biol. 34(2):307–311. doi:10.1007/s00300-010-0872-2.

Crocker FH, Fredrickson JK, White DC, Ringelberg DB, Balkwill DL. 2000. Phylogenetic and physiological diversity of *Arthrobacter* strains isolated from unconsolidated subsurface sediments. Microbiology. 146:1295–1310. doi:10.1099/00221287-146-6-1295.

Crowley DJ, Boubriak I, Berquist BR, Clark M, Richard E, Sullivan L, DasSarma S, McCready S. 2006. The *uvrA*, *uvrB* and *uvrC* genes are required for repair of ultraviolet light induced DNA photoproducts in *Halobacterium* sp. NRC-1. Saline Syst. 2:11. doi:10.1186/1746-1448-2-11.

Cunningham GE, Bodeker PF. 2000. Ground-based measurements of UVB in Namibia. S Afr J Sci. 96(11–12):547–549.

Cunningham PF. 1998. The behaviour of the ozone layer above tropical southern Africa. Transactions of the Zimbabwe Scientific Association. 72:14–17. doi:10.4314/tzsa.v72i1.18492.

Cyronak M, Britton G, Simpson K. 1977. Rhodoxanthin, the red pigment of *Equisetum arvense* sporophytes. Phytochemistry. 16:612–613. doi:10.1016/0031-9422(77)80033-2.

Dana GL, Wharton RA, Dubayah RA. 1998. Solar radiation in the Mcmurdo Dry Valleys, Antarctica. In: Ecosystem dynamics in a polar desert: the Mcmurdo Dry Valleys, Antarctica. American Geophysical Union (AGU). p. 39–64.; [accessed 2020 Nov 21]. https://agupubs.onlinelibrary.wiley.com/doi/abs/10.1029/AR072p0039.

Daood HG, Bencze G, Palotás G, Pék Z, Sidikov A, Helyes L. 2014. HPLC analysis of carotenoids from tomatoes using cross-linked C18 column and MS detection. J Chromatogr Sci. 52(9):985–991. doi:10.1093/chromsci/bmt139.

Dass C. 2007a. Basics of mass spectrometry. In: Fundamentals of contemporary mass spectrometry. New Jersey (NJ): John Wiley & Sons, Ltd. p. 1–14.; [accessed 2021 Feb 22]. https://onlinelibrary.wiley.com/doi/abs/10.1002/9780470118498.ch1.

Dass C. 2007b. Organic mass spectrometry. In: Fundamentals of contemporary mass spectrometry. New Jersey (NJ): John Wiley & Sons, Ltd. p. 195–261.; [accessed 2021 Feb 22]. https://onlinelibrary.wiley.com/doi/abs/10.1002/9780470118498.ch6.

DasSarma S, Kennedy SP, Berquist B, Victor Ng W, Baliga NS, Spudich JL, Krebs MP, Eisen JA, Johnson CH, Hood L. 2001. Genomic perspective on the photobiology of *Halobacterium species* NRC-1, a phototrophic, phototactic, and UV-tolerant haloarchaeon. Photosynth Res. 70(1):3–17. doi:10.1023/A:1013879706863.

Davis SJ, Vener AV, Vierstra RD. 1999. Bacteriophytochromes: phytochrome-like photoreceptors from nonphotosynthetic eubacteria. Science. 286(5449):2517–2520. doi:10.1126/science.286.5449.2517.

Deochand DK, Grove A. 2017. MarR family transcription factors: dynamic variations on a common scaffold. Crit Rev Biochem Mol Biol. 52(6):595–613. doi:10.1080/10409238.2017.1344612.

Di Capua C, Bortolotti A, Farías ME, Cortez N. 2011. UV-resistant *Acinetobacter* sp. isolates from Andean wetlands display high catalase activity. FEMS Microbiol Lett. 317(2):181–189. doi:10.1111/j.1574-6968.2011.02231.x.

Di Mascio P, Kaiser S, Sies H. 1989. Lycopene as the most efficient biological carotenoid singlet oxygen quencher. Arch Biochem Biophys. 274(2):532–538. doi:10.1016/0003-9861(89)90467-0.

Dieser M, Greenwood M, Foreman CM. 2010. Carotenoid pigmentation in Antarctic heterotrophic bacteria as a strategy to withstand environmental stresses. Arct Antarct Alp Res. 42(4):396–405. doi:10.1657/1938-4246-42.4.396.

Dixon SJ, Stockwell BR. 2014. The role of iron and reactive oxygen species in cell death. Nat Chem Biol. 10(1):9–17. doi:10.1038/nchembio.1416.

Doddaiah KM, Narayan A, Gokare Aswathanarayana R, Ravi S. 2013. Effect of metabolic inhibitors on growth and carotenoid production in *Dunaliella bardawil*. J Food Sci Technol. 50(6):1130–1136. doi:10.1007/s13197-011-0429-6.

Doyle CA, Dorsey JG. 1998. Reverse-phase HPLC: preparation and characterisation of reversed-phase stationary phases. In: Corradini D, Katz E, Eksteen R, Schoenmakers P, Miller N, editors. Handbook of HPLC. Florida (FL): CRC Press. p. 293–324.

Dsouza M, Taylor MW, Turner SJ, Aislabie J. 2015. Genomic and phenotypic insights into the ecology of *Arthrobacter* from Antarctic soils. BMC Genom. 16(1):36. doi:10.1186/s12864-015-1220-2.

Dummer AM, Bonsall JC, Cihla JB, Lawry SM, Johnson GC, Peck RF. 2011. Bacterioopsin-mediated regulation of bacterioruberin biosynthesis in *Halobacterium salinarum*. J Bacteriol. 193(20):5658–5667. doi:10.1128/JB.05376-11.

Dundas ID, Larsen H. 1963. A study on the killing by light of photosensitized cells of *Halobacterium salinarium*. Archiv für Mikrobiologie. 46(1):19–28. doi:10.1007/BF00406383.

Eckardt FD, Soderberg K, Coop LJ, Muller AA, Vickery KJ, Grandin RD, Jack C, Kapalanga TS, Henschel J. 2013. The nature of moisture at Gobabeb, in the central Namib Desert. J Arid Environ. 93:7–19. doi:10.1016/j.jaridenv.2012.01.011.

Edge R, McGarvey DJ, Truscott TG. 1997. The carotenoids as anti-oxidants — a review. J Photochem Photobiol B, Biol. 41(3):189–200. doi:10.1016/S1011-1344(97)00092-4.

Ehling-Schulz M, Scherer S. 1999. UV protection in cyanobacteria. Eur J Phycol. 34(4):329–338. doi:10.1080/09670269910001736392.

Eisenstark A. 1998. Bacterial gene products in response to near-ultraviolet radiation. Mutat Res. 422(1):85–95. doi:10.1016/s0027-5107(98)00178-x.

El-Banna AAE-R, El-Razek AMA, El-Mahdy AR. 2012. Isolation, identification and screening of carotenoid-producing strains of *Rhodotorula glutinis*. Food Nutr Sci. 3(5):627–633. doi:10.4236/fns.2012.35086.

El-Sayed WSM, Takaichi S, Saida H, Kamekura M, Abu-Shady M, Seki H, Kuwabara T. 2002. Effects of light and low oxygen tension on pigment biosynthesis in *Halobacterium salinarum*, revealed by a novel method to quantify both retinal and carotenoids. Plant Cell Physiol. 43(4):379–383. doi:10.1093/pcp/pcf044.

Ertl P, Rohde B, Selzer P. 2000. Fast calculation of molecular polar surface area as a sum of fragment-based contributions and its application to the prediction of drug transport properties. J Med Chem. 43(20):3714–3717. doi:10.1021/jm000942e.

Esposito F, Mari S, Pavese G, Serio C. 2003. Diurnal and nocturnal measurements of aerosol optical depth at a desert site in Namibia. Aerosol Science and Technology. 37(4):392–400. doi:10.1080/02786820300972.

Fan L, Vonshak A, Gabbay R, Hirshberg J, Cohen Z, Boussiba S. 1995. The biosynthetic pathway of astaxanthin in a green alga *Haematococcus pluvialis* as indicated by inhibition with diphenylamine. Plant Cell Physiol. 36(8):1519–1524. doi:10.1093/oxfordjournals.pcp.a078916.

Fanali C, Dugo P, Mondello L, D'Orazio G, Fanali S. 2012. Recent developments in high-performance liquid chromatography. In: Toldra F, Nollet LML, editors. Food Analysis by HPLC. Florida (FL): CRC Press. p. 18–49.; [accessed 2021 Feb 21]. https://www.taylorfrancis.com/chapters/recent-developments-high-performance-liquid-chromatography-chiara-fanali-paola-dugo-luigi-mondello-giovanni-orazio-salvatore-fanali/e/10.1201/b13024-5.

Fang FC. 2011. Antimicrobial actions of reactive oxygen species. mBio. 2(5):e00141-11. doi:10.1128/mBio.00141-11.

Farías ME, Fernández-Zenoff V, Flores R, Ordóñez O, Estévez C. 2009. Impact of solar radiation on bacterioplankton in Laguna Vilama, a hypersaline Andean lake (4650 m). J. Geophys. Res. Biogeosci. 114:1–8. doi:10.1029/2008JG000784.

Fekete S, Schappler J, Veuthey J-L, Guillarme D. 2014. Current and future trends in UHPLC. Trends Analyt Chem. 63:2–13. doi:10.1016/j.trac.2014.08.007.

Fernández-Zenoff V, Siñeriz F, Farías ME. 2006. Diverse responses to UV-B radiation and repair mechanisms of bacteria isolated from high-altitude aquatic environments. Appl Environ Microbiol. 72(12):7857–7863. doi:10.1128/AEM.01333-06.

Fernández-Zenoff MV, Estévez MC, Farías ME. 2014. Diurnal variation in bacterioplankton composition and DNA damage in the microbial community from an Andean oligotrophic lake. Rev Argent Microbiol. 46(4):358–362. doi:10.1016/S0325-7541(14)70095-1.

Fierer N, Leff JW, Adams BJ, Nielsen UN, Bates ST, Lauber CL, Owens S, Gilbert JA, Wall DH, Caporaso JG. 2012. Cross-biome metagenomic analyses of soil microbial communities and their functional attributes. PNAS. 109(52):21390–21395. doi:10.1073/pnas.1215210110.

Flegler A, Runzheimer K, Kombeitz V, Mänz AT, Heidler von Heilborn D, Etzbach L, Schieber A, Hölzl G, Hüttel B, Woehle C, et al. 2020. *Arthrobacter* bussei sp. nov., a pink-coloured organism isolated from cheese made of cow's milk. Int J Syst Evol. 70(5):3027–3036. doi:10.1099/ijsem.0.004125.

Flores N, Hoyos S, Venegas M, Galetović A, Zúñiga LM, Fábrega F, Paredes B, Salazar-Ardiles C, Vilo C, Ascaso C, et al. 2020. *Haloterrigena* sp. strain SGH1, a bacterioruberin-rich, perchlorate-tolerant halophilic archaeon isolated from halite microbial communities, Atacama Desert, Chile. Front Microbiol. 11. doi:10.3389/fmicb.2020.00324.

Foissner W, Agatha S, Berger H. 2002. Soil ciliates (*Protozoa, Ciliophora*) from Namibia (Southwest Africa), with emphasis on two contrasting environments, the Etosha Region and the Namib Desert part i: text and line drawings. Linz, Austria: Oberösterreichisches Landesmuseum.

Fong NJC, Burgess ML, Barrow KD, Glenn DR. 2001. Carotenoid accumulation in the psychrotrophic bacterium *Arthrobacter* agilis in response to thermal and salt stress. Appl Microbiol Biotechnol. 56(5–6):750–756. doi:10.1007/s002530100739.

Frank HA, Cogdell RJ. 1993. The photochemistry and function of carotenoids in photosynthesis. In: Young AJ, Britton G, editors. Carotenoids in photosynthesis. Dordrecht (Netherlands): Springer Netherlands. p. 252–326.; [accessed 2020 Sep 26]. https://doi.org/10.1007/978-94-011-2124-8_8.

Friedberg EC. 2003. DNA damage and repair. Nature. 421(6921):436–440. doi:10.1038/nature01408.

Fukuoka S, Ajiki Y, Ohga T, Kawanami Y, Izumori K. 2004. Production of dihydroxy C50-carotenoid by *Aureobacterium* sp. FERM P-18698. Biosci Biotechnol Biochem. 68(12):2646–2648. doi:10.1271/bbb.68.2646.

García-Gómez C, Parages ML, Jiménez C, Palma A, Mata MT, Segovia M. 2012. Cell survival after UV radiation stress in the unicellular chlorophyte *Dunaliella tertiolecta* is mediated by DNA repair and MAPK phosphorylation. J Exp Bot. 63(14):5259–5274. doi:10.1093/jxb/ers185.

Garcia-Pichel F, Castenholz RW. 1993. Occurrence of UV-absorbing, mycosporine-like compounds among cyanobacterial isolates and an estimate of their screening capacity. Appl Environ Microbiol. 59(1):163–169.

Garcia-Pichel F, Sherry ND, Castenholz RW. 1992. Evidence for an ultraviolet sunscreen role of the extracellular pigment scytonemin in the terrestrial cyanobacterium *Chlorogloeopsis* sp. Photochem Photobiol. 56(1):17–23. doi:10.1111/j.1751-1097.1992.tb09596.x.

Girard PM, Francesconi S, Pozzebon M, Graindorge D, Rochette P, Drouin R, Sage E. 2011. UVA-induced damage to DNA and proteins: direct versus indirect photochemical processes. J Phys: Conf Ser. 261:012002. doi:10.1088/1742-6596/261/1/012002.

Giuffrida D, Sutthiwong N, Dugo P, Donato P, Cacciola F, Girard-Valenciennes E, Le Mao Y, Monnet C, Fouillaud M, Caro Y, et al. 2016. Characterisation of the C50 carotenoids

produced by strains of the cheese-ripening bacterium *Arthrobacter arilaitensis*. Int Dairy J. 55:10–16. doi:10.1016/j.idairyj.2015.11.005.

Glaeser J, Klug G. 2005. Photo-oxidative stress in *Rhodobacter sphaeroides*: protective role of carotenoids and expression of selected genes. Microbiology. 151:1927–1938. doi:10.1099/mic.0.27789-0.

Gong Q, Ning W, Tian W. 2016. GoFDR: a sequence alignment based method for predicting protein functions. Methods. 93:3–14. doi:10.1016/j.ymeth.2015.08.009.

Goosen N, Moolenaar GF. 2008. Repair of UV damage in bacteria. DNA Repair. 7(3):353–379. doi:10.1016/j.dnarep.2007.09.002.

Götz D, Paytubi S, Munro S, Lundgren M, Bernander R, White MF. 2007. Responses of hyperthermophilic crenarchaea to UV irradiation. Genome Biol. 8(10):R220. doi:10.1186/gb-2007-8-10-r220.

Goudie A, Viles H. 2015a. Landscapes. In: Goudie A, Viles H, editors. Landscapes and landforms of Namibia. Dordrecht (Netherlands): Springer Netherlands. p. 3–25.; [accessed 2021 Jan 10]. https://doi.org/10.1007/978-94-017-8020-9_1.

Goudie A, Viles H. 2015b. Vegetation, fauna and humans. In: Goudie A, Viles H, editors. Landscapes and landforms of Namibia. Dordrecht: Springer Netherlands. p. 47–51.; [accessed 2021 Jan 10]. https://doi.org/10.1007/978-94-017-8020-9_4.

Grogan DW. 1989. Phenotypic characterization of the archaebacterial genus *Sulfolobus*: comparison of five wild-type strains. J Bacteriol. 171(12):6710–6719.

Gross JH. 2017a. Introduction. In: Gross JH, editor. Mass spectrometry: a textbook. Cham (Switzerland): Springer International Publishing. p. 1–28.; [accessed 2021 Feb 22]. https://doi.org/10.1007/978-3-319-54398-7_1.

Gross JH. 2017b. Tandem mass spectrometry. In: Gross JH, editor. Mass spectrometry: a textbook. Cham (Switzerland): Springer International Publishing. p. 539–612.; [accessed 2021 Mar 19]. https://doi.org/10.1007/978-3-319-54398-7_9.

Gross JH. 2017c. Isotopic composition and accurate mass. In: Gross JH, editor. Mass spectrometry: a textbook. Cham (Switzerland): Springer International Publishing. p. 85–150.; [accessed 2021 Jun 19]. https://doi.org/10.1007/978-3-319-54398-7_3.

Grosvenor AJ, Morton JD, Dyer JM. 2010. Profiling of residue-level photo-oxidative damage in peptides. Amino Acids. 39(1):285–296. doi:10.1007/s00726-009-0440-7.

Guerra AJ, Dann CE, Giedroc DP. 2011. Crystal structure of the zinc-dependent marr family transcriptional regulator AdcR in the Zn(II)-bound state. J Am Chem Soc. 133(49):19614–19617. doi:10.1021/ja2080532.

Gunnigle E, Frossard A, Ramond J-B, Guerrero L, Seely M, Cowan DA. 2017. Diel-scale temporal dynamics recorded for bacterial groups in Namib Desert soil. Sci Rep. 7(1):40189. doi:10.1038/srep40189.

Hammond RK, White DC. 1970. Inhibition of vitamin K2 and carotenoid synthesis in *Staphylococcus aureus* by diphenylamine. J Bacteriol. 103(3):611–615.

Hannay NB, Smyth CP. 1946. Further investigations of polarity in hydrocarbons possessing conjugated systems. J Am Chem Soc. 68(2):244–247. doi:10.1021/ja01206a029.

Haroon S. 2014. Extraction of lycopene from tomato paste and its immobilization for controlled release [dissertation]. Waikato (New Zealand): University of Waikato.

Harrison C. 2003. GrpE, a nucleotide exchange factor for DnaK. Cell Stress Chaperones. 8(3):218–224.

Hashimoto H, Uragami C, Cogdell RJ. 2016. Carotenoids and photosynthesis. In: Stange C, editor. Carotenoids in nature: biosynthesis, regulation and function. Cham (Switzerland): Springer International Publishing. p. 111–139.; [accessed 2020 Sep 26]. https://doi.org/10.1007/978-3-319-39126-7_4.

He Y-Y, Häder DP. 2002a. UV-B-induced formation of reactive oxygen species and oxidative damage of the cyanobacterium *Anabaena* sp.: protective effects of ascorbic acid and N-acetyl-L-cysteine. J Photochem Photobiol B, Biol. 66(2):115–124. doi:10.1016/s1011-1344(02)00231-2.

He Y-Y, Häder DP. 2002b. Reactive oxygen species and UV-B: effect on cyanobacteria. Photochem Photobiol Sci. 1(10):729–736. doi:10.1039/b110365m.

He Y-Y, Häder DP. 2002c. Involvement of reactive oxygen species in the UV-B damage to the cyanobacterium *Anabaena* sp. J Photochem Photobiol B, Biol. 66(1):73–80. doi:10.1016/S1011-1344(01)00278-0.

Heck DE, Vetrano AM, Mariano TM, Laskin JD. 2003. UVB light stimulates production of reactive oxygen species: unexpected role for catalase. J Biol Chem. 278(25):22432–22436. doi:10.1074/jbc.C300048200.

Heider SAE, Peters-Wendisch P, Wendisch VF. 2012. Carotenoid biosynthesis and overproduction in *Corynebacterium glutamicum*. BMC Microbiol. 12(1):198. doi:10.1186/1471-2180-12-198.

Heider SAE, Wolf N, Hofemeier A, Peters-Wendisch P, Wendisch VF. 2014. Optimization of the IPP precursor supply for the production of lycopene, decaprenoxanthin and astaxanthin by *Corynebacterium glutamicum*. Front Bioeng Biotechnol. 2:1–13. doi:10.3389/fbioe.2014.00028.

Henke NA, Austermeier S, Grothaus IL, Götker S, Persicke M, Peters-Wendisch P, Wendisch VF. 2020. *Corynebacterium glutamicum* CrtR and its orthologs in *Actinobacteria*: conserved function and application as genetically encoded biosensor for detection of geranylgeranyl pyrophosphate. Int J Mol Sci. 21(15):e5482. doi:10.3390/ijms21155482.

Henke NA, Heider SAE, Hannibal S, Wendisch VF, Peters-Wendisch P. 2017. Isoprenoid pyrophosphate-dependent transcriptional regulation of carotenogenesis in *Corynebacterium glutamicum*. Front Microbiol. 8. doi:10.3389/fmicb.2017.00633.

Hernández KL, Yannicelli B, Olsen LM, Dorador C, Menschel EJ, Molina V, Remonsellez F, Hengst MB, Jeffrey WH. 2016. Microbial activity response to solar radiation across contrasting environmental conditions in Salar de Huasco, Northern Chilean Altiplano. Front Microbiol. 7:1857. doi:10.3389/fmicb.2016.01857.

Hertzberg S, Liaaen-Jensen S. 1969. The structure of oscillaxanthin. Phytochemistry. 8(7):1281–1292. doi:10.1016/S0031-9422(00)85567-3.

Hescox MA, Carlberg DM. 1972. Photoreactivation in *Halobacterium cutirubrum*. Can J Microbiol. 18(7):981–985. doi:10.1139/m72-152.

Hessling M, Spellerberg B, Hoenes K. 2017. Photoinactivation of bacteria by endogenous photosensitizers and exposure to visible light of different wavelengths - a review on existing data. FEMS Microbiol Lett. 364(2). doi:10.1093/femsle/fnw270.

Heyrman J, Verbeeren J, Schumann P, Swings J, De Vos P. 2005. Six novel *Arthrobacter* species isolated from deteriorated mural paintings. Int J Syst Evol Microbiol. 55(4):1457–1464. doi:10.1099/ijs.0.63358-0.

Hillion M, Antelmann H. 2015. Thiol-based redox switches in prokaryotes. Biol Chem. 396(5):415–444. doi:10.1515/hsz-2015-0102.

Hobman JL. 2007. MerR family transcription activators: similar designs, different specificities. Mol Microbiol. 63(5):1275–1278. doi:10.1111/j.1365-2958.2007.05608.x.

Hodgson DA. 1993. Light-induced carotenogenesis in *Myxococcus xanthus*: genetic analysis of the *carR* region. Mol Microbiol. 7(3):471–488. doi:10.1111/j.1365-2958.1993.tb01138.x.

Hodisan T, Socaciu C, Ropan I, Neamtu G. 1997. Carotenoid composition of *Rosa canina* fruits determined by thin-layer chromatography and high-performance liquid chromatography. J Pharm Biomed Anal. 16(3):521–528. doi:10.1016/s0731-7085(97)00099-x.

Hoffman E, Stroobant V. 2007. Mass spectrometry; principles and applications. 3rd ed. New Jersey (NJ): John Wiley & Sons, Ltd.

Holm E, Jensen V. 1972. Aerobic chemoorganotrophic bacteria of a Danish beech forest. Microbiology of a Danish beech forest. I. Oikos. [accessed 2020 Nov 21]. https://agris.fao.org/agris-search/search.do?recordID=US201302322510.

Hope CK, Strother M, Creber HK, Higham SM. 2016. Lethal photosensitisation of *Prevotellaceae* under anaerobic conditions by their endogenous porphyrins. Photodiagnosis Photodyn Ther. 13:344–346. doi:10.1016/j.pdpdt.2015.07.173.

van der Horst MA, Key J, Hellingwerf KJ. 2007. Photosensing in chemotrophic, non-phototrophic bacteria: let there be light sensing too. Trends Microbiol. 15(12):554–562. doi:10.1016/j.tim.2007.09.009.

Howes CD, Batra PP. 1970. Mechanism of photoinduced carotenoid synthesis. Further studies on the action spectrum and other aspects of carotenogenesis. Arch Biochem Biophys. 137(1):175–180. doi:10.1016/0003-9861(70)90424-8.

Hudon J, Anciães M, Bertacche V, Stradi R. 2007. Plumage carotenoids of the pin-tailed Manakin (*Ilicura militaris*): evidence for the endogenous production of rhodoxanthin from a colour variant. Comp. Biochem. Physiol. B, Biochem. 147(3):402–411. doi:10.1016/j.cbpb.2007.02.004.

Huld T, Suri M, Dunlop E, Albuisson M, Wald L. 2005. Integration of Helioclim-1 database into PV-GIS to estimate solar electricity potential in Africa. In: Proceedings, 20th European Photovoltaic Solar Energy Conference. Barcelone, Spain. [accessed 2021 Jan 14]. https://hal.archives-ouvertes.fr/hal-00091923.

Ii KM, Kono N, Paulino-Lima IG, Tomita M, Rothschild LJ, Arakawa K. 2019. Complete genome sequence of *Arthrobacter* sp. strain MN05-02, a uv-resistant bacterium from a manganese deposit in the Sonoran Desert. J Genomics. 7:18–25. doi:10.7150/jgen.32194.

Ikehata H, Ono T. 2011. The mechanisms of UV mutagenesis. J Radiat Res. 52(2):115–125. doi:10.1269/jrr.10175.

Imhoff JF, Trüper HG, Pfennig N. 1984. Rearrangement of the species and genera of the phototrophic "purple nonsulfur bacteria". Int J Syst Evol. 34(3):340–343. doi:10.1099/00207713-34-3-340.

Imperi F, Caneva G, Cancellieri L, Ricci MA, Sodo A, Visca P. 2007. The bacterial aetiology of rosy discoloration of ancient wall paintings. Environ Microbiol. 9(11):2894–2902. doi:10.1111/j.1462-2920.2007.01393.x.

Jacobs JL, Carroll TL, Sundin GW. 2005. The role of pigmentation, ultraviolet radiation tolerance, and leaf colonization strategies in the epiphytic survival of phyllosphere bacteria. Microb Ecol. 49(1):104–113. doi:10.1007/s00248-003-1061-4.

Jacobs JL, Sundin GW. 2001. Effect of solar UV-B radiation on a phyllosphere bacterial community. Appl Environ Microbiol. 67(12):5488–5496. doi:10.1128/AEM.67.12.5488-5496.2001.

Jagannadham MV, Chattopadhyay MK, Subbalakshmi C, Vairamani M, Narayanan K, Mohan Rao C, Shivaji S. 2000. Carotenoids of an Antarctic psychrotolerant bacterium, *Sphingobacterium antarcticus*, and a mesophilic bacterium, *Sphingobacterium multivorum*. Arch Microbiol. 173(5–6):418–424. doi:10.1007/s002030000163.

Jagannadham MV, Narayanan K, Rao ChM, Shivaji S. 1996. In vivo characteristics and localisation of carotenoid pigments in psychrotrophic and mesophilic *Micrococcus roseus* using photoacoustic spectroscopy. Biochem Biophys Res Commun. 227(1):221–226. doi:10.1006/bbrc.1996.1493.

Jagannadham MV, Rao VJ, Shivaji S. 1991. The major carotenoid pigment of a psychrotrophic *Micrococcus roseus* strain: purification, structure, and interaction with synthetic membranes. J Bacteriol. 173(24):7911–7917.

Jahnke LS. 1999. Massive carotenoid accumulation in *Dunaliella bardawil* induced by ultraviolet-A radiation. J Photochem Photobiol B, Biol. 48(1):68–74. doi:10.1016/S1011-1344(99)00012-3.

Jansen R, Nowak A, Kunze B, Reichenbach H, Höfle G. 1995. Four new carotenoids from *Polyangium fumosum* (myxobacteria): 3,3′,4,4′-tetradehydro-1,1′,2,2′-tetrahydro-1,1′-dihydroxy-Ψ,Ψ-carotene (di-O-demethylspirilloxanthin), its β-glucoside and glucoside fatty acid esters. Liebigs Annalen. 1995(5):873–876. doi:10.1002/jlac.1995199505126.

Johnson RM, Cameron RE. 1973. The physiology and distribution of bacteria in hot and cold deserts. J Ariz-Nev Acad Sci. 8(2):84. doi: 10.2307/40021919

Johnson RM, Ramond J-B, Gunnigle E, Seely M, Cowan DA. 2017. Namib Desert edaphic bacterial, fungal and archaeal communities assemble through deterministic processes but are influenced by different abiotic parameters. Extremophiles. 21(2):381–392. doi:10.1007/s00792-016-0911-1.

Johnsson P, Peerlkamp N, Kamal-Eldin A, Andersson RE, Andersson R, Lundgren LN, Åman P. 2002. Polymeric fractions containing phenol glucosides in flaxseed. Food Chem. 76(2):207–212. doi:10.1016/S0308-8146(01)00269-2.

Jones D, Keddie RM. 2006. The genus *Arthrobacter*. In: Dworkin M, Falkow S, Rosenberg E, Schleifer K-H, Stackebrandt E, editors. The Prokaryotes: Volume 3: *Archaea. Bacteria:*

Firmicutes, Actinomycetes. New York (NY): Springer. p. 945–960.; [accessed 2020 Nov 21]. https://doi.org/10.1007/0-387-30743-5_36.

Jones DL, Baxter BK. 2017. DNA repair and photoprotection: mechanisms of overcoming environmental ultraviolet radiation exposure in halophilic *Archaea*. Front Microbiol. 8:1882. doi:10.3389/fmicb.2017.01882.

Jori G, Fabris C, Soncin M, Ferro S, Coppellotti O, Dei D, Fantetti L, Chiti G, Roncucci G. 2006. Photodynamic therapy in the treatment of microbial infections: basic principles and perspective applications. Lasers Surg Med. 38(5):468–481. doi:10.1002/lsm.20361.

Kajiwara M, Hara K, Takatori K. 1994. Biosynthesis of corrinoids and porphyrinoids. ix. studies on the origin of oxygen of uroporphyrinogen III in *Arthrobacter hyalinus*. Chem Pharm Bull. 42(4):817–820. doi:10.1248/cpb.42.817.

Kajiwara M, Tokiwa S, Takatori K, Kojima I. 1995. Properties of zinc uroporphyrin III produced from isopropanol by *Arthrobacter hyalinus*. J Ferment Bioeng. 79(2):174–176. doi:10.1016/0922-338X(95)94088-9.

Kaminski S, Daminelli G, Mroginski MA. 2009. Molecular dynamics simulations of the chromophore binding site of *Deinococcus radiodurans* bacteriophytochrome using new force field parameters for the phytochromobilin chromophore. J Phys Chem B. 113(4):945–958. doi:10.1021/jp8047532.

Kato F, Hino T, Nakaji A, Tanaka M, Koyama Y. 1995. Carotenoid synthesis in *Streptomyces setonii* ISP5395 is induced by the gene crtS, whose product is similar to a sigma factor. Mol Gen Genet. 247(3):387–390. doi:10.1007/BF00293207.

Kelly M, Norgård S, Liaaen-Jensen S. 1970. Bacterial carotenoids. 31. C50-carotenoids 5. carotenoids of *Halobacterium salinarium*, especially bacterioruberin. Acta Chem Scand. 24(6):2169–2182. doi:10.3891/acta.chem.scand.24-2169.

Kgabi N, Uugwanga M, Ithindi J. 2016. Atmospheric conditions and precipitation in arid environments: a case of Namibia. IJEP. 6(1):148–159. doi:10.5963/IJEP0601017.

Khaengraeng R, Reed RH. 2005. Oxygen and photoinactivation of *Escherichia coli* in UVA and sunlight. J Appl Microbiol. 99(1):39–50. doi:10.1111/j.1365-2672.2005.02606.x.

Khaneja R, Perez-Fons L, Fakhry S, Baccigalupi L, Steiger S, To E, Sandmann G, Dong TC, Ricca E, Fraser PD, et al. 2010. Carotenoids found in *Bacillus*. J Appl Microbiol. 108(6):1889–1902. doi:10.1111/j.1365-2672.2009.04590.x.

Kim S, Jahandar M, Jeong JH, Lim DC. 2018. Recent progress in solar cell technology for low-light indoor applications. Curr Altern Energy. 2(3):1–15. doi:10.2174/1570180816666190112141857.

Kirby JR. 2009. Chemotaxis-like regulatory systems: unique roles in diverse bacteria. Annu Rev Microbiol. 63:45–59. doi:10.1146/annurev.micro.091208.073221.

Klassen JL. 2010. Phylogenetic and evolutionary patterns in microbial carotenoid biosynthesis are revealed by comparative genomics. PLOS ONE. 5(6):e11257. doi:10.1371/journal.pone.0011257.

Knak A, Regensburger J, Maisch T, Bäumler W. 2014. Exposure of vitamins to UVB and UVA radiation generates singlet oxygen. Photochem Photobiol Sci. 13(5):820–829. doi:10.1039/c3pp50413a.

Kopec RE, Cooperstone JL, Cichon MJ, Schwartz SJ. 2012. Analysis methods of carotenoids. In: Analysis of antioxidant-rich phytochemicals. New Jersey (NJ): John Wiley & Sons, Ltd. p. 105–148.; [accessed 2021 Feb 17]. https://onlinelibrary.wiley.com/doi/abs/10.1002/9781118229378.ch4.

Kortstee GJJ. 1969. Porphyrin formation and its regulation in *Arthrobacter*. Wageningen: Veenman. [accessed 2021 Jul 15]. https://www.wur.nl/nl/Publicatie-details.htm?publicationId=publication-way-353235373237.

Kortstee GJJ. 1970. Porphyrin formation by *Arthrobacter* globiformis. Antonie van Leeuwenhoek. 36(1):259–272. doi:10.1007/BF02069028.

Kotilainen T, Aphalo PJ, Brelsford CC, Böök H, Devraj S, Heikkilä A, Hernández R, Kylling A, Lindfors AV, Robson TM. 2020. Patterns in the spectral composition of sunlight and biologically meaningful spectral photon ratios as affected by atmospheric factors. Agric For Meteorol. 291:108041. doi:10.1016/j.agrformet.2020.108041.

Koyama Y, Yazawa Y, Yamagishi S, Arai T. 1974. Photochromogenesis. I. photochromogenicity in genus *Nocardia, Corynebacterium*, *Arthrobacter*, *Brevibacterium*, and *Flavobacterium*. Jpn J Microbiol. 18(1):49–56. doi:10.1111/j.1348-0421.1974.tb00743.x.

Kozak M, Piepho H-P. 2018. What's normal anyway? Residual plots are more telling than significance tests when checking ANOVA assumptions. J Agron Crop Sci. 204(1):86–98. doi:10.1111/jac.12220.

Krinsky NI. 1963. A relationship between partition coefficients of carotenoids and their functional groups. Anal Biochem. 6(4):293–302. doi:10.1016/0003-2697(63)90153-2.

Krinsky NI. 1978. Non-photosynthetic functions of carotenoids. Philos. Trans. R. Soc. Lond., B, Biol. Sci. 284(1002):581–590.

Krinsky NI. 1994. The biological properties of carotenoids. Pure Appl Chem. 66(5):1003–1010.

Krishnan R, Menon RR, Tanaka N, Busse H-J, Krishnamurthi S, Rameshkumar N. 2016. *Arthrobacter pokkalii* sp nov, a novel plant associated *Actinobacterium* with plant beneficial properties, isolated from saline tolerant Pokkali rice, Kerala, India. PLOS ONE. 11(3):e0150322. doi:10.1371/journal.pone.0150322.

Krisko A, Radman M. 2010. Protein damage and death by radiation in *Escherichia coli* and *Deinococcus radiodurans*. PNAS. 107(32):14373–14377. doi:10.1073/pnas.1009312107.

Krubasik P, Kobayashi M, Sandmann G. 2001. Expression and functional analysis of a gene cluster involved in the synthesis of decaprenoxanthin reveals the mechanisms for C50 carotenoid formation. Eur J Biochem. 268(13):3702–3708. doi:10.1046/j.1432-1327.2001.02275.x.

Krügel H, Krubasik P, Weber K, Saluz HP, Sandmann G. 1999. Functional analysis of genes from *Streptomyces griseus* involved in the synthesis of isorenieratene, a carotenoid with aromatic end groups, revealed a novel type of carotenoid desaturase. Biochim Biophys Acta Mol Cell Biol Lipids. 1439(1):57–64. doi:10.1016/S1388-1981(99)00075-X.

Kuluncsics Z, Perdiz D, Brulay E, Muel B, Sage E. 1999. Wavelength dependence of ultraviolet-induced DNA damage distribution: involvement of direct or indirect mechanisms and possible artefacts. J Photochem Photobiol B, Biol. 49(1):71–80. doi:10.1016/S1011-1344(99)00034-2.

Kumar R, Singh D, Swarnkar MK, Singh AK, Kumar S. 2016. Complete genome sequence of *Arthrobacter alpinus* ERGS4:06, a yellow pigmented bacterium tolerant to cold and radiations isolated from Sikkim Himalaya. J Biotechnol. 220:86–87. doi:10.1016/j.jbiotec.2016.01.016.

Kumar S, Stetcher G, Li M, Knyaz C, Tamura K. 2018. MEGA X: Molecular evolutionary genetics analysis across computing platforms. Mol Biol Evol. 35(6):1547–1549.

Kusmita L, Mutiara EV, Nuryadi H, Pratama PA, Wiguna AS, Radjasa OK. 2017. Characterization of carotenoid pigments from bacterial symbionts of soft-coral *Sarcophyton* sp. from North Java Sea. Int Aquat Res. 9(1):61–69. doi:10.1007/s40071-017-0157-2.

Kvam E, Benner K. 2020. Mechanistic insights into UV-A mediated bacterial disinfection via endogenous photosensitizers. J Photochem Photobiol B, Biol. 209:111899. doi:10.1016/j.jphotobiol.2020.111899.

Lacap DC, Warren-Rhodes KA, McKay CP, Pointing SB. 2011. Cyanobacteria and chloroflexi-dominated hypolithic colonization of quartz at the hyper-arid core of the Atacama Desert, Chile. Extremophiles. 15(1):31–38. doi:10.1007/s00792-010-0334-3.

Ladislav F, Vera P, Karel S, Karel V. 2004. Reliability of carotenoid analyses: a review. Curr Anal Chem. 1(1):93–102.

Laity J. 2008. Deserts and desert environments. Chichester (England): Wiley.

Lancaster J, Lancaster N, Seely M. 1984. Climate of the central Namib Desert. Madoqua. 1984(v14i1):5–61.

Lange OL, Meyer A, Zellner H, Ullmann I, Wessels DCJ. 1990. Eight days in the life of a desert lichen: water relations and photosynthesis of *Teloschistes capensis* in the coastal fog zone of the Namib Desert. Madoqua. 17(1):17–30.

Lao Y-M, Xiao L, Ye Z-W, Jiang J-G, Zhou S-S. 2011. In silico analysis of phytoene synthase and its promoter reveals hints for regulation mechanisms of carotenogenesis in *Duanliella bardawil*. Bioinformatics. 27(16):2201–2208. doi:10.1093/bioinformatics/btr371.

Lebedev KS, Cabrol-Bass D. 1998. New computer aided methods for revealing structural features of unknown compounds using low resolution mass spectra. J Chem Inf Comput Sci. 38(3):410–419. doi:10.1021/ci970083b.

Lebre PH, De Maayer P, Cowan DA. 2017. Xerotolerant bacteria: surviving through a dry spell. Nat Rev Microbiol. 15(5):285–296. doi:10.1038/nrmicro.2017.16.

Lee HS, Ohnishi Y, Horinouchi S. 2001. A sigmaB-like factor responsible for carotenoid biosynthesis in *Streptomyces griseus*. J Mol Microbiol Biotechnol. 3(1):95–101.

Lee KC, Archer SDJ, Boyle RH, Lacap-Bugler DC, Belnap J, Pointing SB. 2016. Niche filtering of bacteria in soil and rock habitats of the Colorado Plateau Desert, Utah, USA. Front Microbiol. 7. doi:10.3389/fmicb.2016.01489.

León-Sobrino C, Ramond J-B, Maggs-Kölling G, Cowan DA. 2019. Nutrient acquisition, rather than stress response over diel cycles, drives microbial transcription in a hyper-arid Namib Desert soil. Front Microbiol. 10:1054. doi:10.3389/fmicb.2019.01054.

Leung PM, Bay SK, Meier DV, Chiri E, Cowan DA, Gillor O, Woebken D, Greening C. 2020. Energetic basis of microbial growth and persistence in desert ecosystems. mSystems. 5(2). doi:10.1128/mSystems.00495-19.

Liaaen-Jensen S, Jensen A. 1971. Quantitative determination of carotenoids in photosynthetic tissues. Meth Enzymol. 23:586–602. doi:10.1016/S0076-6879(71)23132-3

Liang M-H, Zhu J, Jiang J-G. 2018. Carotenoids biosynthesis and cleavage related genes from bacteria to plants. Crit Rev Food Sci Nutr. 58(14):2314–2333. doi:10.1080/10408398.2017.1322552.

Libkind D, Pérez P, Sommaruga R, Diéguez M del C, Ferraro M, Brizzio S, Zagarese H, van Broock M. 2004. Constitutive and UV-inducible synthesis of photoprotective compounds (carotenoids and mycosporines) by freshwater yeasts. Photochem Photobiol Sci. 3(3):281–286. doi:10.1039/b310608j.

Lichtenthaler HK, Buschmann C. 2001. Chlorophylls and carotenoids: measurement and characterization by UV-vis spectroscopy. Curr Protoc Food Anal Chem. 1(1):F4.3.1-F4.3.8. doi:10.1002/0471142913.faf0403s01.

Liebler DC, McClure TD. 1996. Antioxidant reactions of β-carotene: identification of carotenoid−radical adducts. Chem Res Toxicol. 9(1):8–11. doi:10.1021/tx950151t.

Llewellyn C, Mantoura R. 1997. A UV absorbing compound in HPLC pigment chromatograms obtained from Icelandic Basin phytoplankton. Mar Ecol Prog Ser. 158:283–287. doi:10.3354/MEPS158283.

Llorente B. 2016. Regulation of carotenoid biosynthesis in photosynthetic organs. In: Stange C, editor. Carotenoids in nature: biosynthesis, regulation and function. Cham (Switzerland): Springer International Publishing. (Subcellular Biochemistry). p. 141–160.; [accessed 2020 Sep 19]. https://doi.org/10.1007/978-3-319-39126-7_5.

Lorantfy B, Renkecz T, Koch C, Horvai G, Lendl B, Herwig C. 2014. Identification of lipophilic bioproduct portfolio from bioreactor samples of extreme halophilic archaea with HPLC-MS/MS. Anal Bioanal Chem. 406(9–10):2421–2432. doi:10.1007/s00216-014-7626-x.

Louie KB, Kosina SM, Hu Y, Otani H, de Raad M, Kuftin AN, Mouncey NJ, Bowen BP, Northen TR. 2020. 6.12 - Mass spectrometry for natural product discovery. In: Liu H-W, Begley TP, editors. Comprehensive natural products III. Oxford (England): Elsevier. p. 263–306.; [accessed 2020 Dec 30]. http://www.sciencedirect.com/science/article/pii/B9780124095472148346.

Lowe WE, Gray TRG. 1972. Ecological studies on coccoid bacteria in a pine forest soil—I. classification. Soil Biol Biochem. 4(4):459–467. doi:10.1016/0038-0717(72)90061-2.

Lowry TM. 1923. XCIX.—Studies of electrovalency. Part I. The polarity of double bonds. J Chem Soc, Trans. 123(0):822–831. doi:10.1039/CT9232300822.

Lucas RM, Norval M, Wright CY. 2016. Solar ultraviolet radiation in Africa: a systematic review and critical evaluation of the health risks and use of photoprotection. Photochem Photobiol Sci. 15(1):10–23. doi:10.1039/c5pp00419e.

Luo J, Song Z, Ning J, Cheng Y, Wang Y, Cui F, Shen Y, Wang M. 2018. The ethanol-induced global alteration in *Arthrobacter simplex* and its mutants with enhanced ethanol tolerance. Appl Microbiol Biotechnol. 102(21):9331–9350. doi:10.1007/s00253-018-9301-1.

Lutnaes BF, Oren A, Liaaen-Jensen S. 2002. New C40-carotenoid acyl glycoside as principal carotenoid in *Salinibacter ruber*, an extremely halophilic eubacterium. J Nat Prod. 65(9):1340–1343. doi:10.1021/np020125c.

Lysenko VS, Chistyakov VA, Zimakov DV, Soier VG, Sazykina MA, Sazykina MI, Sazykin IS, Krasnov VP. 2011. Separation and mass spectrometry identification of carotenoid complex from radioresistant bacteria *Deinococcus radiodurans*. J Anal Chem. 66(13):1281–1284. doi:10.1134/S1061934811130144.

Machmudah S, Goto M. 2013. Methods for extraction and analysis of carotenoids. J Nat Prod. 111:3367–3411. doi:10.1007/978-3-642-22144-6_145.

Makhalanyane TP, Scally SZ de, Cowan DA. 2017. 4. Microbiology of Antarctic edaphic and lithic habitats. In: Steven B, editor. The biology of arid soils. Berlin (Germany): De Gruyter. [accessed 2020 Nov 21]. https://www.degruyter.com/view/book/9783110419047/10.1515/9783110419047-004.xml.

Makhalanyane TP, Valverde A, Gunnigle E, Frossard A, Ramond J-B, Cowan DA. 2015. Microbial ecology of hot desert edaphic systems. FEMS Microbiol Rev. 39(2):203–221. doi:10.1093/femsre/fuu011.

Makhalanyane TP, Valverde A, Lacap DC, Pointing SB, Tuffin MI, Cowan DA. 2013. Evidence of species recruitment and development of hot desert hypolithic communities. Environ Microbiol Rep. 5(2):219–224. doi:10.1111/1758-2229.12003.

Makrodimitris S, van Ham RCHJ, Reinders MJT. 2019. Improving protein function prediction using protein sequence and GO-term similarities. Bioinformatics. 35(7):1116–1124. doi:10.1093/bioinformatics/bty751.

Maleki F, Khosravi A, Nasser A, Taghinejad H, Azizian M. 2016. Bacterial heat shock protein activity. J Clin Diagn Res. 10(3):BE01–BE03. doi:10.7860/JCDR/2016/14568.7444.

Mandelli F, Miranda VS, Rodrigues E, Mercadante AZ. 2012. Identification of carotenoids with high antioxidant capacity produced by extremophile microorganisms. World J Microbiol Biotechnol. 28(4):1781–1790. doi:10.1007/s11274-011-0993-y.

Manitto P, Speranza G, Monti D, Gramatica P. 1987. Singlet oxygen reactions in aqueous solution. Physical and chemical quenching rate constants of crocin and related carotenoids. Tetrahedron Lett. 28(36):4221–4224. doi:10.1016/S0040-4039(00)95585-0.

Marente J, Avalos J, Limón MC. 2020. Controlled transcription of regulator gene *carS* by Tet-on or by a strong promoter confirms its role as a repressor of carotenoid biosynthesis in *Fusarium fujikuroi*. Microorganisms. 9(1). doi:10.3390/microorganisms9010071.

Margesin R, Schumann P, Spröer C, Gounot A-M. 2004. *Arthrobacter psychrophenolicus* sp. nov., isolated from an alpine ice cave. Int J Syst Evol Microbiol. 54(6):2067–2072. doi:10.1099/ijs.0.63124-0.

Matallana-Surget S, Wattiez R. 2013. Impact of solar radiation on gene expression in bacteria. Proteomes. 1(2):70–86. doi:10.3390/proteomes1020070.

Mathews MM. 1963. Studies on the localization, function, and formation of the carotenoid pigments of a strain of *Mycobacterium marinum*. Photochem Photobiol. 2(1):1–8. doi:10.1111/j.1751-1097.1963.tb08114.x.

Mathews MM, Krinsky NI. 1965. The relationship between carotenoid pigments and resistance to radiation in non-photosynthetic bacteria. Photochem Photobiol. 4(4):813–817. doi:10.1111/j.1751-1097.1965.tb07923.x.

Mathews-Roth MM, Krinsky NI. 1970. Studies on the protective function of the carotenoid pigments of *Sarcina Lutea*. Photochem Photobiol. 11(6):419–428. doi:10.1111/j.1751-1097.1970.tb06014.x.

Mathews-Roth MM, Krinsky NI. 1970. Carotenoid pigments and the stability of the cell membrane of *Sarcina lutea*. Biochim Biophys Acta Biomembr. 203(2):357–359. doi:10.1016/0005-2736(70)90155-0.

Mattimore V, Battista JR. 1996. Radioresistance of *Deinococcus radiodurans*: functions necessary to survive ionizing radiation are also necessary to survive prolonged desiccation. J Bacteriol. 178(3):633–637. doi:10.1128/jb.178.3.633-637.1996.

Maurer MM, Mein JR, Chaudhuri SK, Constant HL. 2014. An improved UHPLC-UV method for separation and quantification of carotenoids in vegetable crops. Food Chem. 165:475–482. doi:10.1016/j.foodchem.2014.05.038.

Mei Q, Dvornyk V. 2015. Evolutionary history of the photolyase/cryptochrome superfamily in eukaryotes. PLoS One. 10(9):e0135940. doi:10.1371/journal.pone.0135940.

Meinhardt-Wollweber M, Suhr C, Kniggendorf A-K, Roth B. 2018. Absorption and resonance Raman characteristics of β-carotene in water-ethanol mixtures, emulsion and hydrogel. AIP Adv. 8(5):055320. doi:10.1063/1.5025788.

Meléndez-Martínez AJ, Britton G, Vicario IM, Heredia FJ. 2007. Relationship between the colour and the chemical structure of carotenoid pigments. Food Chem. 101(3):1145–1150. doi:10.1016/j.foodchem.2006.03.015.

Meslier V, Casero MC, Dailey M, Wierzchos J, Ascaso C, Artieda O, McCullough PR, DiRuggiero J. 2018. Fundamental drivers for endolithic microbial community assemblies in the hyperarid Atacama Desert. Environ Microbiol. 20(5):1765–1781. doi:10.1111/1462-2920.14106.

Moeller R, Horneck G, Facius R, Stackebrandt E. 2005. Role of pigmentation in protecting *Bacillus* sp. endospores against environmental UV radiation. FEMS Microbiol Ecol. 51(2):231–236. doi:10.1016/j.femsec.2004.08.008.

Mohana DC, Thippeswamy S, Abhishek RU. 2013. Antioxidant, antibacterial, and ultraviolet-protective properties of carotenoids isolated from *Micrococcus* spp. Radiat Prot Environ. 36(4):168. doi:10.4103/0972-0464.142394.

Moise AR, Al-Babili S, Wurtzel ET. 2014. Mechanistic aspects of carotenoid biosynthesis. Chem Rev. 114(1):164–193. doi:10.1021/cr400106y.

Mongodin EF, Shapir N, Daugherty SC, DeBoy RT, Emerson JB, Shvartzbeyn A, Radune D, Vamathevan J, Riggs F, Grinberg V, et al. 2006. Secrets of soil survival revealed by the genome sequence of *Arthrobacter aurescens* TC1. PLOS Genetics. 2(12):e214. doi:10.1371/journal.pgen.0020214.

Monnet C, Loux V, Gibrat J-F, Spinnler E, Barbe V, Vacherie B, Gavory F, Gourbeyre E, Siguier P, Chandler M, et al. 2010. The *Arthrobacter arilaitensis* Re117 Genome sequence reveals its genetic adaptation to the surface of cheese. PLOS ONE. 5(11):e15489. doi:10.1371/journal.pone.0015489.

Montero-Calasanz M del C, Göker M, Broughton WJ, Cattaneo A, Favet J, Pötter G, Rohde M, Spröer C, Schumann P, Klenk H-P, et al. 2013. *Geodermatophilus tzadiensis* sp. nov., a UV radiation-resistant bacterium isolated from sand of the Saharan desert. Syst Appl Microbiol. 36(3):177–182. doi:10.1016/j.syapm.2012.12.005.

Mortensen A, Skibsted LH. 1996. Kinetics of photobleaching of β-carotene in chloroform and formation of transient carotenoid species absorbing in the near infrared. Free Radic Res. 25(4):355–368. doi:10.3109/10715769609149058.

Mortensen A, Skibsted LH. 1997. Importance of carotenoid structure in radical-scavenging reactions. J Agric Food Chem. 45(8):2970–2977. doi:10.1021/jf970010s.

Mõttus M, Sulev M, Baret F, Lopez-Lozano R, Reinart A. 2013. Photosynthetically active radiation: measurement and modelling. In: Richter C, Lincot D, Gueymard CA, editors. Solar Energy. New York (NY): Springer. p. 140–169.; [accessed 2020 Aug 15]. https://doi.org/10.1007/978-1-4614-5806-7_451.

Müller WJ, Smit MS, van Heerden E, Capes MD, DasSarma S. 2018. Complex effects of cytochrome P450 monooxygenase on purple membrane and bacterioruberin production in an extremely halophilic archaeon: genetic, phenotypic, and transcriptomic analyses. Front Microbiol. 9:2563. doi:10.3389/fmicb.2018.02563.

Multamäki E, Nanekar R, Morozov D, Lievonen T, Golonka D, Wahlgren WY, Stucki-Buchli B, Rossi J, Hytönen VP, Westenhoff S, et al. 2020. Illuminating a phytochrome paradigm – a light-activated phosphatase in two-component signaling uncovered. bioRxiv. doi:10.1101/2020.06.26.173310.

Mulyukin AL, Demkina EV, Kryazhevskikh NA, Suzina NE, Vorob'eva LI, Duda VI, Galchenko VF, El-Registan GI. 2009. Dormant forms of *Micrococcus luteus* and *Arthrobacter globiformis* not platable on standard media. Microbiology. 78(4):407–418. doi:10.1134/S0026261709040031.

Mulyukin AL, Soina V, Demkina E, Kozlova AN, Suzina N, Dmitriev VV, Duda VI, El-Registan G. 2003. Formation of resting cells by non-spore-forming microorganisms as a strategy of long-term survival in the environment. Instruments, Methods and Missions for Astrobiology VI. 4939. doi:10.1117/12.486686.

Navarro-González R, Rainey FA, Molina P, Bagaley DR, Hollen BJ, de la Rosa J, Small AM, Quinn RC, Grunthaner FJ, Cáceres L, et al. 2003. Mars-like soils in the Atacama Desert, Chile, and the dry limit of microbial life. Science. 302(5647):1018–1021. doi:10.1126/science.1089143.

Nguyen M, Francis D, Schwartz S. 2001. Thermal isomerisation susceptibility of carotenoids in different tomato varieties. J Sci Food Agric. 81(9):910–917. doi: 10.1002/jsfa.911.

Niedzwiedzki DM, Dilbeck PL, Tang Q, Mothersole DJ, Martin EC, Bocian DF, Holten D, Hunter CN. 2015. Functional characteristics of spirilloxanthin and keto-bearing analogues in light-harvesting LH2 complexes from *Rhodobacter sphaeroides* with a genetically modified carotenoid synthesis pathway. Biochim Biophys Acta Bioenerg. 1847(6):640–655. doi:10.1016/j.bbabio.2015.04.001.

Niessen WMA. 2006. Liquid chromatography-mass spectrometry. Florida (FL): CRC Press.

Nitzan Y, Kauffman M. 1999. Endogenous porphyrin production in bacteria by δ-aminolaevulinic acid and subsequent bacterial photoeradication. Lasers Med Sci. 14(4):269–277. doi:10.1007/s101030050094.

Nugraheni SA, Khoeri MM, Kusmita L, Widyastuti Y, Radjasa OK. 2010. Characterization of carotenoid pigments from bacterial symbionts of seagrass *Thalassia hemprichii*. J Coast Dev. 14(1):51–60.

Ochsner M. 1997. Photophysical and photobiological processes in the photodynamic therapy of tumours. J Photochem Photobiol B, Biol. 39(1):1–18. doi:10.1016/S1011-1344(96)07428-3.

Oguma K, Katayama H, Ohgaki S. 2002. Photoreactivation of *Escherichia coli* after low- or medium-pressure UV disinfection determined by an endonuclease sensitive site assay. Appl Environ Microbiol. 68(12):6029–6035. doi:10.1128/AEM.68.12.6029-6035.2002.

Oren A. 2009. Microbial diversity and microbial abundance in salt-saturated brines: Why are the waters of hypersaline lakes red? Nat Resour Environ. 15(1). https://digitalcommons.usu.edu/nrei/vol15/iss1/49.

Orset SC, Young AJ. 2000. Exposure to low irradiances favors the synthesis of 9-cis β,β-carotene in *Dunaliella salina* (Teod.). Plant Physiol. 122(2):609–618. doi:10.1104/pp.122.2.609.

Ortiz-Guerrero JM, Polanco MC, Murillo FJ, Padmanabhan S, Elías-Arnanz M. 2011. Light-dependent gene regulation by a coenzyme B12-based photoreceptor. PNAS. 108(18):7565–7570. doi:10.1073/pnas.1018972108.

Panina EM, Mironov AA, Gelfand MS. 2003. Comparative genomics of bacterial zinc regulons: enhanced ion transport, pathogenesis, and rearrangement of ribosomal proteins. Proc Natl Acad Sci USA. 100(17):9912–9917. doi:10.1073/pnas.1733691100.

Parnis JM, Oldham KB. 2013. Beyond the Beer–Lambert law: the dependence of absorbance on time in photochemistry. J Photochem Photobiol A, Chem. 267:6–10. doi:10.1016/j.jphotochem.2013.06.006.

Pathak J, Richa, Rajneesh, Sonker AS, Kannaujiya VK, Sinha RP. 2015. Isolation and partial purification of scytonemin and mycosporine-like amino acids from biological crusts. J Chem Pharm. 7(1).

Paulino-Lima IG, Azua-Bustos A, Vicuña R, González-Silva C, Salas L, Teixeira L, Rosado A, Leitao AA da C, Lage C. 2013. Isolation of UVC-tolerant bacteria from the hyperarid Atacama Desert, Chile. Microb Ecol. 65(2):325–335. doi:10.1007/s00248-012-0121-z.

Paulino-Lima IG, Fujishima K, Navarrete JU, Galante D, Rodrigues F, Azua-Bustos A, Rothschild LJ. 2016. Extremely high UV-C radiation resistant microorganisms from desert environments with different manganese concentrations. J Photochem Photobiol B, Biol. 163:327–336. doi:10.1016/j.jphotobiol.2016.08.017.

Pavlopoulou A, Savva GD, Louka M, Bagos PG, Vorgias CE, Michalopoulos I, Georgakilas AG. 2016. Unraveling the mechanisms of extreme radioresistance in prokaryotes: Lessons from nature. Mutat Res Rev Mutat Res. 767:92–107. doi:10.1016/j.mrrev.2015.10.001.

Peck RF, Graham SM, Gregory AM. 2019. Species widely distributed in halophilic archaea exhibit opsin-mediated inhibition of bacterioruberin biosynthesis. J Bacteriol. 201(2). doi:10.1128/JB.00576-18.

Peck RF, Pleşa AM, Graham SM, Angelini DR, Shaw EL. 2017. Opsin-mediated inhibition of bacterioruberin synthesis in halophilic archaea. J Bacteriol. 199(21):e00303-17. doi:10.1128/JB.00303-17.

Perera IC, Grove A. 2010. Molecular mechanisms of ligand-mediated attenuation of DNA binding by MarR family transcriptional regulators. J Mol Cell Biol. 2(5):243–254. doi:10.1093/jmcb/mjq021.

Pérez V, Hengst M, Kurte L, Dorador C, Jeffrey WH, Wattiez R, Molina V, Matallana-Surget S. 2017. Bacterial survival under extreme UV radiation: a comparative proteomics study of *Rhodobacter* sp., isolated from high altitude wetlands in Chile. Front Microbiol. 8. doi:10.3389/fmicb.2017.01173.

Perez-Fons L, Steiger S, Khaneja R, Bramley PM, Cutting SM, Sandmann G, Fraser PD. 2011. Identification and the developmental formation of carotenoid pigments in the yellow/orange *Bacillus* spore-formers. Biochim Biophys Acta. 1811(3):177–185. doi:10.1016/j.bbalip.2010.12.009.

Pezzoni M, Costa CS, Pizarro RA, Oppezzo OJ. 2011. The relationship between carotenoids and sunlight response in members of the family *Micrococcaceae*. J Basic Microbiol. 51(3):325–329. doi:10.1002/jobm.201000223.

Pfander H. 1994. C45- and C50-carotenoids. Pure Appl Chem. 66(10–11):2369–2374. doi:10.1351/pac199466102369.

Phadwal K. 2005. Carotenoid biosynthetic pathway: molecular phylogenies and evolutionary behavior of *crt* genes in eubacteria. Gene. 345(1):35–43. doi:10.1016/j.gene.2004.11.038.

Pitts DG. 1990. Sunlight as an ultraviolet source. Optom Vis Sci. 67(6):401–406. doi:10.1097/00006324-199006000-00003.

Pointing SB, Belnap J. 2012. Microbial colonization and controls in dryland systems. Nat Rev Microbiol. 10(8):551–562. doi:10.1038/nrmicro2831.

Poole CF. 1999. Planar chromatography at the turn of the century. J Chromatogr A. 856(1):399–427. doi:10.1016/S0021-9673(99)00430-6.

Poole CF. 2003. Thin-layer chromatography: challenges and opportunities. J Chromatogr A. 1000(1–2):963–984. doi:10.1016/s0021-9673(03)00435-7.

Potts M. 1994. Desiccation tolerance of prokaryotes. Microbiol Rev. 58(4):755–805.

Power HC, Mills DM. 2005. Solar radiation climate change over southern Africa and an assessment of the radiative impact of volcanic eruptions. Int J Climatol. 25(3):295–318. doi:10.1002/joc.1134.

Protti S, Ravelli D, Fagnoni M. 2019. Wavelength dependence and wavelength selectivity in photochemical reactions. Photochem Photobiol Sci. 18(9):2094–2101. doi:10.1039/C8PP00512E.

Pudasaini S, Wilson J, Ji M, van Dorst J, Snape I, Palmer AS, Burns BP, Ferrari BC. 2017. Microbial diversity of Browning Peninsula, Eastern Antarctica revealed using molecular and cultivation methods. Front Microbiol. 8:591. doi:10.3389/fmicb.2017.00591.

Purcell EB, Crosson S. 2008. Photoregulation in prokaryotes. Curr Opin Microbiol. 11(2):168–178. doi:10.1016/j.mib.2008.02.014.

Qiu X, Sundin GW, Wu L, Zhou J, Tiedje JM. 2005. Comparative analysis of differentially expressed genes in *Shewanella oneidensis* MR-1 following exposure to UVC, UVB,

and UVA radiation. J Bacteriol. 187(10):3556–3564. doi:10.1128/JB.187.10.3556-3564.2005.

Quek PH, Hu J. 2008. Influence of photoreactivating light intensity and incubation temperature on photoreactivation of *Escherichia coli* following LP and MP UV disinfection. J Appl Microbiol. 105(1):124–133. doi:10.1111/j.1365-2672.2008.03723.x.

Quesada A, Mouget JL, Vincent WF. 1995. Growth of Antarctic cyanobacteria under ultraviolet radiation: UVA counteracts UVB inhibition. J Phycol. 31(2). doi:https://doi.org/10.1111/j.0022-3646.1995.00242.x.

Quesada A, Vincent WF. 1997. Strategies of adaptation by Antarctic cyanobacteria to ultraviolet radiation. Eur J Phycol. 32(4):335–342. doi:10.1080/09670269710001737269.

R Core Team. 2020. R: A language and environment for statistical computing. Vienna, Austria: R Foundation for Statistical Computing. https://www.R-project.org/.

Raisig A, Sandmann G. 2001. Functional properties of diapophytoene and related desaturases of C30 and C40 carotenoid biosynthetic pathways. Biochim Biophys Acta Mol Cell Biol Lipids. 1533(2):164–170. doi:10.1016/S1388-1981(01)00154-8.

Rajagopal L, Sundari CS, Balasubramanian D, Sonti RV. 1997. The bacterial pigment xanthomonadin offers protection against photodamage. FEBS Lett. 415(2):125–128. doi:10.1016/S0014-5793(97)01109-5.

Ramel F, Birtic S, Cuiné S, Triantaphylidès C, Ravanat J-L, Havaux M. 2012. Chemical quenching of singlet oxygen by carotenoids in plants. Plant Physiol. 158(3):1267–1278. doi:10.1104/pp.111.182394.

Ramond J-B, Baxter J, Maggs-Kölling G, Martínez-Alvarez L, Read DA, León-Sobrino C, van der Walt AJ, Cowan DA. 2019. Chapter 6 - Microbial ecology of the Namib Desert. In: Seckbach J, Rampelotto P, editors. Model ecosystems in extreme environments. London (UK): Academic Press. p. 113–143.; [accessed 2021 Jan 10]. http://www.sciencedirect.com/science/article/pii/B9780128127421000064.

Ramond J-B, Woodborne S, Hall G, Seely M, Cowan DA. 2018. Namib Desert primary productivity is driven by cryptic microbial community N-fixation. Sci Rep. 8(1):6921. doi:10.1038/s41598-018-25078-4.

Rampelotto PH. 2013. Extremophiles and extreme environments. Life (Basel). 3(3):482–485. doi:10.3390/life3030482.

Rastogi RP, Richa, Kumar A, Tyagi MB, Sinha RP. 2010. Molecular mechanisms of ultraviolet radiation-induced DNA damage and Repair. J Nucleic Acids. 2010. doi:10.4061/2010/592980.

Reddy GS, Aggarwal RK, Matsumoto GI, Shivaji S. 2000. *Arthrobacter flavus* sp. nov., a psychrophilic bacterium isolated from a pond in McMurdo Dry Valley, Antarctica. Int J Syst Evol Microbiol. 50:1553–1561. doi:10.1099/00207713-50-4-1553.

Reddy GSN, Prakash JSS, Matsumoto GI, Stackebrandt E, Shivaji S. 2002. *Arthrobacter roseus* sp. nov., a psychrophilic bacterium isolated from an Antarctic cyanobacterial mat sample. Int J Syst Evol Microbiol. 52(3):1017–1021. doi:10.1099/00207713-52-3-1017.

Reis-Mansur MCPP, Cardoso-Rurr JS, Silva JVMA, de Souza GR, Cardoso V da S, Mansoldo FRP, Pinheiro Y, Schultz J, Lopez Balottin LB, da Silva AJR, et al. 2019. Carotenoids

from UV-resistant Antarctic *Microbacterium* sp. LEMMJ01. Sci Rep. 9(1):9554. doi:10.1038/s41598-019-45840-6.

Remund J, Müller S, Schmutz M, Graf P. 2020. Meteonorm.

Rettberg P, Rothschild LJ. 2002. Ultraviolet radiation in planetary atmospheres and biological implications. In: Horneck G, Baumstark-Khan C, editors. Astrobiology: the quest for the conditions of life. Berlin (Germany): Springer. p. 233–243.; [accessed 2020 Aug 15]. https://doi.org/10.1007/978-3-642-59381-9_16.

Retzlaff M-G, Hanika J, Beyerer J. 2017. Physically based computer graphics for realistic image formation to simulate optical measurement systems. J Sens Sens Syst. 6(1):171–184. doi:10.5194/jsss-6-171-2017

Rezaeeyan Z, Safarpour A, Amoozegar MA, Babavalian H, Tebyanian H, Shakeri F. 2017. High carotenoid production by a halotolerant bacterium, *Kocuria* sp. strain QWT-12 and anticancer activity of its carotenoid. EXCLI J. 16:840–851. doi:10.17179/excli2017-218.

Rilling HC. 1962. Photoinduction of carotenoid synthesis of a *Mycobacterium* sp. Biochim Biophys Acta. 60:548–556. doi:10.1016/0006-3002(62)90873-9.

Rivera S, Vilaró F, Canela R. 2011. Determination of carotenoids by liquid chromatography/mass spectrometry: effect of several dopants. Anal Bioanal Chem. 400(5):1339–1346. doi:10.1007/s00216-011-4825-6.

Rivera SM, Canela-Garayoa R. 2012. Analytical tools for the analysis of carotenoids in diverse materials. J Chromatogr A. 1224:1–10. doi:10.1016/j.chroma.2011.12.025.

Rivera SM, Christou P, Canela-Garayoa R. 2014. Identification of carotenoids using mass spectrometry. Mass Spectrom Rev. 33(5):353–372. doi:10.1002/mas.21390.

Rochat B. 2018. Quantitative and qualitative LC-high-resolution MS: The technological and biological reasons for a shift of paradigm. IntechOpen. [accessed 2021 Jun 17]. https://www.intechopen.com/books/recent-advances-in-analytical-chemistry/quantitative-and-qualitative-lc-high-resolution-ms-the-technological-and-biological-reasons-for-a-sh.

Rodriguez-Amaya DB. 2016. Structures and analysis of carotenoid molecules. In: Stange C, editor. Carotenoids in nature: biosynthesis, regulation and function. Cham (Switzerland): Springer International Publishing. p. 71–108.; [accessed 2021 Feb 17]. https://doi.org/10.1007/978-3-319-39126-7_3.

Rodriguez-Amaya DB, Kimura M. 2004. HarvestPlus handbook for carotenoid analysis. Washington (D.C.): HarvestPlus.; [accessed 2021 Jan 2]. https://agris.fao.org/agris-search/search.do?recordID=GB2012103733.

Rodriguez-Valera F, Albert FJ, Gibson J. 1982. Effect of light on growing and starved populations of extremely halophilic bacteria. FEMS Microbiol Lett. 14(3):155–158. doi:10.1111/j.1574-6968.1982.tb08654.x.

Romaniuk K, Golec P, Dziewit L. 2018. Insight into the diversity and possible role of plasmids in the adaptation of psychrotolerant and metalotolerant *Arthrobacter* spp. to extreme Antarctic environments. Front Microbiol. 9:3144. doi:10.3389/fmicb.2018.03144.

Roncarati D, Scarlato V. 2017. Regulation of heat-shock genes in bacteria: from signal sensing to gene expression output. FEMS Microbiol Rev. 41(4):549–574. doi:10.1093/femsre/fux015.

Rondanelli R, Molina A, Falvey M. 2015. The Atacama surface solar maximum. Bull Am Meterol Soc. 96(3):405–418. doi:10.1175/BAMS-D-13-00175.1.

Ronnekleiv M. 1995. Bacterial carotenoids 53 C50-carotenoids 23; carotenoids of *Haloferax volcanii* versus other halophilic bacteria. Biochem Syst Ecol. 23(6):627–634. doi:10.1016/0305-1978(95)00047-X.

Rønnekleiv M, Liaaen-Jensen S. 1992. Bacterial carotenoids. 52. C50-carotenoids 22. Naturally occurring geometrical isomers of bacterioruberin. Acta Chem Scand. 46:1092–1095. doi:10.3891/acta.chem.scand.46-1092.

Ruiz Gonzalez C, Simó R, Sommaruga R, Gasol JM. 2013. Away from darkness: a review on the effects of solar radiation on heterotrophic bacterioplankton activity. Front Microbiol. 4. doi:10.3389/fmicb.2013.00131.

Saini RK, Keum Y-S. 2018. Carotenoid extraction methods: A review of recent developments. Food Chem. 240:90–103. doi:10.1016/j.foodchem.2017.07.099.

Saito T, Miyabe Y, Ide H, Yamamoto O. 1997. Hydroxyl radical scavenging ability of bacterioruberin. Radiat Phys Chem. 50(3):267–269. doi:10.1016/S0969-806X(97)00036-4.

Saito T, Terato H, Yamamoto O. 1994. Pigments of *Rubrobacter radiotolerans*. Arch Microbiol. 162(6):414–421. doi:10.1007/BF00282106.

Sajjad W, Din G, Rafiq M, Iqbal A, Khan S, Zada S, Ali B, Kang S. 2020. Pigment production by cold-adapted bacteria and fungi: colorful tale of cryosphere with wide range applications. Extremophiles.1–27. doi:10.1007/s00792-020-01180-2.

Salton MRJ, Ehtisham-ud-Din AFM. 1965. The localization of cytochromes and carotenoids in isolated bacterial membranes and envelopes. Aust J Exp Biol Med Sci. 43(3):255–264. doi:10.1038/icb.1965.24.

Sander LC, Sharpless KE, Pursch M. 2000. C30 stationary phases for the analysis of food by liquid chromatography. J Chromatogr A. 880(1–2):189–202. doi:10.1016/s0021-9673(00)00121-7.

Sander LC, Sharpless KEpler, Craft NE, Wise SA. 1994. Development of engineered stationary phases for the separation of carotenoid isomers. Anal Chem. 66(10):1667–1674. doi:10.1021/ac00082a012.

Sandmann G. 1994. Phytoene Desaturase: Genes, enzymes and phylogenetic aspects. J Plant Physiol. 143(4):444–447. doi:10.1016/S0176-1617(11)81805-5.

Sandmann G. 1995. Carotenoid biosynthesis in microorganisms and plants. In: Christen P, Hofmann E, editors. EJB Reviews 1994. Berlin (Germany): Springer. p. 129–146.; [accessed 2020 Sep 20]. https://doi.org/10.1007/978-3-642-79502-2_10.

Sandmann G. 2019. Antioxidant protection from UV- and light-stress related to carotenoid structures. Antioxidants. 8(7):219. doi:10.3390/antiox8070219.

Sandmann G, Fraser PD. 1993. Differential inhibition of phytoene desaturases from diverse origins and analysis of resistant cyanobacterial mutants. Zeitschrift für Naturforschung C. 48(3–4):307–311. doi:10.1515/znc-1993-3-431.

Sandmann G, Kuhn S, Böger P. 1998. Evaluation of structurally different carotenoids in *Escherichia coli* transformants as protectants against UV-B radiation. Appl Environ Microbiol. 64(5):1972–1974. doi:10.1128/AEM.64.5.1972-1974.1998.

Sanpietro LMD, Kula M-R. 1998. Studies of astaxanthin biosynthesis in *Xanthophyllomyces dendrorhous* (*Phaffia rhodozyma*). Effect of inhibitors and low temperature. Yeast. 14(11):1007–1016. doi:10.1002/(SICI)1097-0061(199808)14:11<1007::AID-YEA307>3.0.CO;2-U.

Santos AL, Gomes NCM, Henriques I, Almeida A, Correia A, Cunha Â. 2012. Contribution of reactive oxygen species to UV-B-induced damage in bacteria. J Photochem Photobiol B, Biol. 117:40–46. doi:10.1016/j.jphotobiol.2012.08.016.

Santos AL, Oliveira V, Baptista I, Henriques I, Gomes NCM, Almeida A, Correia A, Cunha Â. 2013. Wavelength dependence of biological damage induced by UV radiation on bacteria. Arch Microbiol. 195(1):63–74. doi:10.1007/s00203-012-0847-5.

Schabereiter-Gurtner C, Piñar G, Vybiral D, Lubitz W, Rölleke S. 2001. *Rubrobacter*-related bacteria associated with rosy discolouration of masonry and lime wall paintings. Arch Microbiol. 176(5):347–354. doi:10.1007/s002030100333.

Schachtschneider K, February EC. 2010. The relationship between fog, floods, groundwater and tree growth along the lower Kuiseb River in the hyperarid Namib. J Arid Environ. 74(12):1632–1637. doi:10.1016/j.jaridenv.2010.05.027.

Schatzman SS, Culotta VC. 2018. Chemical warfare at the microorganismal level: a closer look at the superoxide dismutase enzymes of pathogens. ACS Infect Dis. 4(6):893–903. doi:10.1021/acsinfecdis.8b00026.

Schenk M, Raffellini S, Guerrero S, Blanco GA, Alzamora SM. 2011. Inactivation of *Escherichia coli*, *Listeria innocua* and *Saccharomyces cerevisiae* by UV-C light: study of cell injury by flow cytometry. LWT - Food Sci Tech. 44(1):191–198. doi:10.1016/j.lwt.2010.05.012.

Schwieterman E, Cockell C, Meadows V. 2015. Nonphotosynthetic pigments as potential biosignatures. Astrobiology. 15(5):341–361. doi:10.1089/ast.2014.1178.

Scola V, Ramond J-B, Frossard A, Zablocki O, Adriaenssens EM, Johnson RM, Seely M, Cowan DA. 2018. Namib Desert soil microbial community diversity, assembly, and function along a natural xeric gradient. Microb Ecol. 75(1):193–203. doi:10.1007/s00248-017-1009-8.

Selvameenal L, Radhakrishnan M, Balagurunathan R. 2009. Antibiotic pigment from desert soil *Actinomycetes*; biological activity, purification and chemical screening. Indian J Pharm Sci. 71(5):499–504. doi:10.4103/0250-474X.58174.

Shahmohammadi H, Asgarani E, Terato H, Saito T, Ohyama Y, Gekko K, Yamamoto O, Ide H. 1998. Protective roles of bacterioruberin and intracellular KCl in the resistance of *Halobacterium salinarium* against DNA-damaging agents. J Radiat Res. 39(4):251–262. doi:10.1269/jrr.39.251.

Shahmohammadi HR, Asgarani E, Terato H, Ide H, Yamamoto O. 1997. Effects of 60Co gamma-rays, ultraviolet light, and mitomycin C on *Halobacterium salinarium* and *Thiobacillus intermedius*. J Radiat Res. 38(1):37–43. doi:10.1269/jrr.38.37.

Sharma N, Hepburn D, Fitt PS. 1984. Photoreactivation in pigmented and non-pigmented extreme halophiles. Biochim Biophys Acta. 799(2):135–142. doi:10.1016/0304-4165(84)90287-3.

Sharp RE, Palmitessa A, Gibney BR, White JL, Moser CC, Daldal F, Dutton PL. 1999. Ubiquinone binding capacity of the *Rhodobacter capsulatus* cytochrome bc1 complex: effect of diphenylamine, a weak binding QO site inhibitor. Biochemistry. 38(11):3440–3446. doi:10.1021/bi982639+.

Sherma J, Fried B, editors. 2003. Handbook of thin-layer chromatography. Florida (FL): CRC Press.; [accessed 2020 Dec 30]. https://www.routledge.com/Handbook-of-Thin-Layer-Chromatography/Sherma-Fried/p/book/9780824708955.

Shiona H, Bodeker G, Scott-Weekly R, Oltmanns K, Chisholm H, Burrowes J, McKenzie R. 2016. NIWA UV Atlas.

Shleeva MO, Savitsky AP, Nikitushkin VD, Solovyev ID, Kazachkina NI, Perevarov VV, Kaprelyants AS. 2019. Photoinactivation of dormant *Mycobacterium smegmatis* due to its endogenous porphyrins. Appl Microbiol Biotechnol. 103(23):9687–9695. doi:10.1007/s00253-019-10197-3.

Sies H, Stahl W. 2004. Carotenoids and UV protection. Photochem Photobiol Sci. 3(8):749–752. doi:10.1039/b316082c.

Silva TR, Tavares RSN, Canela-Garayoa R, Eras J, Rodrigues MVN, Neri-Numa IA, Pastore GM, Rosa LH, Schultz JAA, Debonsi HM, et al. 2019. Chemical characterization and biotechnological applicability of pigments isolated from Antarctic bacteria. Mar Biotechnol. 21(3):416–429. doi:10.1007/s10126-019-09892-z.

Sjursnes BJ, Kvittingen L, Schmid R. 2015. Normal and reversed-phase thin layer chromatography of green leaf extracts. J Chem Educ. 92(1):193–196. doi:10.1021/ed400519v.

Sjuts H, Dunstan MS, Fisher K, Leys D. 2013. Structure of the cobalamin-binding protein of a putative O-demethylase from *Desulfitobacterium hafniense* DCB-2. Acta Crystallogr D Biol Crystallogr. 69:1609–1616. doi:10.1107/S0907444913011323.

Skyring GW, Quadling C. 1969. Soil bacteria: comparisons of rhizosphere and nonrhizosphere populations. Can J Microbiol. 15(5):473–488. doi:10.1139/m69-083.

Smith KC. 1974. The science of photobiology. BioScience. 24(1):45–48. doi:10.1093/bioscience/24.1.45.

Snyder LR, Kirkland JJ, Glajch JL. 1997. Practical HPLC method development. New Jersey (NJ): John Wiley & Sons.

Solovchenko AE, Merzlyak MN. 2008. Screening of visible and UV radiation as a photoprotective mechanism in plants. Russ J Plant Physiol. 55(6):719. doi:10.1134/S1021443708060010.

Solyanikova IP, Suzina NE, Egozarian NS, Polivtseva VN, Prisyazhnaya NV, El-Registan GI, Mulyukin AL, Golovleva LA. 2017. The response of soil *Arthrobacter agilis* lush13 to changing conditions: Transition between vegetative and dormant state. J Environ Sci Health B. 52(10):745–751. doi:10.1080/03601234.2017.1356665.

Song K, Mohseni M, Taghipour F. 2019. Mechanisms investigation on bacterial inactivation through combinations of UV wavelengths. Water Res. 163:114875. doi:10.1016/j.watres.2019.114875.

Squier AH, Hodgson DA, Keely BJ. 2004. A critical assessment of the analysis and distributions of scytonemin and related UV screening pigments in sediments. Org Geochem. 35(11):1221–1228. doi:10.1016/j.orggeochem.2004.07.005.

Squillaci G, Parrella R, Carbone V, Minasi P, La Cara F, Morana A. 2017. Carotenoids from the extreme halophilic archaeon *Haloterrigena turkmenica*: identification and antioxidant activity. Extremophiles. 21(5):933–945. doi:10.1007/s00792-017-0954-y.

Squina FM, Mercadante AZ. 2005. Influence of nicotine and diphenylamine on the carotenoid composition of *Rhodotorula* strains. J Food Biochem. 29(6):638–652. doi:10.1111/j.1745-4514.2005.00030.x.

Stackebrandt E, Fowler VJ, Fiedler F, Seiler H. 1983. Taxonomic studies on *Arthrobacter nicotianae* and related taxa: description of *Arthrobacter uratoxydans* sp. nov. and *Arthrobacter sulfureus* sp. nov. and reclassification of *Brevibacterium protophormiae* as *Arthrobacter protophormiae* comb. nov. Syst Appl Microbiol. 4(4):470–486. doi:10.1016/S0723-2020(83)80005-8.

Stafsnes MH, Josefsen KD, Kildahl-Andersen G, Valla S, Ellingsen TE, Bruheim P. 2010. Isolation and characterization of marine pigmented bacteria from Norwegian coastal waters and screening for carotenoids with UVA-blue light absorbing properties. J Microbiol. 48(1):16–23. doi:10.1007/s12275-009-0118-6.

Stahl W, Sies H. 2002. Carotenoids and protection against solar UV radiation. SPP. 15(5):291–296. doi:10.1159/000064532.

Stark JM, Hart SC. 2003. UV-B radiation and soil microbial communities. Nature. 423(6936):137–138. doi:10.1038/423137a.

Steiger S, Jackisch Y, Sandmann G. 2005. Carotenoid biosynthesis in *Gloeobacter violaceus* PCC4721 involves a single crtI-type phytoene desaturase instead of typical cyanobacterial enzymes. Arch Microbiol. 184(4):207–214. doi:10.1007/s00203-005-0004-5.

Steven B. 2017. 1. An introduction to arid soils and their biology. In: Steven B, editor. The biology of arid soils. Berlin (Germany): De Gruyter; p. 1 – 14.; [accessed 2020 Nov 21]. https://www.degruyter.com/view/book/9783110419047/10.1515/9783110419047-001.xml.

Stomeo F, Valverde A, Pointing SB, McKay CP, Warren-Rhodes KA, Tuffin MI, Seely M, Cowan DA. 2013. Hypolithic and soil microbial community assembly along an aridity gradient in the Namib Desert. Extremophiles. 17(2):329–337. doi:10.1007/s00792-013-0519-7.

Šťovíček A, Kim M, Or D, Gillor O. 2017. Microbial community response to hydration-desiccation cycles in desert soil. Sci Rep. 7:45735. doi:10.1038/srep45735.

Stracy M, Jaciuk M, Uphoff S, Kapanidis AN, Nowotny M, Sherratt DJ, Zawadzki P. 2016. Single-molecule imaging of UvrA and UvrB recruitment to DNA lesions in living *Escherichia coli*. Nat Commun. 7(1):1–9. doi:10.1038/ncomms12568.

Su Y, Liu J, Zhang B, Zhao H, Huang G. 2020. Habitat-specific environmental factors regulate spatial variability of soil bacterial communities in biocrusts across northern China's drylands. Sci Total Environ. 719:137479. doi:10.1016/j.scitotenv.2020.137479.

Sumi S, Mutaguchi N, Ebuchi T, Tsuchida H, Yamamoto T, Suzuki M, Natsuka C, Shiratori-Takano H, Shintani M, Nojiri H, et al. 2020. Light response of *Pseudomonas putida* KT2440 mediated by class II LitR, a photosensor homolog. J Bacteriol. 202(20):e00146-20. doi:10.1128/JB.00146-20.

Sumi S, Shiratori-Takano H, Ueda K, Takano H. 2018. Role and function of class III LitR, a photosensor homolog from *Burkholderia multivorans*. J Bacteriol. 200(24):e00285-18. doi:10.1128/JB.00285-18.

Sumi S, Suzuki Y, Matsuki T, Yamamoto T, Tsuruta Y, Mise K, Kawamura T, Ito Y, Shimada Y, Watanabe E, et al. 2019. Light-inducible carotenoid production controlled by a MarR-type regulator in *Corynebacterium glutamicum*. Sci Rep. 9(1):1–15. doi:10.1038/s41598-019-49384-7.

Sutthiwong N, Caro Y, Milhau C, Valla A, Fouillaud M, Dufossé L. 2014. *Arthrobacter arilaitensis* strains isolated from ripened cheeses: Characterization of their pigmentation using spectrocolorimetry. Food Res Int. 65:184–192. doi:10.1016/j.foodres.2014.06.014.

Sutthiwong N, Dufossé L. 2014. Production of carotenoids by *Arthrobacter arilaitensis* strains isolated from smear-ripened cheeses. FEMS Microbiol Lett. 360(2):174–181. doi:10.1111/1574-6968.12603.

Sutthiwong N, Fouillaud M, Valla A, Caro Y, Dufossé L. 2014. Bacteria belonging to the extremely versatile genus *Arthrobacter* as novel source of natural pigments with extended hue range. Food Res Int. 65:156–162. doi:10.1016/j.foodres.2014.06.024.

Swinehart DF. 1962. The Beer-Lambert Law. J Chem Educ. 39(7):333. doi:10.1021/ed039p333.

Takaichi S. 2014. General methods for identification of carotenoids. Biotechnol Lett. 36(6):1127–1128. doi:10.1007/s10529-014-1479-4.

Takaichi S, Maoka T, Takasaki K, Hanada S. 2009. Carotenoids of *Gemmatimonas aurantiaca* (*Gemmatimonadetes*): identification of a novel carotenoid, deoxyoscillol 2-rhamnoside, and proposed biosynthetic pathway of oscillol 2,2'-dirhamnoside. Microbiology. 156:757–763. doi:10.1099/mic.0.034249-0.

Takaichi S, Shimada K. 1992. Characterization of carotenoids in photosynthetic bacteria. In: Methods in enzymology. Vol. 213. London (UK): Academic Press. p. 374–385.; [accessed 2021 Mar 18]. https://www.sciencedirect.com/science/article/pii/007668799213139O.

Takano H. 2016. The regulatory mechanism underlying light-inducible production of carotenoids in nonphototrophic bacteria. Biosci Biotechnol Biochem. 80(7):1264–1273. doi:10.1080/09168451.2016.1156478.

Takano H, Asker D, Beppu T, Ueda K. 2006. Genetic control for light-induced carotenoid production in non-phototrophic bacteria. J Ind Microbiol Biotechnol. 33(2):88–93. doi:10.1007/s10295-005-0005-z.

Takano H, Beppu T, Ueda K. 2006. The CarA/LitR-family transcriptional regulator: its possible role as a photosensor and wide distribution in non-phototrophic bacteria. Biosci Biotechnol Biochem. 70(9):2320–2324. doi:10.1271/bbb.60230.

Takano H, Kondo M, Usui N, Usui T, Ohzeki H, Yamazaki R, Washioka M, Nakamura A, Hoshino T, Hakamata W, et al. 2011. Involvement of CarA/LitR and CRP/FNR family transcriptional regulators in light-induced carotenoid production in *Thermus thermophilus*. J Bacteriol. 193(10):2451–2459. doi:10.1128/JB.01125-10.

Takano H, Mise K, Hagiwara K, Hirata N, Watanabe S, Toriyabe M, Shiratori-Takano H, Ueda K. 2015. Role and function of LitR, an adenosyl B12-bound light-sensitive regulator of *Bacillus megaterium* QM B1551, in regulation of carotenoid production. J Bacteriol. 197(14):2301–2315. doi:10.1128/JB.02528-14.

Takano H, Mise K, Maruyama T, Hagiwara K, Ueda K. 2016. Role of the semi-conserved histidine residue in the light-sensing domain of LitR, a MerR-type photosensory transcriptional regulator. Microbiology. 162(8):1500–1509. doi:10.1099/mic.0.000321.

Takano H, Obitsu S, Beppu T, Ueda K. 2005. Light-induced carotenogenesis in *Streptomyces coelicolor* A3(2): identification of an extracytoplasmic function sigma factor that directs photodependent transcription of the carotenoid biosynthesis gene cluster. J Bacteriol. 187(5):1825–1832. doi:10.1128/JB.187.5.1825-1832.2005.

Tamura H, Ishikita H. 2020. Quenching of singlet oxygen by carotenoids via ultrafast superexchange dynamics. J Phys Chem A. 124(25):5081–5088. doi:10.1021/acs.jpca.0c02228.

Tan B, Soderstrom DN. 1989. Qualitative aspects of UV-vis spectrophotometry of beta-carotene and lycopene. J Chem Educ. 66(3):258. doi:10.1021/ed066p258.

Tanaka M, Earl AM, Howell HA, Park M-J, Eisen JA, Peterson SN, Battista JR. 2004. Analysis of *Deinococcus radiodurans* transcriptional response to ionizing radiation and desiccation reveals novel proteins that contribute to extreme radioresistance. Genetics. 168(1):21–33. doi:10.1534/genetics.104.029249.

Tang W, Wang Y, Zhang J, Cai Y, He Z. 2019. Biosynthetic pathway of carotenoids in *Rhodotorula* and strategies for enhanced their production. J Microbiol Biotechnol. 29(4):507–517. doi:10.4014/jmb.1801.01022.

Tani C, Maoka T, Tani M, Moritomo Y, Okada T, Kitahara G, Katamoto H. 2014. Accumulation of xanthophylls from the *Phaffia* yeast (*Xanthophyllomyces dendrorhrous*) in calves. J Oleo Sci. 63(9):943–951. doi:10.5650/jos.ess14076.

Tao L, Schenzle A, Odom JM, Cheng Q. 2005. Novel carotenoid oxidase involved in biosynthesis of 4,4′-diapolycopene dialdehyde. Appl Environ Microbiol. 71(6):3294–3301. doi:10.1128/AEM.71.6.3294-3301.2005.

Taylor J-S. 2005. Structure and properties of DNA photoproducts. In: Siede W, Doetsch PW, editors. DNA Damage Recognition. 1st ed. Florida (FL): CRC Press; p. 65–296.

Terao J, Minami Y, Bando N. 2011. Singlet molecular oxygen-quenching activity of carotenoids: relevance to protection of the skin from photoaging. J Clin Biochem Nutr. 48(1):57–62. doi:10.3164/jcbn.11-008FR.

Tescari M, Frangipani E, Caneva G, Casanova Municchia A, Sodo A, Visca P. 2018. *Arthrobacter agilis* and rosy discoloration in “Terme del Foro” (Pompeii, Italy). Int Biodeterior Biodegradation. 130:48–54. doi:10.1016/j.ibiod.2018.03.015.

Thakur K, Tomar SK, Wei Z-J. 2017. Comparative mRNA expression profiles of riboflavin biosynthesis genes in *Lactobacilli* isolated from human feces and fermented bamboo shoots. Front Microbiol. 8. doi:10.3389/fmicb.2017.00427.

Tian B, Sun Z, Shen S, Wang H, Jiao J, Wang L, Hu Y, Hua Y. 2009. Effects of carotenoids from *Deinococcus radiodurans* on protein oxidation. Lett Appl Microbiol. 49(6):689–694. doi:https://doi.org/10.1111/j.1472-765X.2009.02727.x.

Tian B, Xu Z, Sun Z, Lin J, Hua Y. 2007. Evaluation of the antioxidant effects of carotenoids from *Deinococcus radiodurans* through targeted mutagenesis, chemiluminescence, and DNA damage analyses. Biochim Biophys Acta. 1770(6):902–911. doi:10.1016/j.bbagen.2007.01.016.

Tisch D, Schmoll M. 2010. Light regulation of metabolic pathways in fungi. Appl Microbiol Biotechnol. 85(5):1259–1277. doi:10.1007/s00253-009-2320-1.

Tong Y, Lighthart B. 1997. Solar radiation is shown to select for pigmented bacteria in the ambient outdoor atmosphere. Photochem Photobiol. 65(1):103–106. doi: 10.1111/j.1751-1097.1997.tb01884.x.

Tosini G, Ferguson I, Tsubota K. 2016. Effects of blue light on the circadian system and eye physiology. Mol Vis. 22:61–72.

Tuveson RW, Larson RA, Kagan J. 1988. Role of cloned carotenoid genes expressed in *Escherichia coli* in protecting against inactivation by near-UV light and specific phototoxic molecules. J Bacteriol. 170(10):4675–4680. doi:10.1128/jb.170.10.4675-4680.1988.

Tyrrell RM. 1985. A common pathway for protection of bacteria against damage by solar UVA (334 nm, 365 nm) and an oxidising agent (H2O2). Mutat Res DNA Repair Rep. 145(3):129–136. doi:10.1016/0167-8817(85)90019-7.

Tyrrell RM, Keyse SM. 1990. New trends in photobiology the interaction of UVA radiation with cultured cells. J Photochem Photobiol B, Biol. 4(4):349–361. doi:10.1016/1011-1344(90)85014-N.

Unell M. 2008. Physiological, genetic and proteomic characterization of *Arthrobacter chlorophenolicus* during growth on different phenolic substrates or temperatures [dissertation]. Uppsala, Sweden: Swedish University of Agricultural Sciences.

United Nations Environmental Programme. 1992. World atlas of desertification. London: Edward Arnold.

Valverde A, Makhalanyane TP, Seely M, Cowan DA. 2015. Cyanobacteria drive community composition and functionality in rock-soil interface communities. Mol Ecol. 24(4):812–821. doi:10.1111/mec.13068.

Van Goethem MW, Makhalanyane TP, Valverde A, Cary SC, Cowan DA. 2016. Characterization of bacterial communities in lithobionts and soil niches from Victoria Valley, Antarctica. FEMS Microbiol Ecol. 92(4):fiw051. doi:10.1093/femsec/fiw051.

Vásquez-Dean J, Maza F, Morel I, Pulgar R, González M. 2020. Microbial communities from arid environments on a global scale. A systematic review. Biol Res. 53(1):29. doi:10.1186/s40659-020-00296-1.

Veen S van der, Tang CM. 2015. The BER necessities: the repair of DNA damage in human-adapted bacterial pathogens. Nat Rev Microbiol. 13(2):83–94. doi:10.1038/nrmicro3391.

Vega M de la, Sayago A, Ariza J, Barneto AG, León R. 2016. Characterization of a bacterioruberin-producing *Haloarchaea* isolated from the marshlands of the Odiel

River in the southwest of Spain. Biotechnol Prog. 32(3):592–600. doi:10.1002/btpr.2248.

Vikram S, Guerrero LD, Makhalanyane TP, Le PT, Seely M, Cowan DA. 2016. Metagenomic analysis provides insights into functional capacity in a hyperarid desert soil niche community. Environ Microbiol. 18(6):1875–1888. doi:10.1111/1462-2920.13088.

Vila E, Hornero-Méndez D, Azziz G, Lareo C, Saravia V. 2019. Carotenoids from heterotrophic bacteria isolated from Fildes Peninsula, King George Island, Antarctica. Biotechnol Rep. 21:e00306. doi:10.1016/j.btre.2019.e00306.

Vinay Kumar BN, Kampe B, Rösch P, Popp J. 2015. Characterization of carotenoids in soil bacteria and investigation of their photodegradation by UVA radiation via resonance Raman spectroscopy. Analyst. 140(13):4584–4593. doi:10.1039/c5an00438a.

Vitreschak AG, Rodionov DA, Mironov AA, Gelfand MS. 2002. Regulation of riboflavin biosynthesis and transport genes in bacteria by transcriptional and translational attenuation. Nucleic Acids Res. 30(14):3141–3151.

Vollmerhausen TL, Conneely A, Bennett C, Wagner VE, Victor JC, O'Byrne CP. 2017. Visible and UVA light as a potential means of preventing *Escherichia coli* biofilm formation in urine and on materials used in urethral catheters. J Photochem Photobiol B, Biol. 170:295–303. doi:10.1016/j.jphotobiol.2017.04.018.

Wagner JR, Zhang J, von Stetten D, Günther M, Murgida DH, Mroginski MA, Walker JM, Forest KT, Hildebrandt P, Vierstra RD. 2008. Mutational analysis of *Deinococcus radiodurans* bacteriophytochrome reveals key amino acids necessary for the photochromicity and proton exchange cycle of phytochromes. J Biol Chem. 283(18):12212–12226. doi:10.1074/jbc.M709355200.

Walter TH, Andrews RW. 2014. Recent innovations in UHPLC columns and instrumentation. Trends Analyt Chem. 63:14–20. doi:10.1016/j.trac.2014.07.016.

Wang N, Guan B, Kong Q, Sun H, Geng Z, Duan L. 2016. Enhancement of astaxanthin production from *Haematococcus pluvialis* mutants by three-stage mutagenesis breeding. J Biotechnol. 236:71–77. doi:10.1016/j.jbiotec.2016.08.009.

Warren-Rhodes KA, McKay CP, Boyle LN, Wing MR, Kiekebusch EM, Cowan DA, Stomeo F, Pointing SB, Kaseke KF, Eckardt F, et al. 2013. Physical ecology of hypolithic communities in the central Namib Desert: The role of fog, rain, rock habitat, and light. J Geophys Res Biogeosci. 118(4):1451–1460. doi:10.1002/jgrg.20117.

Wass MN, Sternberg MJE. 2008. ConFunc—functional annotation in the twilight zone. Bioinformatics. 24(6):798–806. doi:10.1093/bioinformatics/btn037.

Weeks OB, Saleh FK, Wirahadiku-Sumah M, Berry RA. 1973. Photoregulated carotenoid biosynthesis in non-photosynthetic microorganisms. Pure Appl Chem. 35(1):63–80. doi:10.1351/pac197335010063.

Whittaker JW. 2003. The irony of manganese superoxide dismutase. Biochem Soc Trans. 31(6):1318–1321. doi:10.1042/bst0311318.

Wierzchos J, DiRuggiero J, Vítek P, Artieda O, Souza-Egipsy V, Škaloud P, Tisza M, Davila AF, Vílchez C, Garbayo I, et al. 2015. Adaptation strategies of endolithic chlorophototrophs to survive the hyperarid and extreme solar radiation environment of the Atacama Desert. Front Microbiol. 6. doi:10.3389/fmicb.2015.00934.

Wilkinson F, Ho W-T. 1978. Electronic energy transfer from sinclet molecular oxygen to carotenoids. Spectrosc Lett. 11(7):455–463. doi:10.1080/00387017808067769.

Wilkinson SP, Grove A. 2006. Ligand-responsive transcriptional regulation by members of the MarR family of winged helix proteins. Curr Issues Mol Biol. 8(1):51–62.

Will OH, Reppe CR. 1984. Ultraviolet light sensitivity of carotene-and cytochrome-c-accumulating strains of the smut fungus *Ustilago violacea*. Curr Microbiol. 11(1):31–35. doi:10.1007/BF01567572.

Wong FKY, Lacap DC, Lau MCY, Aitchison JC, Cowan DA, Pointing SB. 2010. Hypolithic microbial community of quartz pavement in the high-altitude tundra of central Tibet. Microb Ecol. 60(4):730–739. doi:10.1007/s00248-010-9653-2.

Woodall AA, Britton G, Jackson MJ. 1997. Carotenoids and protection of phospholipids in solution or in liposomes against oxidation by peroxyl radicals: Relationship between carotenoid structure and protective ability. Biochim Biophys Acta Gen Subj. 1336(3):575–586. doi:10.1016/S0304-4165(97)00007-X.

Woodall AA, Lee SW-M, Weesie RJ, Jackson MJ, Britton G. 1997. Oxidation of carotenoids by free radicals: relationship between structure and reactivity. Biochim Biophys Acta Gen Subj. 1336(1):33–42. doi:10.1016/S0304-4165(97)00006-8.

Wynn-Williams DD, Edwards HGM. 2002. Environmental UV . In: Horneck G, Baumstark-Khan C, editors. Astrobiology. Berlin, Heidelberg: Springer Berlin Heidelberg. p. 245–260.; [accessed 2020 Aug 15]. http://link.springer.com/10.1007/978-3-642-59381-9_17.

Yachai M. 2009. Carotenoid production by halophilic archaea and its applications. [dissertation]. Hat Yai, Thailand: Prince of Songkla University.

Yamane Y, Nakamura Y, Okamoto H, Ooshima H, Kato J. 1995. Overproduction of riboflavin by an *Arthrobacter* sp. mutant resistant to 5-fluorouracil. Appl Biochem Biotechnol. 50(3):317–322. doi:10.1007/BF02788101.

Yang H-S, Hoober JK. 1995. Divergent pathways for δ-aminolevulinic acid synthesis in two species of *Arthrobacter*. FEMS Microbiol Lett. 134(2–3):259–263. doi:10.1111/j.1574-6968.1995.tb07948.x.

Yang Y, Yatsunami R, Ando A, Miyoko N, Fukui T, Takaichi S, Nakamura S. 2015. Complete biosynthetic pathway of the C50 carotenoid bacterioruberin from lycopene in the extremely halophilic archaeon *Haloarcula japonica*. J Bacteriol. 197(9):1614–1623. doi:10.1128/JB.02523-14.

Yatsunami R, Ando A, Yang Y, Takaichi S, Kohno M, Matsumura Y, Ikeda H, Fukui T, Nakasone K, Fujita N, et al. 2014. Identification of carotenoids from the extremely halophilic archaeon *Haloarcula japonica*. Front Microbiol. 5. doi:10.3389/fmicb.2014.00100.

Yoon J-H, Lee C-S, O'Connor TR, Yasui A, Pfeifer GP. 2000. The DNA damage spectrum produced by simulated sunlight. J Mol Biol. 299(3):681–693. doi:10.1006/jmbi.2000.3771.

Yoon J-M, Hahn T-R, Cho M-H, Jeon J-S, Bhoo SH, Kwon Y-K. 2008. The PHY domain is required for conformational stability and spectral integrity of the bacteriophytochrome from *Deinococcus radiodurans*. Biochem Biophys Res Commun. 369(4):1120–1124. doi:10.1016/j.bbrc.2008.03.001.

Young A, Britton G, editors. 1993. Carotenoids in photosynthesis. Dordrecht (Netherlands): Springer Netherlands. [accessed 2021 Jan 9]. https://www.springer.com/gp/book/9789401049429.

Young AJ. 1993. Factors that affect the carotenoid composition of higher plants and algae. In: Young AJ, Britton G, editors. Carotenoids in photosynthesis. Dordrecht (Netherlands): Springer Netherlands; p. 160–205.; [accessed 2020 Oct 12]. https://doi.org/10.1007/978-94-011-2124-8_6.

Young AJ, Lowe GM. 2001. Antioxidant and prooxidant properties of carotenoids. Arch Biochem Biophys. 385(1):20–27. doi:10.1006/abbi.2000.2149.

Yuan M, Chen M, Zhang W, Lu W, Wang J, Yang M, Zhao P, Tang R, Li X, Hao Y, et al. 2012. Genome sequence and transcriptome analysis of the radioresistant bacterium *Deinococcus gobiensis*: insights into the extreme environmental adaptations. PLOS ONE. 7(3):e34458. doi:10.1371/journal.pone.0034458.

Yura T, Nagai H, Mori H. 1993. Regulation of the heat-shock response in bacteria. Annu Rev Microbiol. 47:321–350. doi:10.1146/annurev.mi.47.100193.001541.

Zaghdoudi K, Ngomo O, Vanderesse R, Arnoux P, Myrzakhmetov B, Frochot C, Guiavarc'h Y. 2017. Extraction, identification and photo-physical characterization of Persimmon (*Diospyros kaki* L.) carotenoids. Foods. 6(1). doi:10.3390/foods6010004.

Zamocky M, Furtmüller PG, Obinger C. 2008. Evolution of catalases from bacteria to humans. Antioxid Redox Signal. 10(9):1527–1548. doi:10.1089/ars.2008.2046.

Zdanowski MK, Żmuda-Baranowska MJ, Borsuk P, Świątecki A, Górniak D, Wolicka D, Jankowska KM, Grzesiak J. 2013. Culturable bacteria community development in postglacial soils of Ecology Glacier, King George Island, Antarctica. Polar Biol. 36(4):511–527. doi:10.1007/s00300-012-1278-0.

Zenoff VF, Heredia J, Ferrero M, Siñeriz F, Farías ME. 2006. Diverse UV-B resistance of culturable bacterial community from high-altitude wetland water. Curr Microbiol. 52(5):359–362. doi:10.1007/s00284-005-0241-5.

Zevenhuizen LPTM. 1992. Levels of trehalose and glycogen in *Arthrobacter globiformis* under conditions of nutrient starvation and osmotic stress. Antonie van Leeuwenhoek. 61(1):61–68. doi:10.1007/BF00572124.

Zhang J, Lu L, Yin L, Xie S, Xiao M. 2012. Carotenogenesis gene cluster and phytoene desaturase catalyzing both three- and four-step desaturations from *Rhodobacter azotoformans*. FEMS Microbiol Lett. 333(2):138–145. doi:10.1111/j.1574-6968.2012.02604.x.

Zhang L, Xu C, Chen Z, Li X, Li P. 2010. Photodegradation of pyrene on soil surfaces under UV light irradiation. J Hazard Mater. 173(1–3):168–172. doi:10.1016/j.jhazmat.2009.08.059.

Zhao X, Drlica K. 2014. Reactive oxygen species and the bacterial response to lethal stress. Curr Opin Microbiol. 21:1–6. doi:10.1016/j.mib.2014.06.008.

Zhao Y, Guo L, Xia Y, Zhuang X, Chu W. 2019. Isolation, identification of carotenoid-producing *Rhodotorula* sp. from marine environment and optimization for carotenoid production. Mar Drugs. 17(3):161. doi:10.3390/md17030161.

Ziegelhoffer EC, Donohue TJ. 2009. Bacterial responses to photo-oxidative stress. Nat Rev Microbiol. 7(12):856–863. doi:10.1038/nrmicro2237.

Appendices

Appendix 1: Mass Spectra of HPLC Eluents I – III and V – VIII, corresponding to results of **Section 2.3.3.2.**

A:

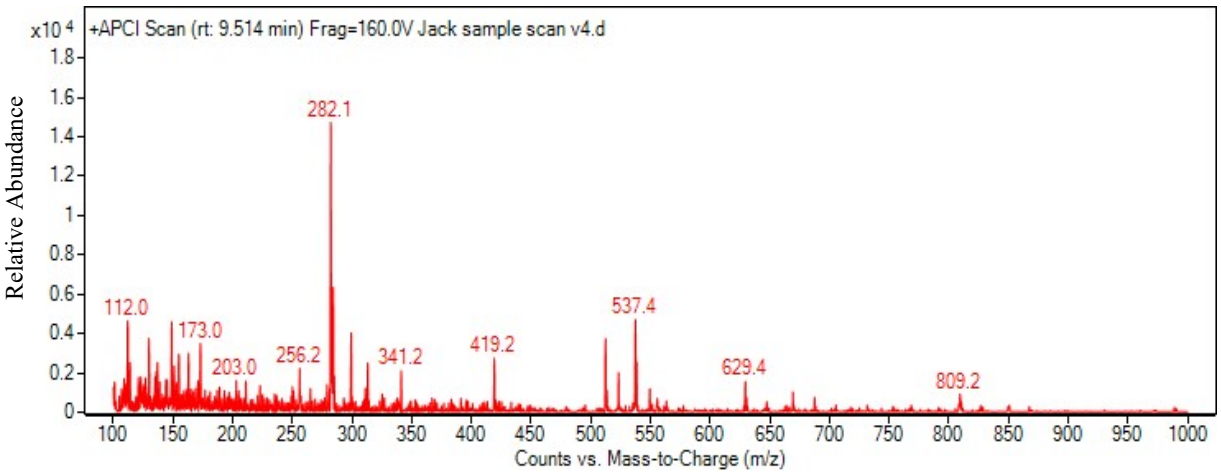

B:

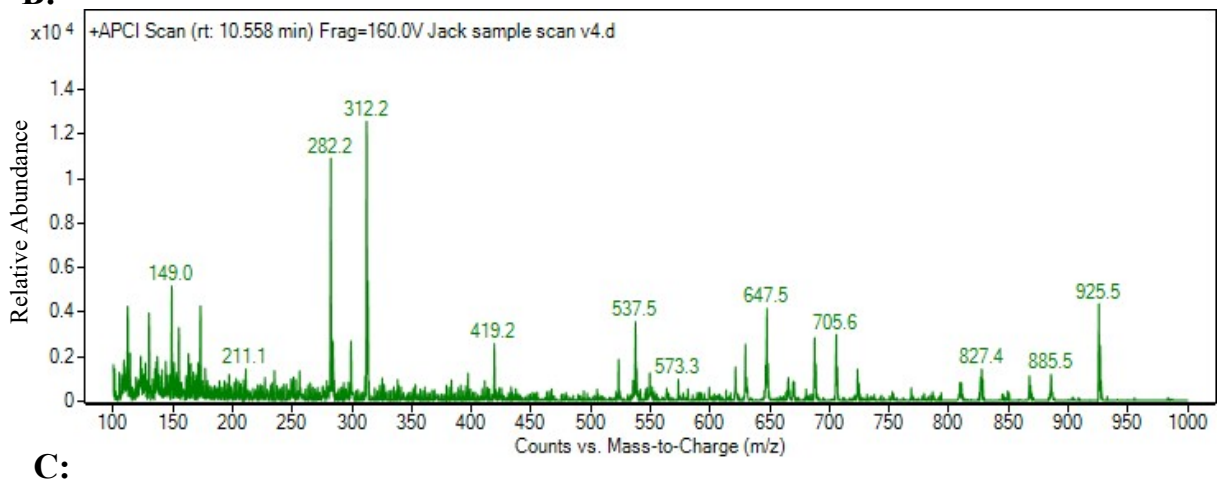

C:

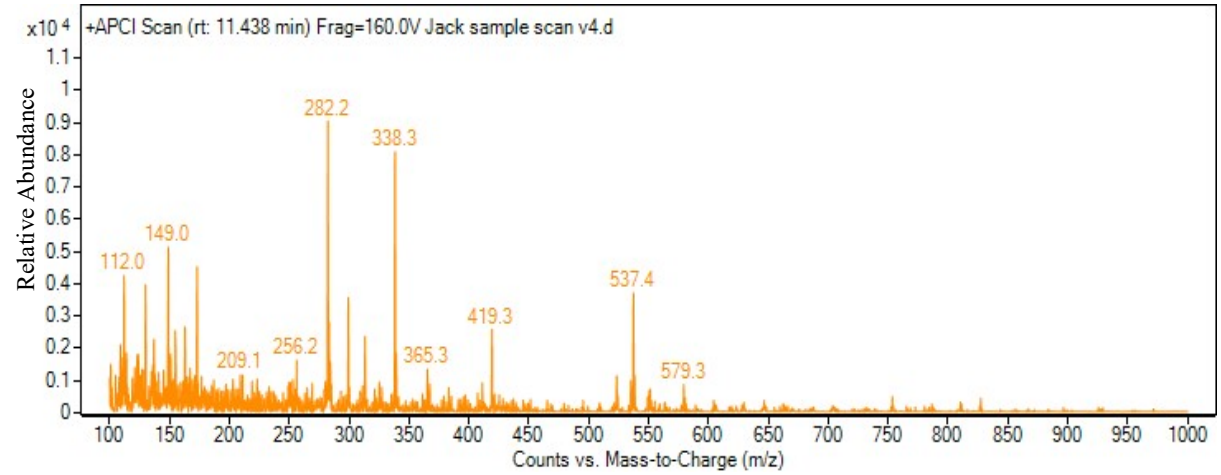

D:

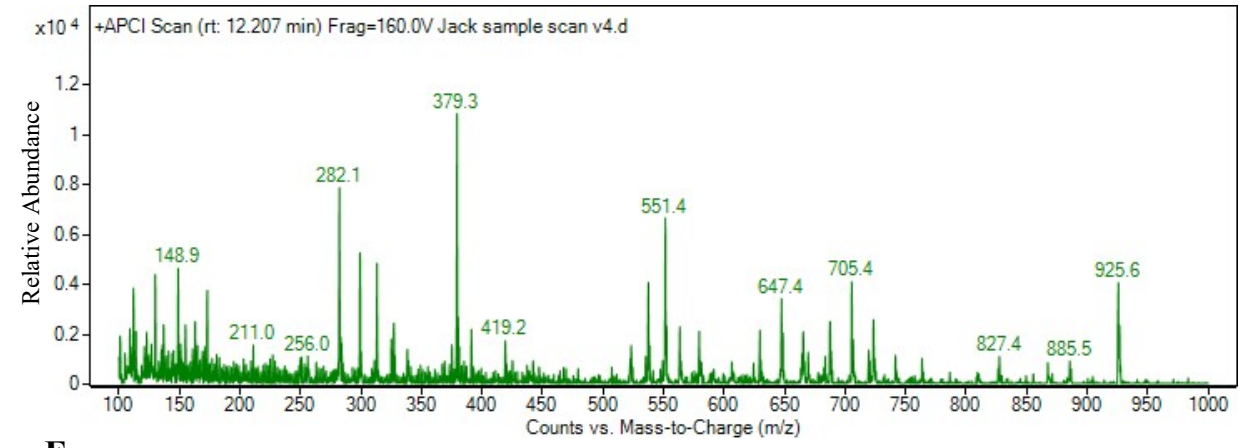
x10 4
+APCI Scan (rt: 12.207 min) Frag=160.0V Jack sample scan v4.d
Relative Abundance
379.3
282.1
551.4
148.9
705.4
647.4
925.6
211.0
256.0
419.2
827.4
885.5
Counts vs. Mass-to-Charge (m/z)

E:

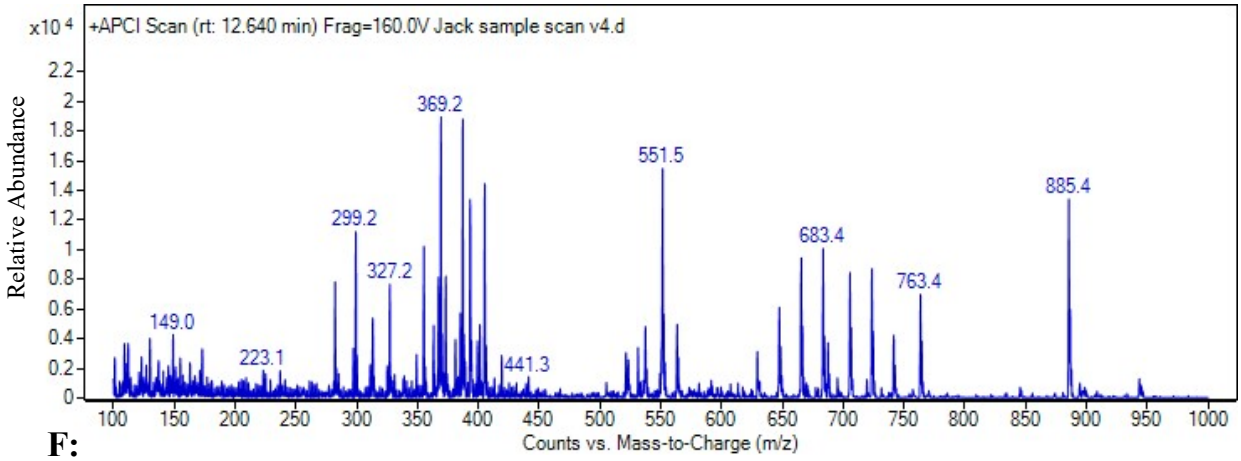
x10 4
+APCI Scan (rt: 12.640 min) Frag=160.0V Jack sample scan v4.d
Relative Abundance
369.2
551.5
885.4
299.2
683.4
327.2
763.4
149.0
223.1
441.3
Counts vs. Mass-to-Charge (m/z)

F:

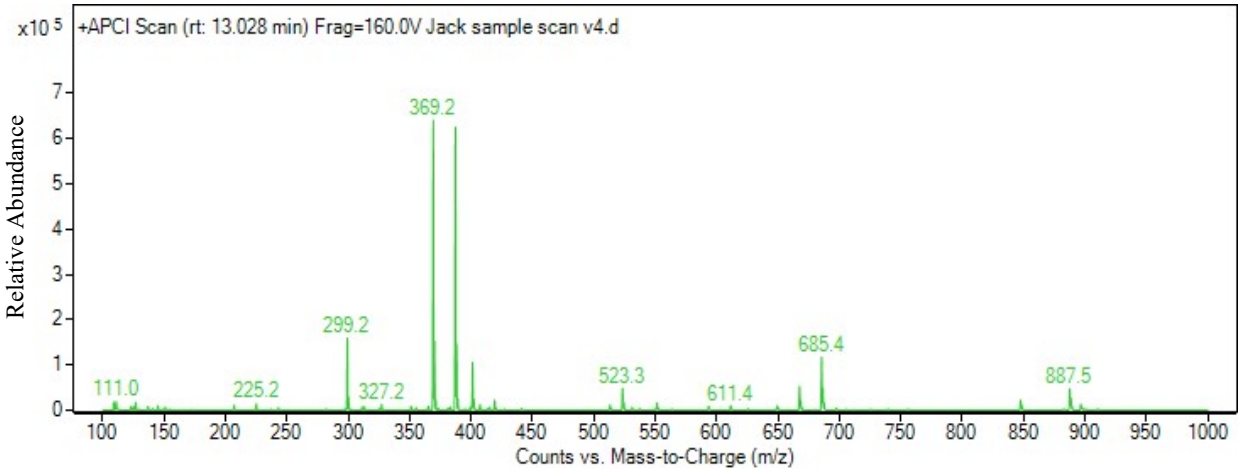
x10 5
+APCI Scan (rt: 13.028 min) Frag=160.0V Jack sample scan v4.d
Relative Abundance
369.2
299.2
685.4
111.0
225.2
327.2
523.3
611.4
887.5
Counts vs. Mass-to-Charge (m/z)

G:

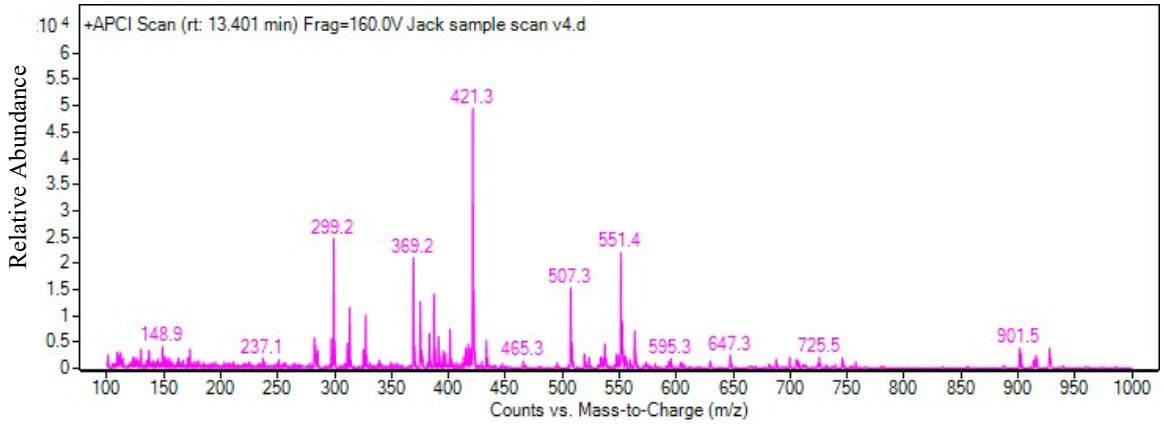

Figure S1: APCI-MS scans of HPLC-eluents. The y axis denotes the relative abundance of fragment ions, and X axis the mass/charge ratio of these fragment ions. The HPLC-eluents analysed via MS here were those presenting retention times of **A:** 9.41 minutes (eluent I); **B:** 10.48 minutes (eluent II); **C:** 11.33 minutes (eluent III); **D:** 11.76 minutes (eluent V); **E:** 12.11 minutes (eluent VI); **F:** 12.93 minutes (eluent VII); **G:** 13.33 minutes (eluent VIII)